(NASA-CR-83089) LAUNCH VEHICLE NO. 8 FLIGHT EVALUATION (Martin Co.) 290 p

N75-75421

Unclas
00/98 23575

GEMINI LAUNCH VEHICLE

GEMINI

CLASSIFICATION CHANGE

TO UNCLASSIFIED ~~CONFIDENTIAL~~

By authority of ~~T.D. No.~~ GDS-Gp 4

Changed by AM Hubbard Date 3/7/75

FOR NASA PERSONNEL ONLY

LAUNCH VEHICLE NO. 8

FLIGHT EVALUATION (U)

U. S. Government Agencies Only

Engineering Report 13227-8

RECEIVED NASA STI FACILITY INPUT BRANCH JUN 1966

Issued as Supplemental Report
to: Gemini Program Mission Report
Gemini VIII
MSC-G-R-66-4

y: Gemini VIII Mission Evaluation Team
National Aeronautics and Space Administration
Manned Spacecraft Center
Houston, Texas

April 1966

PREPARED BY

MARTIN COMPANY

X67-14134
(ACCESSION NUMBER)
290
(PAGES)
CR 83089
(NASA CR OR TMX OR AD NUMBER)
(THRU)
2C
(CODE)
31
(CATEGORY)

UNITED STATES AIR FORCE . . . Los Angeles, California

CY # 312

~~CONFIDENTIAL~~

DIC 66-520-C

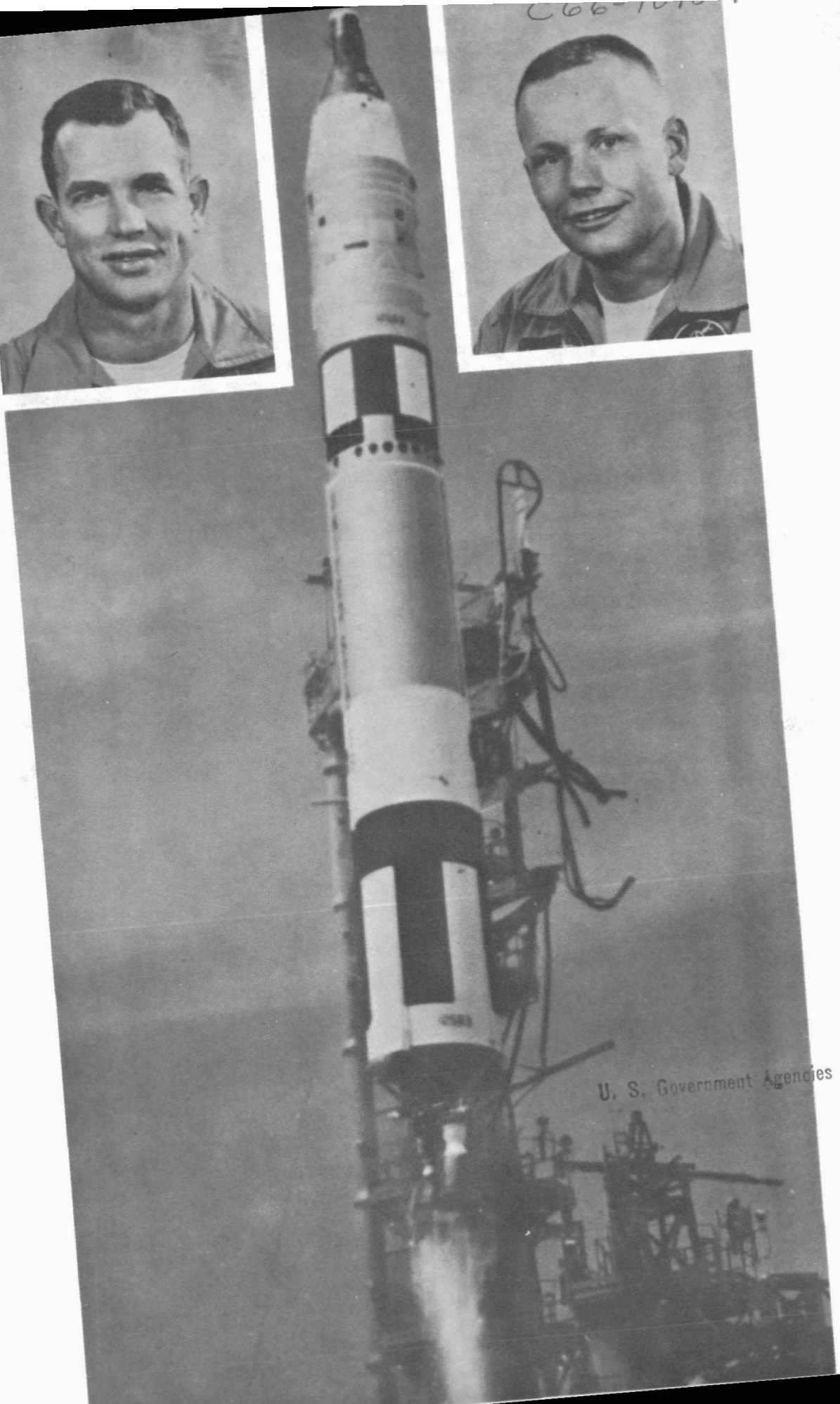

U. S. Government Agencies Only

NASA-MSC-G-R-66-4
Supplemental Report 2

GEMINI LAUNCH VEHICLE

LAUNCH VEHICLE NO. 8 FLIGHT EVALUATION (U)

GROUP 4
Downgraded at 3 year intervals; declassified after 12 years

Approved by

L. J. Rose
Assistant Technical Director
Test Evaluation

NOTICE — THIS DOCUMENT CONTAINS INFORMATION AFFECTING THE NATIONAL DEFENSE OF THE UNITED STATES WITHIN THE MEANING OF THE ESPIONAGE LAWS, TITLE 18, U.S.C. SECTIONS 793 AND 794. ITS TRANSMISSION OR THE REVELATION OF ITS CONTENTS IN ANY MANNER TO AN UNAUTHORIZED PERSON IS PROHIBITED BY LAW.

J. C. Curlander
Technical Director

Issued as Supplemental Report 2
to: Gemini Program Mission Report
Gemini VIII
MSC-G-R-66-4

by: Gemini VIII Mission Evaluation Team
National Aeronautics and Space Administration
Manned Spacecraft Center
Houston, Texas

Prepared by

MARTIN COMPANY, BALTIMORE DIVISION
Baltimore, Maryland 21203

Under CONTRACT AF 04(695)-394
PRIORITY DX-A2

For

SPACE SYSTEMS DIVISION
AIR FORCE SYSTEMS COMMAND

UNITED STATES AIR FORCE
Los Angeles, California

FOREWORD

This report has been prepared by the Gemini Launch Vehicle Program Test Evaluation Section of the Martin Company, Baltimore Division. It is submitted to the Space Systems Division, Air Force Systems Command, in compliance with Contract AF04(695)-394.

CONTENTS

		Page
	Foreword	ii
	Summary	vii
I.	Introduction	I-1
II.	System Performance	II-1
	A. Trajectory Analysis	II-1
	B. Payload Capability	II-39
	C. Staging	II-39
	D. Weight Statement	II-41
III.	Propulsion System	III-1
	A. Engine Subsystem	III-1
	B. Propellant Subsystem	III-22
	C. Pressurization Subsystem	III-66
	D. Environmental Control	III-77
IV.	Flight Control System	IV-1
	A. Stage I Flight	IV-1
	B. Stage II Flight	IV-8
	C. Post-SECO Flight	IV-12
V.	Hydraulic System	V-1
	A. Stage I	V-1
	B. Stage II	V-5
VI.	Guidance Systems	VI-1

CONTENTS (continued)

		Page
	A. Radio Guidance System Performance	VI-1
	B. Spacecraft Inertial Guidance System Ascent Performance	VI-7
VII.	Electrical System Analysis	VII-1
	A. Configuration	VII-1
	B. Countdown and Flight Performance	VII-1
VIII.	Instrumentation System	VIII-1
	A. Airborne Instrumentation	VIII-1
	B. Landline Instrumentation	VIII-1
IX.	Range Safety and Ordnance	IX-1
	A. Command Control Receivers	IX-1
	B. MISTRAM	IX-1
	C. Ordnance	IX-2
X.	Malfunction Detection System	X-1
	A. Configuration	X-1
	B. System Performance	X-2
XI.	Crew Safety	XI-1
	A. Prelaunch Winds Operations	XI-1
	B. Slow Malfunction Monitoring	XI-7
XII.	Airframe System	XII-1
	A. Structural Loads	XII-1
	B. POGO	XII-13

CONTENTS (continued)

		Page
XIII.	AGE and Facilities	XIII-1
	A. Mechanical AGE	XIII-1
	B. Electrical AGE	XIII-1
	C. Master Operations Control Set	XIII-1
	D. Facilities	XIII-1
XIV.	Reliability	XIV-1
XV.	Range Data	XV-1
	A. Launch Data Distribution	XV-1
	B. Film Coverage	XV-6
XVI.	Prelaunch and Countdown Operations	XVI-1
	A. Prelaunch	XVI-1
	B. Launch Countdown	XVI-2
XVII.	Configuration Summary	XVII-1
	A. Launch Vehicle Systems Description	XVII-1
	B. Major Components	XVII-3
XVIII.	References	XVIII-1
	Appendix A: Summary of Gemini Launches	A-1

Page intentionally left blank

Page intentionally left blank

SUMMARY

On 16 March 1966 Gemini-Titan No. 8 (GT-8) was launched successfully and on schedule from Complex 19, Cape Kennedy, Florida. Launch vehicle/spacecraft separation was completed 366 seconds after liftoff. Spacecraft re-entry was accomplished after completion of 6 orbits.

The 240-minute countdown was picked up at 0735 EST on 16 March and progressed smoothly, with astronaut ingress at approximately T-120 minutes. The Atlas-Agena was successfully launched at T-95 minutes (1000 EST). The countdown continued normally, and the programmed hold was initiated automatically at T-3 minutes for 5.9 minutes to adjust for proper liftoff time. The countdown resumed at T-3 minutes (1138 EST), and liftoff occurred on schedule at 1141 EST. The spacecraft was inserted into an elliptical orbit with a perigee of 86.9 nautical miles and an apogee of 148.2 nautical miles, all test objectives for the launch and flight were achieved.

Stages I and II engines operated satisfactorily throughout powered flight. Stage I burning time was 157.9 seconds, with shutdown initiated by fuel exhaustion. Stage II engine operation was terminated by a guidance command after 182.9 seconds of burning.

The flight control system (FCS) maintained satisfactory vehicle stability during Stages I and II flight. The primary FCS was in command throughout the flight. Vehicle rates during Stage I flight did not exceed 2.5 deg/sec, and the maximum attitude error was 1.89 degrees. The maximum rate and attitude error that occurred during staging did not exceed 4.2 deg/sec and 1.8 degrees, respectively.

Performance of the radio guidance system (RGS) was satisfactory. Pitch and yaw steering signals and SECO discrete commands were properly executed.

IGS pitch, yaw and roll performance for the entire flight appeared normal. The dispersions between IGS and primary system attitude errors remained within acceptable limits during powered flight.

The hydraulic system operated satisfactorily during the 240-minute countdown and both stages of flight. There were no significant pressure perturbations at liftoff or during flight.

The electrical system functioned as designed throughout the launch countdown and flight. Power transfer to vehicle batteries was smooth.

All channels of the PCM instrumentation system functioned satisfactorily throughout the flight. The landline instrumentation system also functioned satisfactorily prior to and up to liftoff. All airborne instrumentation hold functions monitored in the blockhouse remained within specification throughout the countdown.

The ordnance system umbilical drop weight release, propulsion system prevalves, explosive launch nuts and stage separation nuts operated as designed.

The performances of the command control receivers and the MISTRAM transponder were satisfactory.

Malfunction detection system (MDS) performance during preflight checkout and flight was satisfactory. There were no switchover commands during the flight.

The flight environment encountered by GT-8 was within design requirements. Flight loads were well within the structural capabilities of the launch vehicle. The most critical loading (which occurred at pre-BECO, aft of Station 320) reached 103% of design limit load in compression.

The longitudinal oscillation (POGO) on GT-8 reached a maximum value at spacecraft-launch vehicle interface of 0.215 g zero-to-peak at a frequency of 12.4 cps at LO + 135.4 seconds. Just prior to BECO, another peak of 0.295 g zero-to-peak was noted for 0.07 second (1 or 2 cycles).

Crew safety monitoring, which was conducted at NASA-MSC, was active during prelaunch and the launch. All guidance monitor parameters were nominal, and no corrective action was required during the flight.

During precount operations, propellant loading was delayed approximately two hours due to troubleshooting of heater and communication circuits in the spacecraft. Propellant loading was completed within the scheduled time span and to the specified load and temperature limit. A momentary malfunction which occurred at T-360 minutes prevented pressurization of the Stage I primary hydraulic system during a rate gain test. This did not cause a countdown delay, since the problem cleared up, did not recur and involved components that are used for ground test only. The T-240 minute countdown was completed on schedule. A calibration problem with the CP 2650 recorder was quickly overcome without delaying the count.

All electrical umbilicals disconnected in the planned sequence and within 0.825 second. Engine blast and heat damage to the launch stand was minor.

GLV-8 Test Objectives and Results

Objective		Results	
Primary			
P-1	Demonstrate satisfactory boost by the Gemini launch vehicle system of a manned Gemini spacecraft into the prescribed orbital insertion conditions.	P-1	Orbit insertion was within the predicted tolerances for V, h and γ.
P-2	Demonstrate performance of GLV subsystems during powered flight, relative to mission success and crew safety.	P-2	All systems performed satisfactorily throughout flight. The POGO oscillation was 0.215 g zero-to peak at a frequency of 12.4 cps at spacecraft-launch vehicle interface.
Secondary			
S-1	Evaluate trajectory performance of the launch vehicle system for refining capability and predictions for future missions.	S-1	Vehicle flight was within the 3-sigma predicted trajectory.
S-2	Demonstrate ability to load propellants to weight and temperature limits imposed by payload and vehicle requirements.	S-2	Tanks were loaded within the required tolerances of weight and temperature.
S-3	Demonstrate effectiveness of combined GLV and GAATV countdown and launch operations, including necessary ground/range support systems to achieve prescribed rendezvous mission launch requirements.	S-3	Atlas-Agena was successfully launched at T-95 minutes, followed by the GT-8 liftoff on schedule. Only a 5.9 minute hold to adjust for proper liftoff time was required.

I. INTRODUCTION

This report presents an engineering evaluation of Gemini Launch Vehicle No. 8 (GLV-8) systems performance during the countdown, launch and powered flight phase of the Gemini 8 mission.

The Gemini-Titan No. 8 (GT-8) vehicle was launched on schedule from Complex 19, Cape Kennedy, Florida at 1141 hours EST on 16 March 1966.

Gemini 8 was the eighth mission and the sixth manned flight of the program, with astronauts Neil A. Armstrong and David R. Scott aboard the spacecraft. The mission, which included a rendezvous with the Agena Target Vehicle (ATV), was completed on 16 March 1966.

The GT-8 vehicle was comprised of the two-stage GLV-8 (similar to GLV-7) and the Gemini 8 spacecraft. The spacecraft was injected into an elliptical orbit having a perigee of 86.9 nautical miles and an apogee of 148.2 nautical miles.

Significant events and tests for GLV-8 at ETR are summarized in Fig. I-1.

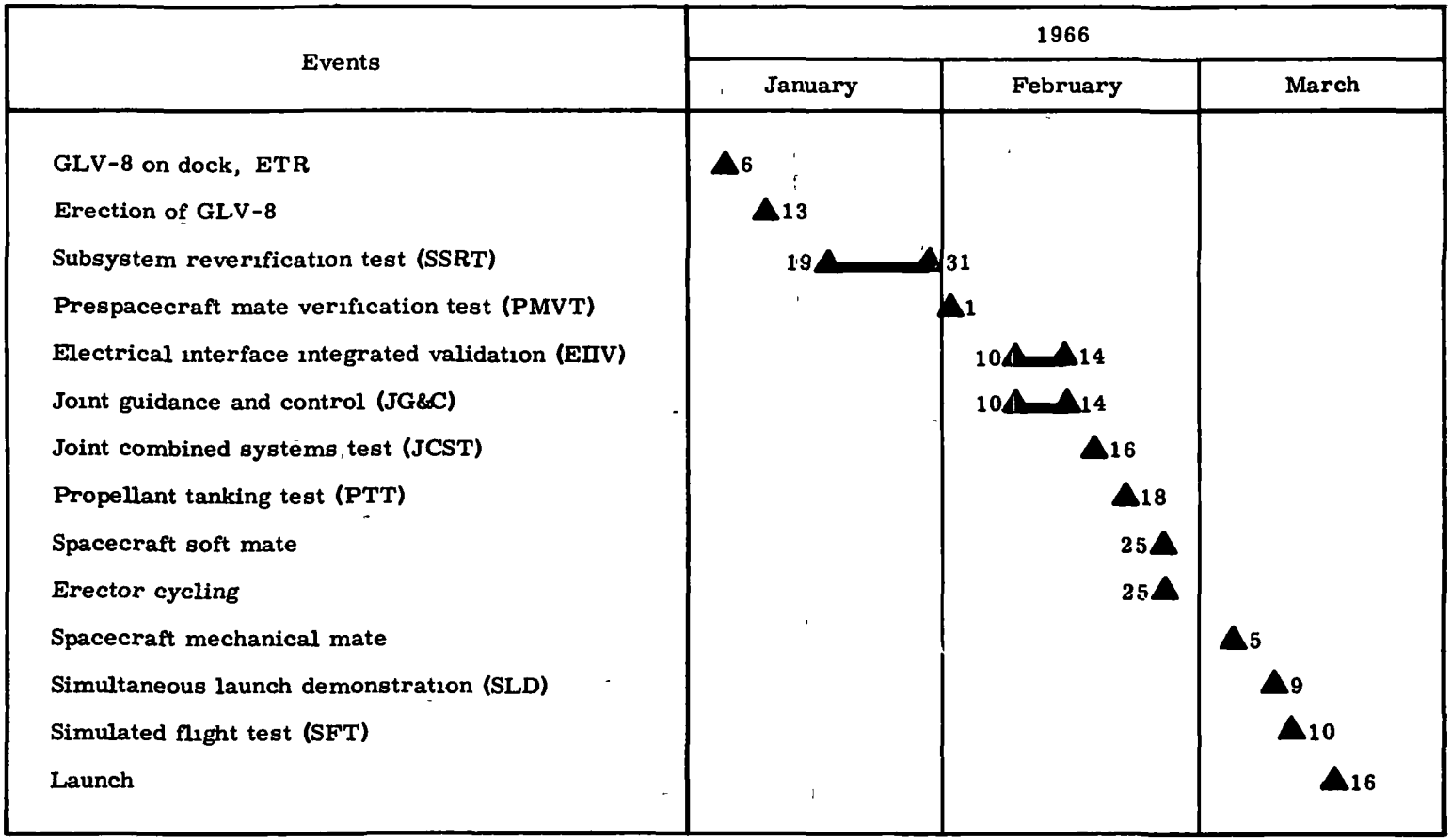

Fig. I-1. Significant Events and Tests at ETR for GT-8

II. SYSTEM PERFORMANCE

A. TRAJECTORY ANALYSIS

1. Orbit Insertion

Gemini Launch Vehicle No. 8 (GLV-8) performed as predicted and inserted the Gemini 8 spacecraft into earth orbit well within the allowable tolerance limits to permit rendezvous with the Agena target vehicle (ATV).

GT-8 was steered in the lateral plane during Stage II flight to a set of ephemeris data referenced to the time of insertion (or targeting). The values of these targeting parameters are given in Table II-1; there are no observed values of these parameters. The targeted and observed inclination angles were 28.868 and 28.92 degrees, respectively. The targeted wedge angle at liftoff was -0.1245 degree. The observed residual wedge angle at insertion was 0.0563 degree, which meant that the total wedge angle steered was -0.0682 degree.

TABLE II-1

Agena Target Vehicle Ephemeris Data

GMTLO	60,062.375 sec
T_R*	147,563.4375
$\imath$	28.868177 deg
Ω	$-0.18775463 \times 10^{-5}$ rad/sec
V_F	25,728.19 fps

A comparison of the predicted and observed insertion conditions is given in Table II-2. In this table and in all succeeding references to a predicted (nominal) trajectory, the data were obtained from the GLV-8 45-day prelaunch report (Ref. 11), updated to reflect the actual spacecraft weight (8351 pounds), guidance constants, T-0 hour wind and atmospheric data, and the -1.34% pitch programmer bias. The observed trajectory parameters are those derived by the Martin Company from the Final GE Mod III-G 2 pps data. These data have been smoothed and corrected for both refraction errors and systematic biases by the General Electric Corporation before submittal to the Martin Company.

CONFIDENTIAL

TABLE II-2

Comparison of Insertion Conditions at SECO + 20 Seconds

	Predicted Nominal	GE MOD III-G	Observed Minus Planned	Preliminary Tolerance
Altitude (naut mi)	86.734	86.667	-0.067	±0.394
Inertial velocity (fps)	25,729	25,736	+7	±29.7
Inertial flight path angle (deg)	0.001	-0.020	-0.021	±0.134

2. Derivation of Trajectory Uncertainties

The expected maximum vehicle dispersions and RGS dispersions at BECO and at SECO + 20 seconds were obtained from Refs. 12 and 13, respectively. A root sum square (RSS) of these dispersions is termed the preliminary tolerance. After determination of the preliminary tolerance, the total tolerance may be computed by the arithmetic addition of the preliminary tolerance to the 3-sigma data error of the instrumentation source being considered. Thus,

$$\text{Preliminary tolerance} = \sqrt{(\text{vehicle dispersions})^2 + (\text{RGS dispersions})^2}$$

Total tolerance = preliminary tolerance + 3-sigma data error.

The resulting preliminary tolerance is shown in Table II-3. Because the actual insertion conditions were within the preliminary tolerance, the data error estimates are not needed and, therefore, have been excluded from this report.

3. Flight Plan

The primary objective for GLV-8 was to place the Gemini 8 spacecraft into an elliptical earth orbit with an 87-nautical mile perigee* and 146-nautical mile apogee.* Having achieved orbital insertion at 25,730 fps,** the spacecraft then separates from Stage II (adding 10 fps to spacecraft velocity in the process) and coasts to the desired apogee. The following flight plan was employed to attain the desired conditions.

A vertical rise is planned for the first 23.04 seconds following liftoff, during which time a programmed roll rate of 1.25 deg/sec is initiated to roll the vehicle from a pad orientation of 84.933 degrees to the flight azimuth of 99.9 degrees.

*Relative to Complex 19.
**Does not include the separation velocity imparted by the spacecraft.

CONFIDENTIAL

TABLE II-3

Predicted Dispersions at BECO and SECO + 20 Seconds

Performance Parameter	Predicted Nominal Value* (Ref. 11)	Predicted Dispersions		
		Vehicle Dispersion (Ref. 12)	RGS Dispersion (Ref. 13)	RSS of RGS and Vehicle Dispersions
BECO				
Time from liftoff (sec)	153.847	±4.58	N/A	±4.58
Geocentric radius (ft)	21,117,565	±13,230		±13,230
Inertial velocity (fps)	9,971	±192		±192
Crossrange (ft)	2695	±15,802		±15,802
Crossrange velocity (fps)	25	±396		±396
Ground range (naut mi)	50.94	±3.33		±3.33
Inertial flight path angle (deg)	19.17	±2.51	N/A	±2.51
SECO + 20 seconds				
Time from liftoff (sec)	356.486	±7.57	±0.081	±7.57
Geocentric radius (ft)	21,438,572	±1935	±1410	±2392
Inertial velocity (fps)	25,729	±17.3	±24.09	±29.65
Crossrange (ft)	77,938	±71,720	±498	±71,720
Crossrange velocity (fps)	942	±32.16	±9.90	±33.65
Ground range (naut mi)	538.3	±14.94	±0.1416	±15.04
Inertial flight path angle (deg)	0.0005	±0.0721	±0.1125	±0.1338

N/A: Not applicable.

*Updated to reflect actual spacecraft weight (8351 pounds), guidance constants, T-0 hour wind and atmospheric data, and -1.34% pitch programmer bias.

CONFIDENTIAL

CONFIDENTIAL

At this time, an open-loop pitch program is begun (via a three-step rate command) which terminates at 162.56 seconds. The nominal commanded pitch rates and their times of application are shown in Table II-4.

Guidance commands from the radio guidance system (RGS) are initiated at LO + 168.35 seconds and continue until two seconds prior to SECO, however, velocity cutoff computations continue to SECO. Between SECO and SECO + 20 seconds, the engine shutdown impulse continues to add velocity to the vehicle (approximately 81 fps), and the spacecraft is separated from the sustainer after SECO + 20 seconds.

TABLE II-4

Planned GLV Pitch Program

Program	Rate (deg/sec)	Time from Liftoff (sec)
Step 1	-0.709	23.04 to 88.32
Step 2	-0.516	88.32 to 119.04
Step 3	-0.235	119.04 to 162.56

A comparison of the planned and actual sequences of events is contained in Table II-5, and a profile of the GTA-8 flight superimposed on the range planning map appears in Fig. II-1.

4. Trajectory Results

Analysis of the range data and Mod III-G radar data indicates that the performance of GLV-8 was normal and the vehicle flew close to the prescribed ascent trajectory throughout Stages I and II.

Table II-6 shows a reconstruction of the BECO condition by considering the actual engine data, weather conditions, propellant loading, engine misalignments, wind and guidance errors. This table is comprised of those items which can be measured and those which can only be estimated due to lack of suitable instrumentation. The primary factors contributing to the pitch and yaw plane trajectory dispersions at BECO are listed and the effect of each is summarized.

A Y_F coordinate displacement at BECO results in an approximate amplification of five on the Y_F coordinate displacement at SECO + 20 seconds. The differences shown in the apparent and measured increments of Table II-6 are well within the allowable tolerance limits presented in Table II-3.

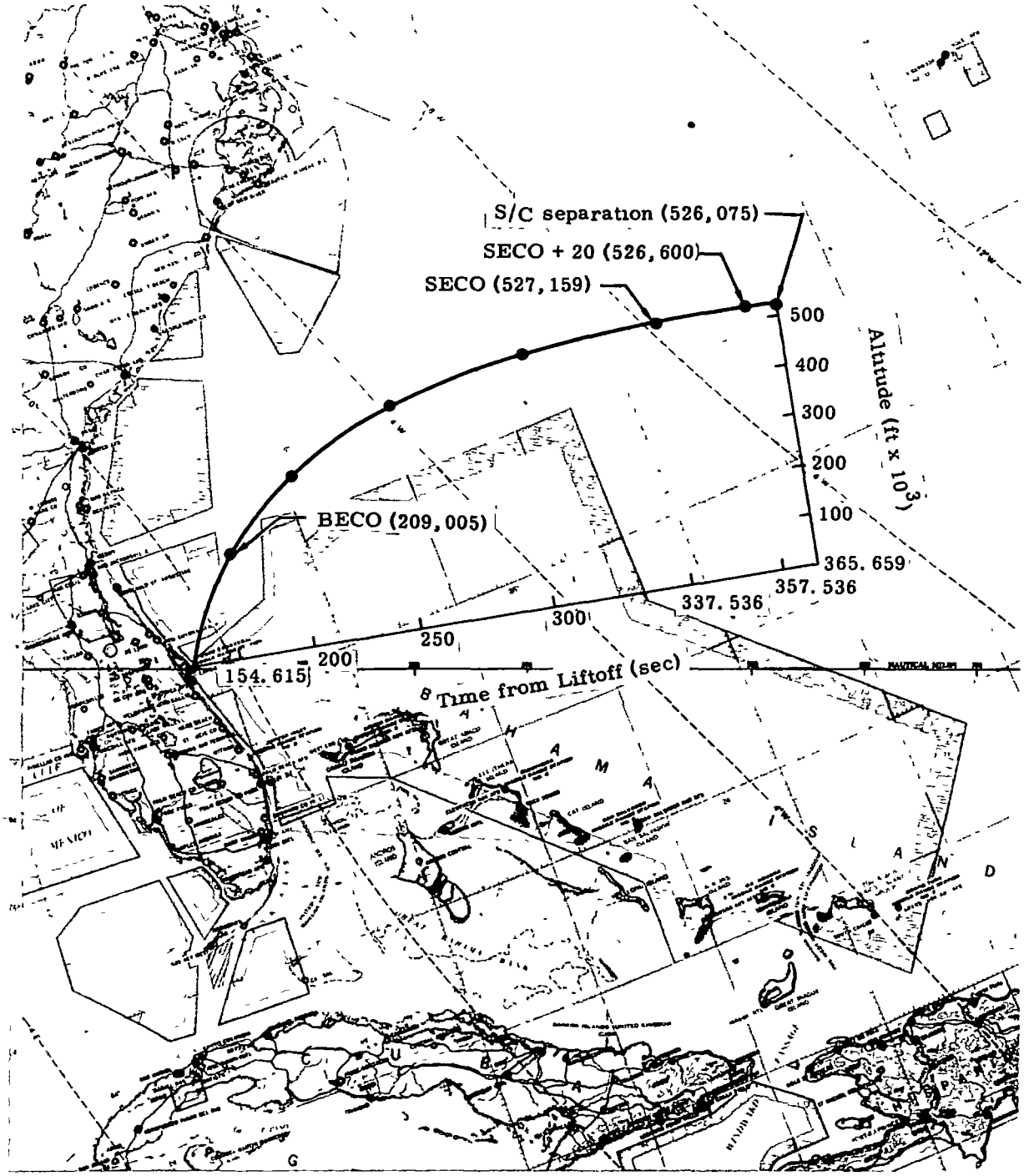

Fig. II-1. GT-8 Boost Flight Path Profile

TABLE II-5

GT-8 Flight Events Summary

Measurement	Event	GMT (hr-min-sec)	Time from Liftoff (sec)	
			Actual	Planned
0800/0801	Power Transfer	1639:33.4	-89.0	-89
FC B-10	MOCS T-0	1640.59.037	-3.352	-3.46
2104	$87FS_1$ (T-0)	:59.088	-3.301	-3.37
0356	Stage I S/A-1 MDTCPS Make	1641.00.030	-2.359	-2.27
0357	Stage I S/A-2 MDTCPS Make	:00.021	-2.368	-2.27
2101	TCPS S/A-1 & S/A-2	:00.098	-2.291	-2.20
0169	Launch Nuts	:02.206	-0.183	-0.20
4421	First Motion	:02.280	-0.109	-0.10
4422	Shutdown Lockout (backup)	:02.290	-0.099	-0.10
4423	Liftoff	02.389	0	0
0734	Start Roll Program	.10.87	8.48	8.48
0734	End Roll Program	:22.86	20.47	20.48
0732	Start Pitch Program No. 1	25.43	23.04	23.04
0732	Stop Pitch Program No. 1	1642 30.63	88.24	88.32
0732	Start Pitch Program No. 2	:30.63	88.24	88.32
0728	FCS Gain Change No. 1	.47.15	104.76	104.96
0732	Stop Pitch Program No. 2	1643 01.26	118.87	119.04
0732	Start Pitch Program No. 3	01.26	118.87	119.04
0735	Staging Enable (TARS discrete)	26.80	144.41	144.64
0741	IPS Staging Arm Timer	26.96	144.57	145.00
0356	Stage I S/A-1 MDTCPS Break	:36.969	154.580	153.79
0357	Stage I S/A-2 MDTCPS Break	:36.980	154.591	153.79
0032	$87FS_2/91FS_1$ (BECO)	37.004	154.615	153.85
0502	Start PC_3 Rise	37.650	155.261	154.50
0169	Stage Separation	:37.688	155.299	154.58
0855	Stage II MDFJPS Make	37.661	155.272	154.75
0732	Stop Pitch Program No. 3	.44.11	161.72	162.56
0740	RGS Enable	44.04	161.65	162.56
0755/0756	First Guidance Command	50.79	168.40	168.35
0739	Stage II Shutdown Enable	1646:18.68	316.29	317.44
0777	Guidance SECO	.39.905	337.516	336.73
0519	$91FS_2$	39.925	337.536	336.75
0522	Shutdown Valve Relay	.39.96	337.57	336.77
0521	Shutdown Squib	:39.95	337.56	336.77
0799	ASCO	39.97	337.58	336.78
0855	Stage II MDFJPS Break	:40.065	337.676	337.07
0699	Spacecraft Separation	1647 08.048	365.659	356.75

TABLE II-6

GT-8 BECO Conditions

	Δ Time (sec)	Δ Altitude (ft)	Δ Velocity (fps)	$\Delta\gamma$ (deg)	ΔY_F (ft)	$\Delta \dot{Y}_F$ (fps)
Measured Parameters						
Thrust Stage I (-0.31%)	0.442	-877	- 0.4	-0.155	-4	- 0.2
Outage (mean = 600 lb) (348 lb)	0.201	596	33.2	-0.018	-7	- 0.2
Wind and weather	--	-2367	63.3	-0.197	1864	9.0
Propellant loading (361 lb)	0.223	-110	7.7	-0.062	-6	- 0.2
Trend Indications						
TARS pitch programmer (-0.68%)	--	1715	- 15.9	0.364	--	--
TARS roll programmer (-1.24%)	--	--	--	--	1290	42.9
TARS pitch gyro drift (7.5 deg/hr)	--	-1050	10.1	-0.230	-50	- 1.1
TARS yaw gyro drift (-7.0 deg/hr)	--	-37	- 0.8	-0.005	1210	31.6
TARS roll gyro drift (14.3 deg/hr/g)	--	--	--	--	-683	-17.1
Engine misalignment in pitch (-0.032 deg)	--	460	- 4.8	0.115	70	1.3
Engine misalignment in yaw (-0.032 deg)	--	41	--	0.007	-615	-17.8
Engine misalignment in roll (-0.17 deg)	--	-13	- 4.2	0.006	4460	116.5
Specific impulse (0.11%)	0.169	237	12.5	0.029	-5	--
Apparent increments	1.035	-1406	100.7	-0.146	7524	164.7
Measured increments	0.768	-917	9.9	-0.03	2933	40.6

Table II-7 presents the trajectory parameters computed from the GE Mod III-G, MISTRAM I and MISTRAM I and II data. At BECO and insertion, the two data sources yielded comparable results with the exception of the crossrange position (Y_F) and the crossrange velocity ($\dot{Y}_F$) parameters as both flight events.

The actual, as well as the predicted, nominal trajectory is presented in graphical form in Figs. II-2 through II-24. On these graphs, the nominal trajectory is that documented in Ref. 11, updated to reflect the actual spacecraft weight (8351 pounds), guidance constants, T-0 hour wind and atmospheric data, and the -1.34% pitch programmer bias. The observed flight data were obtained from the Mod III-G 2-pps data, smoothed and corrected for refraction errors and systematic biases.

A list of the primary tracking sources with the trajectory time interval covered by each is contained in Table II-8.

5. Geodetic and Weather Parameters

Significant geodetic and weather parameters are shown in Table II-9. The atmospheric pressure and temperature variation with altitude is depicted in Fig. II-25, the pressure and temperature were essentially standard. Figure II-26 presents the altitude history of the magnitude and direction of the wind. At low altitudes the winds were light, increasing to a peak of 125 knots at 37,500 feet. The wind was nearly a side wind up to approximately 7,000 feet then shifted to essentially a tail wind.

6. Look Angles

The maximum look angle in pitch (LAP) occurred at LO + 336 seconds, when it attained a value of 20.7 degrees. This maximum value was within the boundary existing at that time, as shown in Fig. II-27. The corresponding look angle in yaw (LAY) was also within the established limitation, as shown in Fig. II-28. The maximum value of LAY was 4.8 degrees, which occurred 159 seconds after liftoff.

TABLE II-8

Data Available for Trajectory Analysis

Source	Type	Station	Flight Coverage (sec from range-0)
AFETR	MISTRAM position, velocity and acceleration	Valkaria I Eleuthera II	65 to 374.8 132.4 to 374.8
GE	Mod III-G radar position, velocity	Cape Kennedy	LO to + 424
NASA-MSC	Spacecraft IGS ascent parameters		LO to + 380

TABLE II-7

Comparison of GT-8 Predicted and Observed Performance at BECO and at SECO + 20 seconds

	Predicted Nominal Trajectory (Ref. 11)*	Tracking Facility			
		GE Mod III-G (2 pps)	MISTRAM I	MISTRAM I and II	BET
BECO					
Time from LO (sec)	153.847	154.615	154.615	154.615	154.615
Inertial velocity (fps)	9970.8	9917.4	9906.7	9910.	9918.
Altitude (ft)	207,556.	209,005.	209,081.	209,066	209,074
Inertial flight path angle (deg)	19.173	19.34	19.34	19.34	19.35
Ground range (naut mi)	50.938	50.93	50.931	50.934	50.933
Geocentric radius (ft)	21,117,565.	21,119,011.	21,119,085.	21,119,070.	21,119,078.
Downrange position X_F (ft)	312,770.	312,690.	312,709	312,720.	312,716
Crossrange Position, Y_F (ft)	2695.	3764.	4278.	4286.	4282.
Vertical position, Z_F (ft)	205,211.	206,660.	206,737	206,720.	206,728
Downrange velocity, $\dot{X}_F$ (fps)	8128.	8067.	8056.	8057.	8067.
Crossrange velocity, $\dot{Y}_F$ (fps)	25.1	56.8	69.8	70.	70.
Vertical velocity, $\dot{Z}_F$ (fps)	3151.	3161.	3159.	3158.	3163.
Yaw steering velocity, $\dot{V}_Y$ (fps)	---	213.	---	---	---
Biased yaw steering velocity, $\dot{V}_Y$ (fps)	---	---	---	---	---
SECO + 20 seconds					
Time from LO (sec)	356.486	357.536	357.536	357.536	357,536
Inertial velocity (fps)	25,729.1	25,736	25,735	25,737	25,736
Altitude (ft)	527,005.	526,600.	526,951	526,248	526,472
Inertial flight path angle (deg)	0.0005	-0.0200	-0.0110	-0.0448	-0.0330
Ground range (naut mi)	538.330	538.68	538.59	538.71	538.88
Geocentric radius (ft)	21,438,572.	21,438,152.	21,438,488.	21,437,787	21,438,008
Downrange position, X_F (ft)	3,340,309.	3,342,304.	3,342,158.	3,342,217.	3,342,200
Crossrange position, Y_F (ft)	77,938.	84,057.	89,811.	89,878.	89,818
Vertical position, Z_F (ft)	265,329.	264,585.	264,937.	264,218.	264,446
Downrange velocity, $\dot{X}_F$ (fps)	24,045.	24,049.	24,047	24,046	24,046.
Crossrange velocity, $\dot{Y}_F$ (fps)	942.0	960.2	996.9	997.	997.
Vertical velocity, $\dot{Z}_F$ (fps)	-3,805.	-3,818.	-3,814.	-3,829.	-3824.
Yaw steering velocity, $\dot{V}_Y$ (fps)	3.26	-16.0	---	---	---
Biased yaw steering velocity, $\dot{V}_Y$ (fps)	-1.26	---	---	---	---

*Updated to reflect actual spacecraft weight (8351 pounds), guidance constants, T-0 hour wind and atmospheric data, and the -1.34% pitch programmer bias.

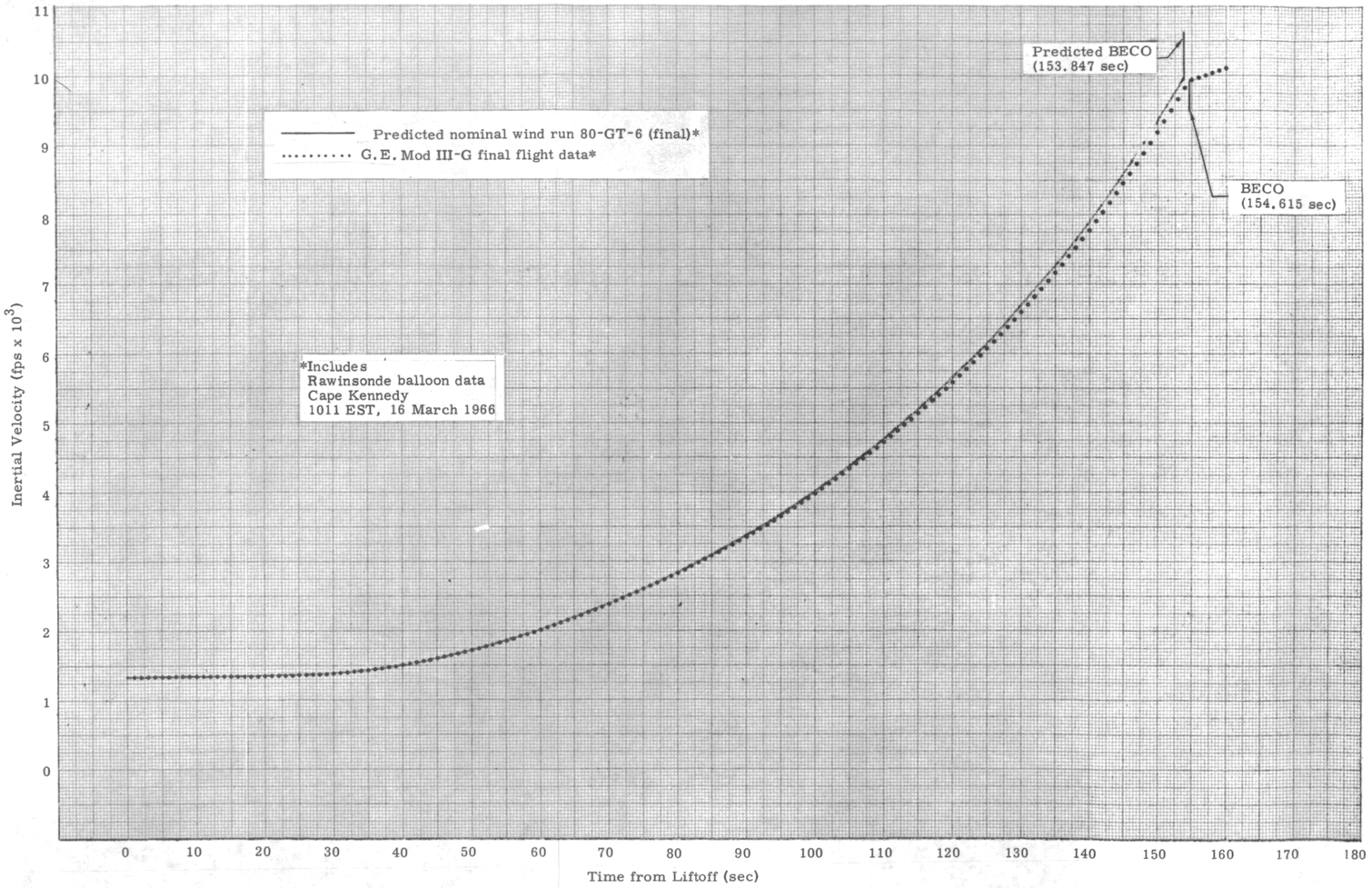

Fig. II-2. Inertial Velocity Versus Time: Stage I Flight

II-11-1

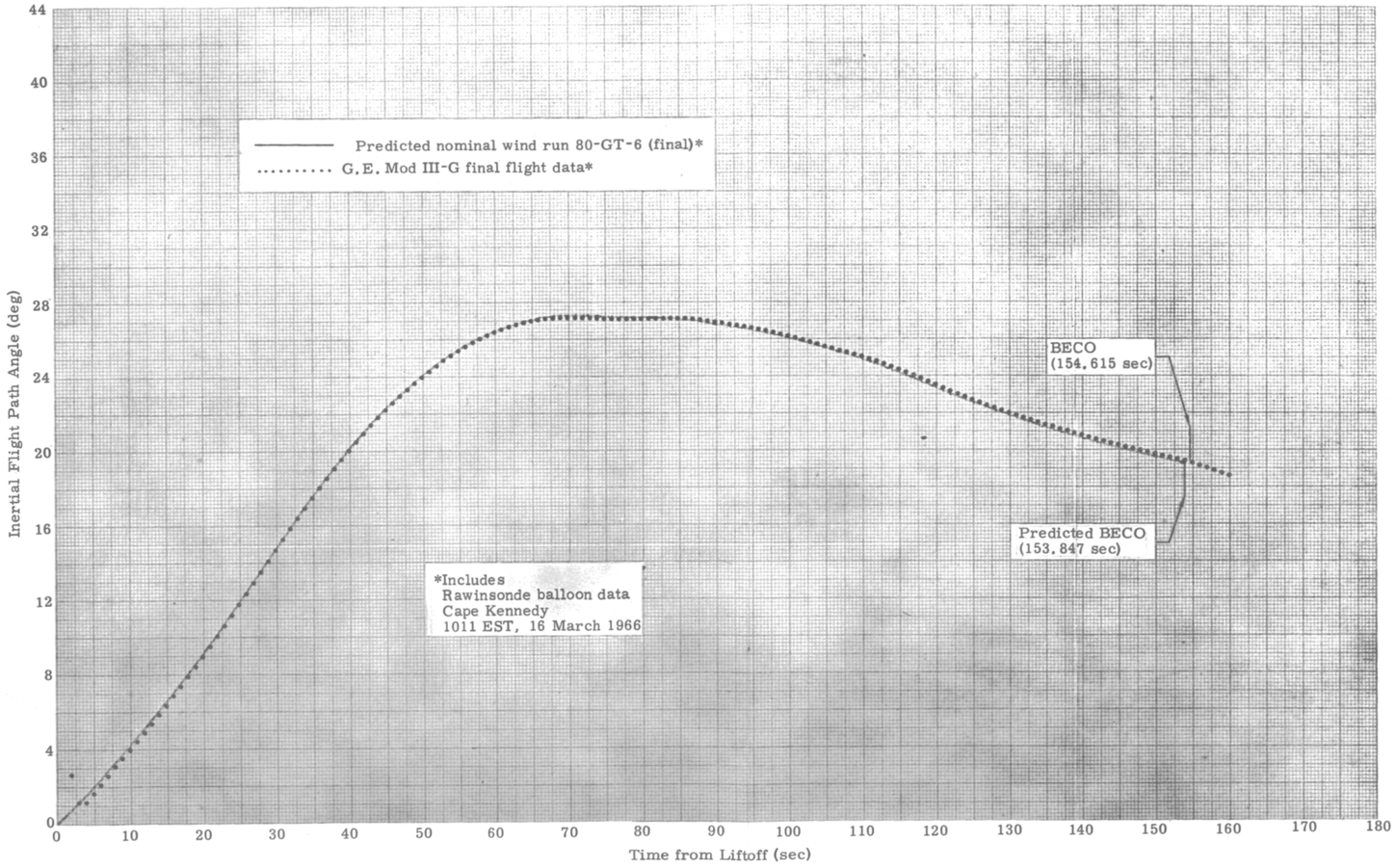

Fig. II-3. Inertial Flight Path Angle Versus Time: Stage I Flight

CONFIDENTIAL

CONFIDENTIAL

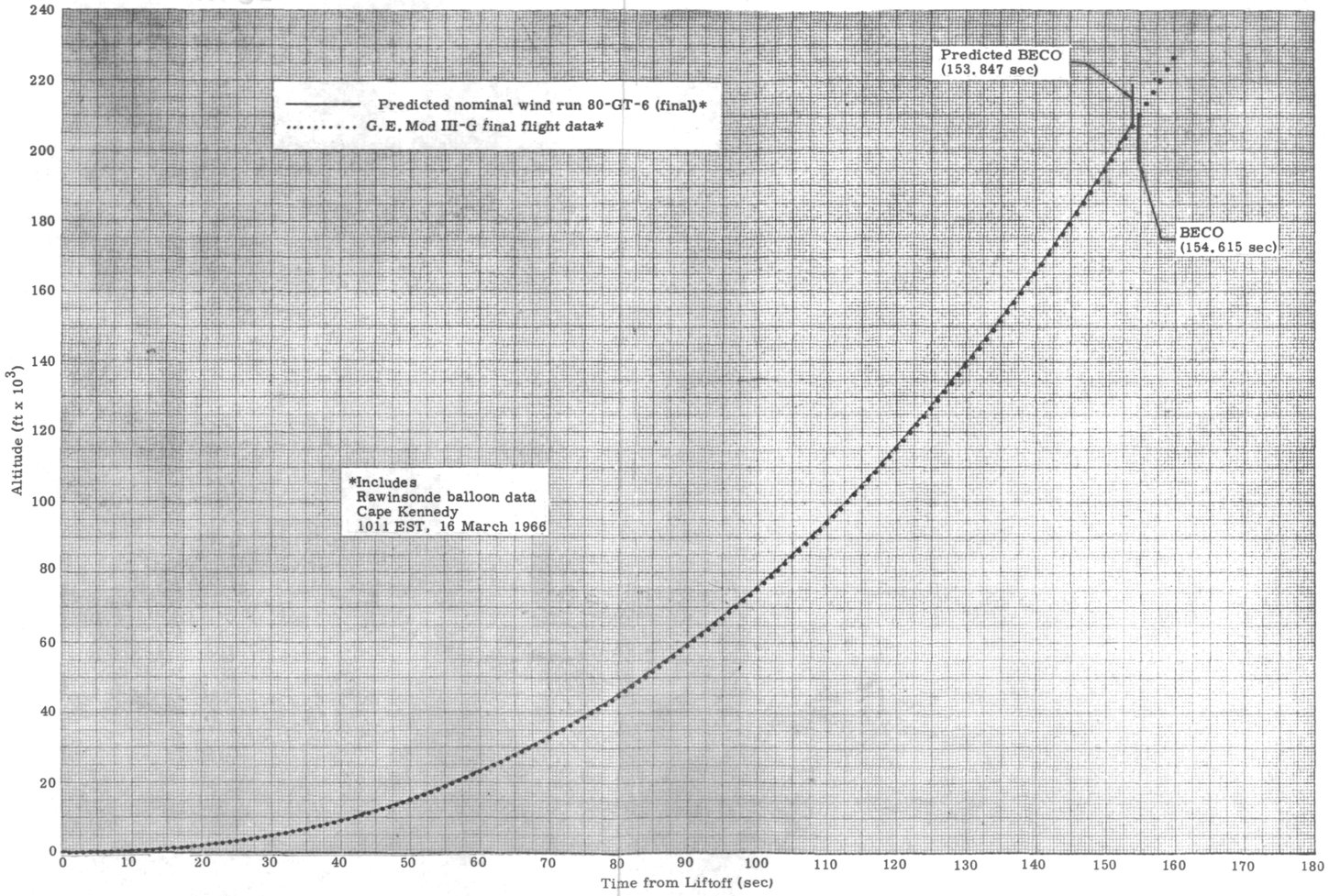

Fig. II-4. Altitude (h) Versus Time: Stage I Flight

CONFIDENTIAL

CONFIDENTIAL

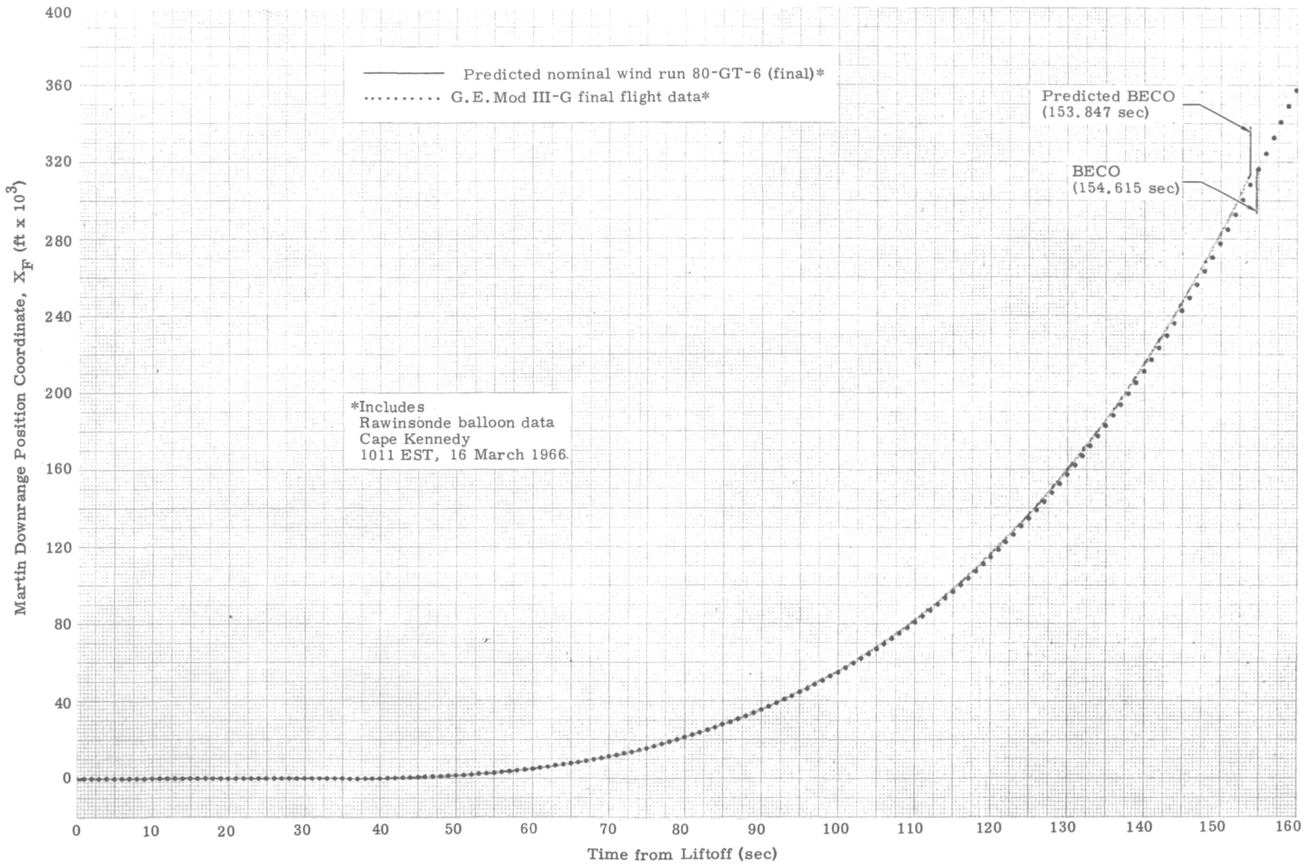

Fig. II-5. Downrange Position Coordinate (X_F) Versus Time: Stage I Flight

CONFIDENTIAL

CONFIDENTIAL

CONFIDENTIAL

II-14-1

CONFIDENTIAL

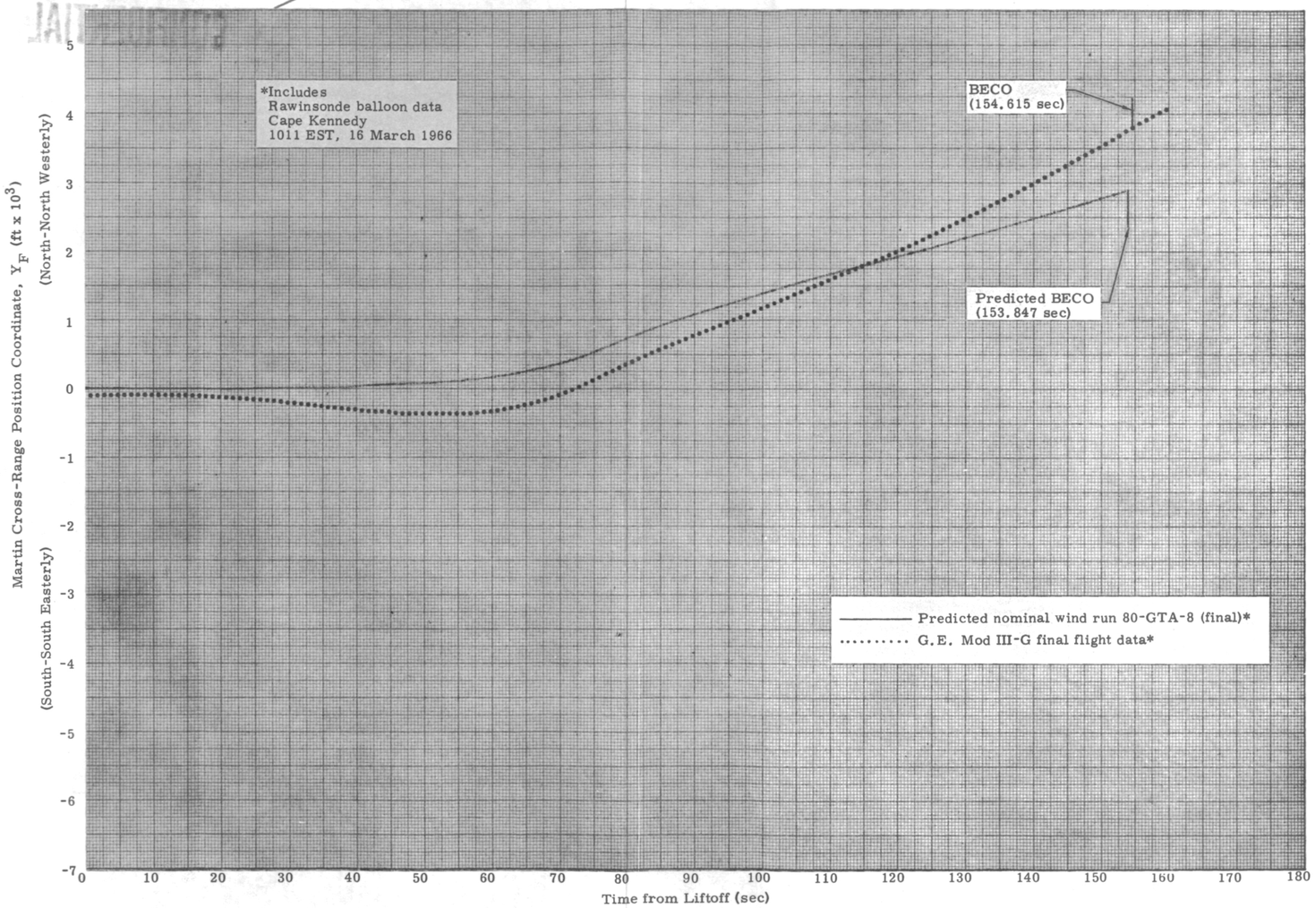

Fig. II-6. Cross-Range Position Coordinate (Y_F) Versus Time: Stage I Flight

CONFIDENTIAL

II-15-1

CONFIDENTIAL

II-15-2

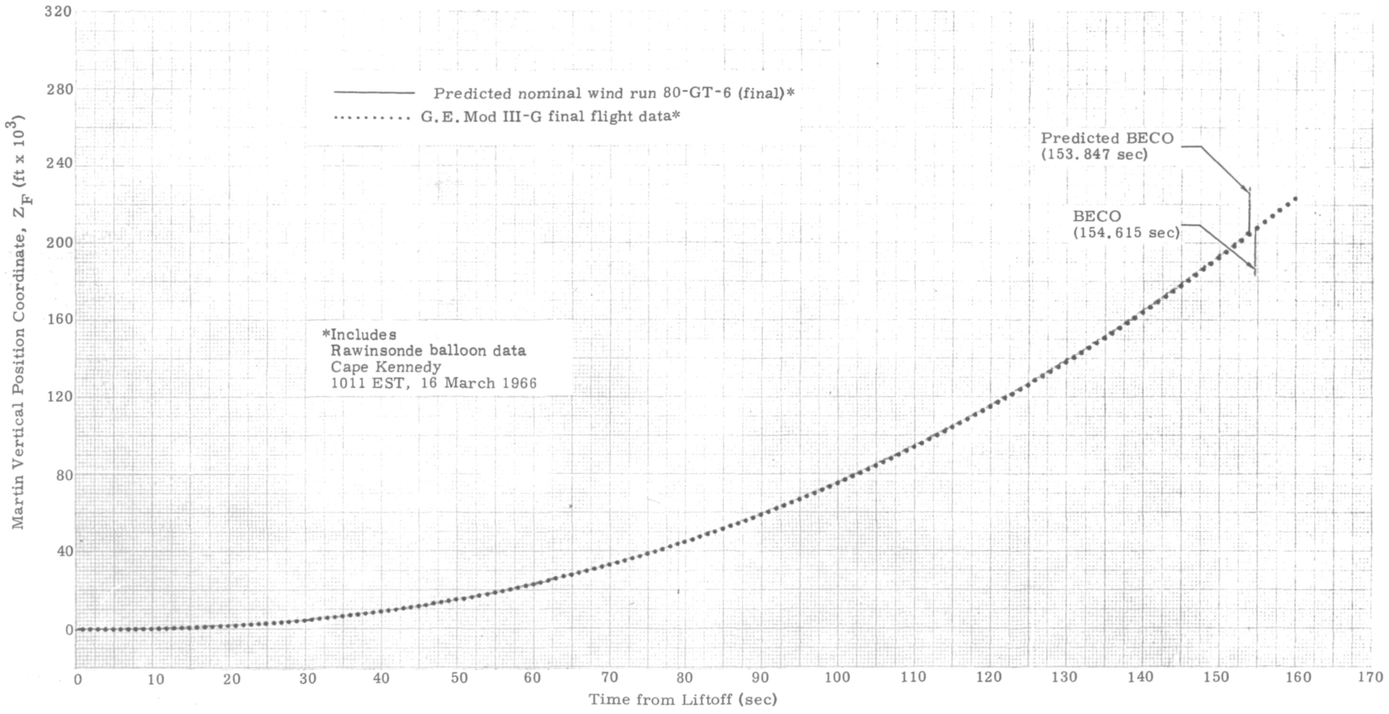

Fig. II-7. Vertical Position Coordinate (Z_F) Versus Time: Stage I Flight

CONFIDENTIAL

CONFIDENTIAL

CONFIDENTIAL

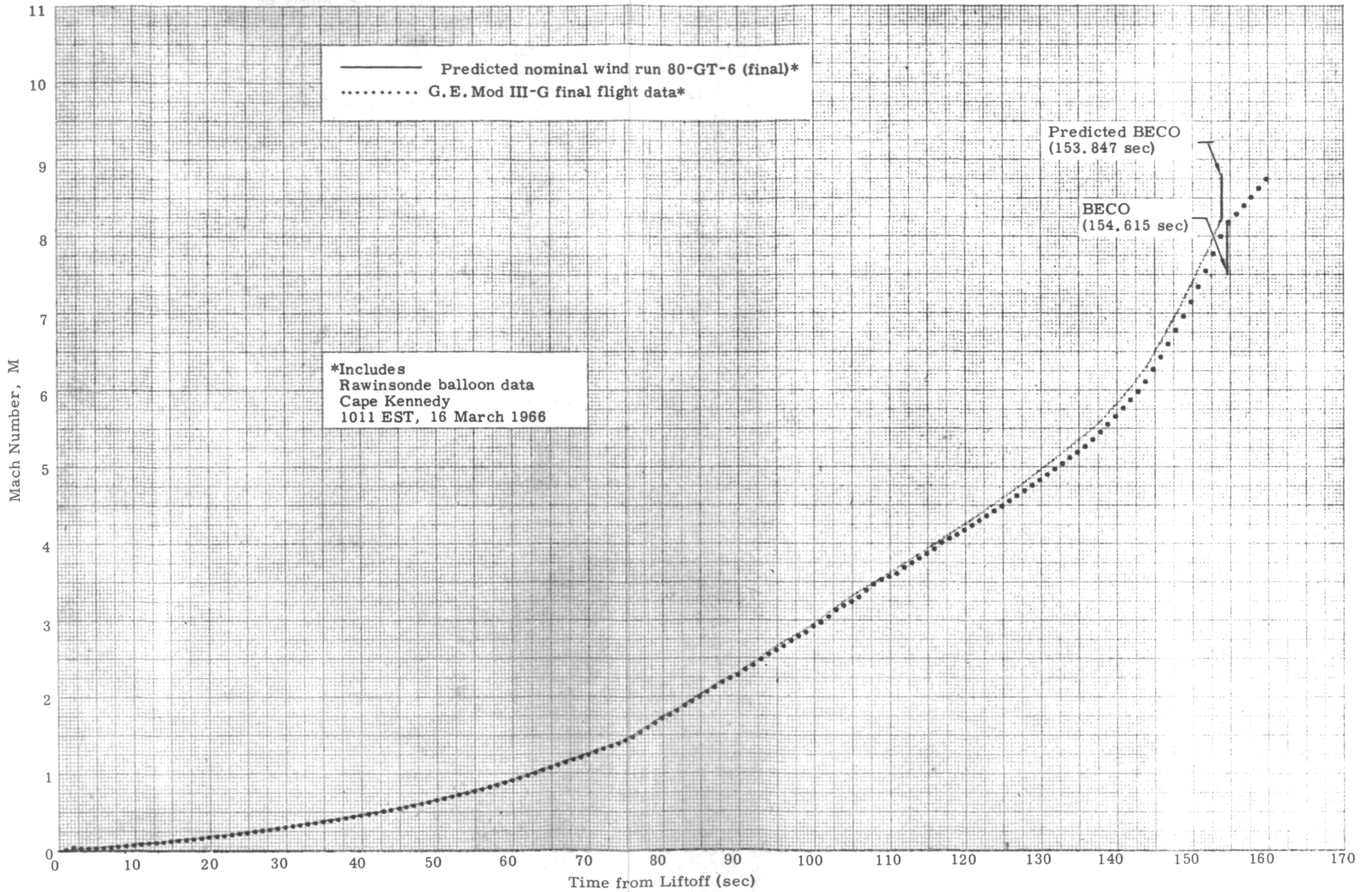

Fig. II-8. Mach Number (M) Versus Time: Stage I Flight

CONFIDENTIAL

II-17-1 CONFIDENTIAL

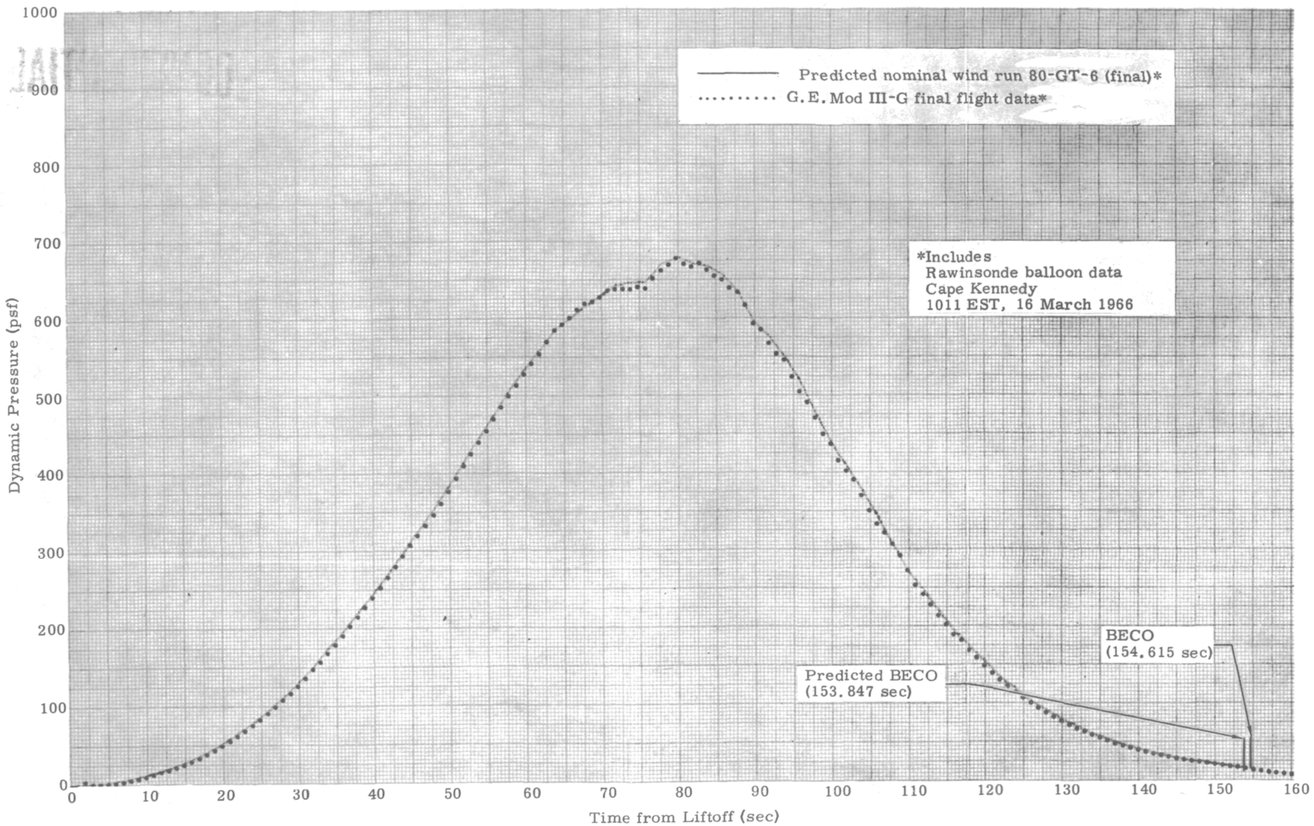

Fig. II-9. Dynamic Pressure (q) Versus Time: Stage I Flight

CONFIDENTIAL

CONFIDENTIAL

II-18-1

CONFIDENTIAL

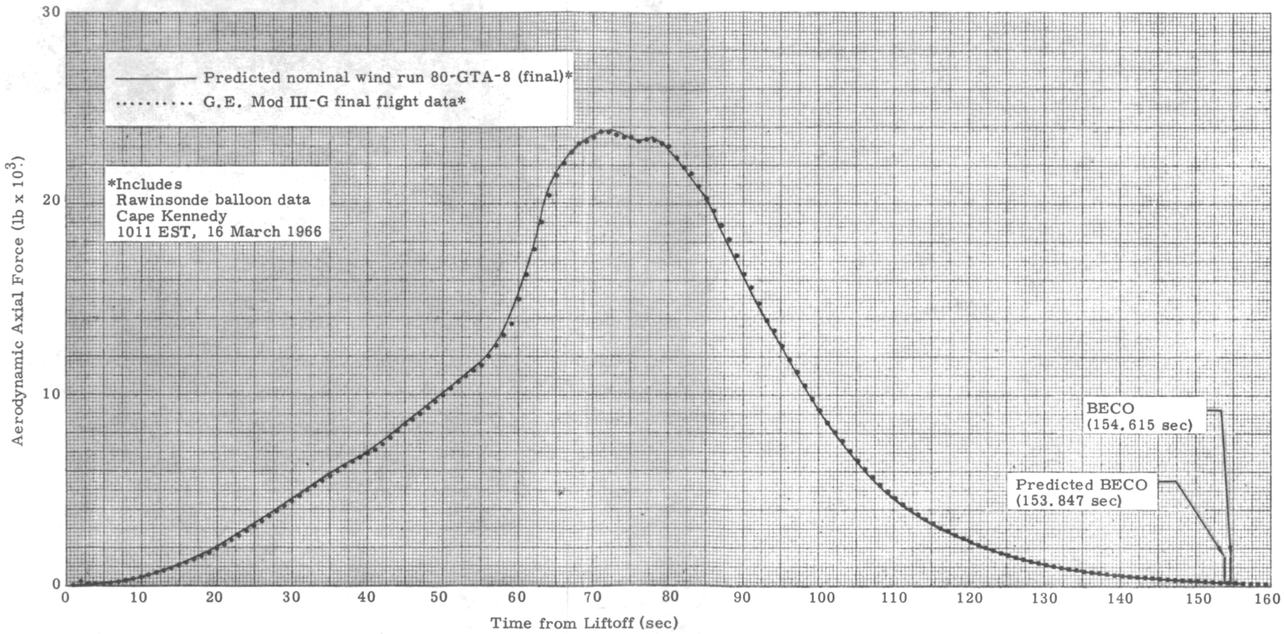

Fig. II-10. Axial Force Versus Time: Stage I Flight

CONFIDENTIAL

CONFIDENTIAL

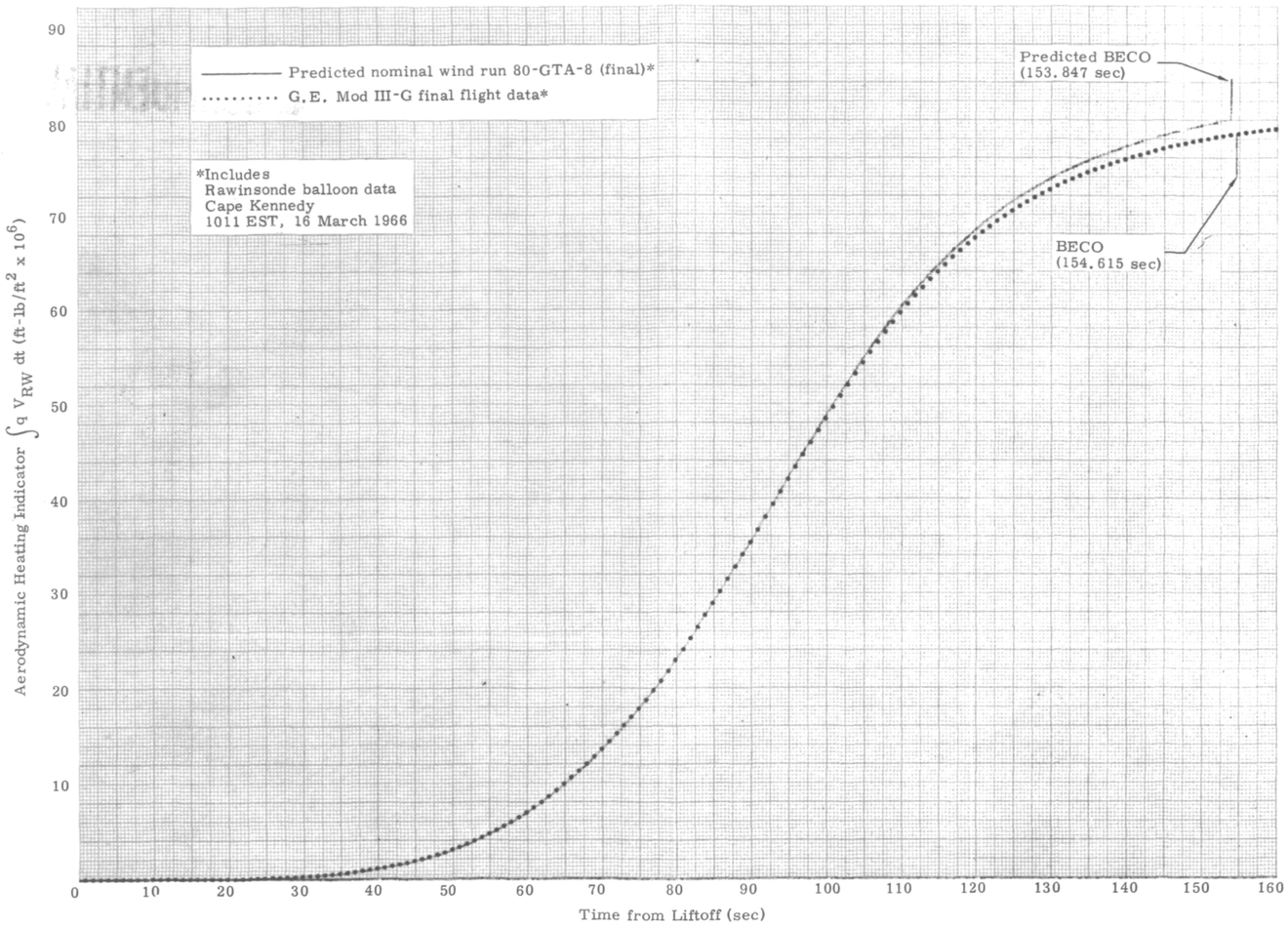

Fig. II-11. Aerodynamic Heating Indicator Versus Time: Stage I Flight

CONFIDENTIAL

II-20-1

CONFIDENTIAL

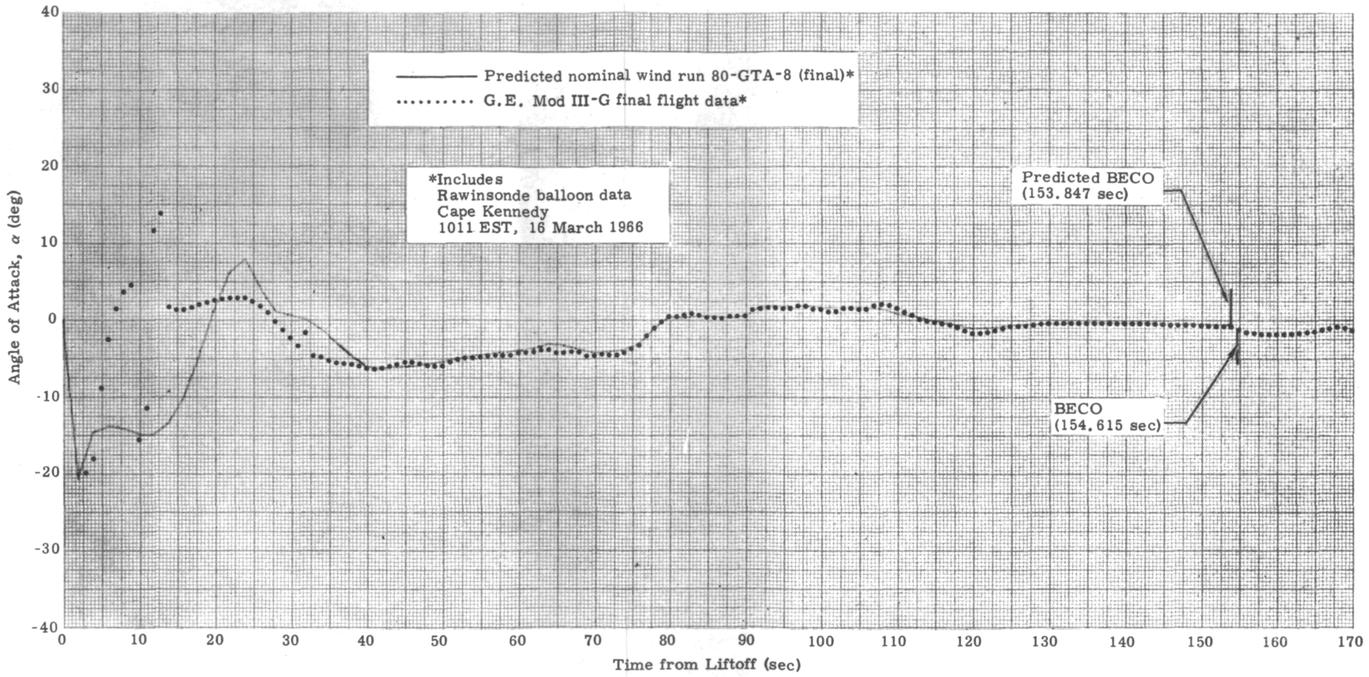

Fig. II-12. Stage I Angle of Attack History

CONFIDENTIAL

CONFIDENTIAL

II-21-1

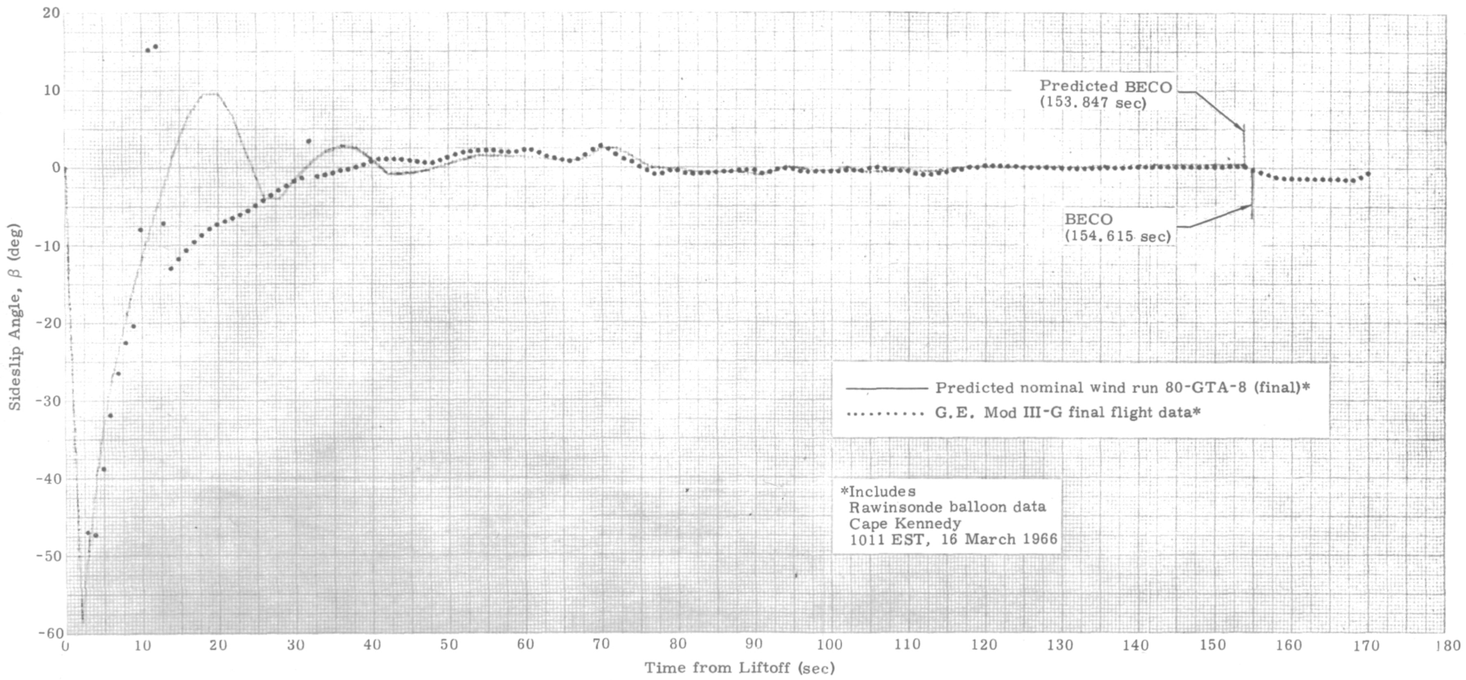

Fig. II-13. Stage I Angle of Sideslip History

CONFIDENTIAL

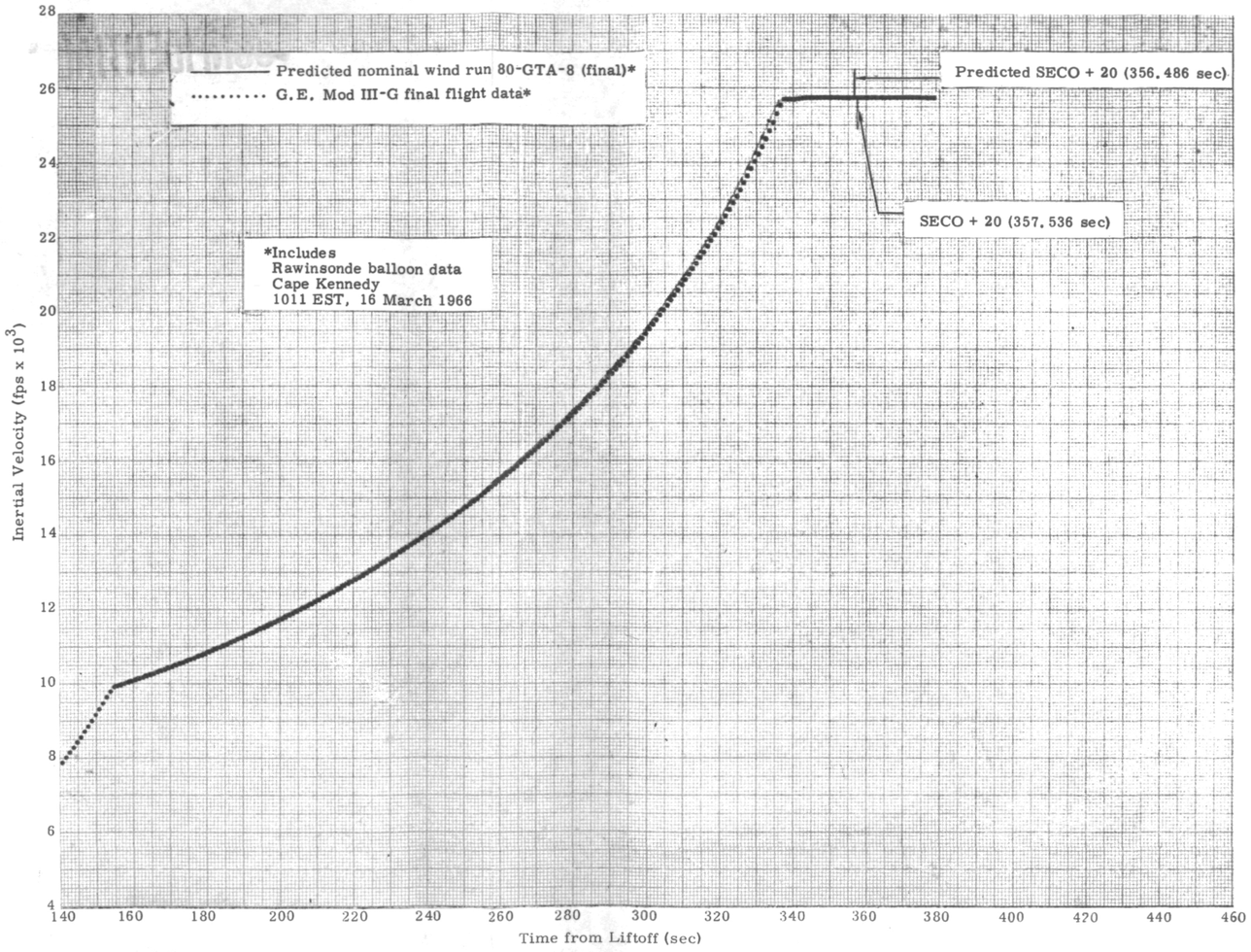

Fig. II-14. Resultant Inertial Velocity (V_I) Versus Time: Stage II Flight

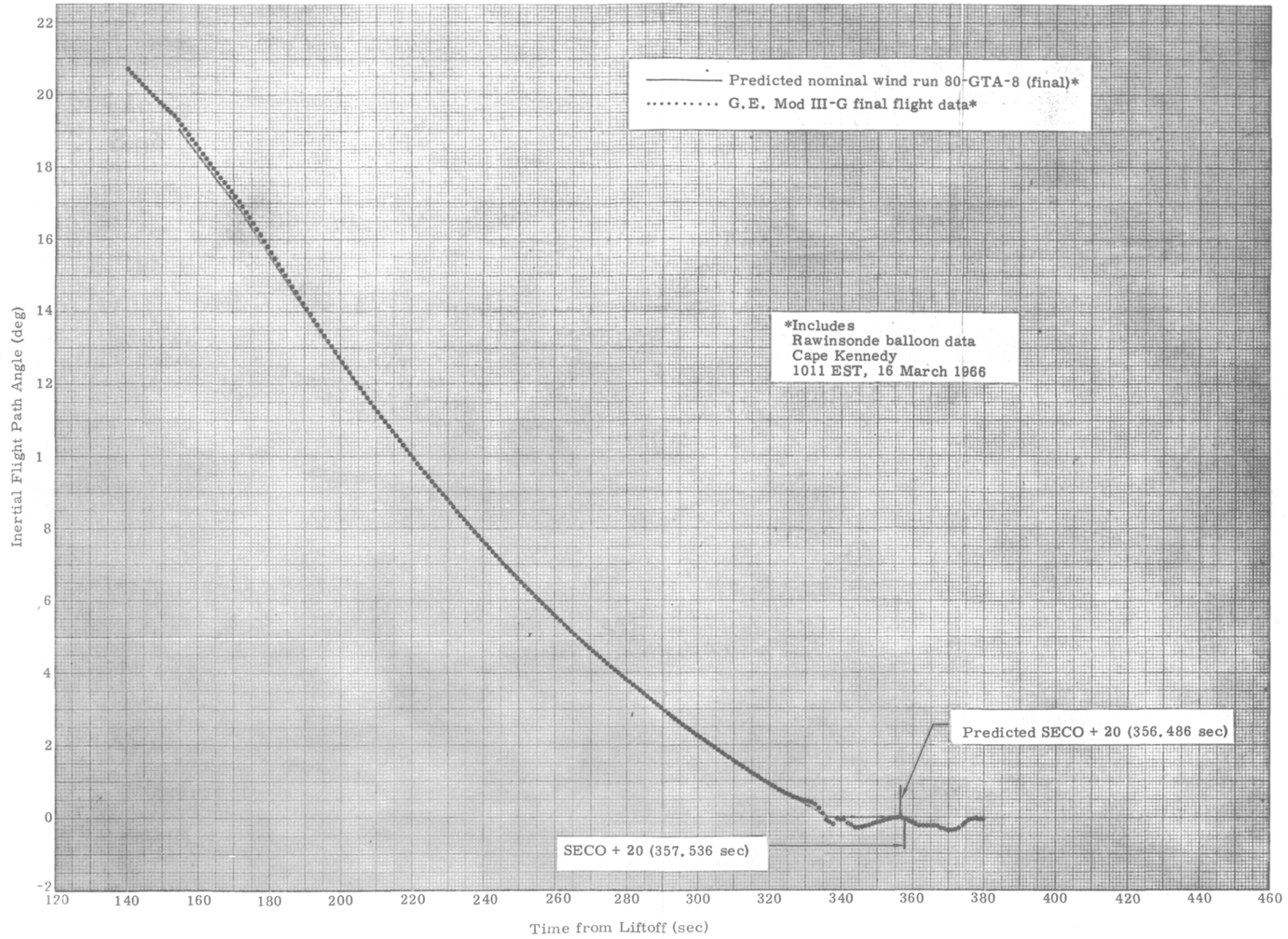

Fig. II-15. Inertial Flight Path Angle (γ_I) Versus Time: Stage II Flight

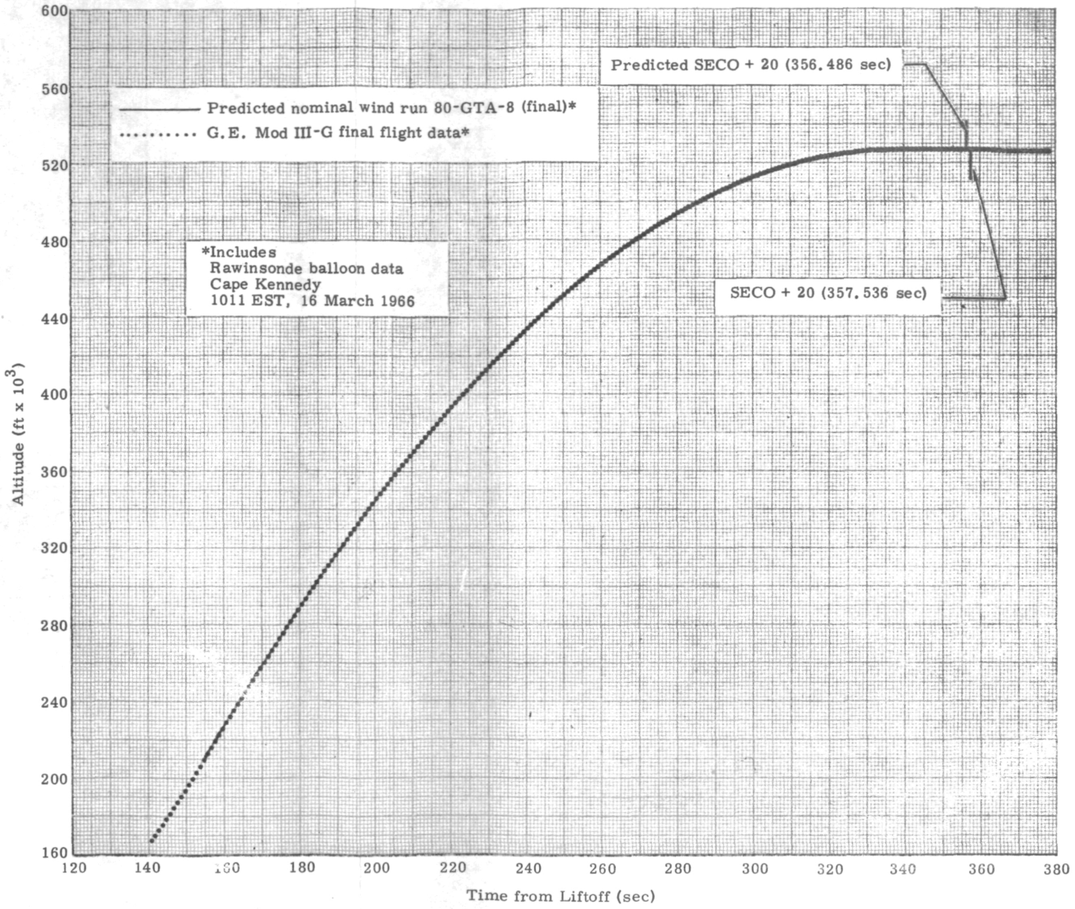

Fig. II-16. Altitude Versus Time: Stage II Flight

II-25-1

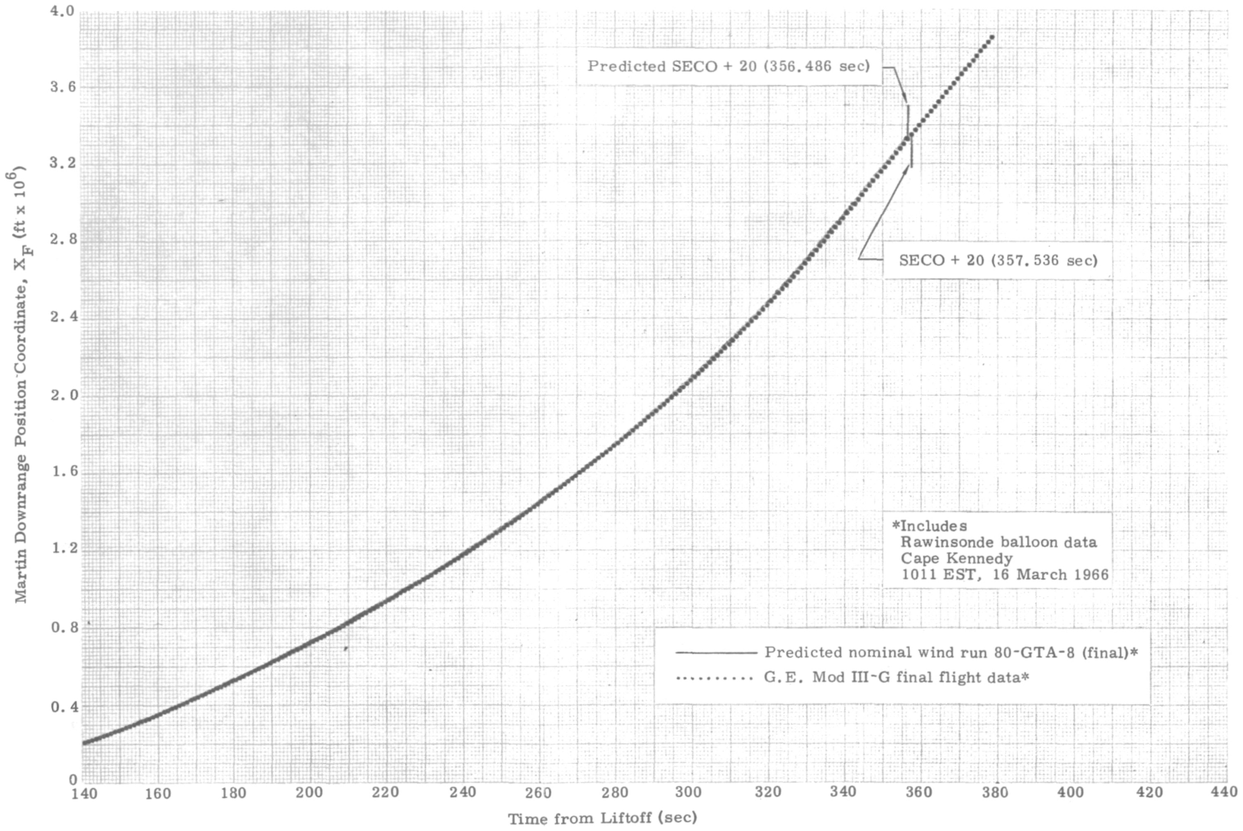

Fig. II-17. Downrange Position Coordinate (X_F) Versus Time: Stage II Flight

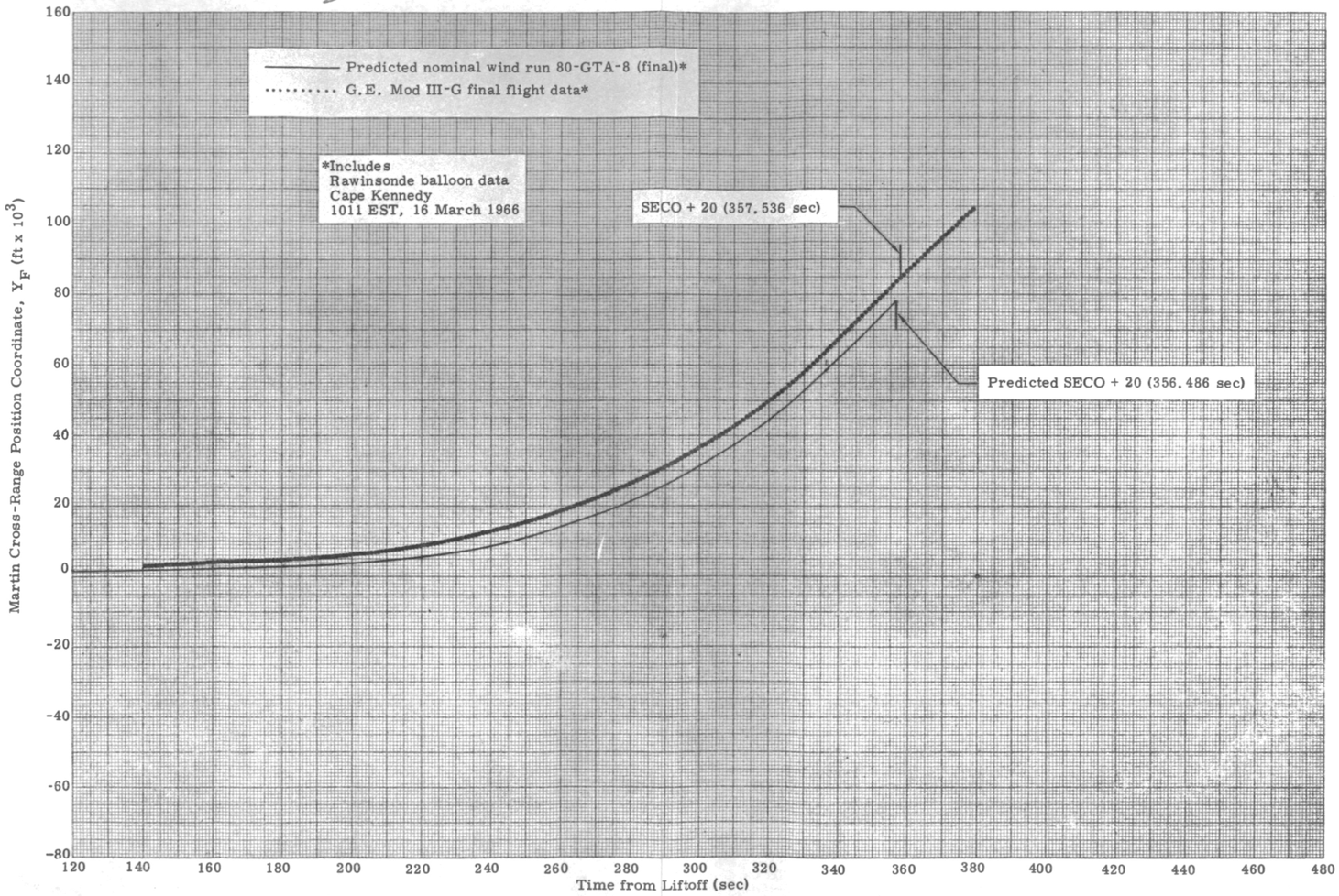

Fig. II-18. Cross-Range Position Coordinate (Y_F) Versus Time: Stage II Flight

II-27-1

CONFIDENTIAL

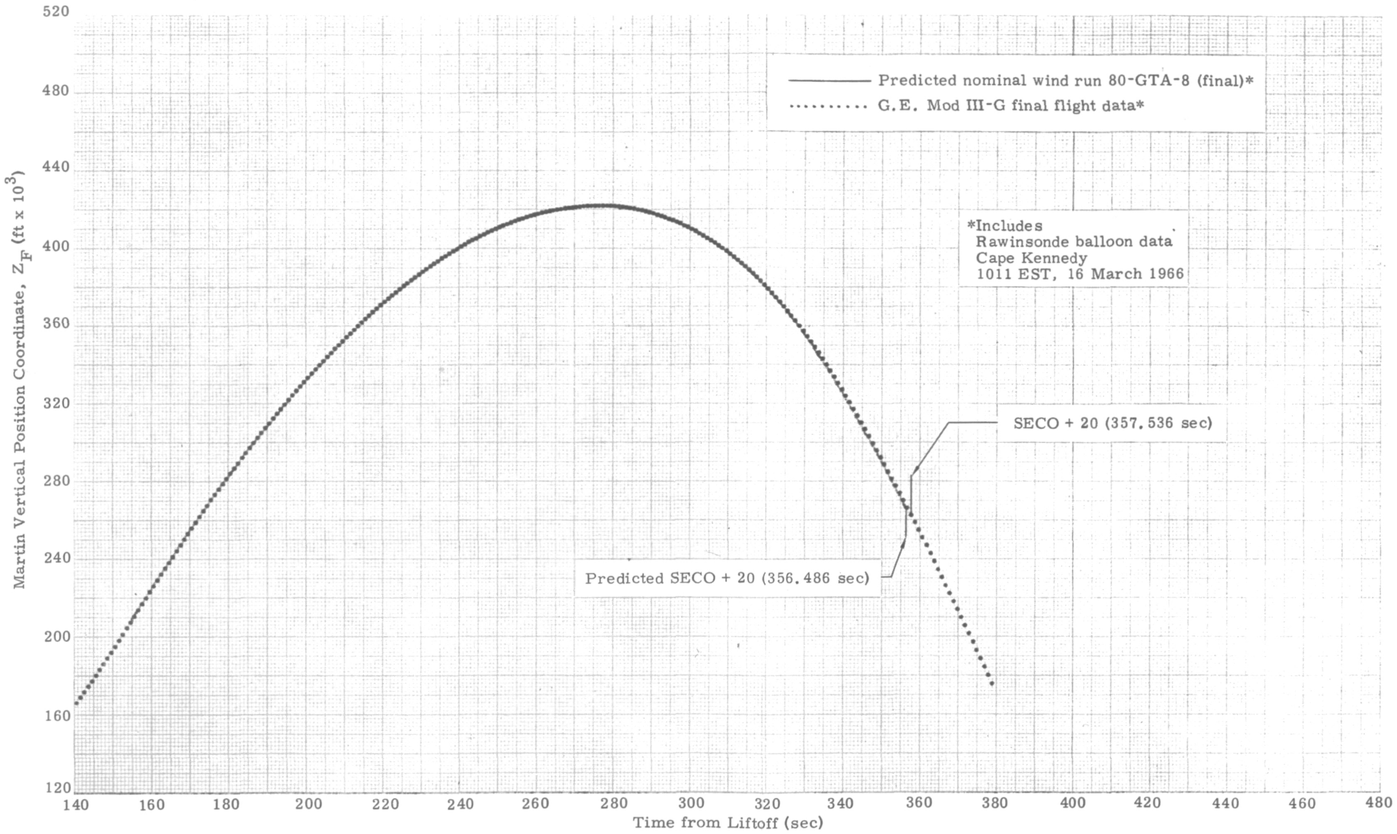

Fig. II-19. Vertical Position Coordinate (Z_F) Versus Time: Stage II Flight

CONFIDENTIAL

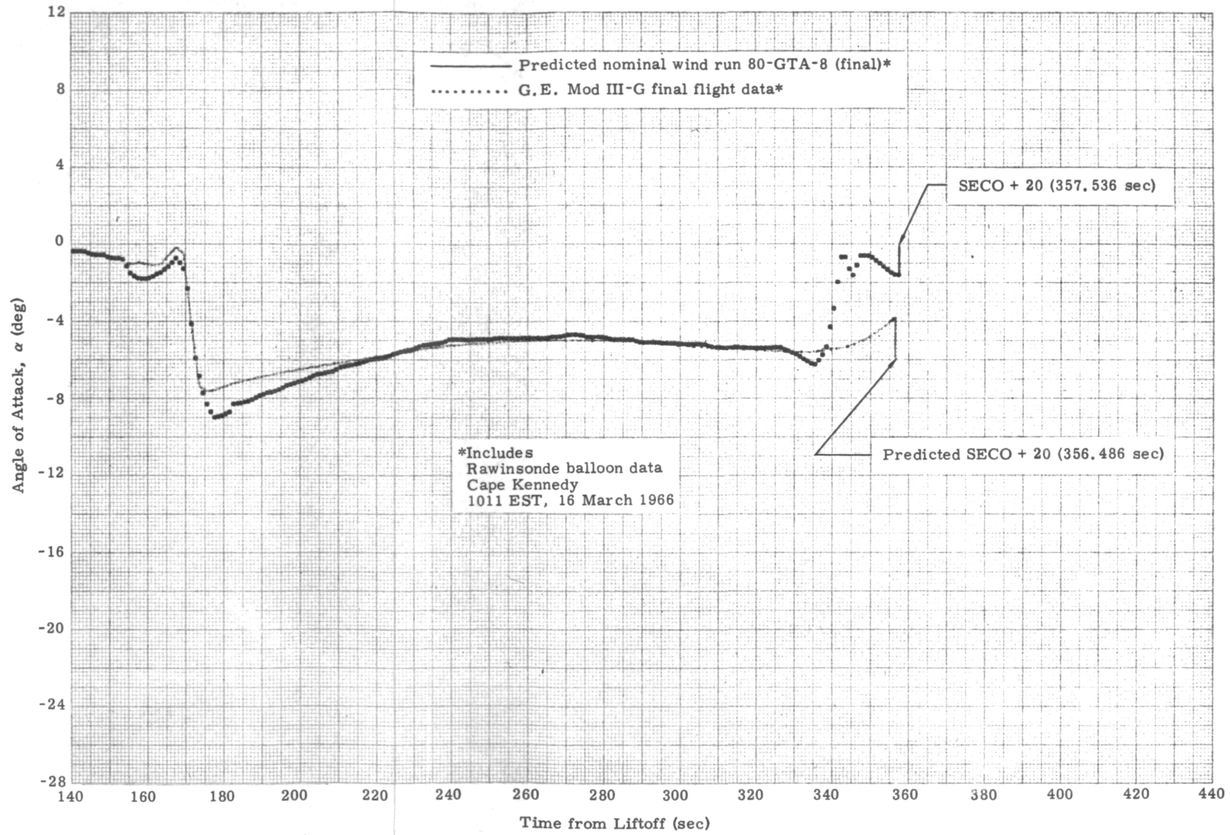

Fig. II-20. Stage II Angle of Attack History

II-29

CONFIDENTIAL

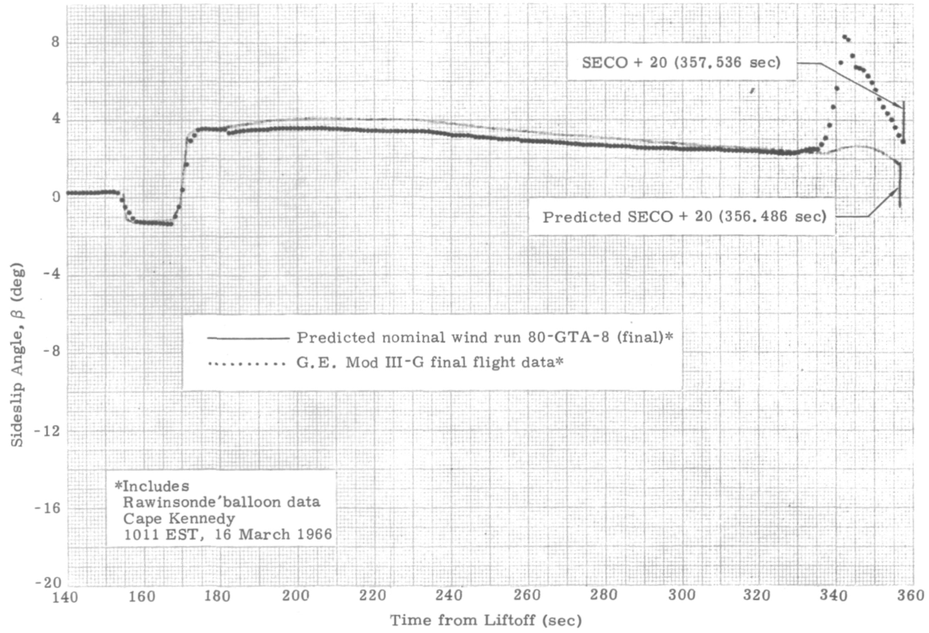

Fig. II-21. Angle of Sideslip Versus Time: Stage II Flight

CONFIDENTIAL

CONFIDENTIAL

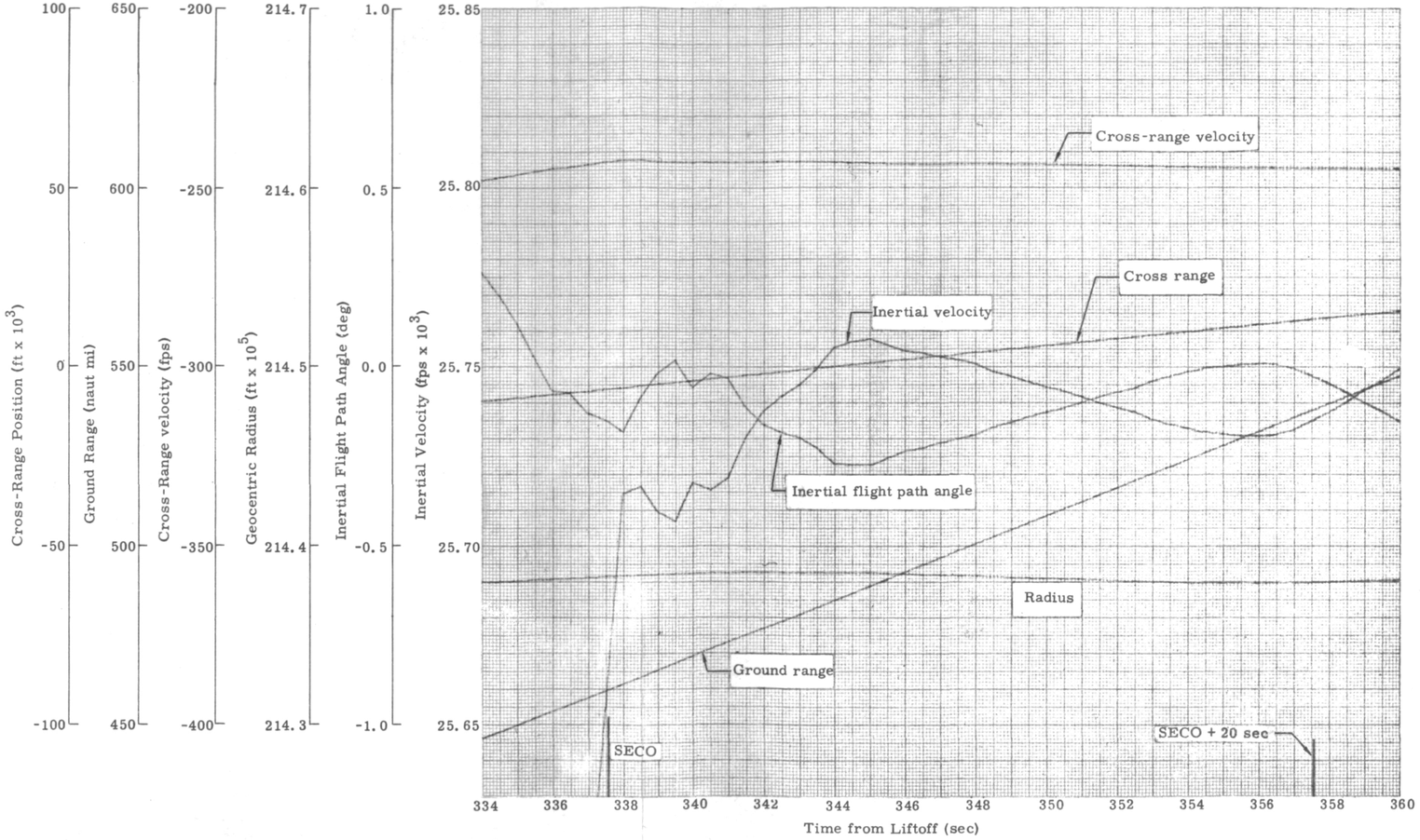

Fig. II-22. GE Mod III-G Flight Data from SECO to SECO + 20 Seconds

CONFIDENTIAL

CONFIDENTIAL

II-31-1

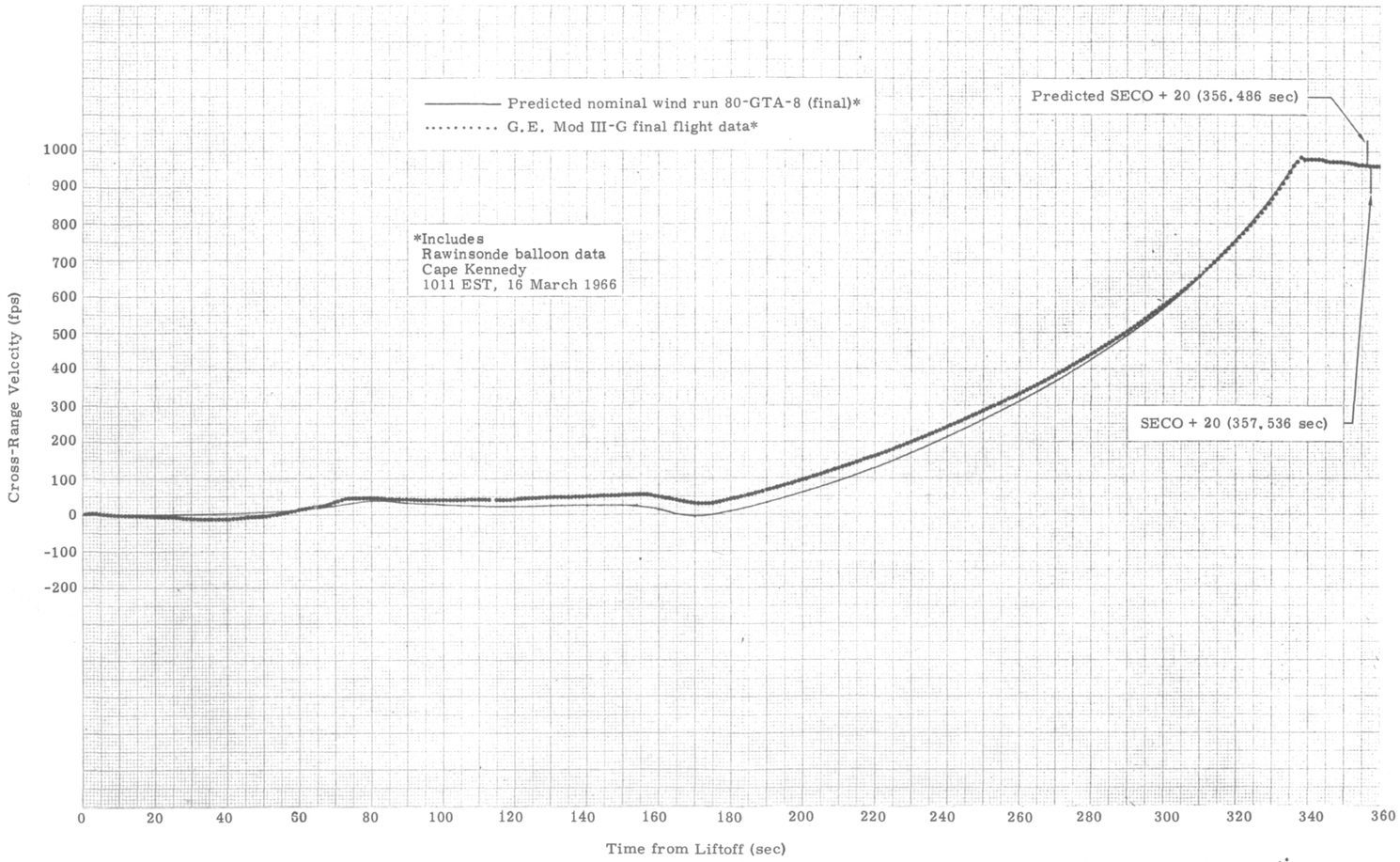

Fig. II-23. Cross-Range Velocity ($\dot{Y}_F$) Versus Time

CONFIDENTIAL

CONFIDENTIAL

II-32-1

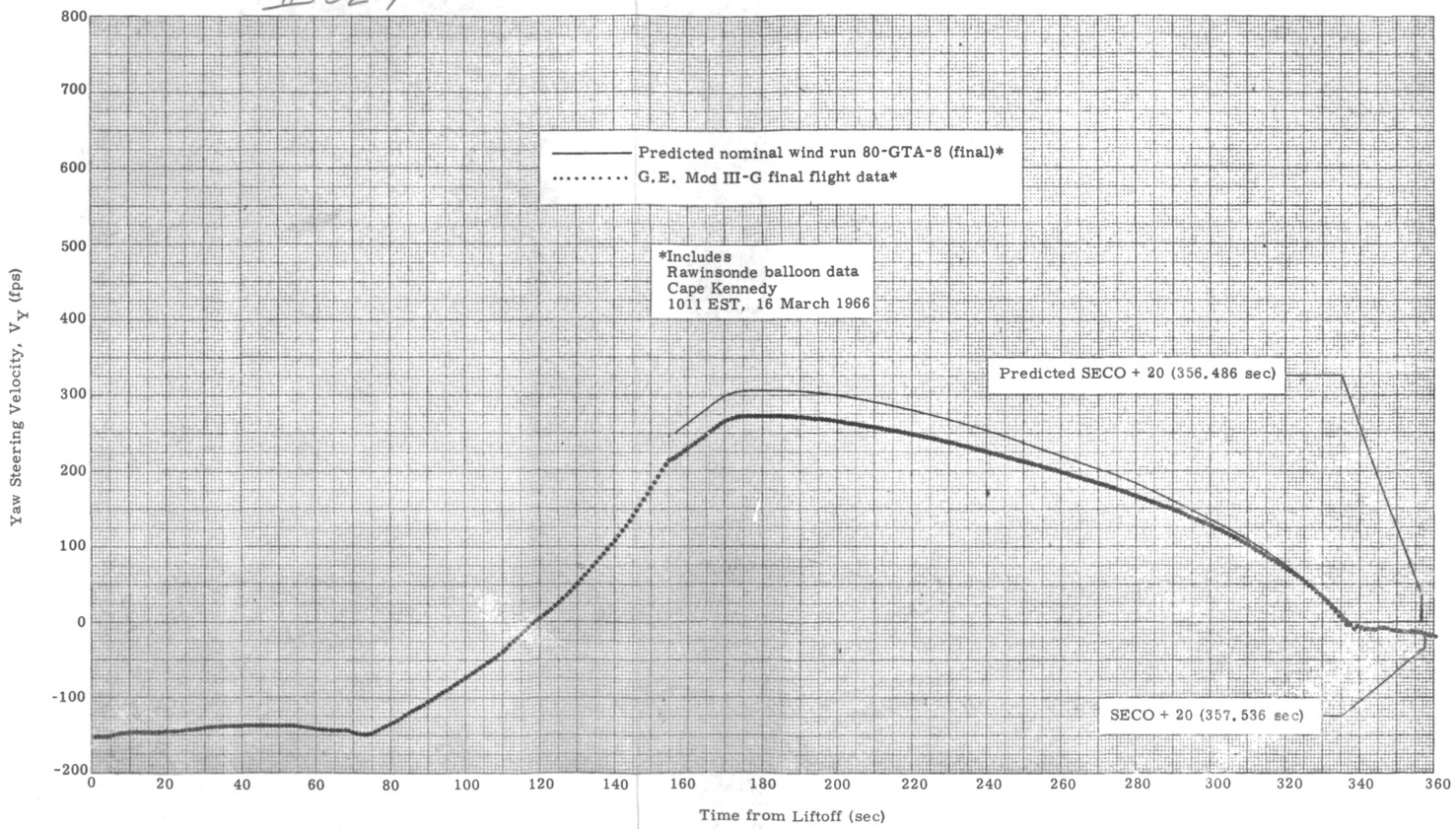

Fig. II-24. Yaw Steering Velocity (V_Y) Versus Time

CONFIDENTIAL

CONFIDENTIAL

TABLE II-9

Geographic and Weather Conditions at Launch

Location	
Site	Complex 19
Site coordinates:	
Latitude (deg)	28.507 N
Longitude (deg)	80.554 W
Pad orientation (deg)	84.933 true azimuth
Weather	
Ambient pressure (psi)	14.76
Ambient temperature (°F)	70
Dew point (°F)	59
Relative humidity (%)	69
Surface wind:	
Speed (fps)	30
Direction (deg)	350
Winds aloft (max):	
Altitude (ft)	37,500
Speed (fps)	211
Direction (deg)	268 true azimuth
Cloud cover	0.3 strato-cumulus
Reference Coordinate System	
Type	Martin reference coordinate system
Origin	Center of launch ring, Complex 19
Positive X-axis	Downrange along flight azimuth tangent to ellipsoid
Positive Y-axis	To left of flight azimuth tangent to ellipsoid and $\perp$ X-axis
Positive Z-axis	Forms a right-handed orthogonal system
Reference ellipsoid	Fischer
Launch	
Initial flight azimuth (deg)	99.9 true azimuth
Roll program (deg)	15.0 ccw

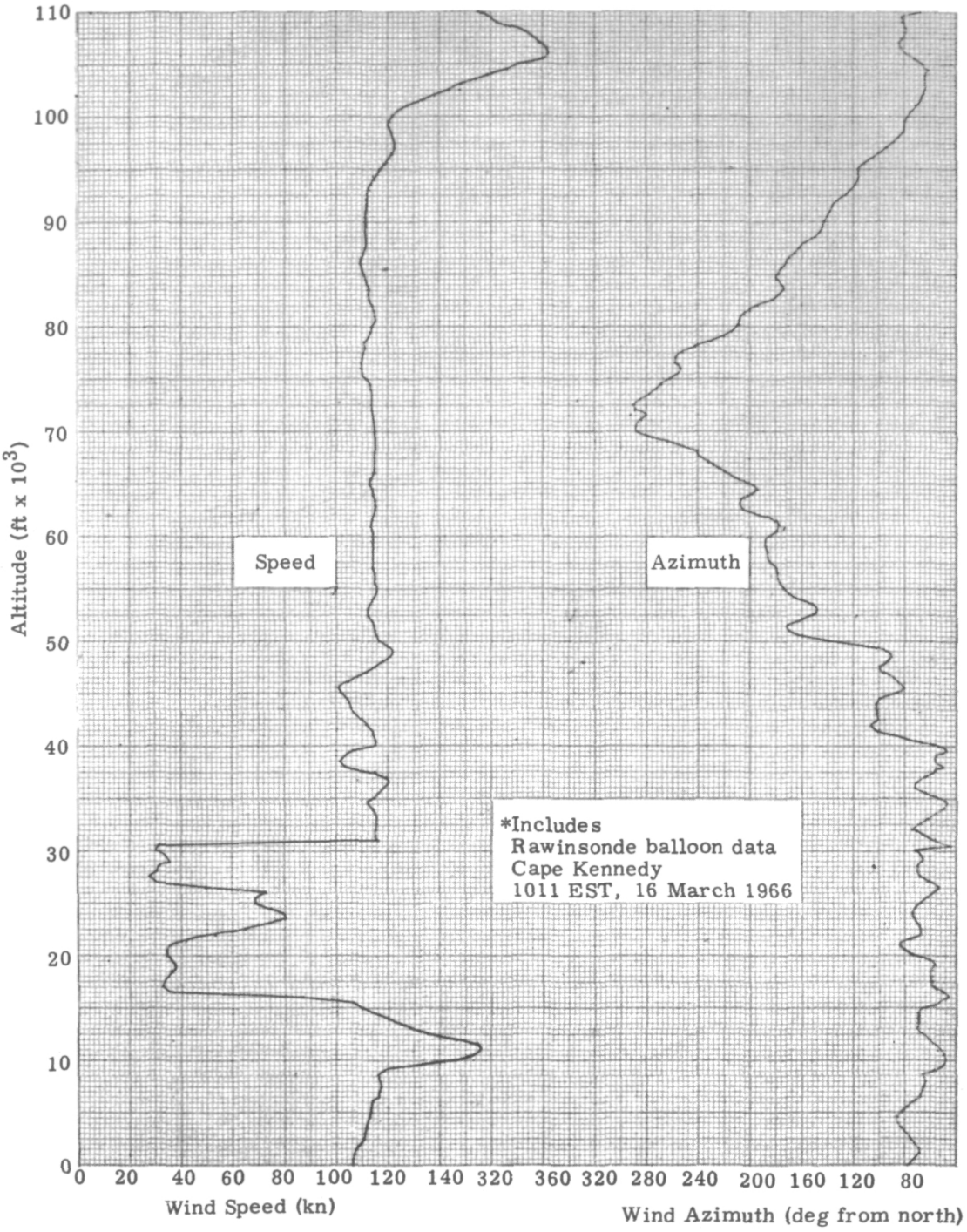

Fig. II-25. Wind Speed and Azimuth Versus Altitude

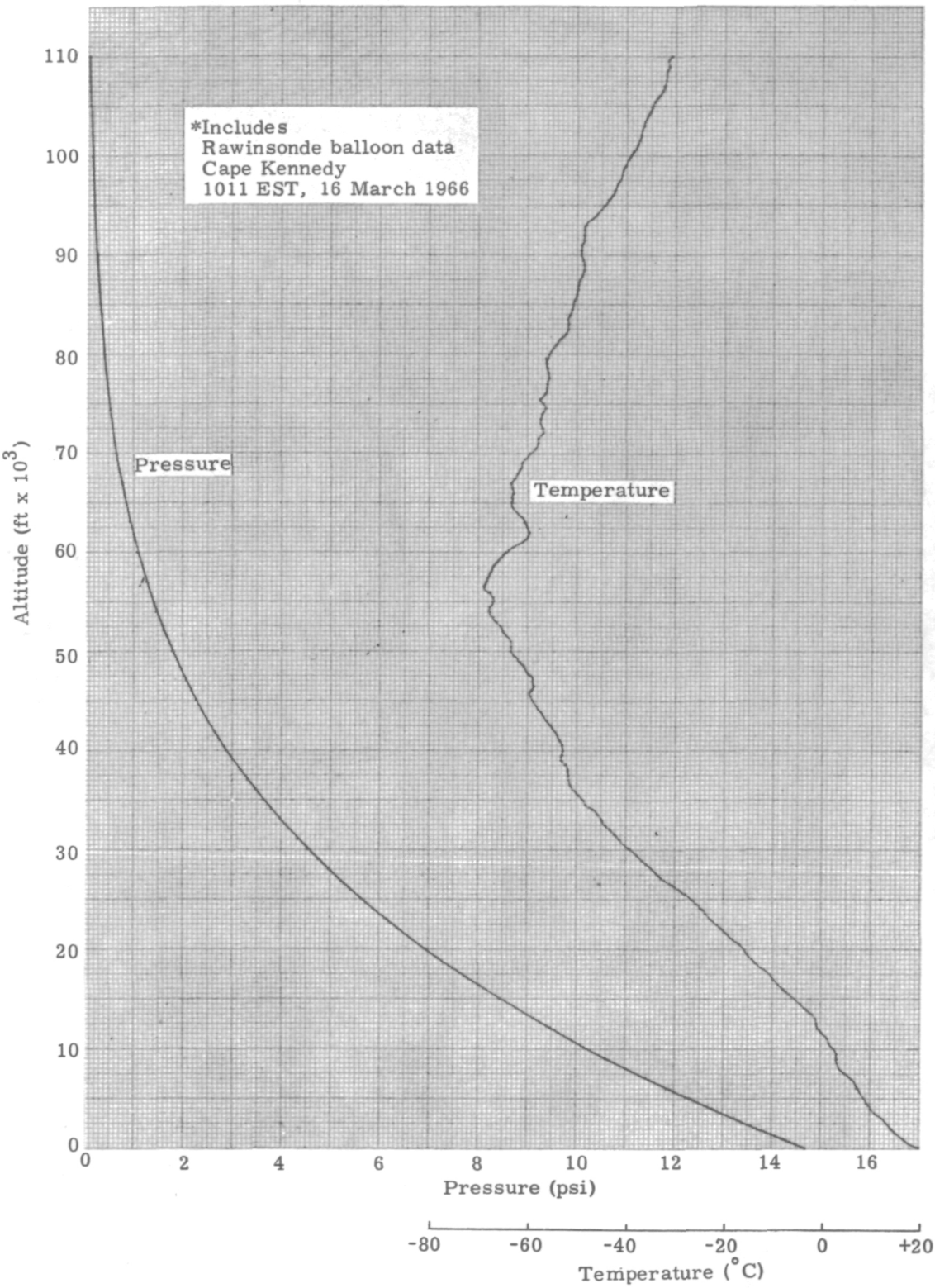

Fig. II-26. Ambient Temperature and Pressure Versus Altitude

CONFIDENTIAL

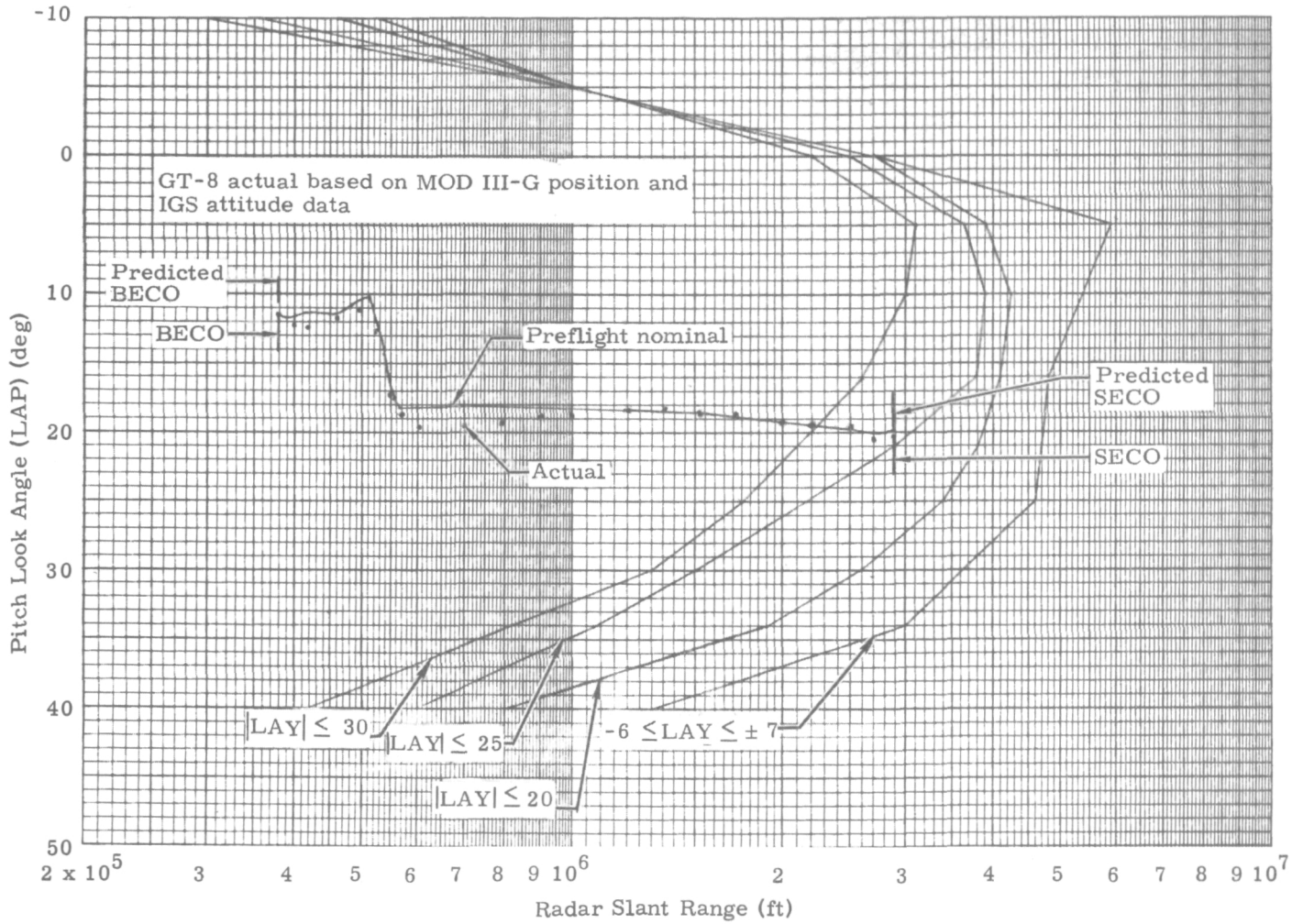

Fig. II-27. Permissible Pitch Look-Angle Envelope

CONFIDENTIAL

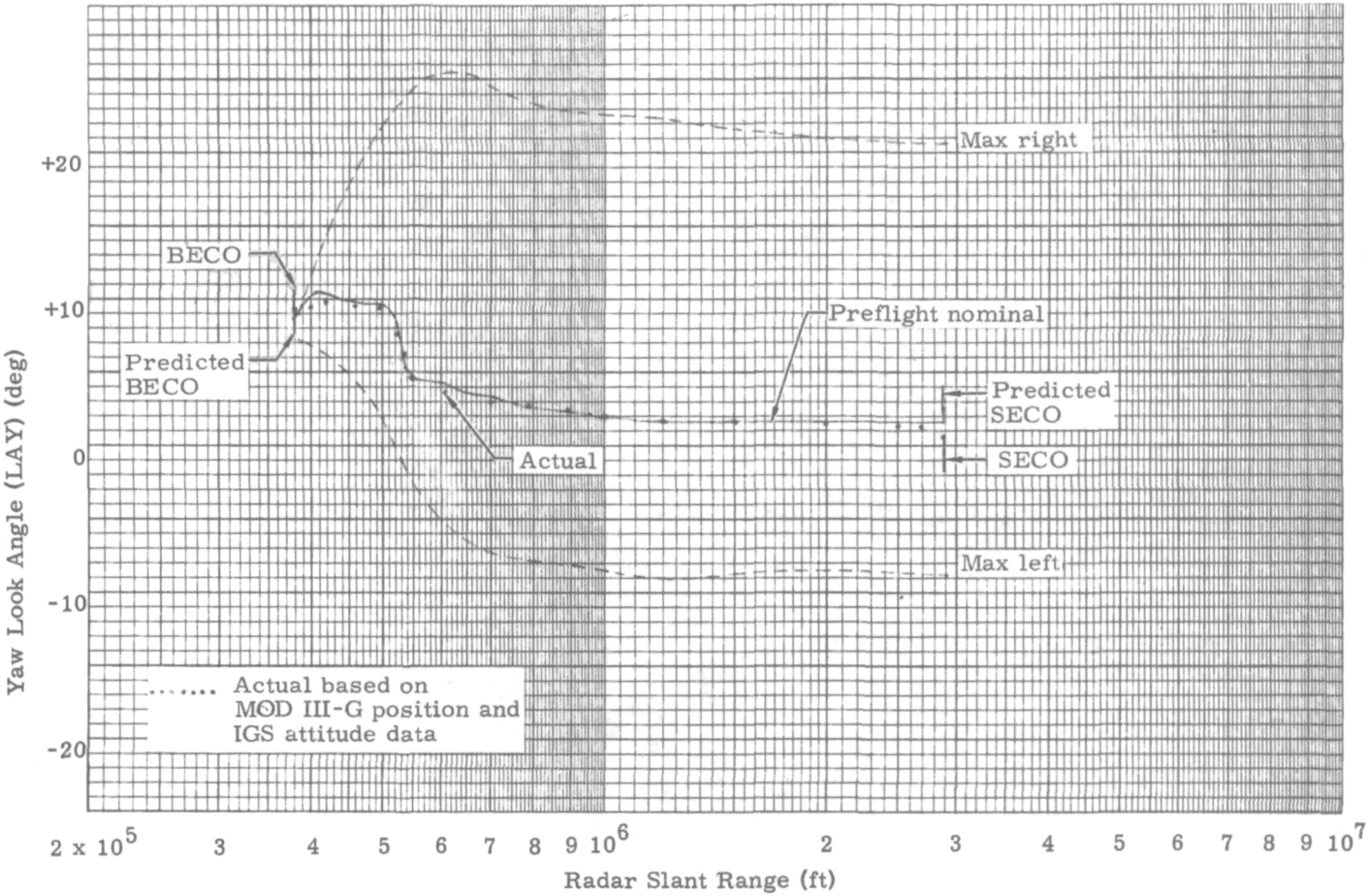

Fig. II-28. Permissible Yaw Look-Angle Envelope

CONFIDENTIAL

7. Maximum Dynamic Pressure

The maximum dynamic pressure for the GTA-8 trajectory was less than design limits. Table II-10 compares the predicted and observed conditions associated with the maximum dynamic pressure. The predominantly tail wind environment for this flight in itself reduces the maximum dynamic pressure. A predicted trajectory computation for a no-wind condition showed that the maximum dynamic pressure would be 743.4 psi, and the predicted trajectory with T-0 winds, from Table II-10, shows a value of 681.3 psi, verifying the effect of a tail wind.

TABLE II-10

Trajectory Parameters at Maximum Dynamic Pressure

	Predicted* (nominal)	Observed**
Dynamic pressure (psf)	681.3	678.3
Time from liftoff (sec)	79.62	80.12
Mach number	1.73	1.74
Altitude (ft)	45,000	45,306
Relative flight path angle (deg)	47.52	47.45
Relative wind velocity (fps)	1665.	1673
Wind velocity (fps)	135	136
Wind azimuth (deg from north)	266	267
Angle of attack (deg)	0.35	0.65
Angle of sideslip (deg)	-0.09	-0.35

*Ref. 11, updated (see footnote to Table II-7)
**Mod III-G 2 pps radar data

CONFIDENTIAL

8. Angles of Attack and Sideslip

Predicted and observed histories of angles of attack and sideslip during the ascent are shown in Figs. II-12, II-13, II-20 and II-21. The predicted values were obtained from a digital run utilizing wind and atmospheric information obtained from the 1011 EST Rawinsonde sounding. Observed angles of attack and sideslip were derived using the Mod III-G position and velocity information, IGS attitude data and the aforementioned weather data.

B. PAYLOAD CAPABILITY

Propellants remaining onboard after Stage II low level sensor uncover indicated that a burning time margin (BTM) of 1.327 seconds existed to a command shutdown. The total propellant weight margin was 437 pounds, and the corresponding GLV payload capability was 8826 pounds. These values and the predicted nominal and minimum values appear in Fig. II-29. The predicted capability curves were obtained from the real-time propellant temperature monitoring digital program (Run 14) adjusted to reflect the pre-liftoff temperature changes and the actual Agena ephemeris data used in the guidance equations at launch. The predicted propellant weight and burning time margins are based on the difference between these curves and the 8351-pound spacecraft weight.

The last payload prediction indicated that the minimum payload capability was 215 pounds less than the spacecraft weight, and the nominal payload capability was 393 pounds greater than the spacecraft weight at the predicted launch time. The actual (postflight reconstructed) GLV capability was 475 pounds greater than the spacecraft weight.

C. STAGING

The staging sequence was normal and physical stage separation occurred as planned. The time interval from staging signal ($87FS_2/91FS_1$) to start of Stage II engine chamber pressure (P_{c_3}) rise was 0.646 second. This compares favorably with the nominal expected time of 0.70 ± 0.08 second. Stage separation occurred 0.029 second following start of P_{c_3} rise.

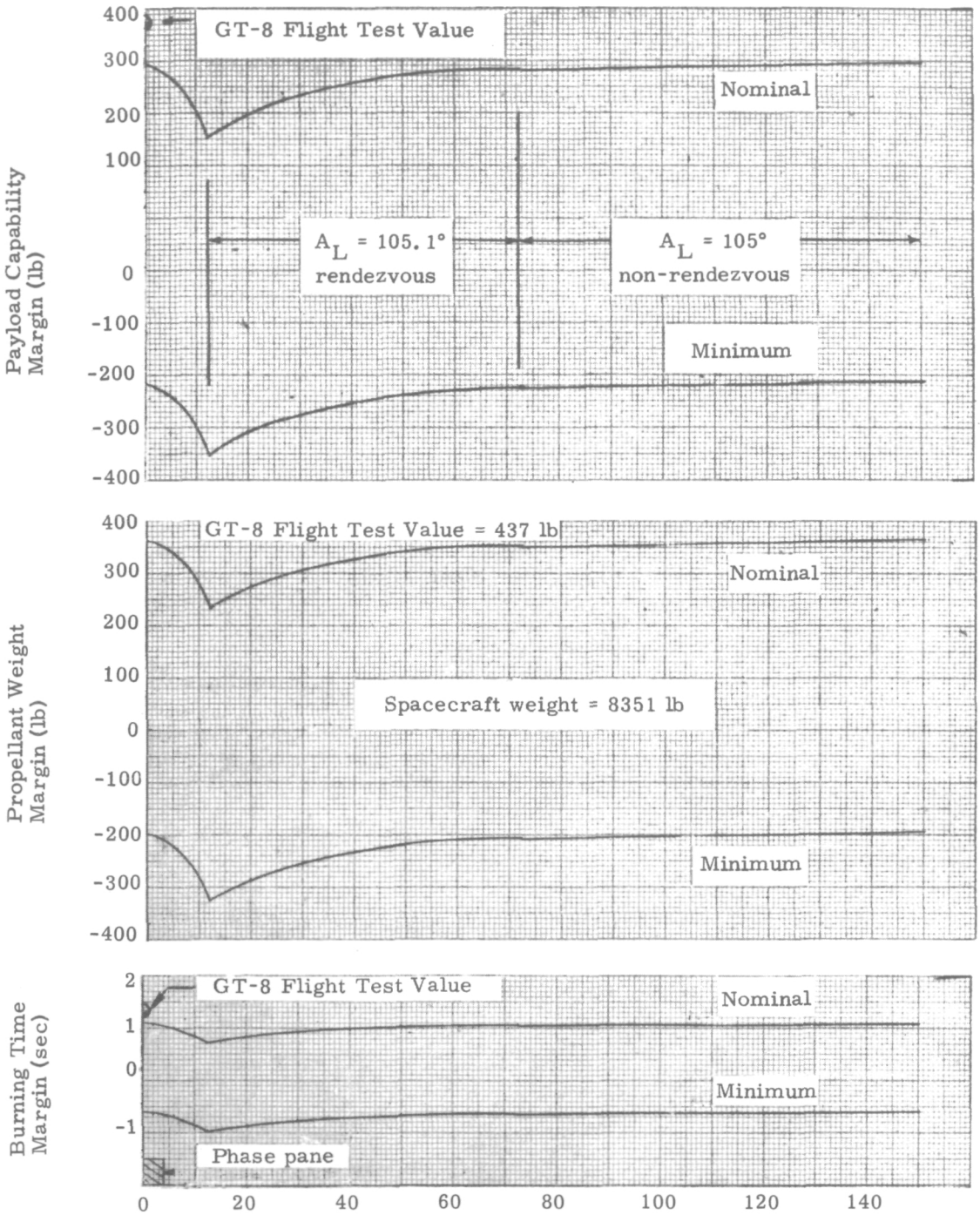

Fig. II-29. Payload Capability

D. WEIGHT STATEMENT

Table II-11 shows the GT-8 weight history from launch to orbital insertion.

The postflight weight report (Ref. 12) provides the background data for this summary. The report includes a list of dry weight empty changes at ETR and shows a derivation of weight empty from the actual vehicle weighing. Other items covered include the derivation of burnout, BECO, SECO and shutdown weights; weight comparisons with the BLH data; and the center of gravity travel envelope as a function of burn time for the horizontal, vertical and lateral planes.

TABLE II-11

GT-8 Weight Summary

	Weight (lb)			
	Step I	Step II	Step III	Stage Total
Loaded weight	271,366	65,642	8,351(2)	345,359
Start and grain losses	- 3,688(1)			
Trajectory LO weight	267,678	65,642	8,351	341,671
Propellant consumed to BECO	256,384	11		
Coolant water	0	0	0	
Weight at BECO	11,294	65,631	8,351	85,276
Shutdown propellant	353			
Weight Stage I burnout	10,941(3)	65,631(3)	8,351	84,923
Stage II engine start	10,941	192		
Stage II LO		65,439	8,351	73,790
Propellant consumed to SECO		59,422		
Ablative, covers and coolant water		42		
Stage II at SECO		5,975	8,351	14,326(4)
Shutdown propellant		136		
Weight at SECO + 20 seconds		5,839	8,351	14,190(4)

NOTES:

(1) Event: TCPS + 2 seconds (launch bolts blown)

(2) Information from NASA-Houston (3/15/66)

(3) Includes outage: 252-lb Stage I, 261-lb Stage II

(4) Includes 437 lb of burning margin

III. PROPULSION SYSTEM

A. ENGINE SUBSYSTEM

The Stages I and II engines operated satisfactorily throughout the flight, and all launch objectives were met. Stage I burning time was 157.918 seconds, and shutdown was initiated by fuel exhaustion. Stage II operation was terminated by a guidance command at $91FS_1$ + 182.921 seconds.

Several anomalies occurred during the flight, none of which adversely affected engine performance. These were:

(1) The Stage I oxidizer pressurant pressure switch (OPPS) cycled once prior to final actuation at T + 1.674 seconds. Approximately 7.5 milliseconds after initial actuation the switch deactuated for 7.5 milliseconds before final "make." Pressure fluctuations were not observed in the oxidizer pressurant orifice inlet pressure (POPOI), although the low sampling rate may have obscured a perturbation. It is assumed that the OPPS chattering on GLV-8 was a random event. Chattering of OPPS cannot influence an engine shutdown prior to the interrogation time of T + 2.2 seconds.

(2) The Stage II thrust chamber pressure start transient indicated an abnormally slow rise rate. The most probable cause was a temporary obstruction in the sensing line or transducer cavity.

(3) Stage II engine performance began to decay and exhibited an unusual time-dependent characteristic after $91FS_1$ + 90 seconds. The unusual operation was predominant in oxidizer flow rate, mixture ratio and thrust. Examination of flight data indicates abnormal oxidizer pump operation.

(4) Five disturbances were noted in accelerometer data after SECO and before spacecraft separation. The disturbances were not characteristic of the post-SECO disturbances observed on previous GLV and Titan II flights. A correlation of the disturbances with thrust chamber pressures cannot be established. A post-SECO disturbance, characteristic of previous flights, was observed after spacecraft separation.

The only significant configuration change affecting performance was the incorporation of the Stage II Gemini Stability Improvement Program (GEMSIP) thrust chamber injector. Analysis of the flight data indicated

satisfactory performance of this injector. Although several anomalies occurred during Stage II operation, none appeared related to injector performance.

1. Stage I Engine (YLR87-AJ-7, S/N 1008)

a. Configuration and special procedures

The GLV-8 Stage I engine differed from that of GLV-7 by the retrofit replacement of the rigid tube between the lubricating oil heat exchanger and the fuel pump with a flexible line in order to minimize excessive vibration and tube failures (Aerojet ECP-076).

The thrust-chamber valve through-bolts were torqued to only 100 inch-pounds at Martin-Baltimore, then retorqued to the final 300 to 320 inch-pounds at ETR. This procedure was invoked to preclude a possible stress corrosion problem.

All propulsion system breaks of integrity were reviewed to verify that procedures were adequate to ensure that closures had not inadvertently been left in the engine during reassembly.

The pressure sequence valve (PSV) drain line engine attachment configuration was modified to prevent a recurrence of the premature separation of the drain lines from the vehicle which occurred during the GT-6 shutdown. On the GT-6 launch attempt, the resultant fire in the flame pit area created a hazard and delayed astronaut egress. The slip-fit polyethylene tube to the engine drain line as previously used was replaced with a clamped configuration incorporating a weak link V-notch in the polyethylene tube.

b. Start transient

The S/A 1 and S/A 2 thrust chamber pressure start transients were normal and are presented in Figs. III-1 and III-2. The ignition spikes indicated 88% (687 psia) and 81% (634 psia) of rated thrust for S/A 1 and S/A 2, respectively, which are above the engine model specification allowable (75%). However, the GLV engine chamber pressure instrumentation has characteristically shown undamped oscillations which obscure the true transient performance and prevent accurate determination of the ignition spikes.

Significant start events are presented in Table III-1.

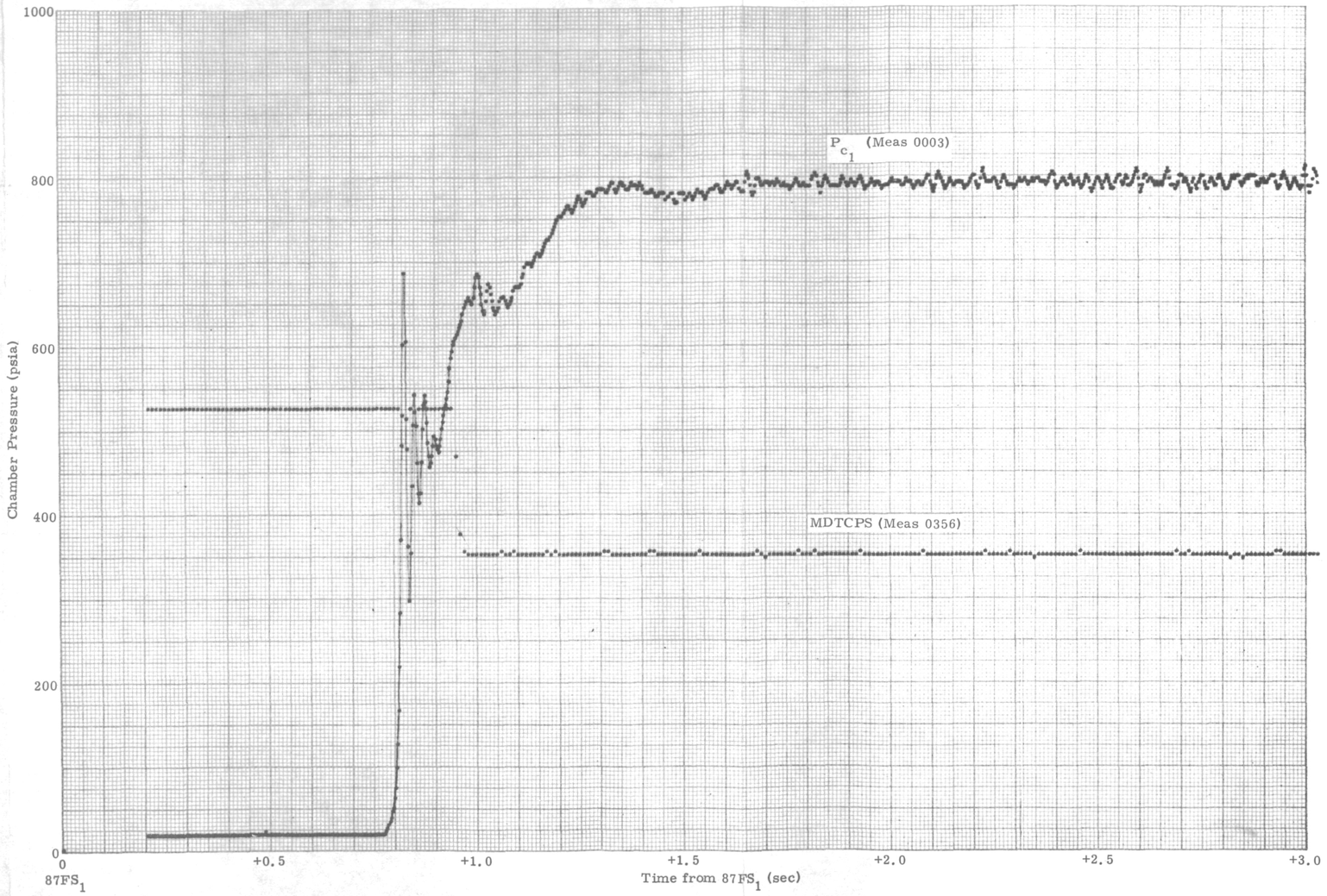

Fig. III-1. S/A 1 Start Transient

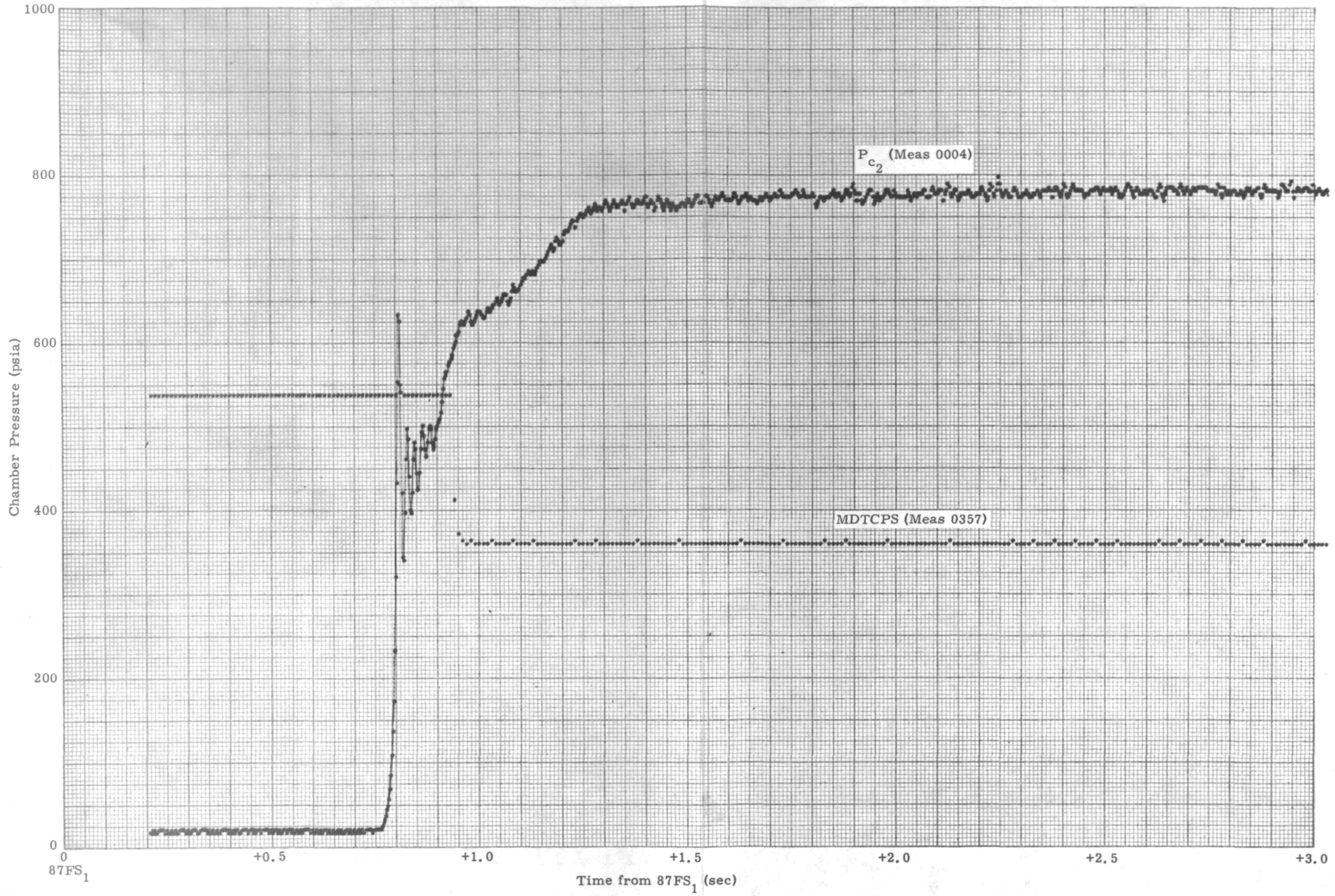

Fig. III-2. S/A 2 Start Transient

TABLE III-1

Stage I Engine Start Parameters

Parameter	S/A 1	S/A 2
FS_1 to initial P_c rise (sec)	0.773	0.766
P_c ignition spike (psia)	687	634
P_c step--approximate (psia)	455	440
P_c overshoot (psia)	None	None

c. Steady-state performance

Stage I engine flight performance agreed closely with the preflight prediction. Flight integrated average performance parameters were within 0.8% of the preflight predictions.

From measured flight data, engine performance was calculated with the Martin-Baltimore PRESTO computer program, using the Stage I thrust coefficient relationship as modified by Martin-Baltimore. The modification increased thrust and specific impulse by approximately 3400 pounds and 2.0 seconds, respectively, above the values calculated using the Aerojet thrust coefficient relationship. The Martin-Baltimore modified thrust coefficient was also used for preflight predictions.

The Stage I engine average flight performance, integrated from liftoff to $87FS_2$, is compared with the preflight prediction in Table III-2.

TABLE III-2

Predicted and Flight Performance Comparison--Stage I Engine

Parameter	Preflight Predicted Average*	Flight Average*	Difference (%)
Thrust, engine (lb)	462,508	461,233	-0.28
Specific impulse, engine (sec)	278.14	278.51	+0.13
Mixture ratio, engine	1.9443	1.9290	-0.79
Oxidizer flow rate, overboard (lb/sec)	1097.78	1090.33	-0.68
Fuel flow rate, overboard (lb/sec)	565.11	565.74	+0.11

*Martin-Baltimore modified thrust coefficient relationship used.

The engine performance calculated throughout the Stage I flight is presented in Fig. III-3. The preflight prediction is shown for comparison.

On GLV-8, the thrust chamber pressure transducers were wrapped with twice the normal amount of thermal insulation in order to minimize P_c instrumentation drift. Reconstructed flight data showed that the drift was delayed from the previous average time of approximately $87FS_1$+ 75 seconds to approximately $87FS_1$ + 90 seconds. Although P_c drift for the Stage I engine subassemblies reached -2.8% on this flight as compared to a previous average of -1.5%, it is recommended that the additional wrap be continued for the remaining flights.

The preflight prediction for GLV-8 was the first to use the final acceptance test time-dependent biases directly rather than to apply the acceptance-to-flight family correction (derived from Titan II data). GLV flight experience has shown better correlation with acceptance biases. Figure III-3 shows the close time-dependent agreement of the flight results with the preflight prediction.

Stage I engine flight performance calculated at the $87FS_1$ + 55-second time slice and corrected to standard inlet conditions is shown in Table III-3. This is compared with the acceptance test and the predicted flight performance, at standard inlet conditions, and the nominal time as used in the preflight prediction. The predicted flight performance at standard conditions was obtained by modifying the nominal acceptance test data for a 4850-pound acceptance-to-flight thrust growth obtained from analysis of previous Titan II and GLV flights. The 55-second time slice performance corrected to standard inlet conditions is not representative of the total acceptance or flight performance; however, it is the nominal time used for quoting rated performance. The data, therefore, are indicative of the corrected performance at 55 seconds only because of variations in the time-dependent biases and engine inlet conditions throughout flight.

d. Shutdown transient

Stage I engine shutdown was initiated by fuel exhaustion. Figures III-4 and III-5 show the S/A 1 and S/A 2 chamber pressure decays. All engine parameters were normal for a fuel exhaustion shutdown. The engine thrust at staging was approximately 57,000 pounds. Significant events during shutdown are presented in Table III-4.

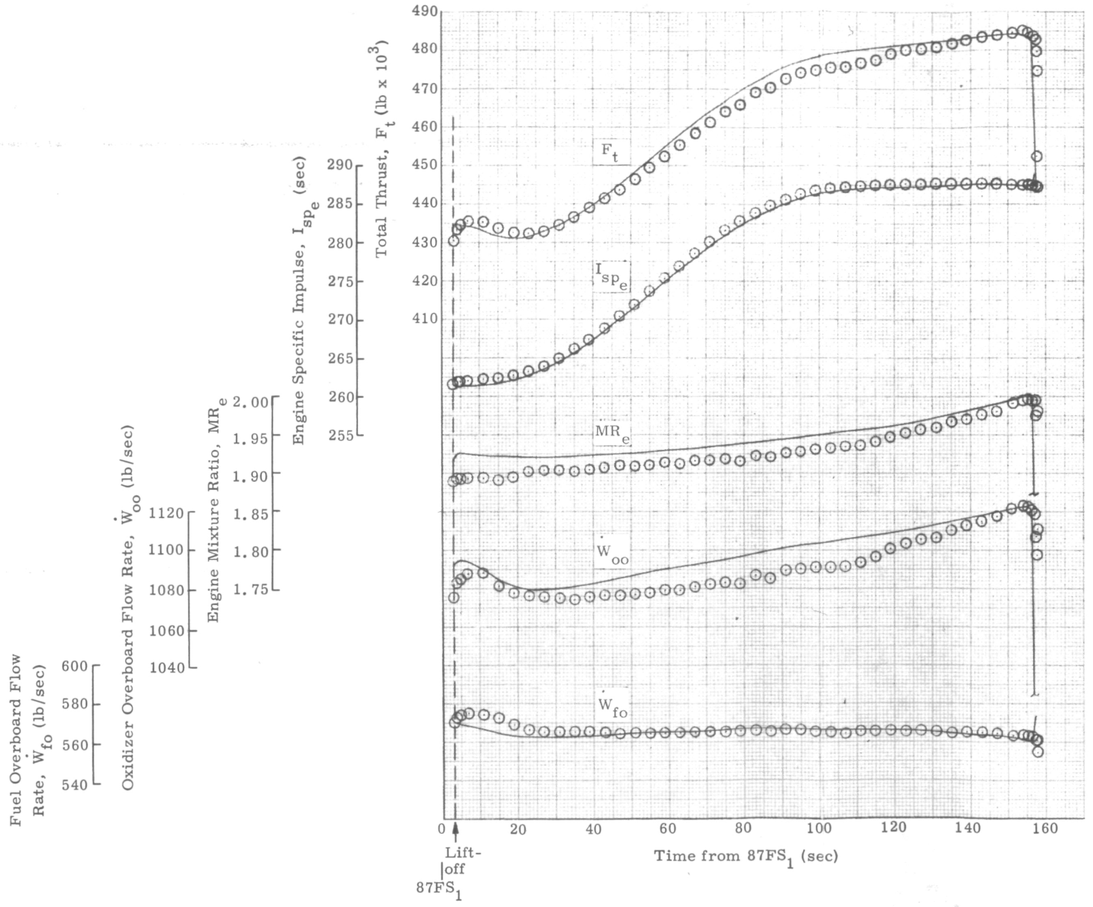

Average Engine Performance Integrated from Liftoff to $87FS_2$

Symbol	Preflight Prediction	Flight Average
F_t(lb)	462,508	461,233
I_{sp_e}(sec)	278.14	278.51
MR_e	1.9443	1.9290
$\dot{W}_{oo}$(lb/sec)	1097.78	1090.33
$\dot{W}_{fo}$(lb/sec)	565.11	565.74

——— Preflight prediction
○ Flight performance

Fig. III-3. Stage I Engine Flight Performance

CONFIDENTIAL

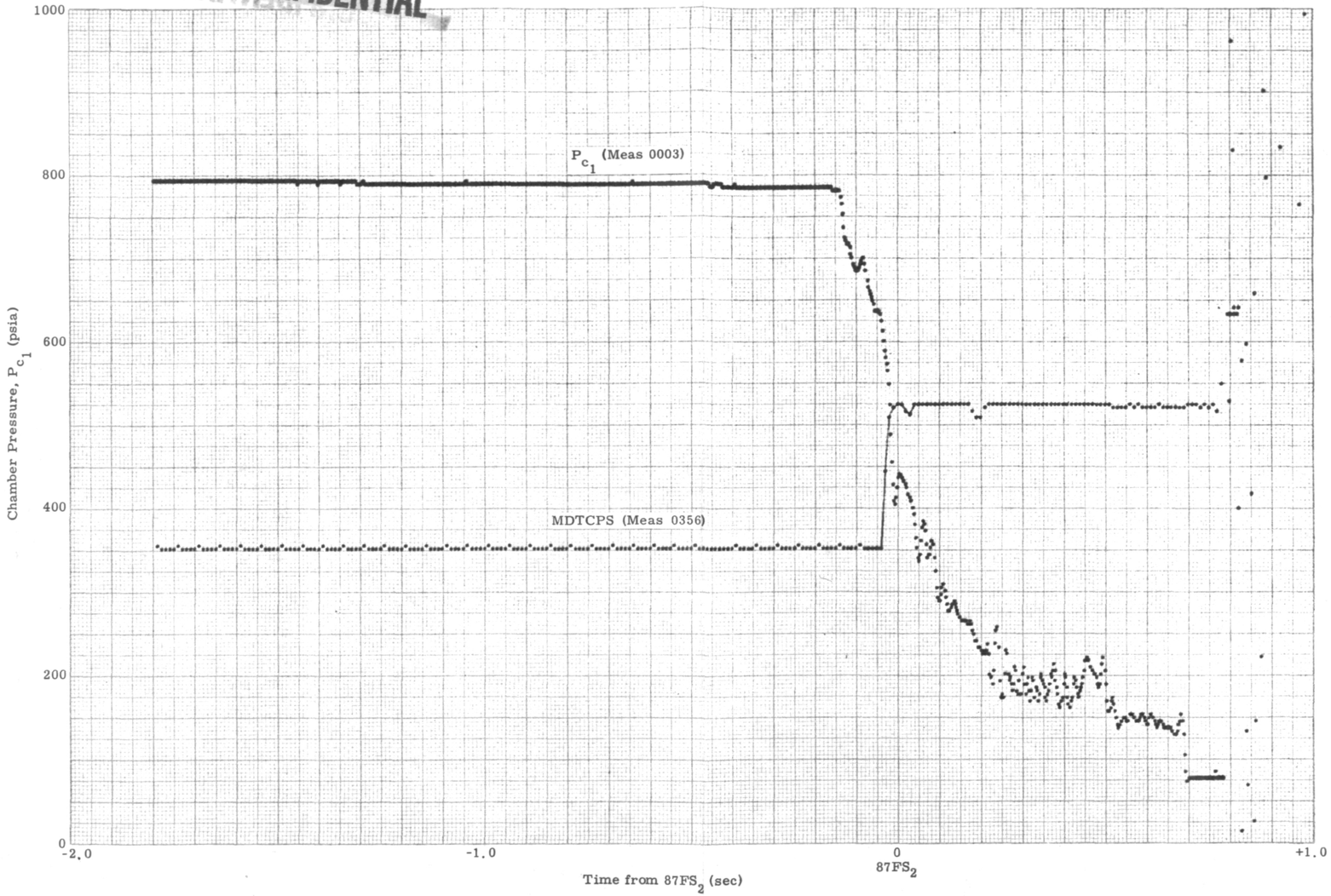

Fig. III-4. S/A 1 Shutdown Transient

CONFIDENTIAL

CONFIDENTIAL

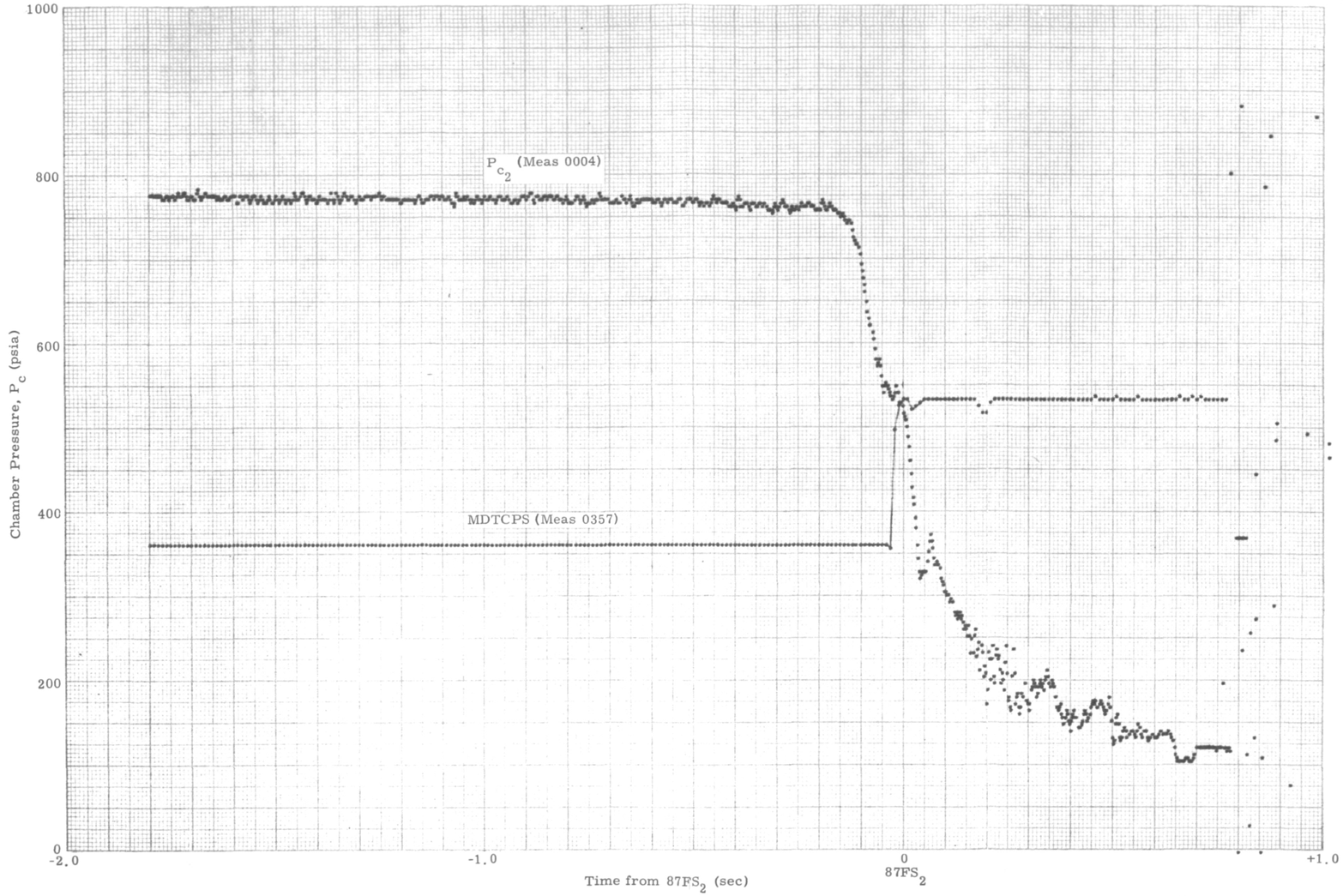

Fig. III-5. S/A 2 Shutdown Transient

CONFIDENTIAL

CONFIDENTIAL

TABLE III-3

Stage I Engine Performance Corrected to Standard Inlet Conditions at $87FS_1$ + 55 Seconds

Parameter	Acceptance Test*	Predicted Flight (including 4850-lb thrust growth)*	Flight Performance*
Thrust, engine (lb)	432,603	437,453	434,328
Specific impuse, engine (sec)	261.42	261.42	261.45
Mixture ratio, engine	1.9519	1.9519	1.9421
Oxidizer flow rate, overboard (lb/sec)	1093.87	1106.13	1096.26
Fuel flow rate, overboard (lb/sec)	560.94	567.22	564.97

*Martin-Baltimore modified thrust coefficient relationship used.

TABLE III-4

Stage I Engine Shutdown Parameters

Parameter	S/A 1	S/A 2
Time from P_c decay to $87FS_2$ (sec)	0.13	0.17
P_c at $87FS_2$ (psia)	440	525
Time from FS_2 to data dropout (sec)	0.7	0.7
P_c at data dropout (psia)	145	105

e. Engine malfunction detection system (MDS)

The Stage I engine MDS operated satisfactorily and within specified limits throughout the flight. Figures III-1 and III-2 illustrate response times and actuation pressure levels of the malfunction detection thrust chamber pressure switches (MDTCPS) during engine start for S/A 1 and S/A 2, respectively. Figures III-4 and III-5 show deactuation times and pressure levels during shutdown for S/A 1 and S/A 2, respectively.

A summary of the operating characteristics of the switches is tabulated in Table III-5.

TABLE III-5

Stage I MDTCPS Operation

	Actuation		Deactuation	
Switch	Time (sec)	Pressure*(psia)	Time (sec)	Pressure*(psia)
S/A 1	FS_1 + 0.945	600	FS_2 - 0.035	585
S/A 2	FS_1 + 0.935	580	FS_2 - 0.025	535

Specification Requirements	
Actuation	540 to 600 psia
Deactuation	585 to 515 psia

*Low sampling rate of the MDTCPS actuation times precludes accurate determination of pressure.

f. Engine prelaunch malfunction detection system (PMDS)

All PMDS switches actuated within the specified times and pressures as shown in Table III-6. However, the oxidizer pressurant pressure switch (OPPS) cycled once, prior to final actuation at MOCS T_0 + 1.674 seconds ($87FS_1$ + 1.623 seconds) at a pressure of 414 psia. Approximately 7.5 milliseconds after initial actuation, the switch was deactivated for 7.5 milliseconds before final "make," as shown in Fig. III-6. The flight "make" pressure (414 psia) agreed closely with the preflight checkout "make" pressure (410 psia).

TABLE III-6

Stage I PMDS Operation

	TCPS	OPPS	FPDSP
Actuation time			
Measured time from $87FS_1$ (sec)	1.012	1.623	0.902
Measured time from T_0 (sec)	1.063	1.674	0.953
Required time (sec)*	T_0+ 2.2	T_0 + 2.2	T_0+ 2.2
Actuation pressure			
Measured (psia)	**	414	**
Required (psia)	600 to 640	360 to 445	46 to 79 psid

*The shutdown timers start from T_0; $87FS_1$ is 70 to 100 milliseconds after T_0.

**Not instrumented.

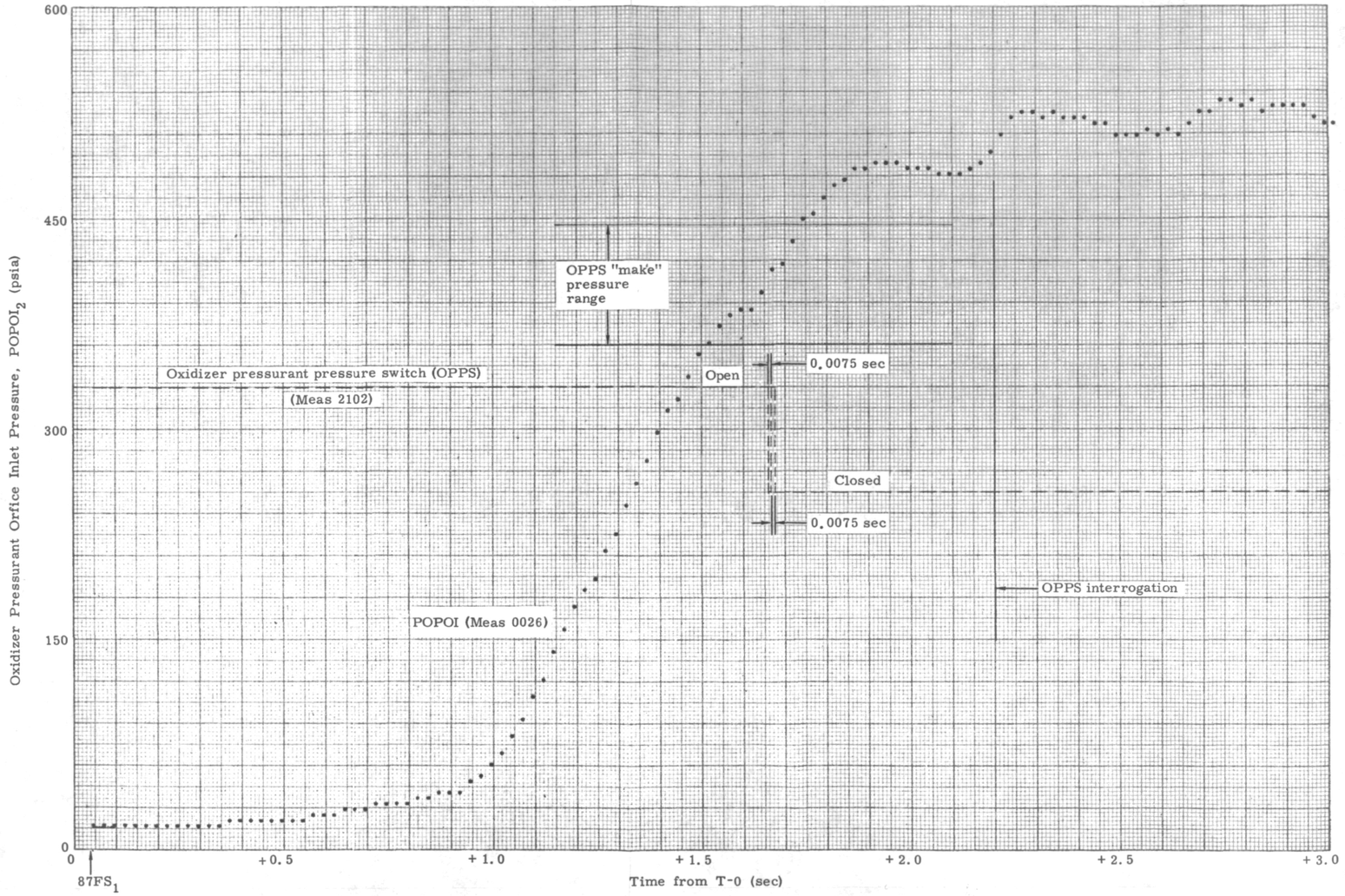

Fig. III-6. S/A 2 Start Transient

A review of oxidizer pressurant orifice inlet pressure (POPOI) failed to disclose fluctuations which may have contributed to the cycling of the switch. The slow sampling rate of POPOI (40 samples/second) makes observation of such pressure fluctuations difficult. There is no history of pressure fluctuations during POPOI buildup on previous GLV flights or during engine acceptance tests. It is highly improbable, therefore, that switch cycling resulted from pressure changes.

Another possible cause of switch oscillations may be sensitivity of the switch to the vibrational environment when pressure is held steady at or near the actuation level of the switch. A test history for this situation does not exist; therefore, a firm evaluation of this cause is not possible at the present time. Implementation of a test program to verify the validity of this assumption is under consideration.

An indication of switch oscillation could be the result of the generation of a spurious electrical signal in the landline circuit. However, this assumption does not appear valid since the instrumentation system shows no evidence of a transient.

Prior to the start of the interrogation period, at MOCS T_0 + 2.2 seconds, chattering of the OPPS has no effect upon engine operation and cannot produce an engine shutdown. OPPS chatter after initiation of interrogation can result in an engine shutdown if the duration of switch dropout exceeds 40 milliseconds. This time interval is necessary for "make" and latching of the holdfire monitoring relay (HFMR), which would then initiate a shutdown.

The very short duration of OPPS dropout (7.5 milliseconds) on GLV-8 and its occurrence prior to MOCS T_0 + 2.2 seconds precluded an inadvertent engine shutdown.

2. Stage II Engine (YLR91-AJ-7 S/N 2009)

a. Configuration and special procedures

The GLV-8 Stage II engine was different from that of GLV-7 in two areas. The lockwire on the turbine rotor retaining bolts was replaced with a lockring for increased bolt security (ECP-059). Secondly, the configuration of the thrust chamber injector was changed (ECP-157). The new GEMSIP injector (effective for GLV-8 and up) is less susceptible to combustion instability and provides essentially the same performance as the replaced production quadlet injector.

The propulsion system break-of-integrity review showed that the redundant engine shutdown valve had been removed at Martin-Baltimore and that retest procedures were not adequate to verify that closures

were not inadvertently left in during reassembly. The valve was removed at ETR for inspection and closures were not found in the unit.

As on Stage I, the thrust chamber valve through-bolts were retorqued to the final 300 to 320 inch-pounds at ETR.

b. Start transient

The engine start transient, as illustrated by the thrust chamber pressure history in Fig. III-7, showed an abnormally slow P_c rise rate from thrust chamber ignition time to staging blackout. Following telemetry blackout, normal P_c operation was observed. The slow P_c rise rate is not indicative of engine operation, since the pump discharge pressures, turbine speed, and MDFJPS actuation exhibited normal characteristics. A similar phenomenon was observed on GLV-5. The most likely cause of the GLV-5 and GLV-8 occurrences was moisture freezing in the P_c sensing line or transducer cavity during Stage I flight. Other possibilities include contamination or an improperly sized transducer orifice.

Significant engine start events are presented in Table III-7.

TABLE III-7

Stage II Engine Start Parameters

Parameter	S/A 3
FS_1 to initial P_{c_3} rise (sec)	0.65
P_{c_3} ignition spike (psia)	Invalid
P_{c_3} step (psia)	Invalid
P_{c_3} overshoot (psia)	Not available*

*Staging blackout period.

c. Steady-state performance

Stage II engine steady-state flight performance was satisfactory throughout flight. The average Stage II engine performance integrated over steady-state operation (from FS_1 + 1.2 seconds to $91FS_2$) agreed closely with preflight predictions. Average flight performance is compared in Table III-8.

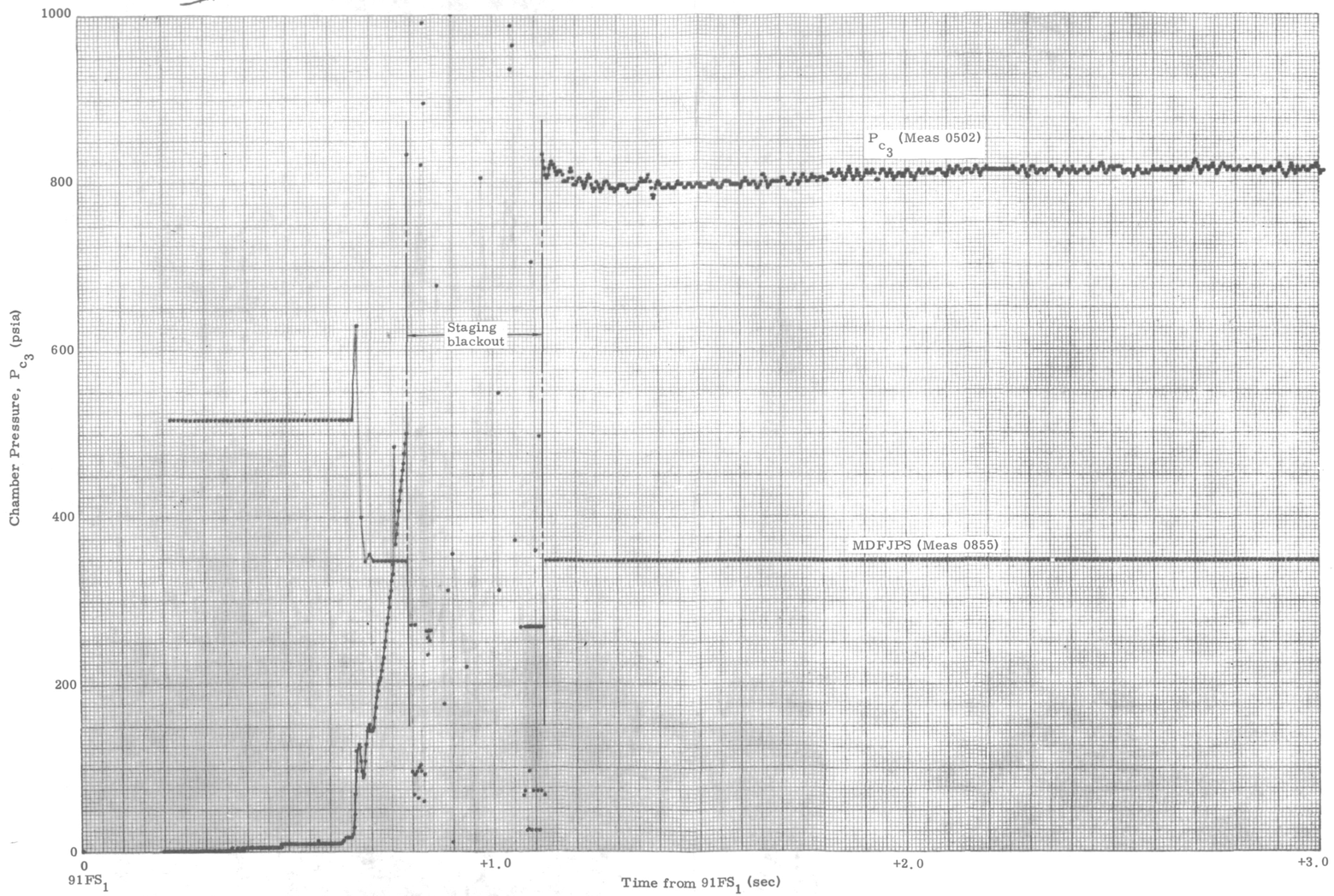

Fig. III-7. S/A 3 Start Transient

TABLE III-8

Predicted and Flight Performance Comparison--Stage II Engine

Parameter	Preflight Predicted Average	Flight Average	Difference (%)
Thrust, chamber (lb)	101,750	101,820	+0.07
Specific impulse, engine (sec)	311.84	311.38	-0.15
Mixture ratio, engine	1.7680	1.7901	+1.25
Oxidizer flow rate, overboard (lb/sec)	208.57	209.96	+0.67
Fuel flow rate, overboard (lb/sec)	117.72	117.04	-0.58

The engine flight performance calculated with the Martin-Baltimore PRESTO computer program is shown in Fig. III-8 as a function of time from $91FS_1$. The preflight prediction is presented for comparison.

Flight performance (Fig. III-8) shows unusual operation of the Stage II engine beginning at approximately $91FS_1$ + 90 seconds. A decay in performance and an unusual time-dependent characteristic are predominant in oxidizer flow rate, mixture ratio, and thrust. amination of the data indicates that the oxidizer pump performance was abnormal after $91FS_1$ +90 seconds. After this time, oxidizer and fuel pump discharge pressures, thrust chamber pressure, and turbine speed are normally expected to increase. At approximately $91FS_2$ + 90 seconds, P_{od_3} and P_{c_3} started to decline. The pressure decline lasted approximately 30 seconds and then erratically followed the expected trend (increase) but at the lower level. Turbine speed and P_{fd_3} remained essentially constant during this period; however, P_{fd_3} showed some response to the fluctuations in P_{od_3} and P_{c_3}.

Thrust chamber pressure also indicated larger pressure oscillations than noted on previous GLV flights, beginning at approximately $91FS_1$ + 140 seconds and continuing until the end of Stage II flight. Prior to this time, the P_{c_3} pressure fluctuations were approximately $\pm$15 psi, increasing to a maximum of approximately $\pm$40 psi near $91FS_1$ + 150 seconds. These steady-state abnormalities are under investigation.

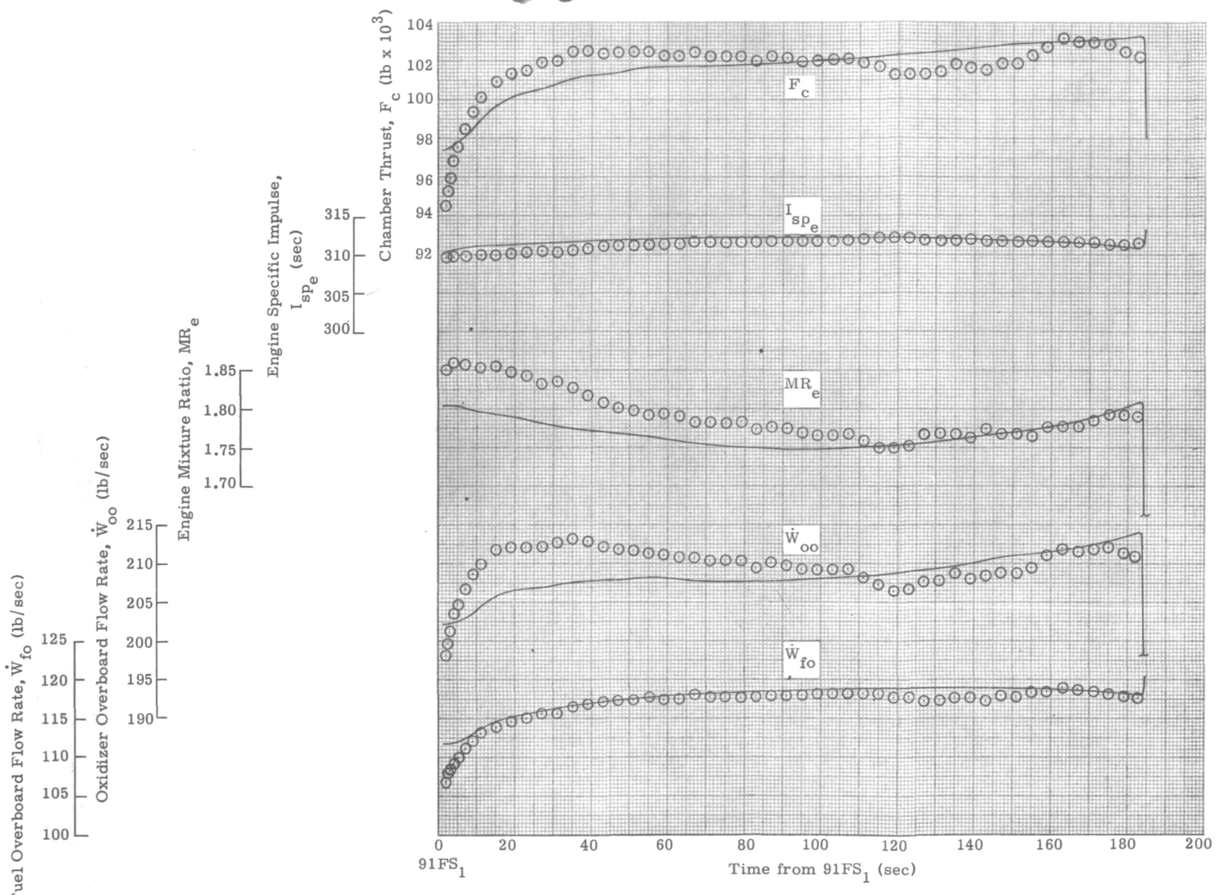

Average Engine Performance Integrated from First Steady-State to $91FS_2$

Symbol	Preflight Prediction	Flight Average
F_c (lb)	101,750	101,820
I_{sp_e} (sec)	311.84	311.38
MR_e	1.7680	1.7901
$\dot{W}_{oo}$ (lb/sec)	208.57	209.96
$\dot{W}_{fo}$ (lb/sec)	117.72	117.04

——— Preflight prediction
○ Flight performance

Fig. III-8. Stage II Engine Flight Performance

CONFIDENTIAL

CONFIDENTIAL

CONFIDENTIAL

The Stage II engine final acceptance test time-dependent biases were used directly in the preflight prediction rather than applying the acceptance-to-flight family correction that had previously been used. Figure III-8 indicates that prior to $91FS_1$ + 90 seconds the flight time-dependent characteristic correlates with the prediction although not as well as for the Stage I engine. After $91FS_1$ +90 seconds, the unusual time-dependent characteristics resulted from the abnormal oxidizer pump performance.

Engine flight performance corrected at the $91FS_1$ + 55-second time slice to standard inlet conditions is shown in Table III-9. This is compared with the acceptance test and the predicted flight performance at standard inlet conditions and the nominal time as used in the preflight prediction. The predicted flight performance at standard inlet conditions was obtained by adjusting the nominal acceptance test data for a 900-pound acceptance-to-flight thrust growth obtained from analysis of previous Titan II and GLV flights. The 55-second time slice performance corrected to standard inlet conditions is not representative of the total acceptance or flight performance. This is the nominal time used for quoting rated performance and the data indicates a comparison of corrected performance at 55 seconds only. The differences in performance indicated below are not necessarily compatible with the flight average performance summary previously shown because of the differences in time-dependent biases and engine inlet conditions throughout flight.

TABLE III-9

Stage II Engine Performance Corrected to Standard Inlet Condition at $91FS_1$ + 55 Seconds

Parameter	Acceptance Test	Predicted Flight (including 900-lb thrust growth)	Flight Performance
Thrust, chamber (lb)	100,642	101,542	102,386
Specific impulse, engine (sec)	311.02	311.02	310.80
Mixture ratio, engine	1.8071	1.8071	1.8204
Oxidizer flow rate, overboard (lb/sec)	208.48	210.34	212.79
Fuel flow rate, overboard (lb/sec)	115.11	116.14	116.64

CONFIDENTIAL

d. Shutdown transient

Stage II engine shutdown was initiated by a guidance command, with $91FS_2$ occurring at $91FS_1$ + 182.921 seconds. The calculated shutdown impulse from $91FS_2$ to $91FS_2$ + 20 seconds was 35,535 lb-sec; predicted impulse was 36,100 ± 7000 lb-sec. The impulse obtained from the ±10 g accelerometer data was 24,536 lb-sec using an average spacecraft plus Stage II weight of 14,280 pounds over the time interval from $91FS_2$ to $91FS_2$ + 0.665 second. The initial portion of the shutdown transient is illustrated by the P_{c_3} decay in Fig. III-9. Impulse from $91FS_2$ + 0.665 second to $91FS_2$ + 20 seconds was 10,999 lb-sec, obtained from the ±0.5 g accelerometer data and an average combined weight of 14,212 pounds. Zero thrust occurred at approximately $91FS_2$ + 14.35 seconds.

The thrust tailoff, calculated from the ± 0.5 g accelerometer data, is illustrated in Fig. III-10, which shows that the accelerometer recorded disturbances at approximately $91FS_2$ + 3.3, 3.8, 4.4, 5.3 and 7.1 seconds. These disturbances were not reflected in actuator motions characteristic of the post-SECO disturbances observed on previous GLV and Titan II flights. There is no firm correlation of the GLV-8 disturbances with thrust chamber pressure, although P_{c_3} indicated activity during the first two perturbations.

A post-SECO disturbance characteristic of those observed on previous flights (i.e., motion of actuators) did occur after spacecraft separation at approximately $91FS_2$ + 34.6 seconds.

e. Engine malfunction detection systems (MDS)

The Stage II engine MDS operated satisfactorily throughout flight. Figures III-7 and III-9 illustrate the response times and chamber pressure correlation of the malfunction detection fuel injector pressure switches (MDFJPS) during the start and shutdown transients, respectively. The fuel injector pressure is not shown since this parameter is not measured. A summary of the significant switch parameters is presented in Table III-10.

III-20-2 CONFIDENTIAL

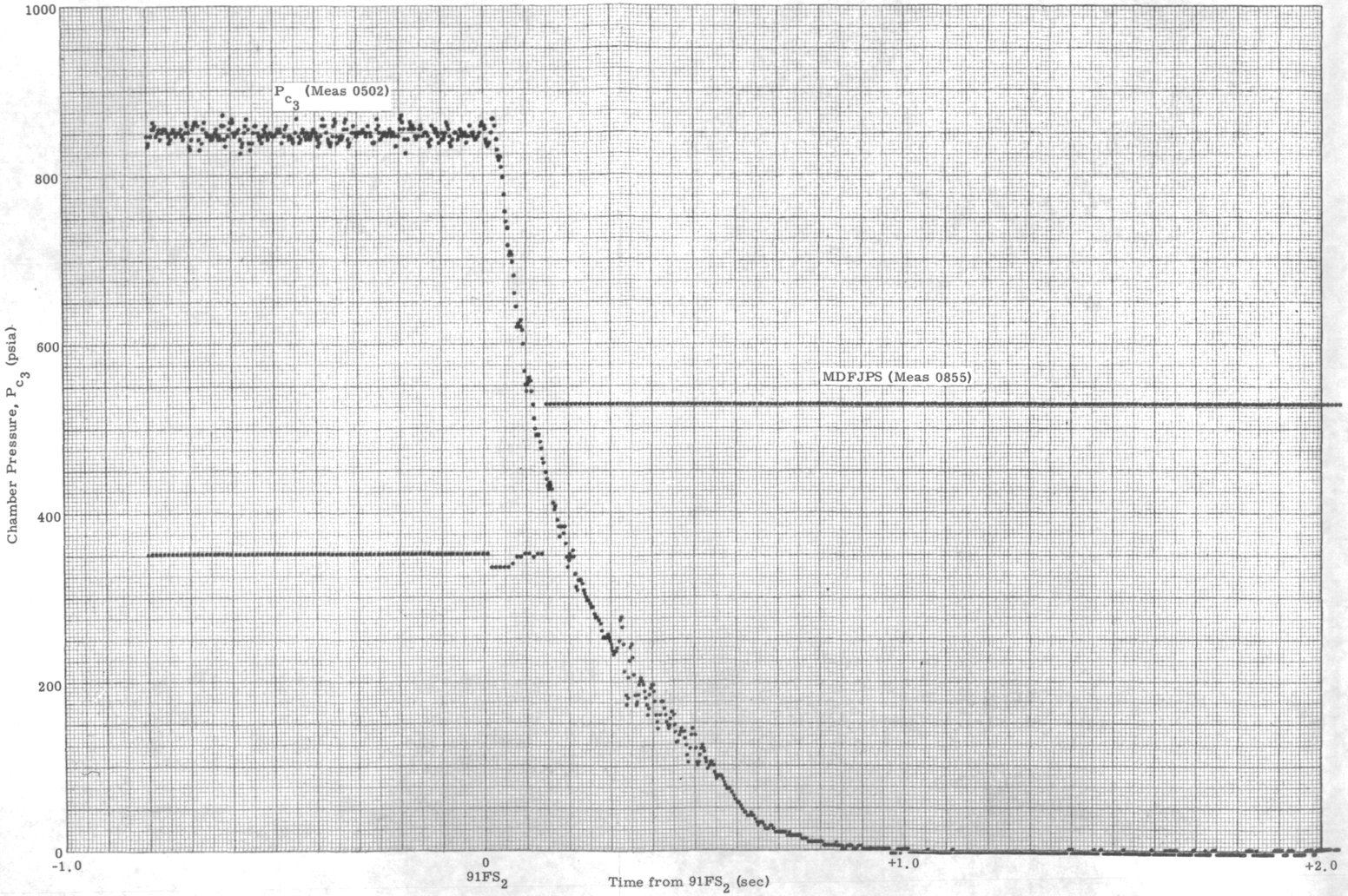

Fig. III-9. S/A 3 Shutdown Transient

CONFIDENTIAL

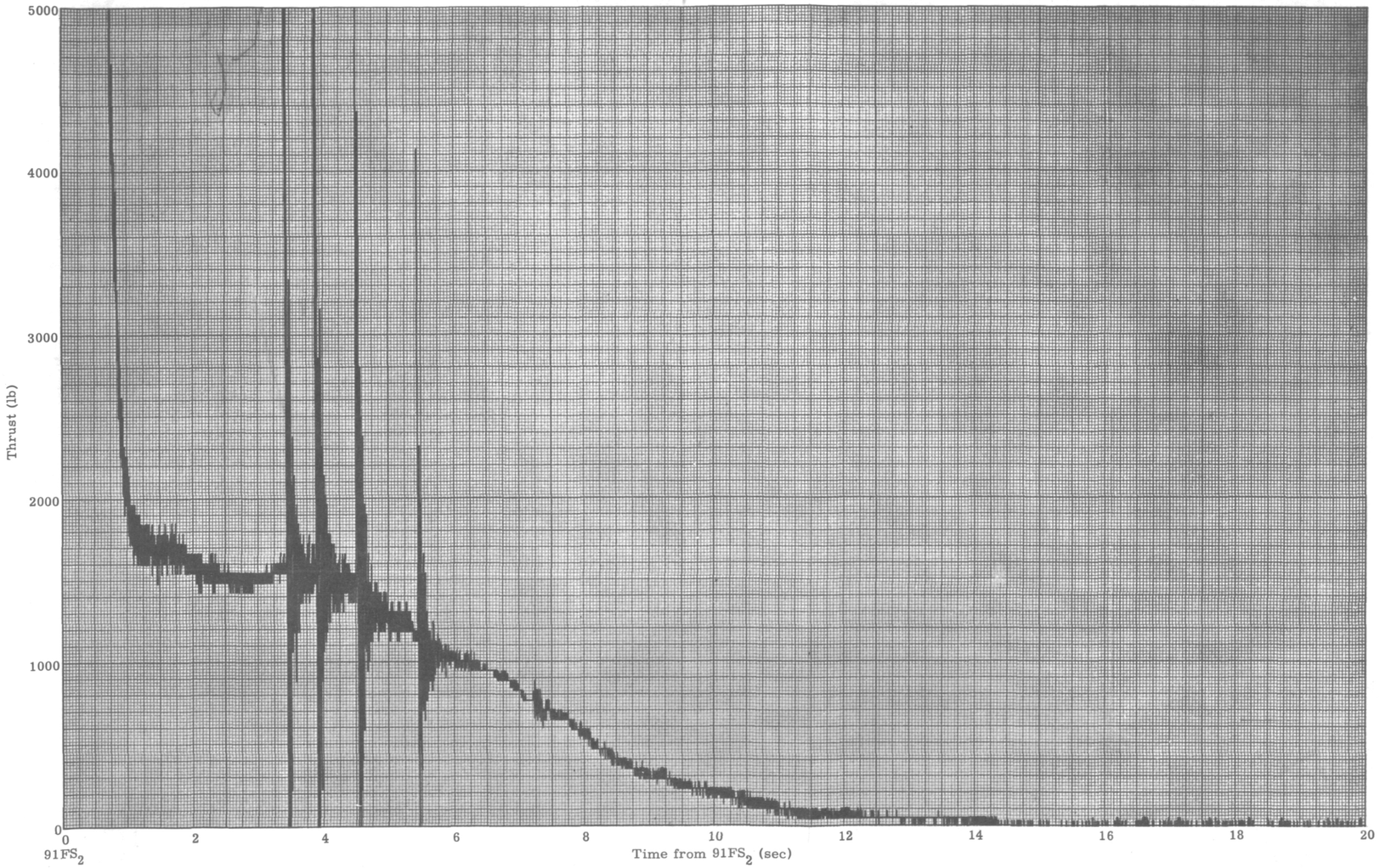

Fig. III-10. Stage II Engine Thrust Tail-Off

CONFIDENTIAL

TABLE III-10

Stage II MDS Operation

Parameter	
Actuation time (sec)	$91FS_1 + 0.67$
P_c at actuation (psia)	*
Deactuation time (sec)	$91FS_2 + 0.142$
P_c at deactuation (psia)	450

*P_c start transient invalid.

B. PROPELLANT SUBSYSTEM

1. Propellant Loading

a. Loading operations

Two propellant loadings were performed on GLV-8, consisting of a special loading on 17 February 1966 and the launch loading on 16 March. During the special loading, each tank was loaded individually up to highlight, with the quantity measured by all four flowmeters. Stage II oxidizer tank was filled to mission load to verify the new, no automatic temperature compensation (ATC) loading procedures. For the launch loading the tanks were dual-loaded to mission load using this procedure.

Both propellant loadings were made using the new, no ATC, no gear changer flowmeters with redesigned counter baseplate seals. The meters read in gallons, and the loading procedures were changed in accordance with the methods outlined in Ref. 18.

Due to problems during the GLV-8 tank calibrations, the volume to the highlight for the launch loading was shifted to agree with the average of the meter readings during the special loading. A -0.2% bias was incorporated in the oxidizer readings to compensate for a known calibration bias existing between the Wyle and Denver calibration facilities. The final total shift in the tab run from the original calibration volume is given in Table III-11.

CONFIDENTIAL

TABLE III-11

Total Tab Run Volume Shifts

Stage I Oxidizer	Stage I Fuel	Stage II Oxidizer	Stage II Fuel
+0.137%	-0.045%	-0.634%	-0.534

The sequence of launch propellant loading events is shown in Table III-12.

TABLE III-12

GLV-8 Launch Propellant Loading Schedule

Event	Time (EST) 16 March 1966			
	Stage I Oxidizer	Stage II Oxidizer	Stage I Fuel	Stage II Fuel
Start prechill	0031	0031	0300	0300
Start load	0047	0047	0315	0315
Highlight	0210	0130	0412	0349
Load complete	0233	0148	0423	0357

Table III-13 contains pertinent data for each loading of GLV-8. During the special loading, a delay between leak check and highlight on Stage II oxidizer caused the actual delta between average flowmeter temperature and highlight temperature to be 2.6° F instead of the predicted 0.7° F. If a delay of this nature occurs during a launch loading, present procedures dictate a detanking and reloading to obtain the proper mission load.

The launch loading went smoothly despite a few problems. These are:

(1) During oxidizer loading Stage I oxidizer meter S/N 199174 experienced a +0.6% shift in accuracy after prechill. The shift was noted at highlight when the highlight flowmeter comparison showed +0.837% instead of the anticipated +0.2%. A check of mechanical counters showed that tandem Stage I oxidizer meter S/N 206359 was performing properly; hence, it was electrically connected to the blockhouse totalizer instead of Stage I oxidizer meter S/N 199174. The existing

III-24
-2

TABLE III-13

Summary of Propellant Load Verification at Highlight

CONFIDENTIAL

Loading Event	Tank	Flowmeter				High-light Temperature (° F)	Average FM Temperature to High-light (° F)	Difference Between FM and Original Tab Run (%)(2)	Difference Between FM and Corrected Tab Run (%)(2)	Observed FM Tab Run Difference at Time of Test (%)	Average Loading Rate (gpm)
		Serial No.	PTPS No.	Stage	Calibration Facility						
Special Loading	Stage II oxidizer (through 4 meters)	199174	442	I	Wyle	34.9	32.3	-0.264	+0.370		94
		206359	4412	I	Wyle	34.9	32.3	-0.319	+0.315		
		204277	446	II	Wyle	34.9	32.3	-0.397	+0.237		
		199173(1)	4420	II	Wyle	34.9	32.3	-0.369	+0.265	-0.602	
	Stage I oxidizer (through 4 meters)	199174	442	I	Wyle	32.4	31.9	+0.297	+0.177		184
		206359(1)	4412	I	Wyle	32.4	31.9	+0.249	+0.129	+0.313	
		204277	446	II	Wyle	32.4	31.9	+0.371	+0.251		
		199173	4420	II	Wyle	32.4	31.9	+0.236	+0.116		
	Stage II fuel (through 4 meters)	206362	441	I	Denver	33.6	32.1	-0.530	+0.004		
		202146	4411	I	Denver	33.6	32.1	-0.554	-0.020		
		206361	445	II	Denver	33.6	32.1	-0.554	-0.020		
		199171(1)	4419	II	Denver	33.6	32.1	-0.549	-0.015	-0.533	
	Stage I fuel (through 4 meters)	206362	441	I	Denver	32.3	32.0	-0.057	-0.012		212
		202146(1)	4411	I	Denver	32.3	32.0	-0.079	-0.033	-0.067	
		206361	445	II	Denver	32.3	32.0	-0.014	+0.031		
		199171	4419	II	Denver	32.3	32.0	-0.043	+0.004		
Launch	Stage I oxidizer	199174(1)	442	I	Wyle	26.9	26.1		+0.814(4)	+0.837	184
		206359	4412	I	Wyle	26.9	26.1	(3)	+0.217	+0.289(4)	
	Stage I fuel	206362	441	I	Denver	30.8	30.1	(3)	+0.022		219
		202146(1)	4411	I	Denver	30.8	30.1		+0.000	-0.001	
	Stage II oxidizer	204277	446	II	Wyle	28.1	27.0	(3)	+0.125		78
		199173(1)	4420	II	Wyle	28.1	27.0		+0.186	+0.093	
	Stage II fuel	206361	445	II	Denver	31.9	30.7	(3)	+0.032		109
		199171(1)	4419	II	Denver	31.9	30.7		-0.001	+0.004	

(1)Meter connected to CP 2500 totalizer in blockhouse.

(2)Flowmeter readings corrected for temperature and flow rates.

(3)Original tab run not applicable for launch loading.

(4)Topping above highlight dome with meter S/N 206359.

CONFIDENTIAL

counter readings were corrected, and a new preset value was established using the K-factor equation. Loading was then completed without incident. Postlaunch oxidizer flow verification confirmed the +0.6% shift between the other Stage I meter and the two Stage II meters. Flowmeter S/N 199174 was removed from the system and failure analyzed. It was found to have excessive rotor scoring, indicative of having passed a piece of foreign material. Accuracy checks showed that, while it had a bias error, its performance was adequate. Investigation into the possible relationship of the scoring and the +0.6% shift is continuing.

(2) Postflight analysis of Stage I oxidizer pulser data indicated that there was a flowback of about one gallon when flow was stopped at highlight and when loading was complete. This was caused by a sluggish response of the pump outlet check valve. The questionable valve will be verified during the normal leak check procedures prior to performing the propellant tanking test for GLV-9. Replacement, if necessary, will be made before launch loading.

(3) During the Stage II fuel loading there was an overshoot of two gallons greater than normal. The automatic pump shutoff signal was not sent by the CP 2500 counter and the normal manual pump stop was initiated, preventing a large overload.

b. Total propellant loads

Total mission loads for the launch, as determined from flowmeters, are shown in Table III-14. The flowmeter readings were corrected by subtracting propellants vaporized and propellants remaining in the fill lines. Stage I oxidizer flowmeter load reflects the use of the K-factor ratio method to obtain mission load. Total propellant loads as determined by flight verification are also shown in Table III-14. The flight verification loads were calculated from a propellant inventory, using actual level sensor uncover times and tank calibration data to determine flow rates. Total, integrated, in-flight overboard propellant consumption was found using the engine analytical model. Engine start transient consumptions were derived from Aerojet summary reports. Other transient propellant consumptions and pressurization gas weights were calculated from flight data (Tables III-37 and III-38).

In Table III-14 the large discrepancy in the Stage II oxidizer load should be noted. This discrepancy is not consistent with the excellent agreement in the Stage I oxidizer load. An investigation is currently under way to determine the causes for the indicated overload as well as for the overloads indicated on Stage II of GLV-4, -5, -6 and -7. It appears that the reconstruction technique, not the loadings, is in error.

CONFIDENTIAL

TABLE III-14

Verification of Mission Loads

Tank	Flowmeter Indicated Load (gal.)	Flowmeter Indicated Load (lb)	Requested Load (lb)	Flight Verification Load (lb)	Difference Between Flight Verification and Flowmeter Load (%)
Stage I oxidizer	13,777*	172,134	172,155	172,356	+0.129
Stage I fuel	11,589	89,222	89,145	89,299	+0.086
Stage II oxidizer	3,084	38,509	38,491	38,678	+0.439
Stage II fuel	2,849	21,931	21,909	21,873	-0.264

*K-factor equation used to obtain mission load.

CONFIDENTIAL

c. Propellant assay

Prelaunch data from the propellant assay report (sampled on 4 March 1966) for oxidizer and fuel are presented in Table III-15. Specification values are also listed. Satisfactory agreement between the analysis and specification requirements was obtained. Data are from the primary RSV propellants which were used to load the vehicle.

TABLE III-15

Propellant Assay Summary

Fuel MIL-P-27402 (USAF)	Test	Requirement
Hydrazine	51.4 %	51 ± 0.9%
UDMH	47.7%	46.9% min
H_2O	0.9%	2.0% max
Total N_2H_4 + UDMH	99.1%	98% min
Solids	0.6 mg/liter	25 mg/liter
Particles on 50 mesh screen	0	0
Density (gm/cc) at 77° F	0.8978	0.89826 ± 0.5%
Oxidizer MIL-P-26539 (USAF)		
Nitrogen tetroxide (N_2O_4)	99.6%	99.4% min
Chloride as NOCl	*	--
H_2O equivalent	0.10%	0.2%
Solids	0	10 mg/liter
Nonvolatile ash	0	0
Particles on 50 mesh screen	0	0

*Not reported.

2. Propellant Temperature

a. Weather

Table III-16 presents the F-45 day prediction, the F-1 day 1200 EST prediction and the 16 March actual launch weather for GLV-8. The F-45 day prediction was based on a hot December through March day. Actual temperatures were in close agreement with those predicted on F-1 day. Wind speed forecasts were as much as 8 knots below the actual velocity, however.

CONFIDENTIAL

ER 13227-8

TABLE III-16

Predicted and Actual Weather Conditions for GT-8 Launch

Time (EST)		Dry Bulb Temperature (° F)			Dew Point Temperature (° F)			Wind Speed (kn)			Cloud Cover		
		F-45	F-1	Actual	F-45	F-1	Actual	F-45	F-1	Actual (kn)/ Direction (deg)	F-45	F-1	Actual
2100	15 March	71.2			65.8			7			0.5		
2200		70.7			65.3			7			0.5		
2300		70.1			64.9			7			0.5		
0000	16 March	69.8	66.0	63.4	64.6	52.0	55.0	7	16.0	10/303	0.4	0.2	0.1
0100		69.5		62.9	64.4		55.0	7		9/300	0.5		0.1
0200		69.3		62.2	64.2		55.0	7		9/309	0.5		0.1
0300		69.0	64.0	61.4	64.0	52.0	55.0	7	14.0	11/316	0.5	0.2	0.1
0400		68.8		60.8	63.9		55.0	7		8/309	0.5		0.1
0500		68.7		60.0	63.7		56.0	7		8/317	0.5		0.1
0600		68.5	62.0	60.9	63.6	52.0	57.0	7	13.0	8/318	0.5	0	0.1
0700		68.4		64.3	64.9		59.0	7		16/341	0.6		0.1
0800		70.9		64.8	66.1		58.0	7		18/345	0.6		0.2
0900		72.8	66.0	65.7	67.2	53.0	57.0	9	13.0	19/339	0.6	0	0.2
1000		75.0		65.1	68.2		57.0	10		17/336	0.6		0.2
1100		76.4		65.7	68.8		58.0	12		20/336	0.6		0.2
1200		77.2	68.0	65.5	69.2	56.0	58.0	12	12.0	20/337	0.6	0	0.2

CONFIDENTIAL

b. Propellant loading temperatures

Table III-17 compares the requested propellant temperatures in the RSV (at start of loading) and at the tank bottom probe (at highlight) with the measured values.

TABLE III-17

Propellant Loading Temperature Comparison--
RSV and Tank Bottom Probe

System	RSV			Tank Bottom Probe		
	Required*	Actual	ΔTemperature (° F)	Required*	Actual	ΔTemperature (° F)
Stage I oxidizer	23.6	23.6	0	26.0	26.9	+0.9
Stage II oxidizer	23.6	23.6	0	27.8	28.1	+0.3
Stage I fuel	28.9	28.5	-0.4	30.6	30.8	+0.2
Stage II fuel	28.9	28.5	-0.4	31.6	31.9	+0.3

*Required values were for loading start times of 2300 EST for oxidizer and 0230 EST for fuel. Similar requirements for actual loading start times of 0100 EST for oxidizer and 0330 EST for fuel are as shown in Table III-18.

TABLE III-18

Revised Propellant Loading Temperature Comparison--
RSV and Tank Bottom Probe

System	RSV			Tank Bottom Probe		
	Required*	Actual	ΔTemperature (° F)	Required*	Actual	ΔTemperature (° F)
Stage I oxidizer	26.2	23.6	-2.6	28.6	26.9	-1.7
Stage II oxidizer	26.2	23.6	-2.6	30.3	28.1	-2.2
Stage I fuel	29.9	28.5	-1.4	31.5	30.8	-0.7
Stage II fuel	29.9	28.5	-1.4	32.5	31.9	-0.6

*For loading start time of 0100 EST.

The two-hour delay in loading oxidizer, while maintaining the same RSV temperature, was the start of a chain of events which caused a breakdown of the propellant temperature monitoring program. Other problems with weather forecast, erector curtain configuration and thermal stratification prediction resulted in an unnecessarily low minimum payload capability forecast. Changes to the computer program are expected to improve the situation on future flights. RSV and flowmeter temperatures recorded during loading are shown in Figs. III-11 and III-12.

c. Liftoff temperatures

A comparison of predicted, actual and reconstructed propellant bulk temperatures appears in Table III-19. Positions of the reconstructed, actual and predicted temperatures in the mixture ratio band are shown in Figs. III-13 and III-14.

TABLE III-19

Propellant Bulk Temperature Comparison

System	F-45 Day Prediction (° F)	F-1 Day Prediction (° F)	Actual* (° F)	Reconstructed (° F)
Stage I oxidizer	41.5	41.8	42.4	44.0
Stage I fuel	41.8	42.8	43.2	43.9
Stage II oxidizer	43.7	43.5	43.2	42.9
Stage II fuel	39.0	38.9	41.9	39.5

*Actual bulk temperatures obtained from average flight temperature profiles adjusted for differences listed in Table III-21.

Figures III-15 through III-18 show a comparison of the F-1 day, reconstructed and actual tank bottom probe temperatures for each propellant tank from loading to liftoff.

Correlation of actual, F-1 day predicted and reconstructed bulk temperature was good, except in the case of the Stage II fuel tank on which the actual bulk rise was 25% greater than the reconstructed. The discrepancy in this tank was similar to the one experienced on GLV-1, which was the only other flight on which erector curtains were

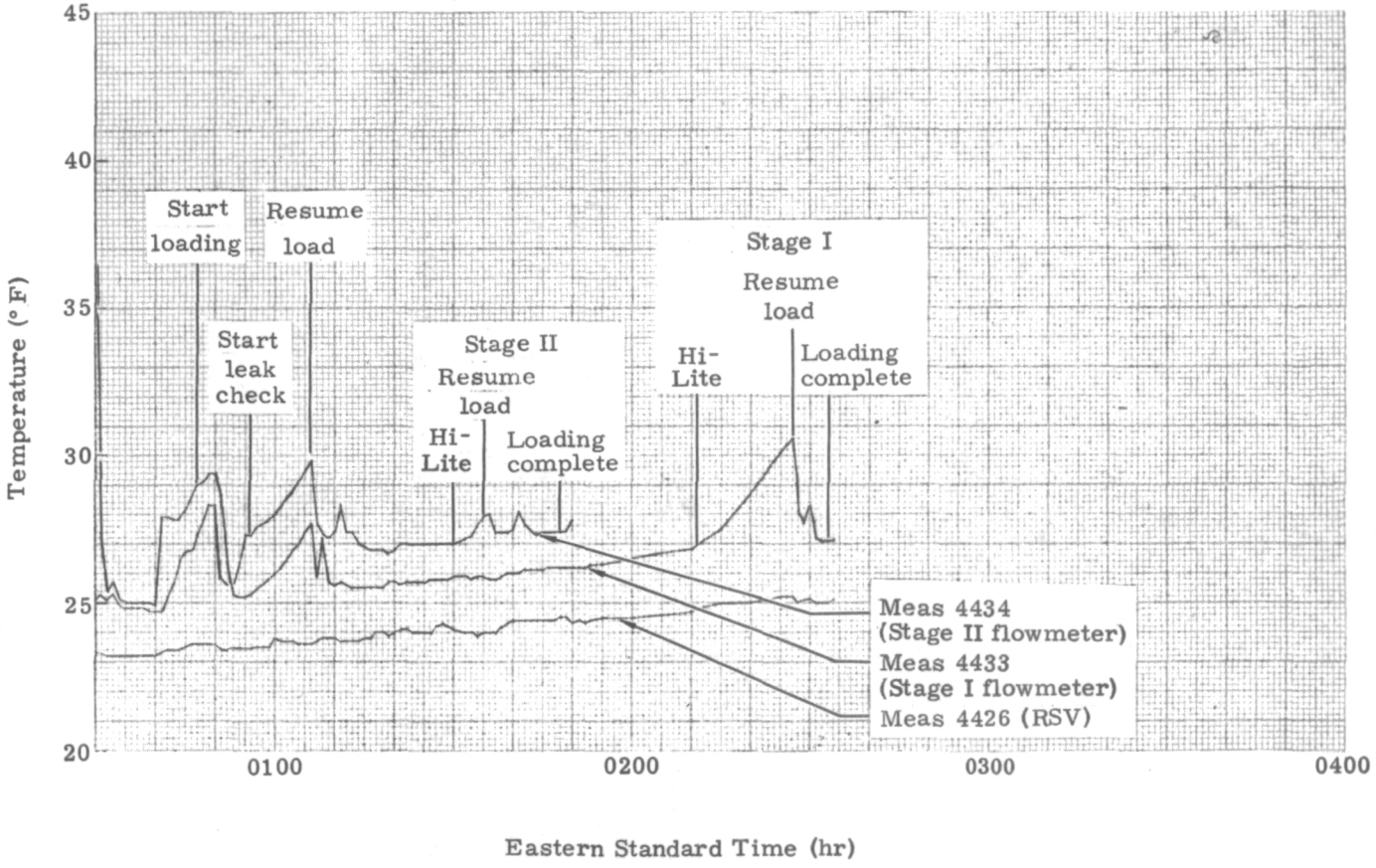

Fig. III-11. Oxidizer Temperatures During Loading

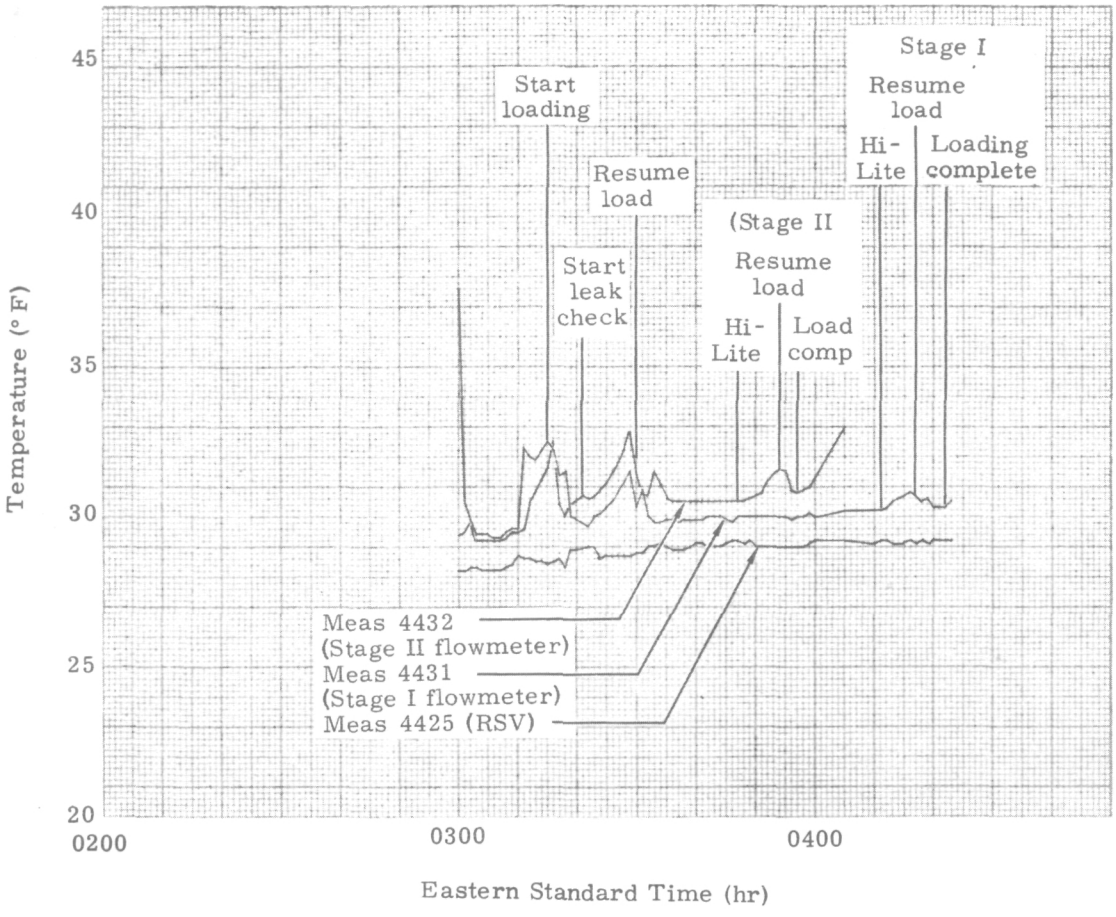

Fig. III-12. Fuel Temperature During Loading

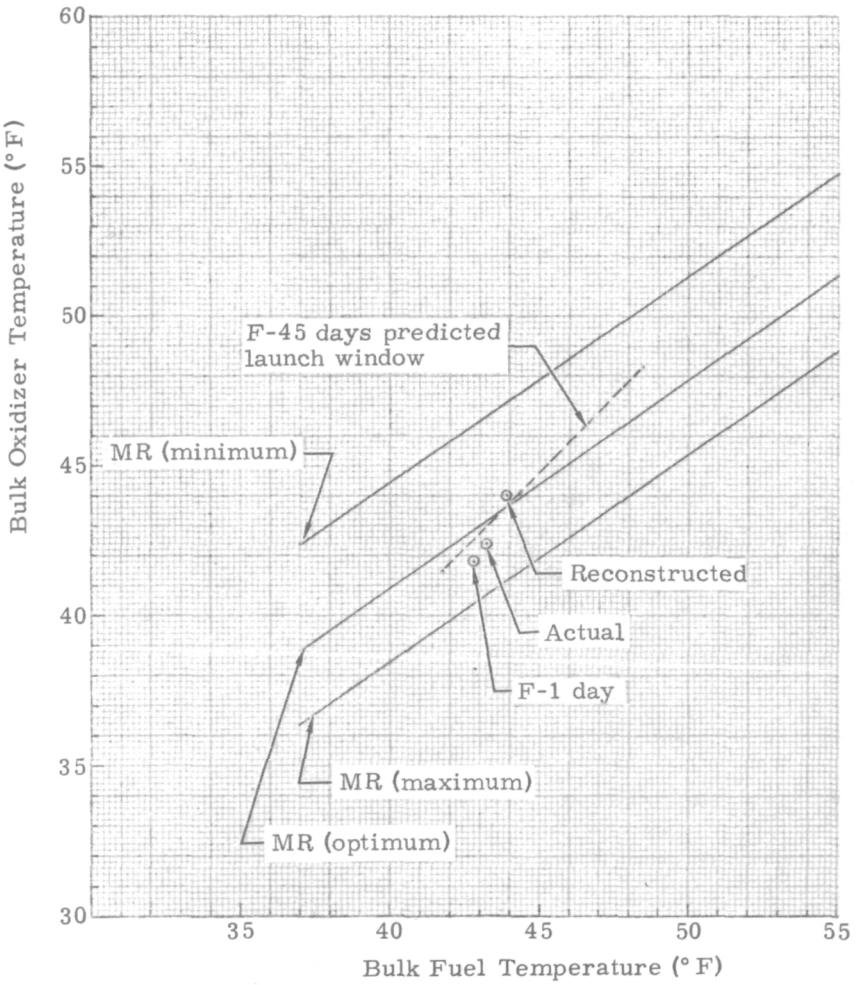

Fig. III-13. Propellant Bulk Temperatures at Liftoff, Stage I

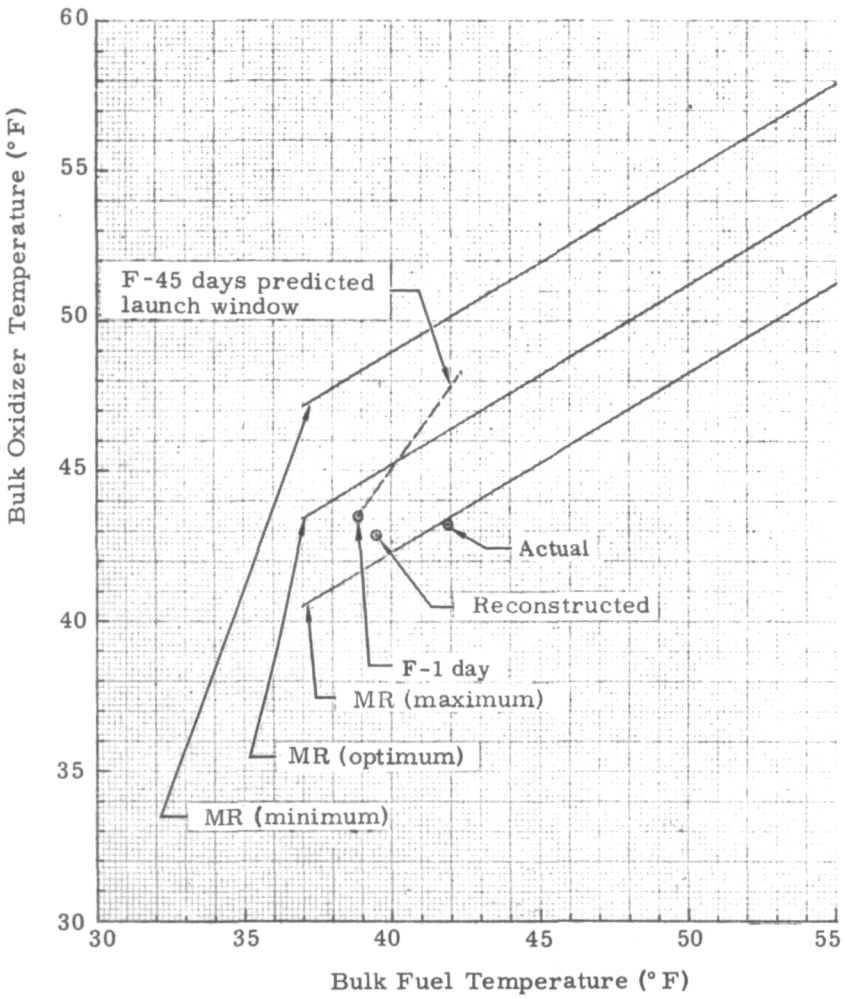

Fig. III-14. Propellant Bulk Temperatures at Liftoff, Stage II

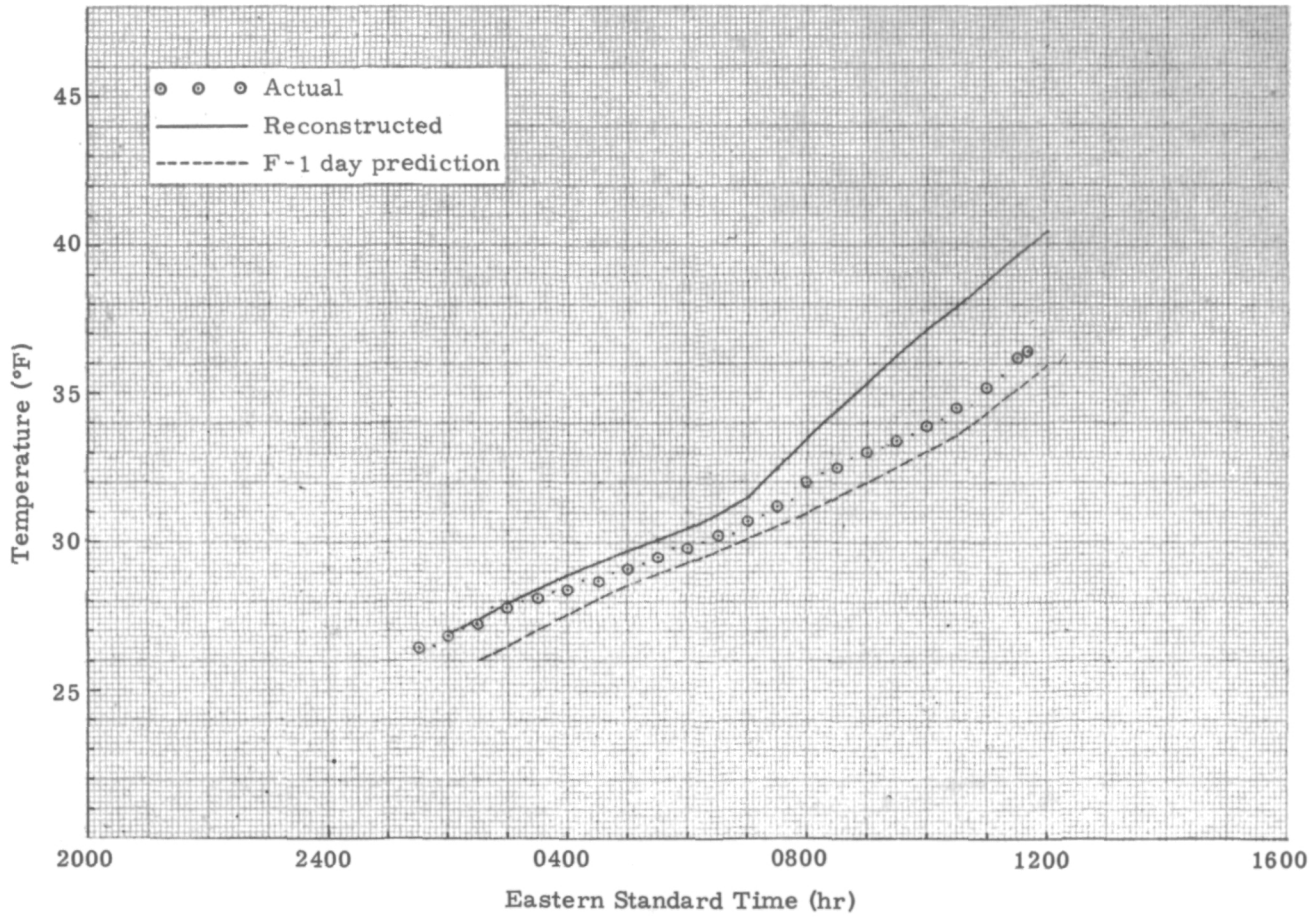

Fig. III-15. Stage I Oxidizer Tank Bottom Probe Temperature (Meas 4128)

CONFIDENTIAL

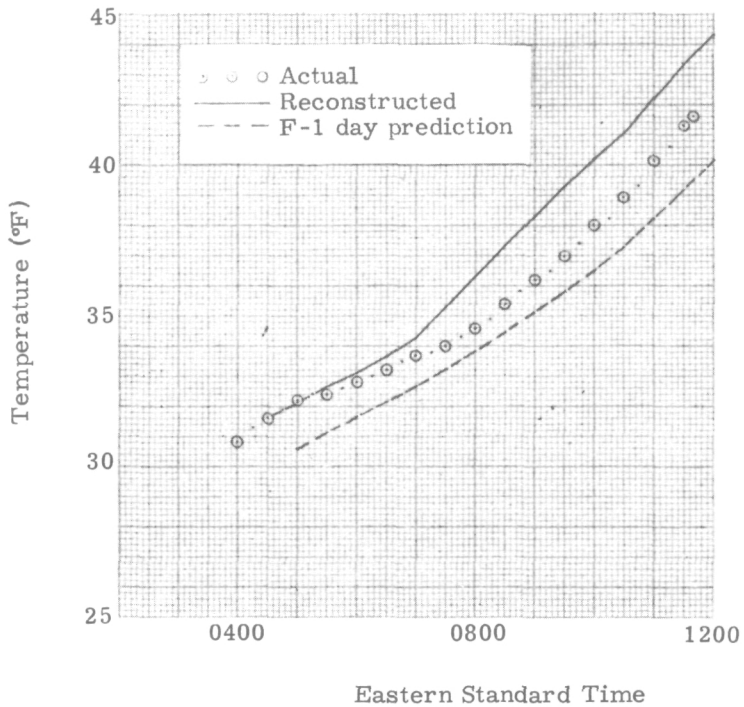

Fig. III-16. Stage I Fuel Tank Bottom Probe Temperature (Meas 4124)

CONFIDENTIAL

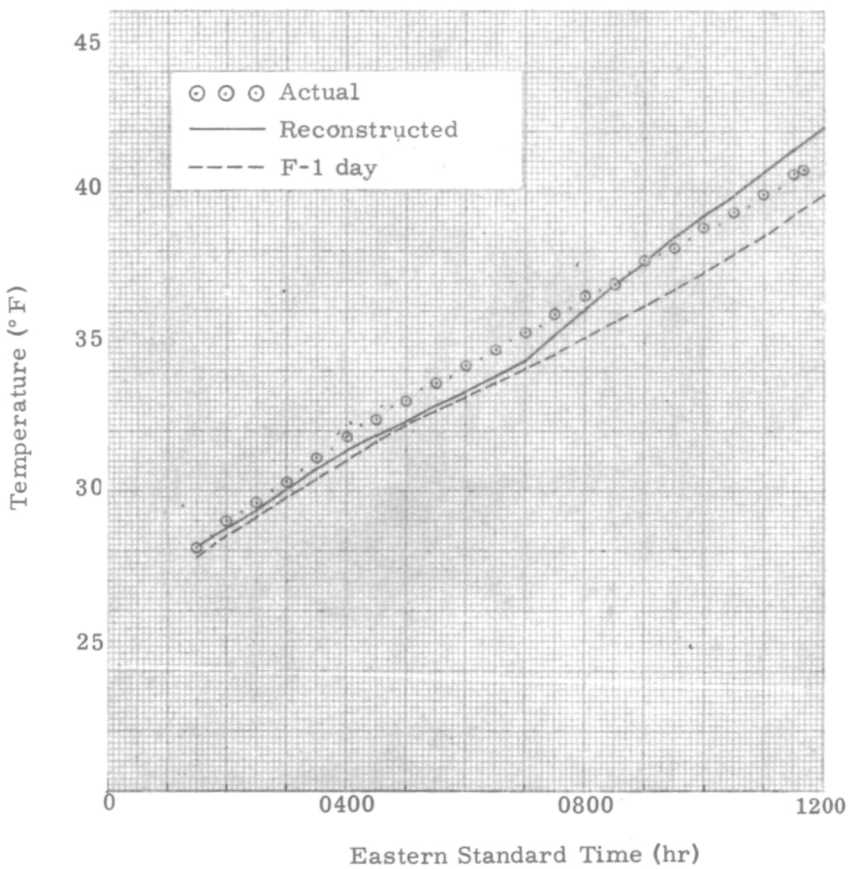

Fig. III-17. Stage II Oxidizer Tank Bottom Probe Temperature (Meas 4604)

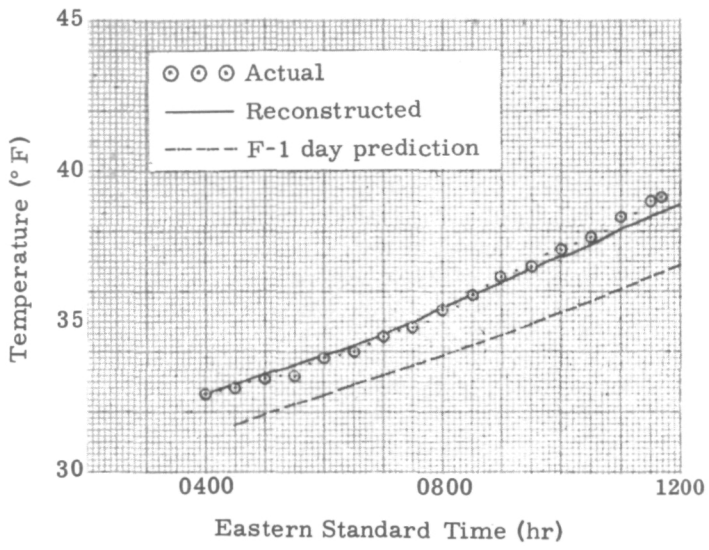

Fig. III-18. Stage II Fuel Tank Bottom Probe Temperature (Meas 4601)

opened. It is indicated that higher-than-predicted heat transfer coefficients are incurred in the Stage II fuel tank when the curtains are opened. Changes to the propellant temperature prediction program will be made to cover this situation, thereby making erector curtain deployment a more predictable variable when forecasting propellant temperatures.

The lack of correlation of the tank bottom probe readings with predictions after the curtains were opened was also similar to the GLV-1 experience. Analysis of previous flights shows that the thermal stratification experienced on GLV-1 and GLV-8 was as much as 15% greater than predicted. Table III-20 shows the predicted and actual stratification for GLV-1, GLV-5 and GLV-8; GLV-5 is typical of the "no curtains opened" operation.

TABLE III-20

Thermal Stratification--Predicted and Actual

System	Predicted	GLV-1	GLV-5	GLV-8
Stage I				
Oxidizer	25%	31%	23%	39%
Fuel	5%	18%	5%	15%
Stage II				
Oxidizer	10%	19%	10%	17%
Fuel	15%	32%	19%	30%

It is believed that a large increase in stratification occurred when the Stages I and II oxidizer curtains were opened at 0700 EST. This would explain why the probe temperature rise rate failed to respond to the wind increase which occurred coincident with the curtain opening. Changes in the rise rate program to cover this situation will also be made for GLV-9 and up.

d. Suction temperatures

The actual pump inlet temperatures were in good agreement with the predicted temperature profiles. These data are shown in Figs. III-19 through III-22. The trends of the actual temperature curves are in fair agreement with those predicted. Deviations may be ascribed to differences in predicted and actual weather and the differences between predicted and actual thermal stratification. Thermal stratification differences (predicted versus actual), while large for propellant temperature monitoring uses, are not reflected as large on a propellant temperature profile basis.

CONFIDENTIAL

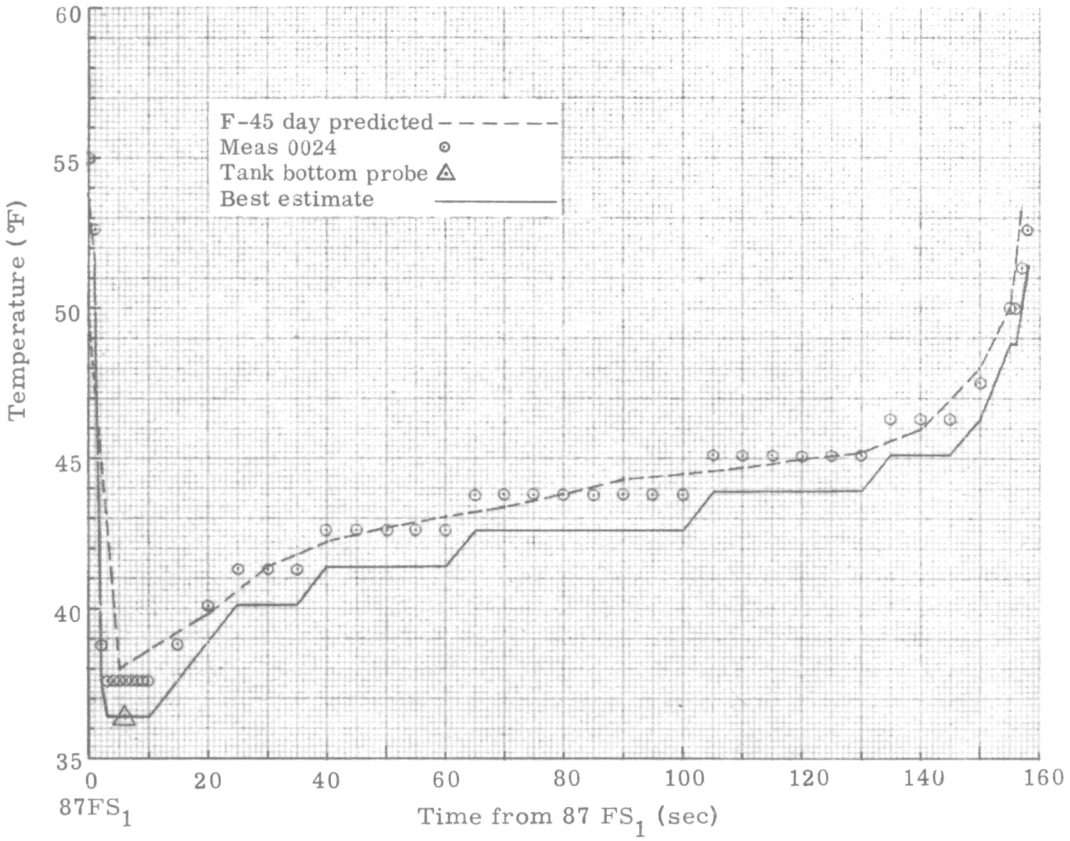

Fig. III-19. Stage I Oxidizer Pump Inlet Temperature (Meas 0023 and 0024)

CONFIDENTIAL

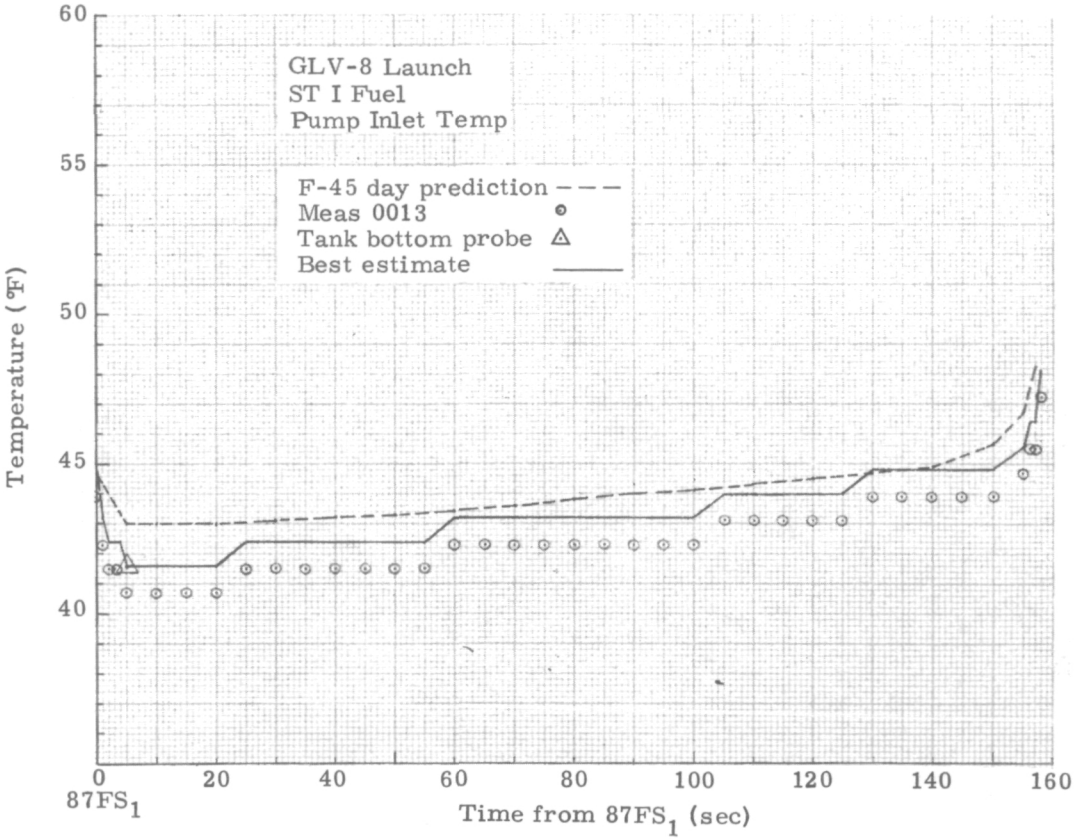

Fig. III-20. Stage I Fuel Pump Inlet Temperature

CONFIDENTIAL

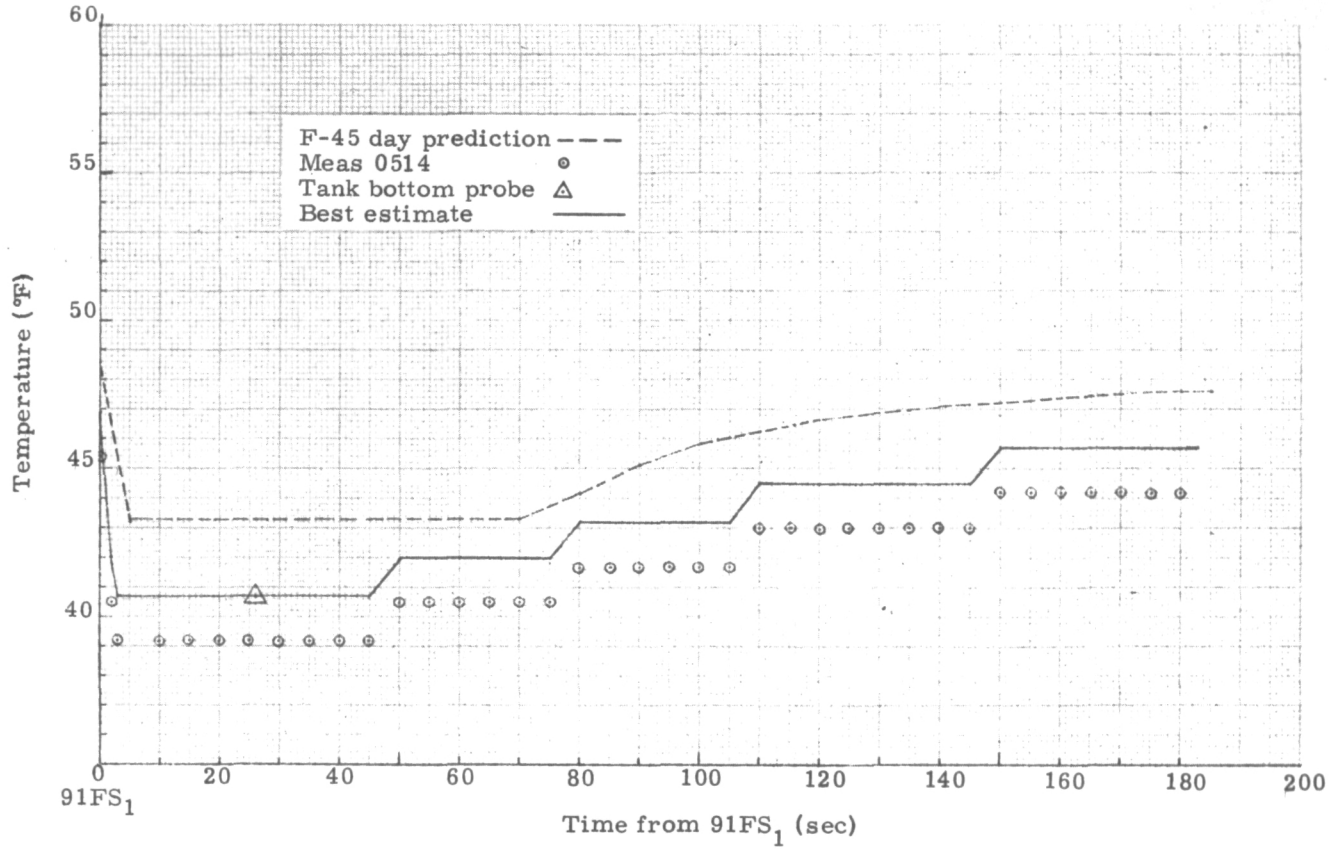

Fig. III-21. Stage II Oxidizer Pump Inlet Temperature

CONFIDENTIAL

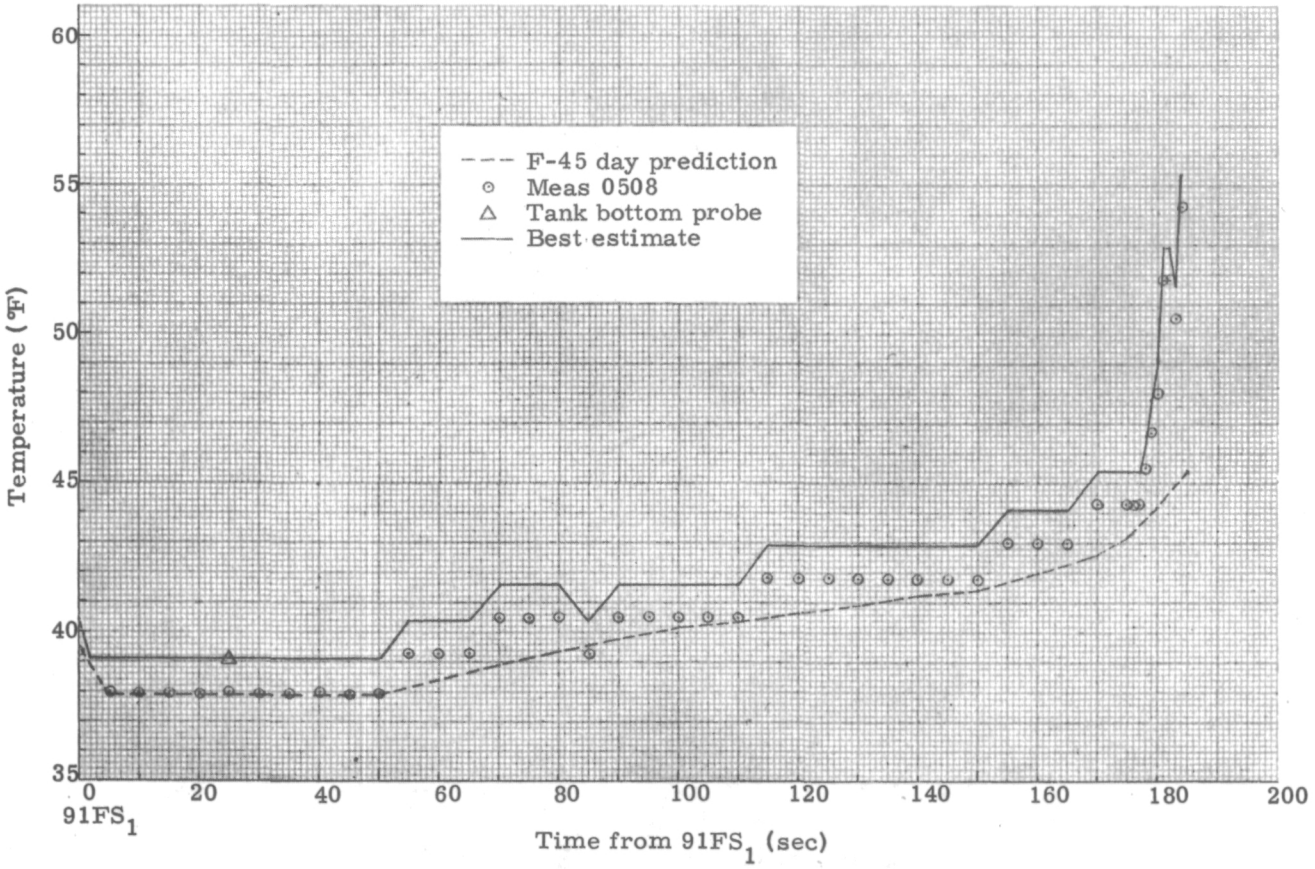

Fig. III-22. Stage II Fuel Pump Inlet Temperature

A comparison between the suction and tank bottom probes at various times after FS_1 is made in Table III-21.

TABLE III-21

Propellant Temperature Comparison--
Tank Bottom Probe and Pump Inlet

System	Time (sec)	Suction Probe Temperature (° F)	Tank Bottom Probe Temperature (° F)	Delta Temperature (° F)
Stage I fuel	FS_1 + 5	40.7	41.6	-0.9
Stage II fuel	FS_1 + 25	38.0	39.1	-1.1
Stage I oxidizer	FS_1 + 6	37.6	36.4	+1.2
Stage II oxidizer	FS_1 + 22	39.2	40.7	-1.5

Due to the greater accuracy of the tank bottom probes, the best estimate propellant temperatures are those that would be obtained if the suction probe profile were shifted to agree with the tank bottom probe. In the postflight propellant temperature analyses this shift has been applied to all four tanks.

3. Propellant Feed System

a. Feedline transients

The maximum transient pressures recorded at the pump inlet instrumentation bosses are listed in Table III-22.

TABLE III-22

Maximum Transient Pressures at Pump Inlet

Meas	At Prevalve Opening* (psia)	At Initial Pressure Wave	At Ignition (psia)	At TCV Closing	Design Operating Pressure (psia)
Stage I oxidizer (0017)	No data	Negligible	134	Negligible	215
Stage I fuel (0014)	46	Negligible	Negligible	Negligible	55
Stage II oxidizer (0510)	No data	Negligible	*	psia	260
Stage II fuel (0507)	No data	Negligible	*	Negligible	80

* Not available due to telemetry staging blackout.

Ignition transient pressures were, in general, similar to those of GLV-6 and GLV-7 flights. Telemetry blackout normally experienced during Stage II ignition prevents obtaining data on sustainer engine ignition transients.

b. Pump inlet suction pressures

Stages I and II static suction pressures at the suction measurement boss locations are shown in Figs. III-19 through III-22, which present preflight predicted, postflight reconstructed and best estimates of actual flight pressures.

The postflight reconstructed curves were based on flight measured values of ullage gas pressure, axial load factors, propellant temperatures and propellant loadings.

The Stage I oxidizer best estimate curve of the static suction pressures at the measurement boss (Meas 0017) consists of an average of the measured pressure and the two oxidizer standpipe pressures (Meas 0033 and 0034) adjusted to the Meas 0017 boss location. The Stage I fuel suction pressure best estimate at Meas 0014 boss location is an average of measured pressure and the two fuel accumulator pressures (Meas 0037 and 0038) adjusted to the Meas 0014 boss location. The Stage II oxidizer and fuel best estimate suction pressures are the pressures measured by Meas 0510 and 0507, respectively.

Agreement between measured and reconstructed curves in Figs. III-23 through III-26 was generally better than on previous flights. The difference between measured and predicted curves on Stages I and II fuel figures is due largely to differences between predicted and actual tank ullage gas pressures.

c. NPSH supplied

The NPSH supplied at the engine turbopump inlet during the start phase and during steady-state operation is shown in Table III-23.

TABLE III-23

Minimum NPSH Supplied

System	Minimum NPSH Supplied During Start Transient (psia)	Starting NPSH Required ① (psia)	Limited Operation NPSH Required ②	Minimum Steady-State NPSH Supplied (psia)	Unlimited Operation NPSH Required ① (psia)
Stage I oxidizer	24.2	④	28.2 psia for 135 sec	53.2	46.1
Stage I fuel	30.5	17.1	17.1 psia for 120 sec	30.2	23.1
Stage II oxidizer	③	38.4	19.2 psia for 120 sec	28.0	22.4
Stage II fuel	③	39.8	39.8 psia for 120 sec	47.5	43.4

① Extracted from SCNP S75015, page 1, and SCNP S85008, page 1. Oxidizer values represent NPSH required at FS_1 and fuel values at engine start.

② Time given in table represents maximum cumulative operating time from engine acceptance at the given NPSH levels. The data were extracted from source ①

③ Not available due to telemetry blackout.

④ 38.4 psia required at FS_1. No specific requirement during start transient.

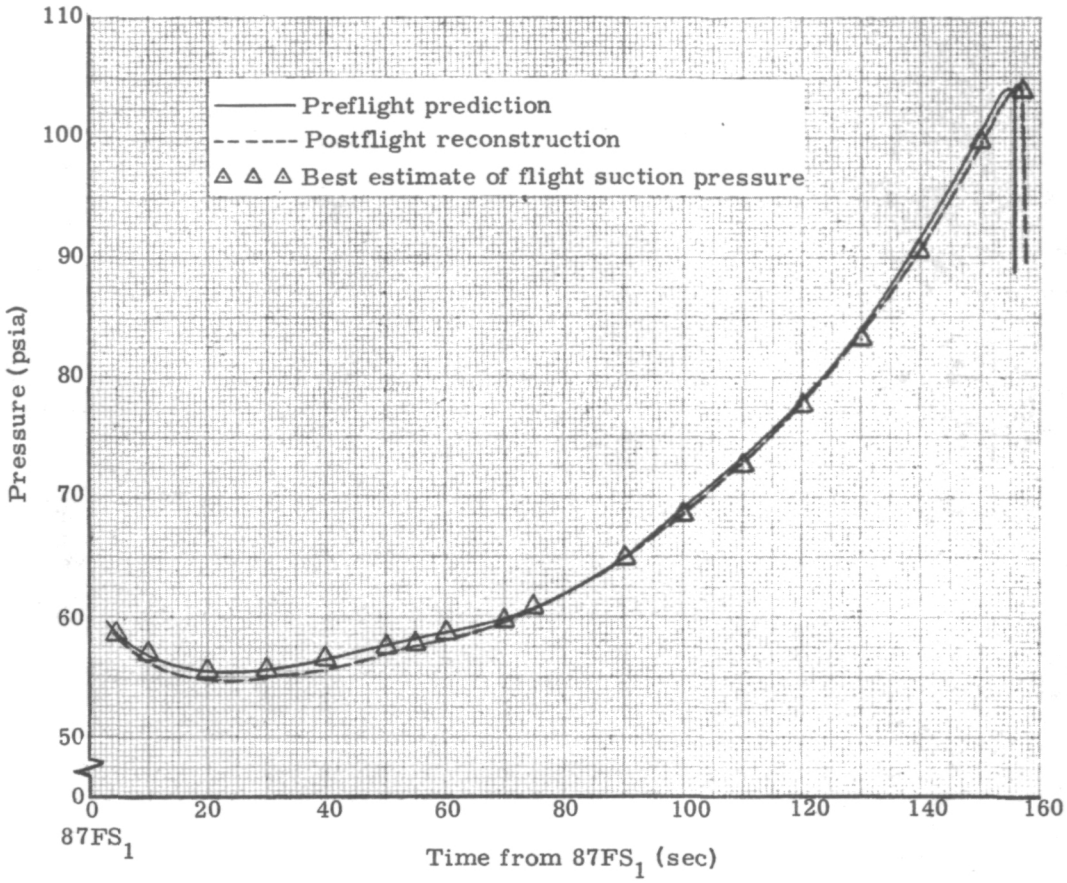

Fig. III-23. Stage I Oxidizer Suction Pressure (Meas 0017)

CONFIDENTIAL

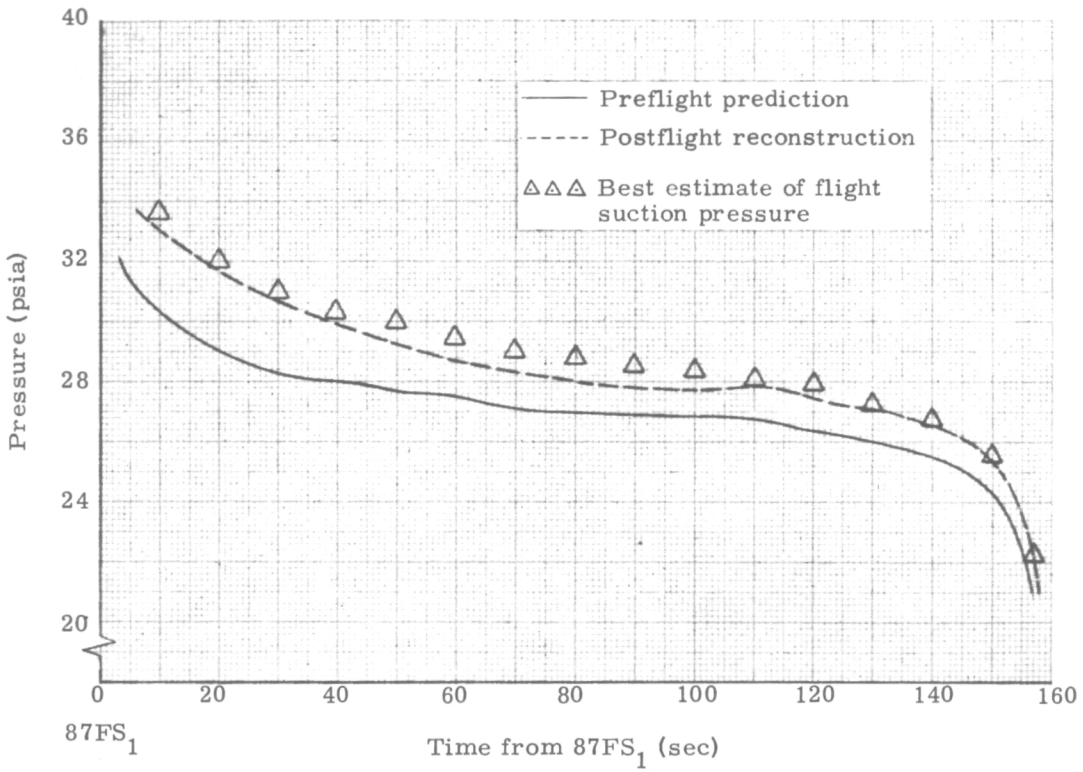

Fig. III-24. Stage I Fuel Suction Pressure (Meas 0014)

CONFIDENTIAL

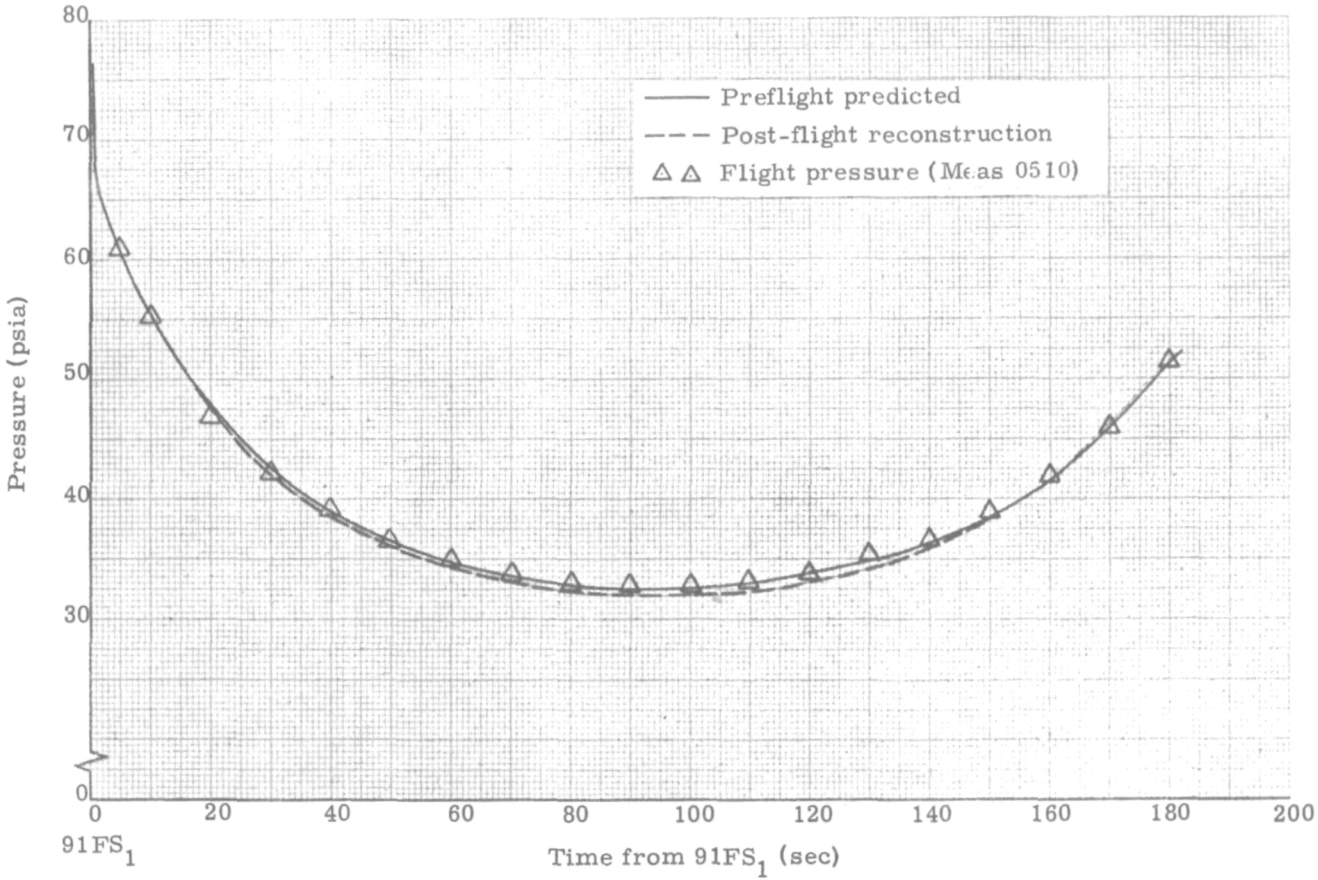

Fig. III-25. Stage II Oxidizer Suction Pressure (Meas 0510)

CONFIDENTIAL

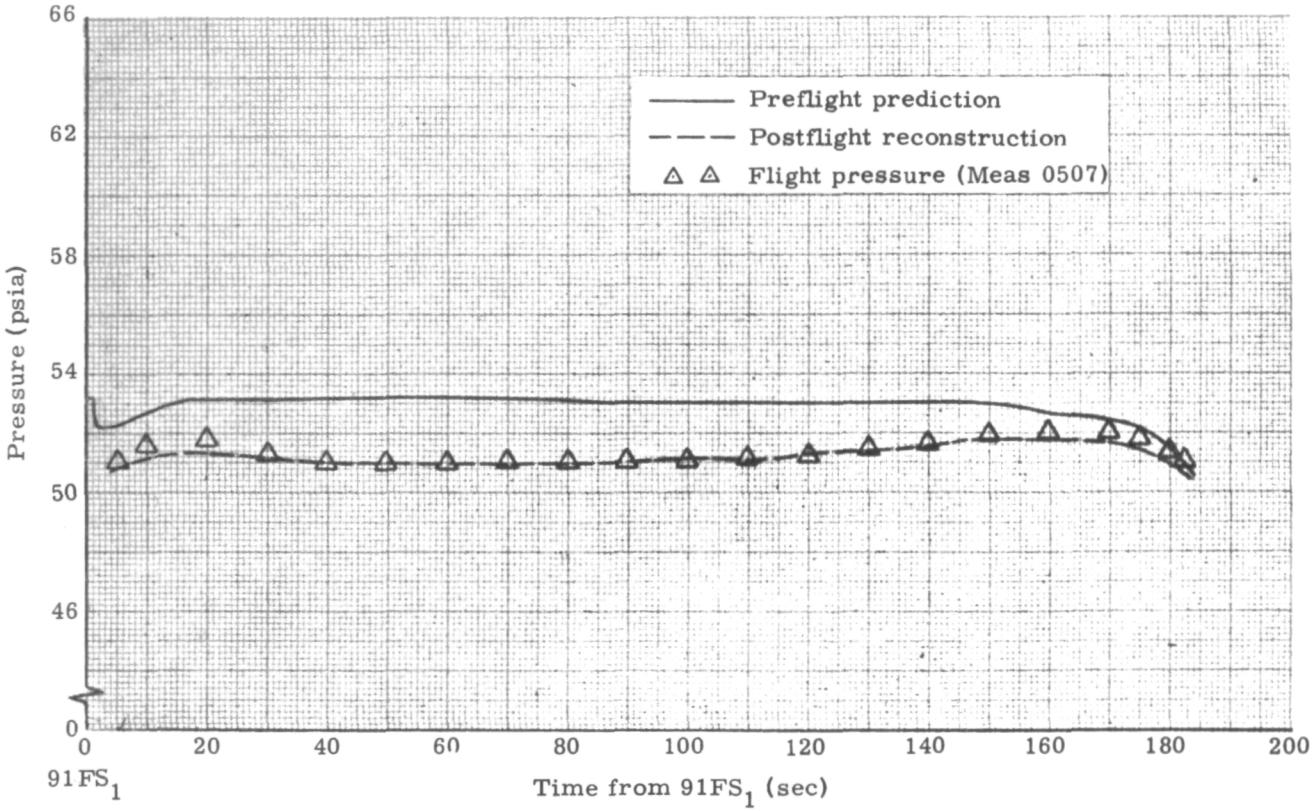

Fig. III-26. Stage II Fuel Suction Pressure (Meas 0507)

CONFIDENTIAL

TABLE III-24

Measured Level Sensor Uncover Times

Meas	Sensor	Uncover Time (GMT)	Average Uncover Time (GMT)	T (sec)	Remarks
0056	Stage I oxidizer high	1641:13.272		Refer to Table III-25	Clean
0058	Stage I oxidizer outage	1643:34.371	1643:34.396		Clean
0059	Stage I oxidizer outage	1643:34.421			Clean
0054	Stage I fuel high	1641:15.372			Clean
0052	Stage I fuel outage	1643:30.471	1643:30.446		Clean
0053	Stage I fuel outage	1643:30.421			Clean
0050	Stage I fuel shutdown	1643:36.221	1643:36.246		Clean
0060	Stage I fuel shutdown	1643:36.271			Clean
0542	Stage II oxidizer high	1644:35.621			Clean
0548	Stage II oxidizer outage	1646:31.522	1646:31.547		Clean
0549	Stage II oxidizer outage	1646:31.572			Clean
0540	Stage II fuel high	1643:54.071			Clean
0546	Stage II fuel outage	1646:35.022	1646:35.072		Clean
0547	Stage II fuel outage	1646:35.122			Clean
0545	Stage II oxidizer shutdown	1646:39.022			Clean
0550	Stage II oxidizer shutdown	1646:39.072			Clean
0544	Stage II fuel shutdown				Did not uncover
0551	Stage II fuel shutdown				Did not uncover

CONFIDENTIAL

TABLE III-25

Best Estimate Average Sensor Uncover Time

Quadrant	Meas	Sensor	Average Uncover Time (GMT)	Δt (sec)
I	0056	Stage I oxidizer high	1641:13.214	141.124
I/IV	0058	Stage I oxidizer outage	1643:34.338	
II/III	0059	Stage I oxidizer outage		
I	0054	Stage I fuel high	1641:15.314	135.074
III	0052	Stage I fuel outage	1643:30.388	
II	0053	Stage I fuel outage		
I	0050	Stage I fuel shutdown	1643:36.188	
III	0060	Stage I fuel shutdown		
IV	0542	Stage II oxidizer high	1644:35.563	115.920
I/IV	0548	Stage II oxidizer outage	1646:31.489	
II/III	0549	Stage II oxidizer outage		
I	0540	Stage II fuel high	1643:54.013	161.001
I	0546	Stage II fuel outage	1646:35.014	
III	0547	Stage II fuel outage		
II	0545	Stage II oxidizer shutdown	1646:38.989	
IV	0550	Stage II oxidizer shutdown		
II	0544	Stage II fuel shutdown	Did not uncover	
IV	0551	Stage II fuel shutdown	Did not uncover	

System	Integrated Average Temperature (between uncoverings) (° F)	Corresponding Density (lb/ft^3)
Stage I oxidizer	42.8	92.170
Stage I fuel	43.4	57.341
Stage II oxidizer	44.1	92.068
Stage II fuel	42.1	57.220

CONFIDENTIAL

4. Propellant Utilization

a. Level sensor uncover

Figures III-27 and III-28 show the predicted, actual and reconstructed level sensor uncover times for Stages I and II. Measured level sensor uncover times are tabulated in Table III-24.

Slosh, as indicated by on and off signals at the time of level sensor uncovering, was minimal on this flight. All sensor uncoverings were clean.

b. Best estimate level sensor uncover times

Table III-25 contains the best estimate average level sensor uncover times for the GT-8 flight. Also shown are the integrated average temperatures between level sensor uncoverings and the corresponding densities. The measured average uncover times shown in Table III-24 were decreased by 0.058 second to allow for the built-in level sensor delay of 0.033 second and for the PCM digital sampling rate of 0.05 second.

Table III-26 contains the level sensor volumes and delta volumes used in the level sensor flow rate analysis. The Stages I and II oxidizer and fuel high level sensor volumes were reconstructed to reflect the volumes which were determined by calibration at Cape Kennedy using the propellant transfer and pressurization system. The Stages I and II outages and shutdown level sensor volumes were calculated using the actual counts of flowmeter pulses during the special loading.

TABLE III-26

Averaged Volumes at Level Sensor Locations

Tank	Sensor	Averaged Volumes (stretch included) (ft^3)	Delta Volumes (ft^3)
Stage I oxidizer	High-level	1710.07	1672.27
	Outage	37.80	
Stage I fuel	High-level	1403.00	1336.98
	Outage	66.02	
Stage II oxidizer	High-level	286.34	263.65
	Outage	22.69	
Stage II fuel	High-level	349.32	331.56
	Outage	17.76	

CONFIDENTIAL

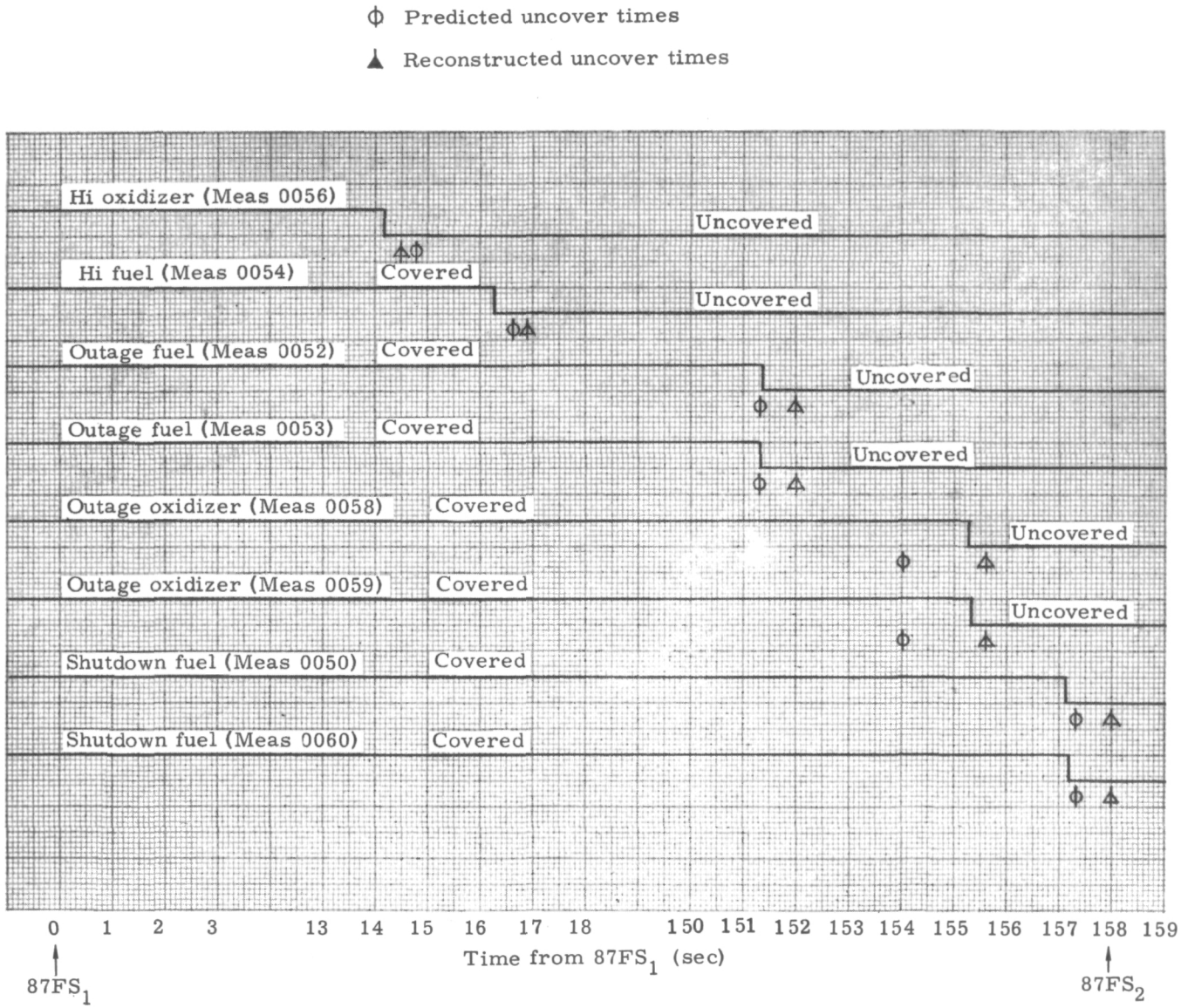

Fig. III-27. Stage I Level Sensor Operation

CONFIDENTIAL

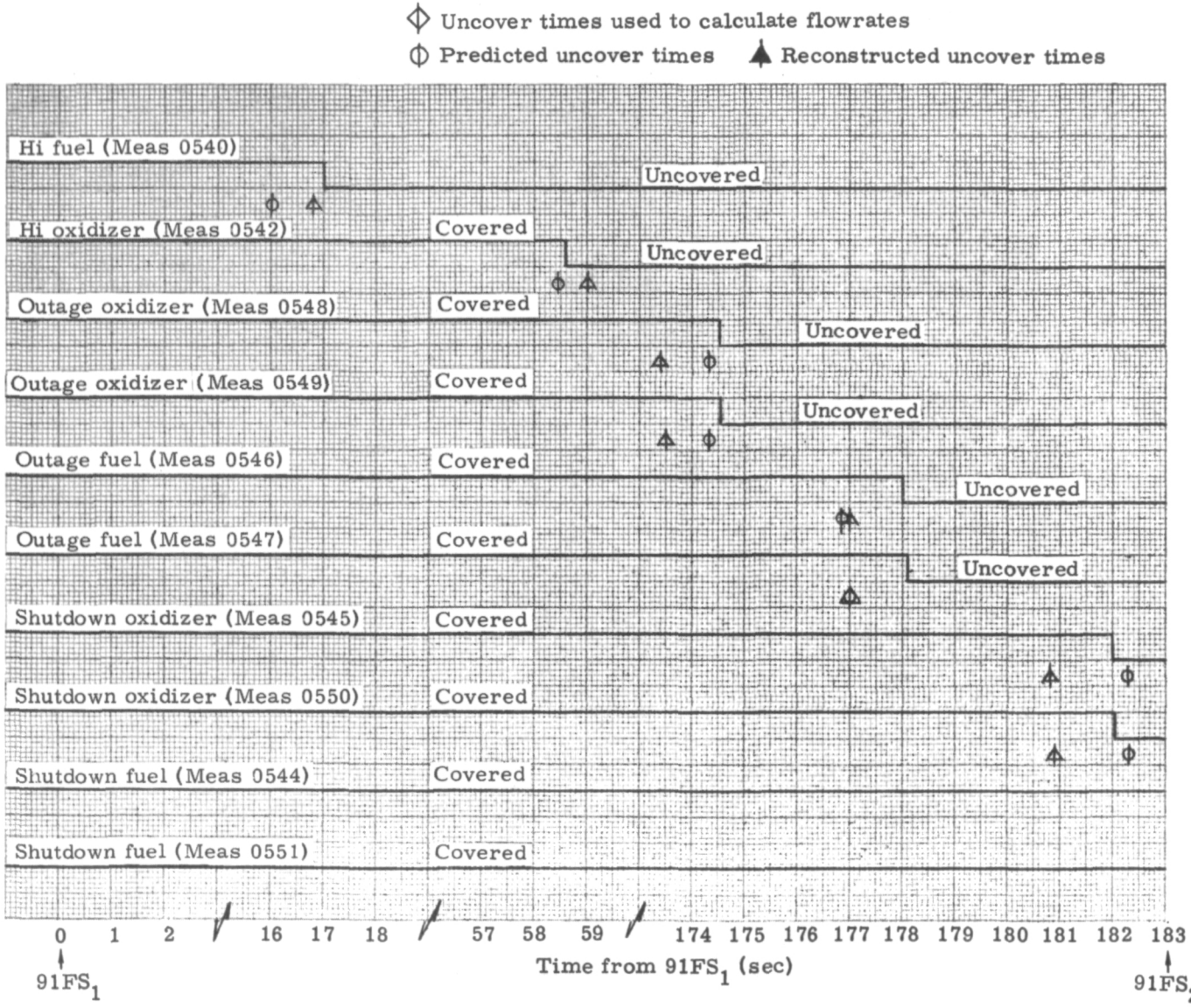

Fig. III-28. Stage II Level Sensor Operation

CONFIDENTIAL

c. Flow rates

Table III-27 presents the predicted and the actual volumetric flow rates between level sensors.

TABLE III-27

Propellant Volumetric Flow Rate

Tank	Predicted (ft^3/sec)	Actual (ft^3/sec)
Stage I oxidizer	10.529	11.850
Stage I fuel	10.067	9.898
Stage II oxidizer	2.097	2.274
Stage II fuel	2.115	2.059

d. Mixture ratio

Table III-28 shows the Stages I and II predicted and actual in-flight average engine mixture ratios for GLV-8.

TABLE III-28

Engine Mixture Ratio

System	Mixture Ratio	
	Predicted	Actual
Stage I	1.9443	1.9290
Stage II	1.7680	1.7901

Sensitivity coefficients applied to the delta between the predicted and actual variations in average suction pressure and temperature between sensor uncoverings yield the information shown in Table III-29.

TABLE III-29

Mixture Ratio Pressure and Temperature

System	ΔPressure (psi)	ΔMixture Ratio (press.)	ΔTemperature (° F)	ΔMixture Ratio (temp)	ΔMixture Ratio (total)
Stage I					
Oxidizer	0.0	-0.0	-1.3	+0.003013	+0.003013
Fuel	+1.8	-0.006336	-0.7	-0.001139	-0.007475
Total Stage I		-0.006336		+0.001874	-0.004462

CONFIDENTIAL

TABLE III-29 (continued)

System	ΔPressure (psi)	ΔMixture Ratio (press.)	ΔTemperature (° F)	ΔMixture Ratio (temp)	ΔMixture Ratio (total)
Stage II					
Oxidizer	0.0	+0.0	-2.0	+0.005230	+0.005230
Fuel	-2.0	+0.008850	+1.9	+0.003162	+0.012012
Total Stage II		+0.008850		+0.008392	+0.017242

By applying the delta mixture ratio (total) shown in Table III-29 to the predicted (F-45 day) between-sensors mixture ratios, the run-to-run variation can be calculated. The mixture ratio deviation along with the allowable run-to-run dispersions is shown in Table III-30.

TABLE III-30

Mixture Ratio Deviation

System	Predicted Mixture Ratio*	Actual Mixture Ratio	Deviation (%)	Allowable Run-to-Run Dispersion (%)
Stage I	1.9398	1.9290	-0.56	±1.38
Stage II	1.7852	1.7901	+0.27	±2.28

*Corrected for pressure and temperature variations.

e. Outage and trapped propellant

Table III-31 shows the mean and maximum (99%) outages predicted for GLV-8. Also shown are the actual outages as calculated using the information contained in the reconstructed propellant inventories of Tables III-37 and III-38.

TABLE III-31

Outage Prediction

System	Predicted (F-45 day)		Predicted (F-0 day)		
	Mean	Max (99%)	Mean	Max (99%)	Actual
Stage I	0.220% 566 lb	0.643% 1652 lb	0.315% 810 lb	0.744% 1910 lb	0.098% oxidizer 252 lb

CONFIDENTIAL

TABLE III-31 (continued)

System	Predicted (F-45 day)		Predicted (F-0 day)		
	Mean	Max (99%)	Mean	Max (99%)	Actual
Stage II	0.344% 206 lb	1.026% 615 lb	0.517% 310 lb	1.217% 730 lb	0.436% fuel 261 lb

All outages are presented as percent of total steady-state propellants (taken from Ref. 11) and in pounds. The values used for total steady-state propellants are: 256,737 pounds for Stage I and 59,966 pounds for Stage II.

The trapped propellants for Stages I and II are given in Table III-32.

TABLE III-32

Trapped Propellants

System	Oxidizer (lb)	Fuel (lb)
Stage I		
Above interface	0	20
Below interface	235	309
Stage II		
Above interface	0	0
Below interface	20	14

f. Start and propellant consumptions

The predicted and actual propellant consumptions during the Stage I start period are shown in Table III-33.

TABLE III-33

Stage I Ignition and Propellant Consumption

Stage I	Oxidizer (lb)		Fuel (lb)	
	Predicted	Actual	Predicted	Actual
Start consumption ($87FS_1$ to TCPS)	209	209	44	44
Holddown consumption (TCPS to liftoff)	2157	2218	1128	1184

CONFIDENTIAL

The predicted and actual start consumptions listed in Table III-33 were selected from Ref. 15 and were modified to allow for the difference between propellant out of the tanks (as listed in the report) and propellant overboard. The predicted holddown consumption was derived from the engine analytical model and previous flight test data, while the actual value was derived from the Post-test Rocket Engine System Total Operation (PRESTO) engine performance reconstruction program.

The Stage II propellant consumptions between $91FS_1$ and $91FS_1$ + 1.2 seconds are listed in Table III-34.

TABLE III-34

Stage II Start Propellant Consumption

	Oxidizer (lb)	Fuel (lb)
Start consumption ($91FS_1$ to $91FS_1$ + 1.2 sec)	135	53

The consumptions were obtained from Ref. 15 and modified as on the Stage I start consumption.

g. Vapor retained

The predicted and actual values of vapor retained in the tanks as a result of pressurization gases and propellant vaporization during flight are shown in Table III-35.

TABLE III-35

Pressurization Gas Inventory

System	Oxidizer (lb)		Fuel (lb)	
	Predicted	Actual*	Predicted	Actual*
Stage I				
Vapor retained:				
Oxidizer tank	318	322	0	0
Fuel tank	8	8	90	91
Vaporized	6	6	0	0
Stage II				
Pressurization				
Fuel tank	5	4	50	49
Vaporization				
Oxidizer tank	9	9	-	-

*Actual values were obtained from reconstructed flight pressure profile of pressurization computer program runs.

CONFIDENTIAL

h. Shutdown

Stage I shutdown was due to fuel exhaustion. The predicted and actual values for the propellants consumed during shutdown are presented in Table III-35. The actual values were obtained by integrating a curve (derived from PRESTO) of flight flow rate versus time after $87FS_2$.

Stage II shutdown was initiated by a guidance command; therefore, the propellants were not exhausted as in Stage I. The predicted and actual values for the propellants consumed during shutdown are shown in Table III-36. The actual values were computed using altitude shutdown impulse data.

TABLE III-36

Propellant Shutdown Consumption

	Oxidizer (lb)		Fuel (lb)	
	Predicted	Actual	Predicted	Actual
Stage I	446	312	27	41
Stage II	76	76	60	60

i. Propellant inventory

The reconstructed propellant inventories for GT-8 are shown in Tables III-37 and III-38 for Stages I and II, respectively. The inventory consists of both nonusable and usable propellants. The burning time margin for Stage II was 1.327 seconds.

5. Components

a. Prevalves

During the launch countdown, all prevalve functions were performed without incident. Prevalves installed for the flight are identified in Table III-39.

CONFIDENTIAL

TABLE III-37

GLV-8 Stage I Reconstructed Propellant Loading

Predicted in-flight engine mixture ratio			1.9443 ± 1.54%
Average in-flight mixture ratio (engine)			1.9290 ± 1.71%
Outage (percent of total usable propellants)			0.098%
	Oxidizer (lb)	Fuel (lb)	Total (lb)
Nonusable propellants			
A. Fuel bleed	0	23	23
B. Start consumption ($87FS_1$ to TCPS)	209	45	254
C. Holddown (TCPS to liftoff (-2 sec))	2,218	1,184	
D. Trapped above interface at shutdown	0	20	20
E. Trapped below interface at shutdown	235	309	544
F. Vapor retained at shutdown			
1. For pressurization			
a. Oxidizer tank	317		317
b. Fuel tank	8	92	100
2. Vaporized	6		6
G. Total nonusable	2,993	1,673	4,666
Usable propellants			
A. Steady-state overboard (liftoff to $87FS_2$)	168,799	87,585	256,384
B. Shutdown transient (FS_2 to 0% thrust)	312	41	353
C. Outage	252		252
D. Total usable	169,363	87,626	256,989
Total propellant loaded	172,356	89,299	261,655
Propellant load at liftoff	169,929	88,047	257,976
Weight of initial pressurizing gas			
A. Fuel tank (N_2)			11
B. Oxidizer tank ($N_2 + NO_2$)			17

TABLE III-38

GLV-8 Stage II Reconstructed Propellant Loading

Predicted in-flight engine mixture ratio			1.7680 ± 2.52%
Average in-flight mixture ratio (engine)			1.7901 ± 1.55%
Outage (percent of total usable propellants)			±0.436%
Burning time margin			1.327 sec
	Oxidizer (lb)	Fuel (lb)	Total (lb)
Nonusable propellants			
A. Fuel bleed	0	11	11
B. Trapped above interface at FS_2 + 20 sec (0% thrust)	0	0	0
C. Trapped below interface at FS_2 + 20 sec (0% thrust)	20	14	34
D. Vapor retained after FS_2			
1. Pressurization (fuel tank)	4	49	53
2. Vaporization (oxidizer tank)	9		9
E. Total nonusable	33	74	107
Usable propellants			
A. Start consumption (FS_1 to 90% thrust)	135	54	189
B. Steady-state overboard (90% thrust to FS_2)	38,154	21,268	59,422
C. Shutdown consumption (FS_2 to 0% thrust)	76	60	136
D. Steady-state residuals (after FS_2)			
1. Burning time margin	281	156	437
2. Outage		261	261
E. Total usable	38,646	21,799	60,445
Total propellants loaded	38,679	21,873	60,552
Weight of initial pressurizing gas			
A. Fuel tank (N_2)			5
B. Oxidizer tank (N_2 + NO_2)			31

TABLE III-39

Prevalve Identification

Description	Part No.	Serial No.
Stage I oxidizer S/A 1 (fill and drain)	PS47510007-139	0700025
Stage I oxidizer S/A 2 (drain)	PS47510007-159	0700029
Stage II oxidizer S/A 3 (fill and drain)	PS47510005-199	0600022
Stage I fuel S/A 1 (fill and drain)	PS47510005-159	0600023
Stage I fuel S/A 2 (drain)	PS47510005-169	0600099
Stage II fuel S/A 3 (fill and drain)	PS47510006-059	0400013

b. Level sensors

GLV-8 incorporated 18 Bendix optical type propellant level sensors. These are identified in Table III-40. All sensors performed satisfactorily during propellant loadings and in flight.

c. Oxidizer standpipe

The oxidizer suction line standpipes were charged with the remote charge system at T-59 minutes. No problems were encountered during the charging operation. Flight data obtained from pressure Meas 0033 and 0034, located in the standpipes, show surge chamber performance to be normal and consistent with the low longitudinal oscillatory levels experienced on this flight.

d. Fuel accumulators

Accumulator piston response on this flight was similar to that of other flights utilizing the same configuration (GLV-3 through GLV-6). This response is presented in Fig. III-29.

Dynamic friction levels for dry accumulators were measured prior to installation of accumulator assemblies at Martin-Baltimore and again prior to flight at ETR. A summary of these friction measurements is presented in Table III-41 as peak-to-peak values (twice the equivalent friction force in one direction).

CONFIDENTIAL

TABLE III-40

GLV-8 Propellant Level Sensor Identification

Location	Stage I					Stage II				
	Meas	Quadrant	Volume* (ft)	Configuration	Serial No.	Meas	Quadrant	Volume* (ft^3)	Configuration	Serial No.
Oxidizer tank										
High level	0056	I	1710.07	-039	000488	0542	IV	286.34	039	000478
Outage	0058	I/IV	37.82	-039	000354	0548	I/IV	22.72	-039	000494
Outage	0059	II/III	37.77	-039	000486	0549	II/III	22.65	-039	000484
Shutdown	--	--		--	--	0545	II	5.05	-039	000485
Shutdown	--	--		--	--	0550	IV	5.18	-039	000483
Fuel tank										
High level	0054	I	1403.00	-059	000479	0540	I	349.32	-049	000318
Outage	0052	III	66.03	-049	000317	0546	I	17.52	-049	000468
Outage	0053	I	66.03	-049	000480	0547	III	18.00	-049	000481
Shutdown	0050	I	8.03	-049	000487	0544	II	2.32	-049	000464
Shutdown	0060	III	7.63	-049	000306	0551	IV	2.34	-059	000495

*Volume to interface including tank stretch at uncover time.

CONFIDENTIAL

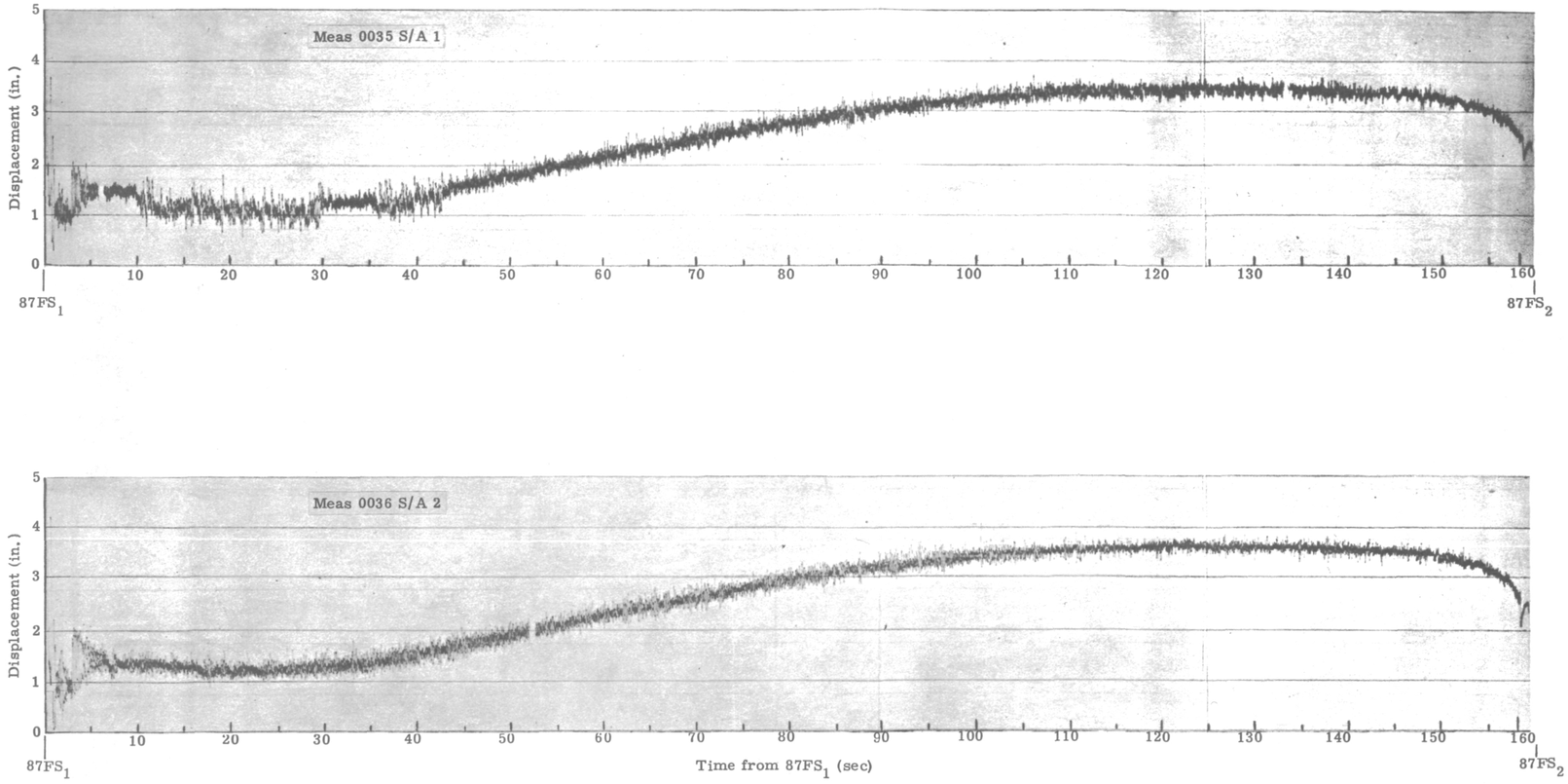

Fig. III-29. Fuel Accumulator Piston Travel

CONFIDENTIAL

TABLE III-41

Dynamic Friction Levels for Dry Accumulators

S/A	Serial	Peak-to-Peak Friction* (psi)	
		Bench	Preflight
1	B019	0.8	0.6
2	B018	1.2	0.6

*Maximum acceptable value = 2.0 psi

Observed flight data do not indicate significant differences in friction levels between accumulators.

6. POGO Performance

Flight data indicate no significant structural responses in propulsion measurements. At BECO-3 seconds, the oxidizer suction pressure (Meas 0017) and oxidizer standpipe pressure (Meas 0033 and 0034) show a response at the structural frequency. This response was observed on previous flights and is predictable analytically. This flight was slightly different only in that amplitudes of the oxidizer feed system pressures were no greater at pre-BECO than at other times of Stage I flight.

Additional details on POGO will be found in Chapter XII.

C. PRESSURIZATION SUBSYSTEM

1. Prelaunch Pressurization

At approximately T-185 minutes, all four propellant tanks were pressurized, through AGE, from blanket pressure level to flight pressure levels. The resultant time-pressure profiles (Fig. III-30) indicate that the process was normal. The tank ullage lockup pressures obtained from landline measurements made at T-0 and the related normal operating pressure ranges are presented in Table III-42.

CONFIDENTIAL

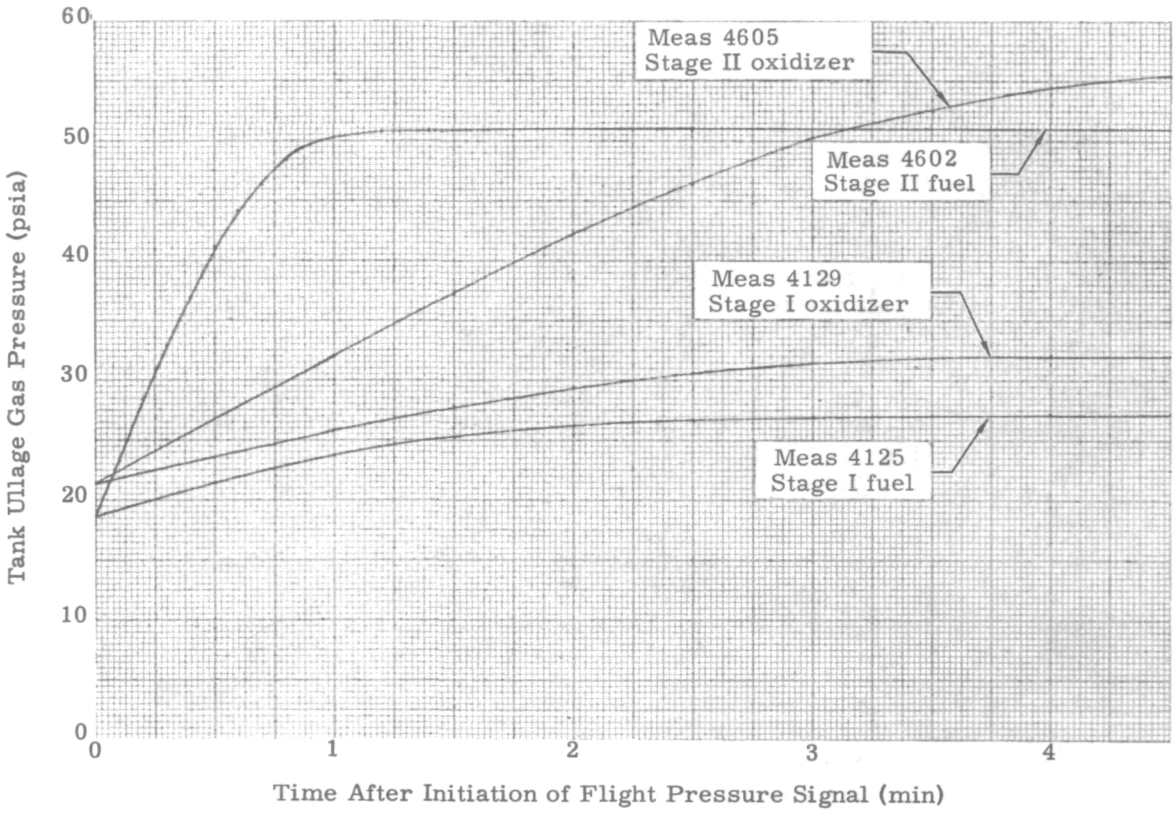

Fig. III-30. Tank Pressurization Cycle (blanket to flight pressure)

CONFIDENTIAL

TABLE III-42

Tank Ullage Lockup Pressures

Meas	Parameter	Normal Range (psia)	Measured (psia)
4125	Stage I fuel tank	27.5 to 31.5	29.7
4129	Stage I oxidizer tank	30.5 to 34.5	32.0
4602	Stage II fuel tank	49.5 to 54.5	51.7
4605	Stage II oxidizer tank	53.5 to 57.5	56.2

2. Flight Pressurization

Stages I and II ullage gas pressure time histories appear in Figs. III-31 through III-34. These plots show flight-measured pressures, preflight predicted pressures and postflight reconstructed pressures. The flight-measured pressures were obtained by averaging the telemetered output from each pair of pressure transducers in the individual tanks; the preflight predicted curves were taken from Ref. 11; and the postflight reconstruction was based on flight measured values of engine performance, propellant temperatures and propellant loadings. A comparison of significant pressurization system parameters taken at FS_1 + 100 seconds is shown in Table III-43.

TABLE III-43

Comparison of Significant Pressurization System Parameters at FS_1 + 100 Seconds

	Preflight Predicted	Flight Data	Postflight Reconstructed
Stage I Fuel Tank (1)			
Tank pressure, P_{FT} (psia)	21.9	22.72	22.7
Nozzle inlet temp, T_{FPOI} (° F)	213.0	--	212.9 (2)
Flow ratio, W_{FP}/Q_{FS} (lb/ft^3)	0.0638	--	0.0653
Stage I Oxidizer Tank (3)			
Tank pressure, P_{OT} (psia)	18.4	17.68	16.5
Orifice inlet specific enthalpy, H_{OPOI} (Btu/lb)	336.4	--	332.6 (2)
Flow ratio, W_{OP}/Q_{OS}, (lb/ft^3)	0.1704	--	0.1729

CONFIDENTIAL

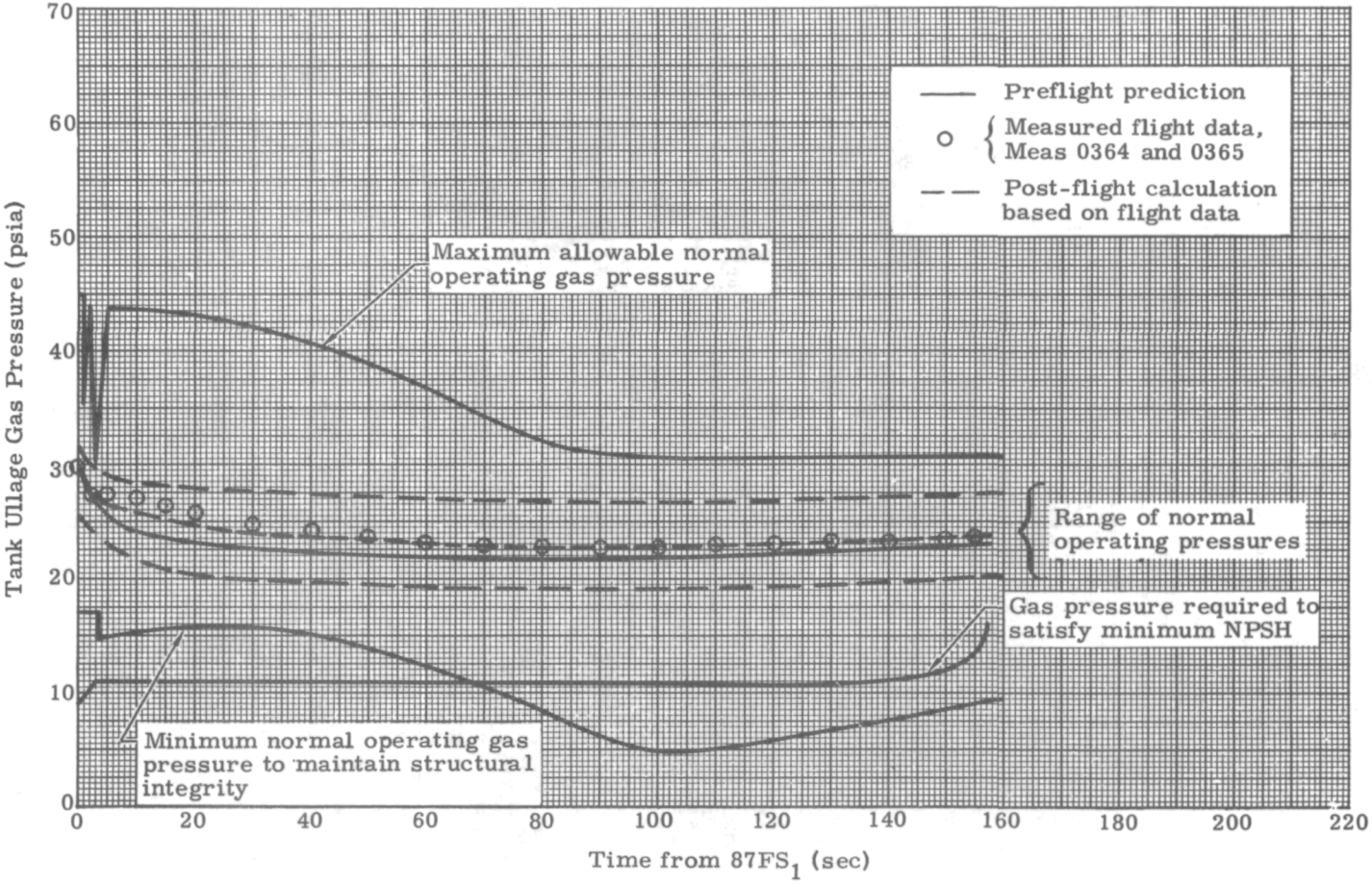

Fig. III-31. Stage I Fuel Tank Ullage Pressure History

CONFIDENTIAL

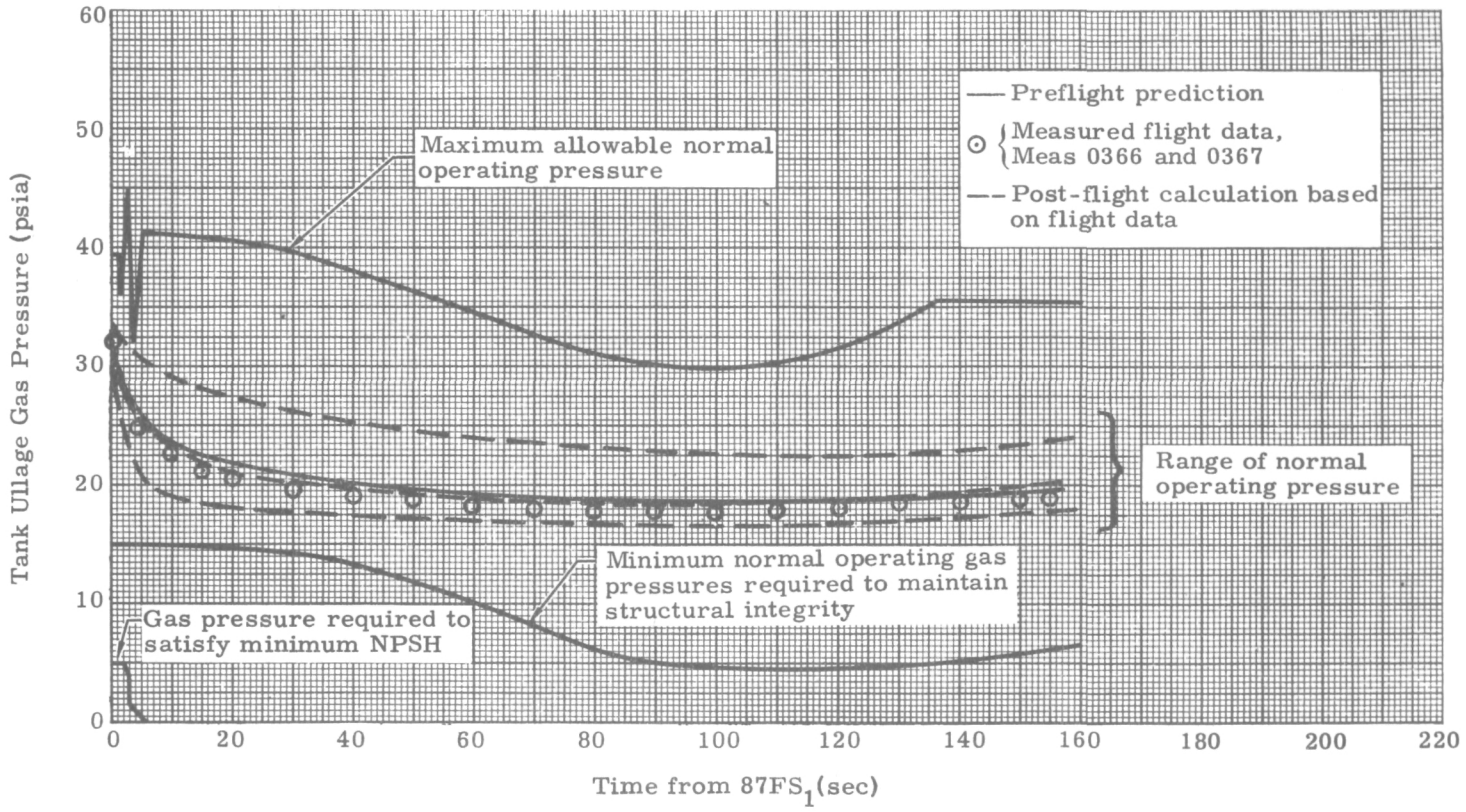

Fig. III-32. Stage I Oxidizer Tank Ullage Pressure History

CONFIDENTIAL

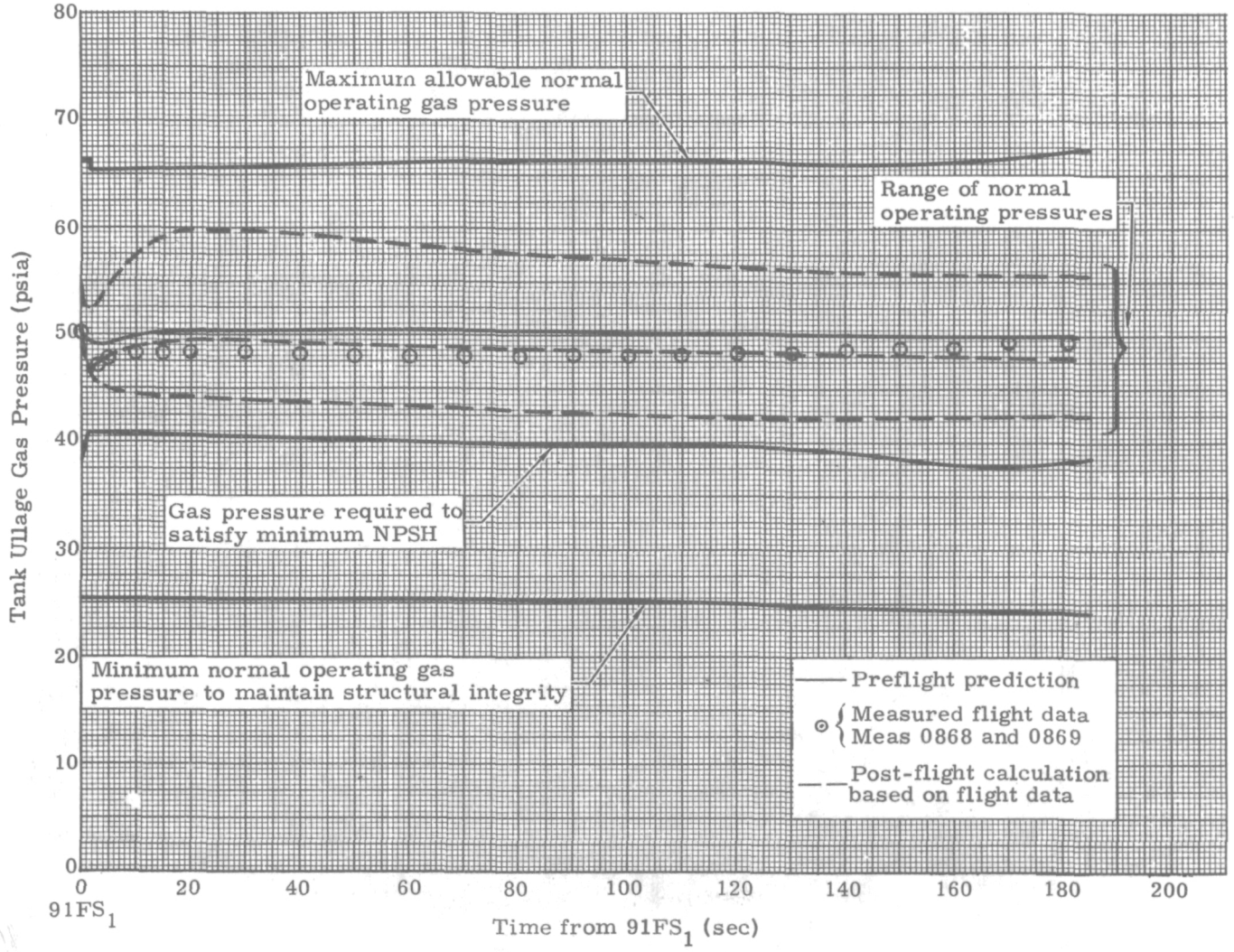

Fig. III-33. Stage II Fuel Tank Ullage Pressure History

CONFIDENTIAL

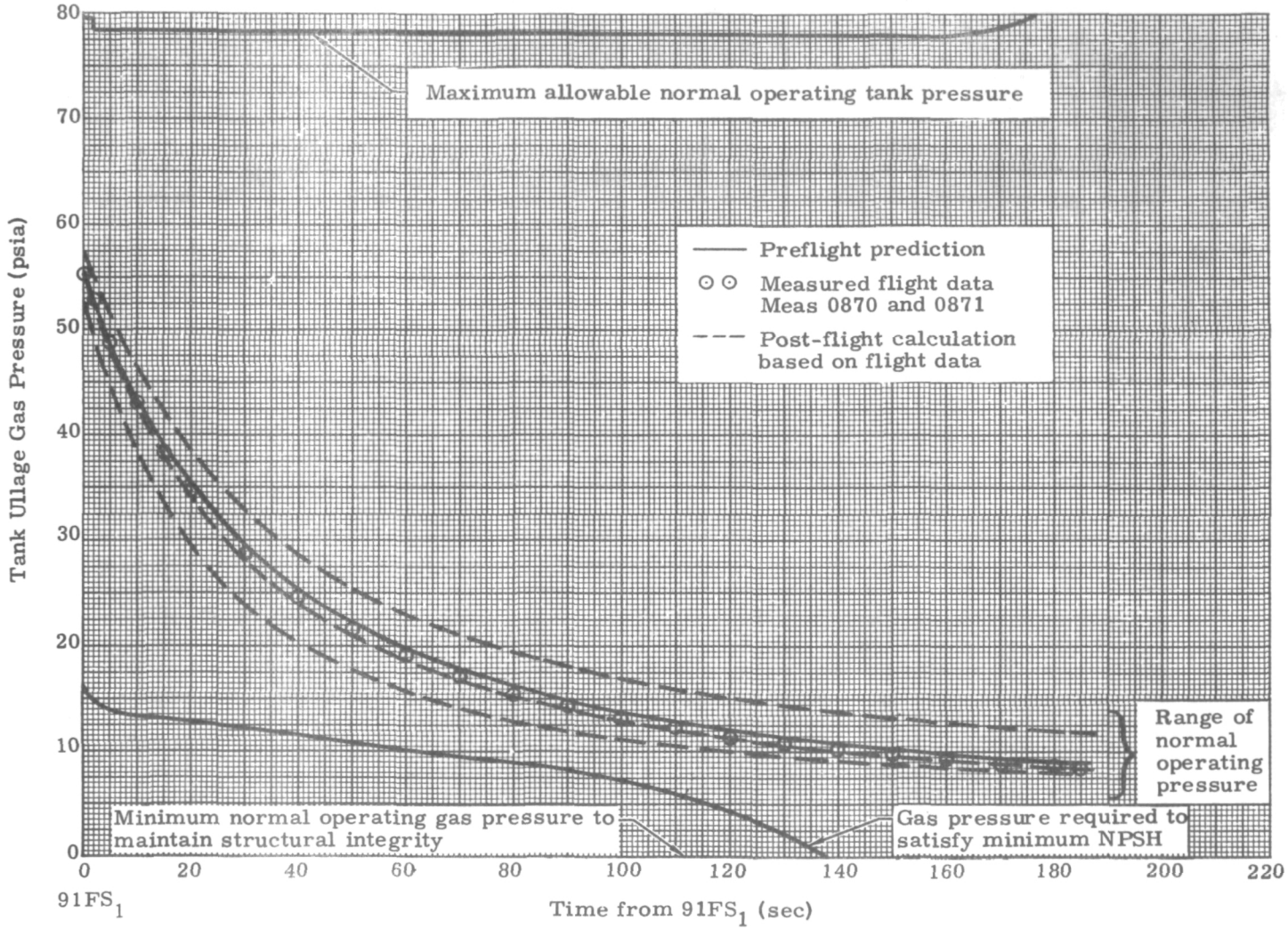

Fig. III-34. Stage II Oxidizer Tank Ullage Pressure History

CONFIDENTIAL

TABLE III-43 (continued)

	Preflight Predicted	Flight Data	Postflight Reconstructed
Stage II Fuel Tank④			
Tank pressure P_{FT} (psia)	50.4	48.14	48.5
Nozzle inlet temp T_{FPOI} (° F)	227.3	--	227.3②
Flow ratio, W_{FP}/Q_{FS} (lb/ft^3)	0.1458	--	0.1428
Stage II Oxidizer Tank			
Tank pressure, P_{OT} (psia)	13.7	13.29	13.2
Propellant flow rate, Q_{OS} (ft^3/sec)	2.2643	--	2.2706

①Nozzle diameter, FPN Stage I fuel--0.490 in.

②Estimated, temperature not instrumented.

③Flow control venturi coefficient--0.0509.

④Nozzle diameter, FPN Stage II fuel--0.260 in.

Figures III-35, III-36 and III-37 present the preflight-predicted and the in-flight-estimated pressurization gas characteristics at the orifice or nozzle inlet.

3. Component Performance

All tank pressure sensors functioned normally. The maximum and mean pressure differences between pairs of sensors in each of the individual propellant tanks are shown in Table III-44.

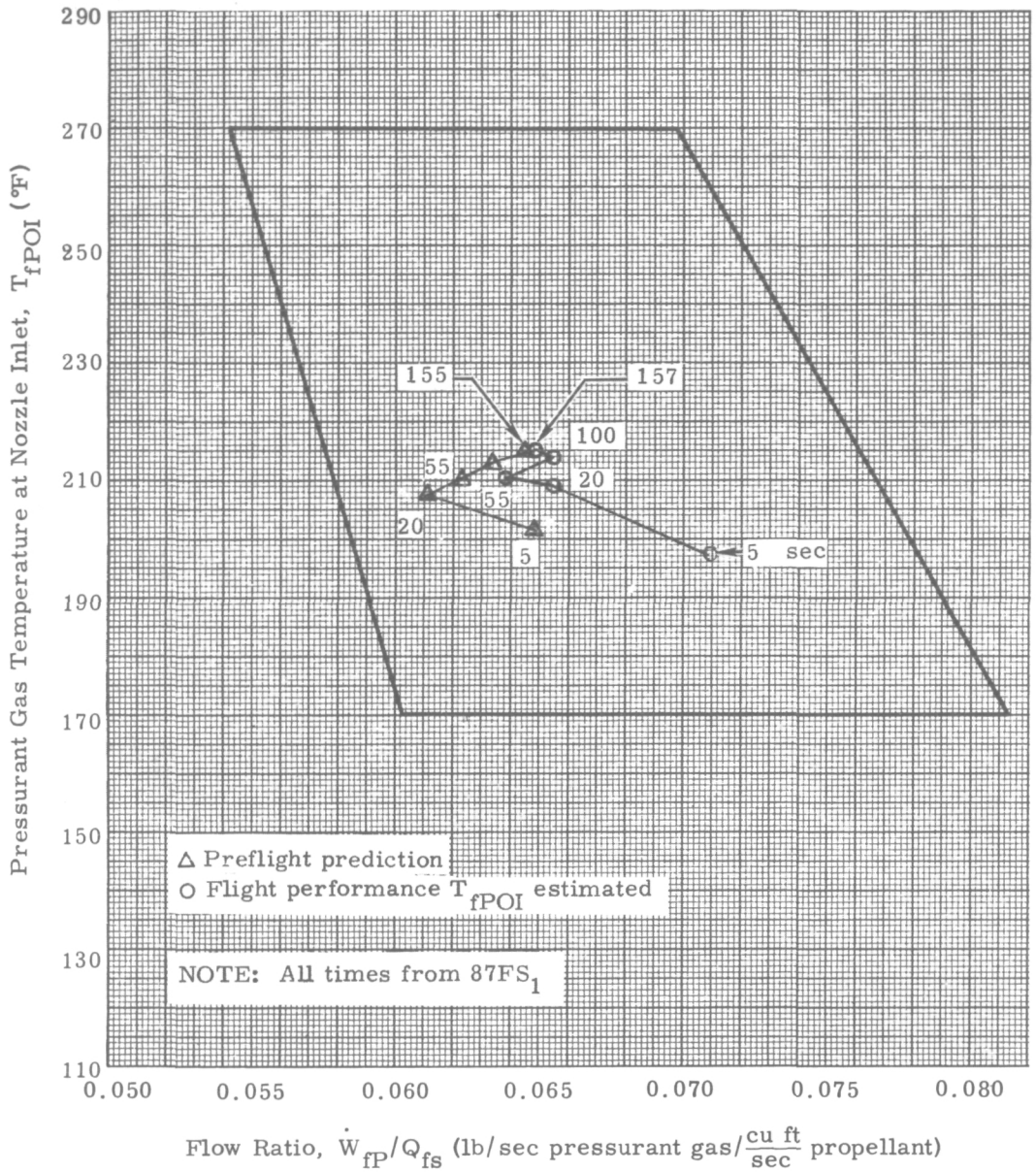

Fig. III-35. Stage I Fuel Tank Pressurant Performance

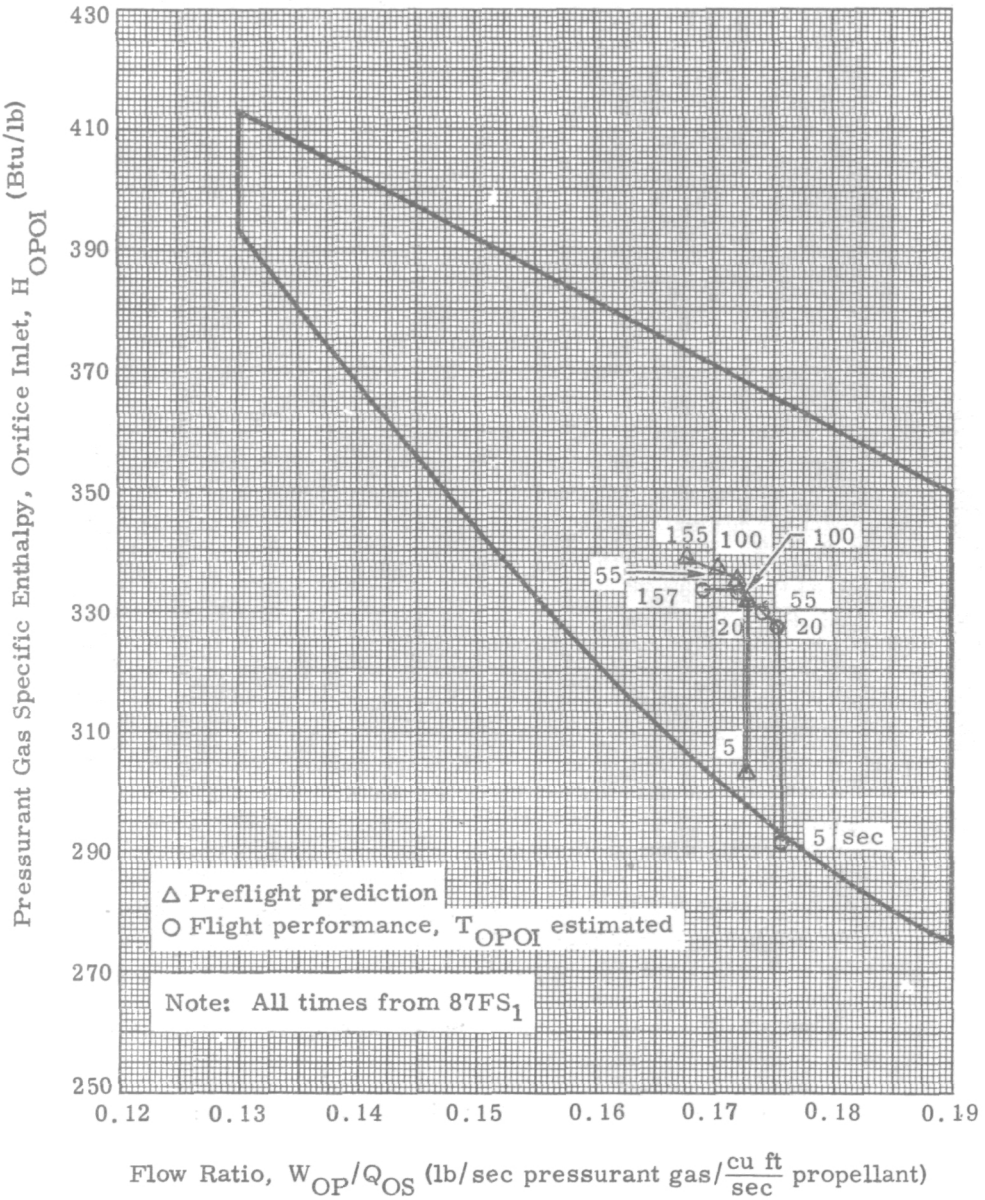

Fig. III-36. Stage I Oxidizer Tank Pressurant Performance

CONFIDENTIAL

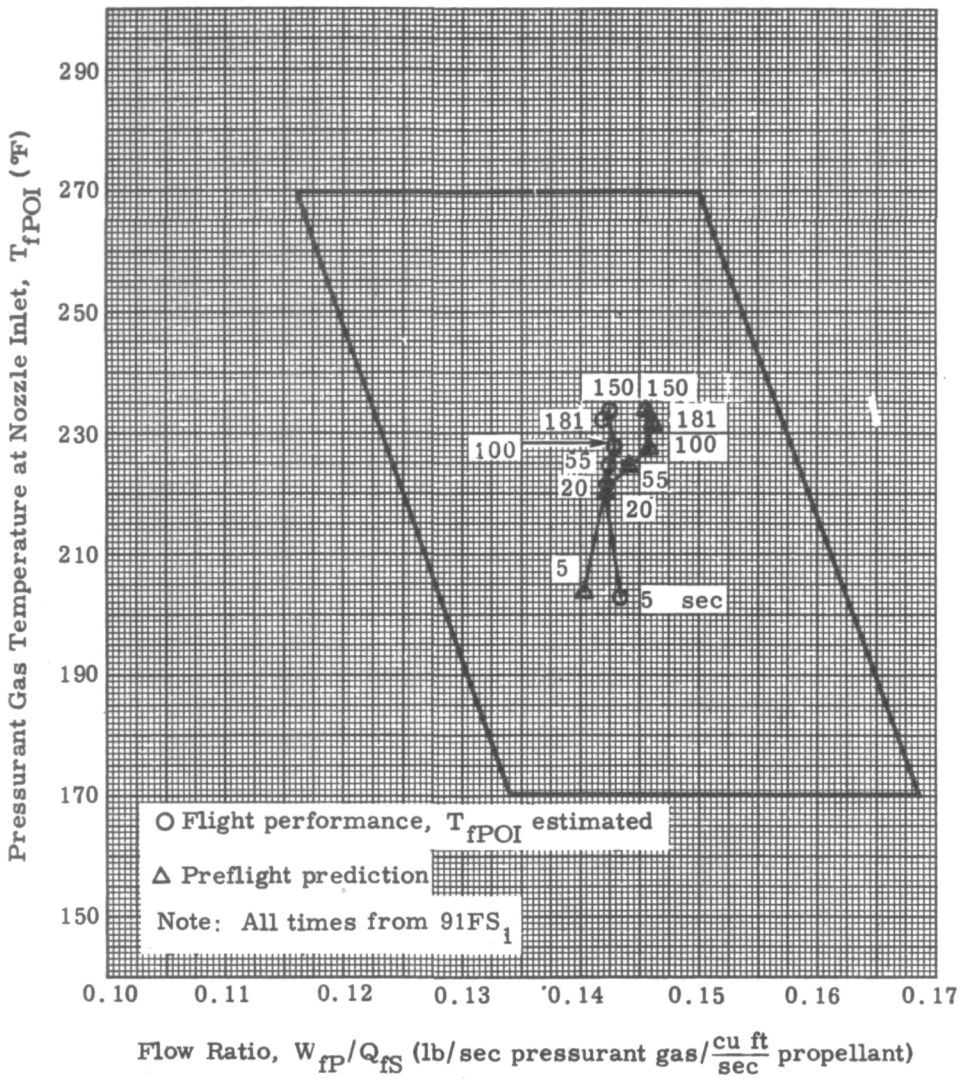

Fig. III-37. Stage II Fuel Tank Pressurant Performance

CONFIDENTIAL

TABLE III-44

Pressure Difference Between Tank Pressure Transducer Pairs

Tank	Maximum Difference (psi)	Mean Difference (psi)	Maximum Allowable Difference (psi)
Stage I oxidizer	0.32	0.16	1.50
Stage I fuel	0.28	0.10	1.50
Stage II oxidizer	0.78	0.36	2.25
Stage II fuel	0.42	0.14	2.25

D. ENVIRONMENTAL CONTROL

Launch vehicle air-conditioning system. This system, which serves launch vehicle Compartment 2 and all engine start cartridges, was operative continuously during the prelaunch activities until vehicle liftoff. The system operated satisfactorily. Table III-45 presents a summary of the system parameters.

TABLE III-45

Air-Conditioning System Performance Summary

Meas	Description	Observed Range	Specified Range	Remarks
4403	GLV supply air temperature	48° to 55° F	48° to 56° F (Compartment 2), 48° to 58° F (engine start cartridges)	Temperature of air supplied to GLV Compartment 2 and the engine start cartridges
4405	Compartment 2 supply air mass flow rate	Approximately 99.8 lb/min	82 lb/min (minimum)	
4418	Compartment 2 exhaust air temperature	57° to 61° F (61° F at liftoff)	40° to 75° F	Manual hold parameter
4045	Start cartridge temperature S/A 1	51.5° F (at liftoff)	35° to 80° F	S/N 0000487 manual hold parameter
4046	Start cartridge temperature S/A 2	53.5° F (at liftoff)	35° to 80° F	S/N 0000801 manual hold parameter
4612	Start cartridge temperature S/A 3	57° F (at liftoff)	36° to 88° F	S/N 0859182 manual hold parameter

IV. FLIGHT CONTROL SYSTEM

Analysis of the GT-8 flight control system (FCS) measured parameters indicated proper system operation during both Stages I and II flight. The primary FCS was in command throughout, and no switchover to the secondary system was required.

A. STAGE I FLIGHT

1. Ignition and Liftoff Transients

Peak actuator travels and rate gyro disturbances recorded during the ignition and holddown period are presented in Table IV-1.

TABLE IV-1

Transients During Stage I Holddown Period

Actuator Designation	Maximum During Ignition		Maximum During Holddown Null Check (in.)
	Travel (in.)	Time from LO (sec)	
Pitch, 1_1	-0.120	-2.52	±0.01
Yaw/roll, 2_1	+0.250	-2.47	+0.01
Yaw/roll, 3_1	+0.275	-2.47	+0.01
Pitch, 4_1	-0.060	-2.52	±0.01
Axis	Maximum Rate, Stage I (deg/sec)		Maximum Rate, Stage II (deg/sec)
Pitch	±0.3		-0.3
Yaw	±0.2		+0.3
Roll	±0.3		--

The combination of thrust and engine misalignments at full thrust initiated a roll transient at liftoff. To correct this offset, the response of the FCS, Shown in Fig. IV-1, kept the roll rate to a maximum of 2.4 deg/sec clockwise (CW) at 0.03 second after liftoff. The roll rate oscillation basic frequency of 5.7 rad/sec damped out in 1.8 seconds. After the initial transient, the FCS responded to three extraneous disturbances

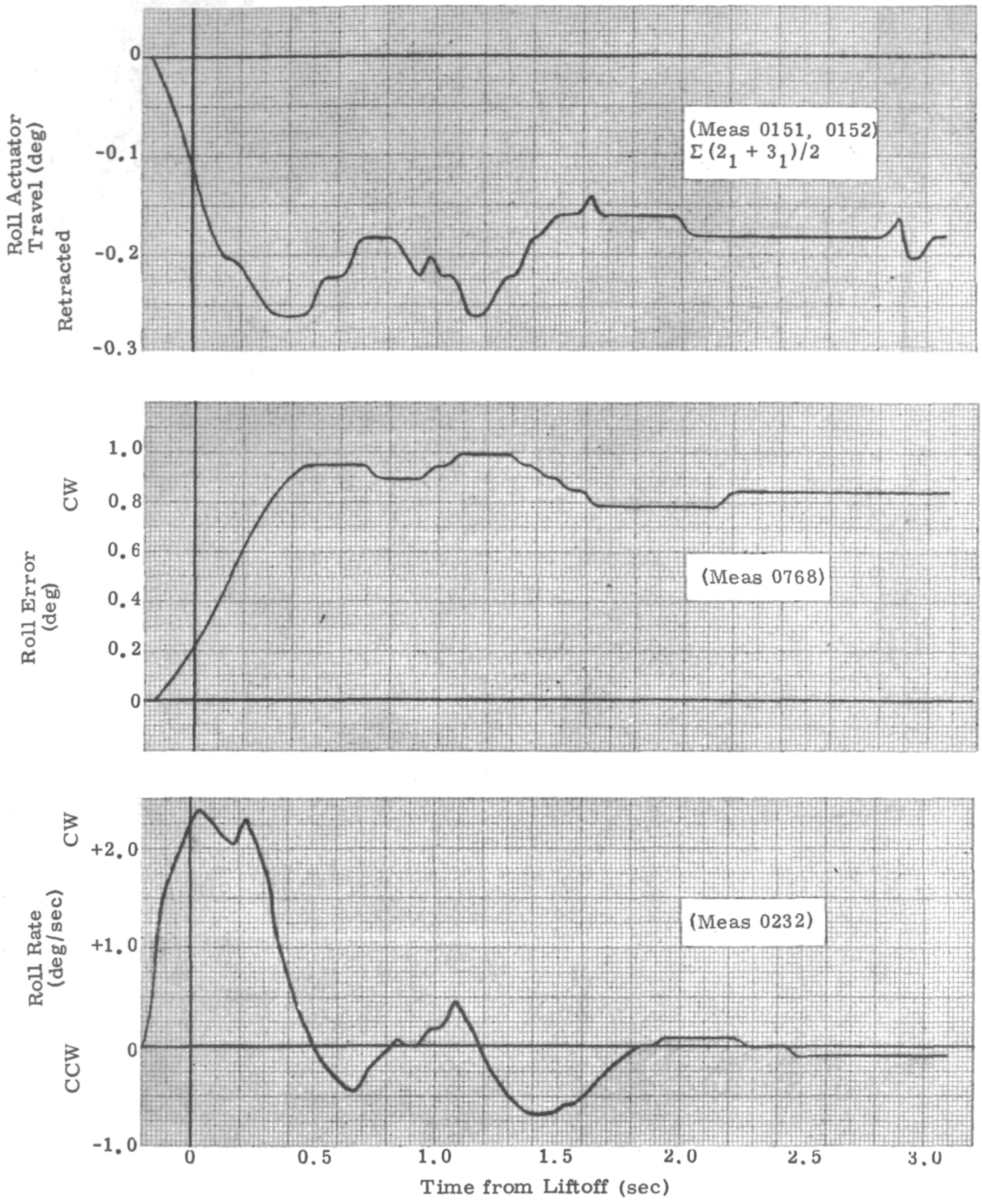

Fig. IV-1. Liftoff Roll Transients

as indicated by the roll rate gyro at 0.2, 0.6 and 1.0 second after liftoff. A roll bias of 0.84 degree CW was introduced at liftoff by the equivalent engine misalignment of 0.17 degree.

2. Roll and Pitch Programs

The TARS roll and pitch programs performed nominally as shown in Table IV-2. The maximum roll and pitch overshoots which occurred at the initiation of their respective programs were 1.6 deg/sec counter-clockwise (CCW) for roll and 0.9 deg/sec nose-down for pitch.

TABLE IV-2

TARS Roll and Pitch Programs

Program	Time from LO (sec)	Nominal Time (sec)	Rate Gyro Average (deg/sec)	Torquer Monitor Indication (deg/sec)	Nominal Rate (deg/sec)
Roll					
Start	8.48	8.48	-1.28	-1.25	-1.25
Stop	20.48	20.48			
Pitch Step 1					
Start	23.04	23.04	-0.71	-0.69	-0.709
Pitch Step 2					
Start	88.24	88.32	-0.52	-0.50	-0.516
Pitch Step 3					
Start	118.87	119.04	-0.24	-0.25	-0.235
Stop	161.72	162.56			

3. TARS-IGS Comparison (Stage I)

The TARS and IGS attitude error signals during Stage I flight for the pitch, yaw and roll axes are presented in Figs. IV-2, IV-3 and IV-4, respectively. The dispersion between the TARS and IGS signals was caused by a combination of TARS gyro and IGS-IMU drifts, errors in open-loop guidance programs, and reference axis cross-coupling. The dispersion (TARS attitude minus IGS attitude) at BECO was -1.10 degrees in the pitch axis, +0.28 degree in the yaw axis, and +1.94 degrees in the roll axis.

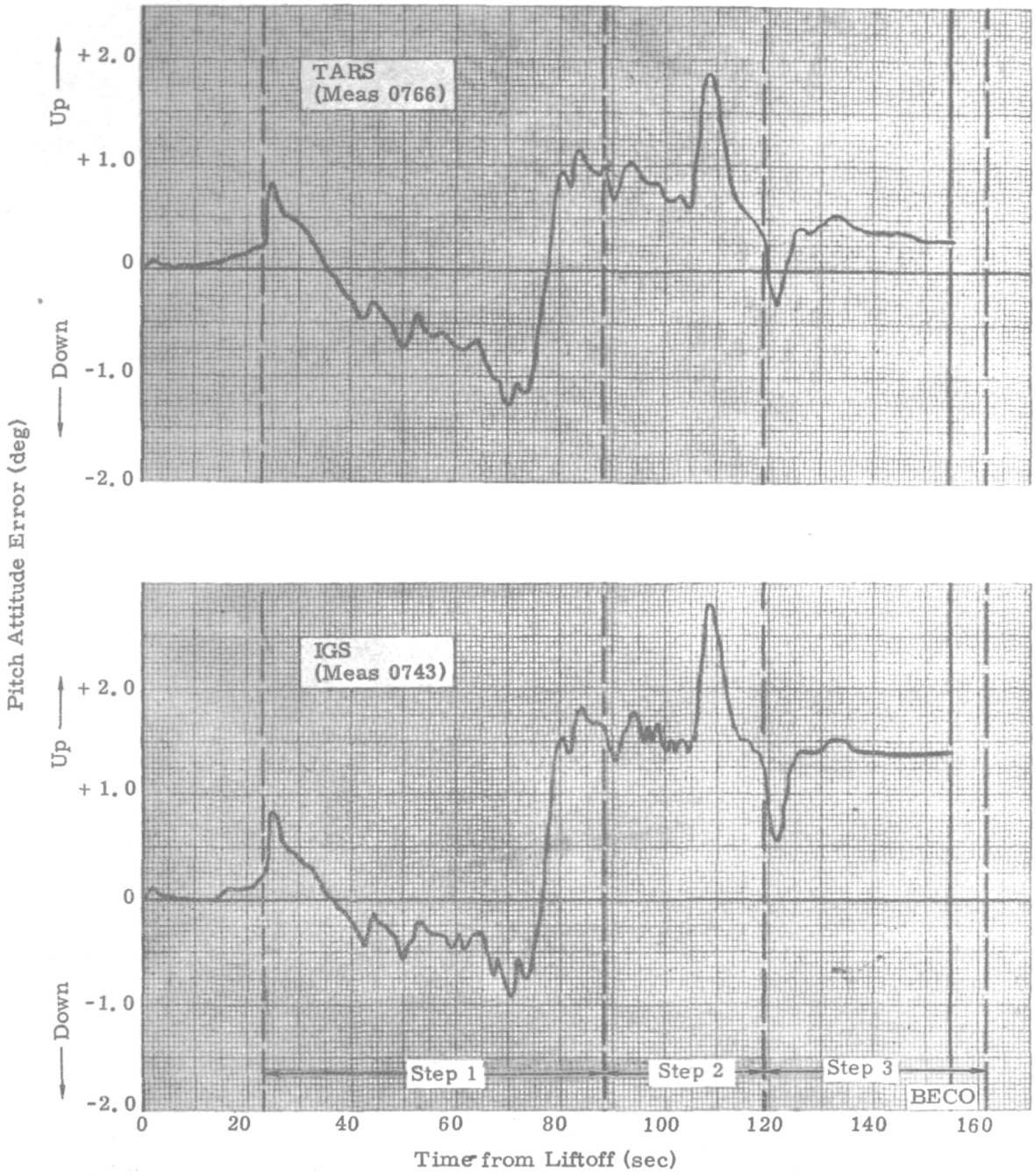

Fig. IV-2. Pitch Attitude Error History During Stage I Flight

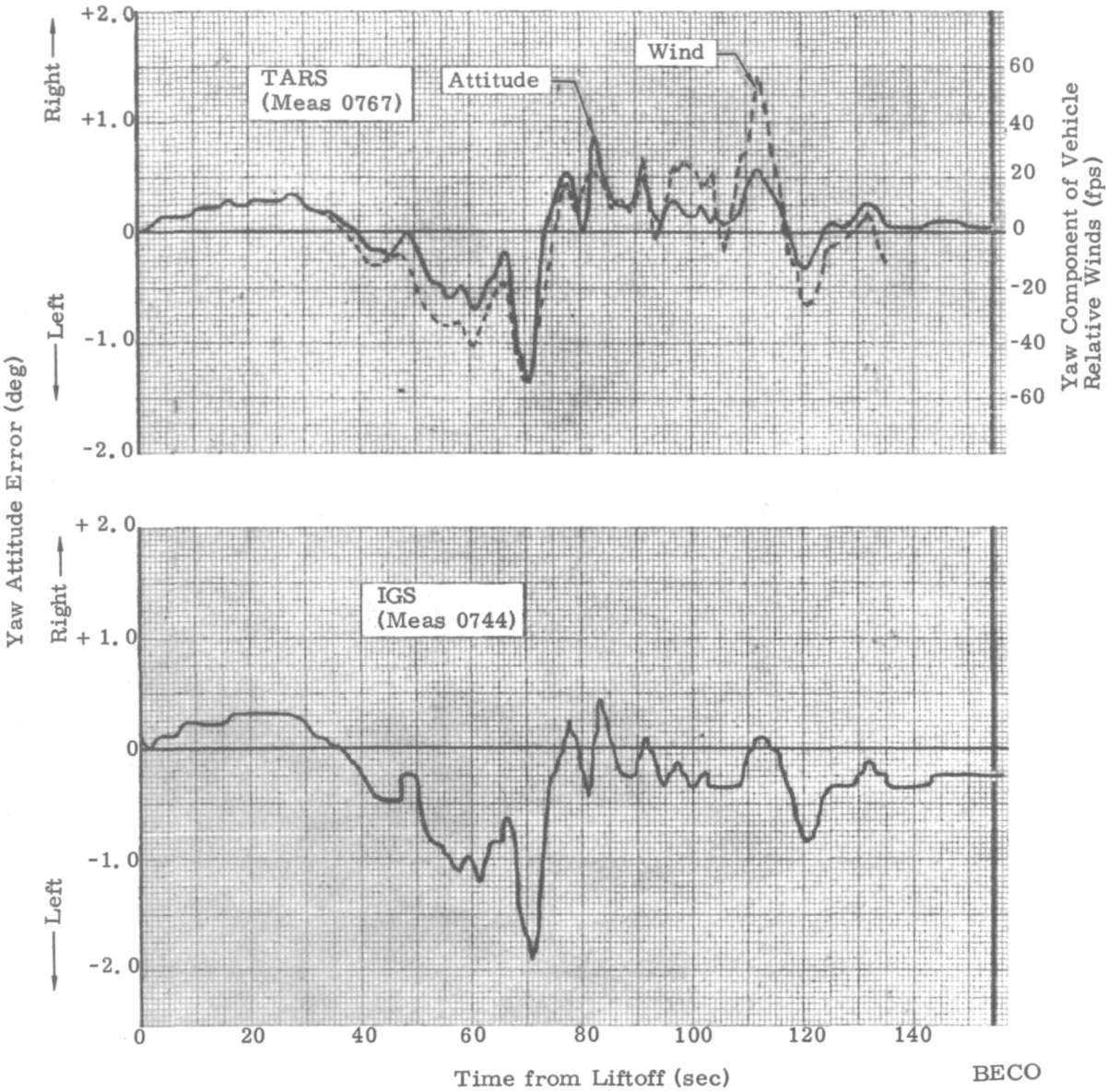

Fig. IV-3. Yaw Attitude Error History During Stage I Flight

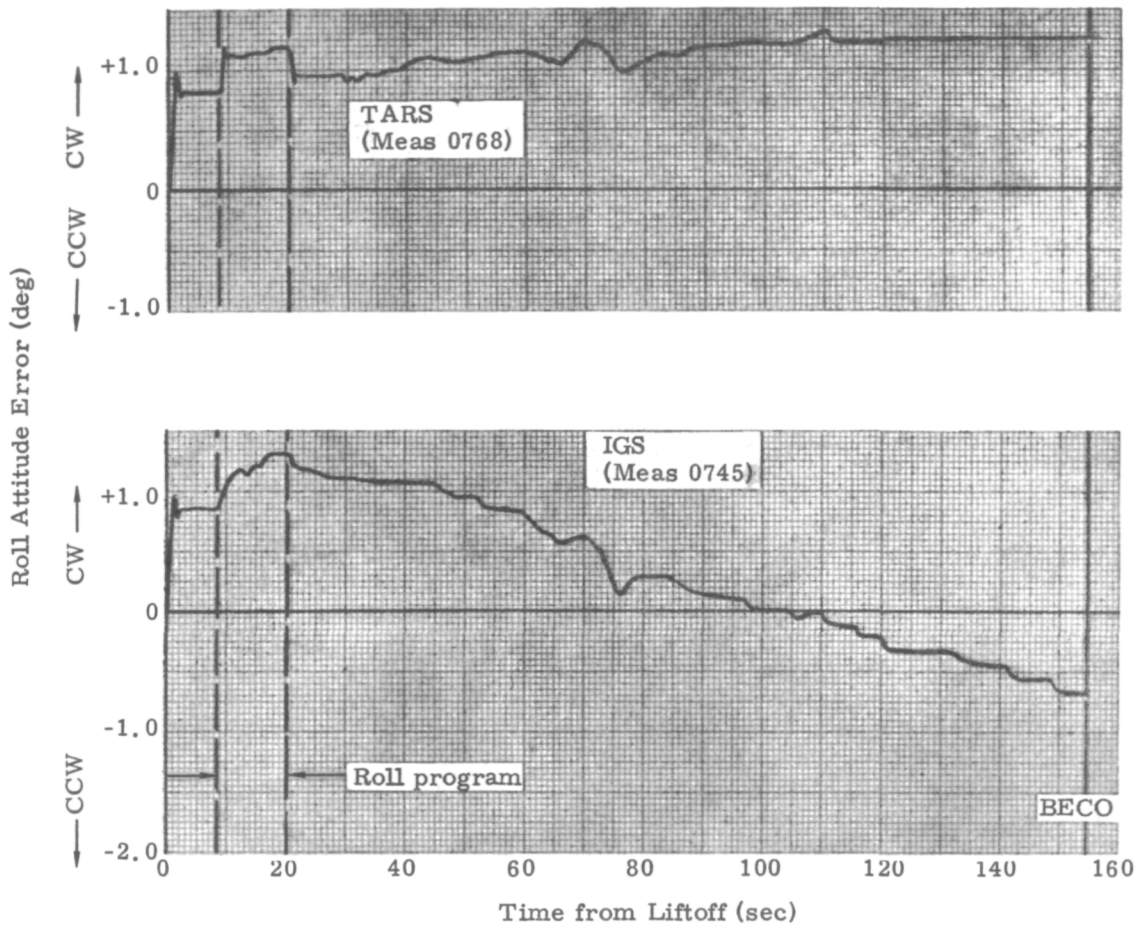

Fig. IV-4. Roll Attitude Error History During Stage I Flight

4. Stage I Flight Disturbances

Analysis of the FCS attitude error signals shown in Figs. IV-2, IV-3 and IV-4 shows response to guidance programs and to vehicle disturbances caused by prevailing winds aloft. The control system response to these disturbances was normal and well controlled. During the wind disturbances, oscillations between 1.0 and 1.6 rad/sec with an average peak-to-peak overshoot amplitude of less than 0.4 degree of attitude error occurred in both pitch and yaw at the predicted GT-8 rigid body oscillatory mode frequencies, varying with flight condition. The level of pitch and yaw excitations was of high magnitude, causing up to two degree peak-to-peak pitch and yaw attitude errors during the max q region and producing inertial coupling excitation in the roll axis. The maximum change in the roll attitude error during the period of excitation never exceeded 0.3-degree peak to peak. The maximum rates and attitude errors recorded during Stage I flight are shown in Table IV-3.

TABLE IV-3

Maximum Rate and Attitude Errors During Stage I Flight

		Primary Gyros		Secondary Gyros	
	Axis	Maximum Rates* (deg/sec)	Time from LO (sec)	Maximum Rates* (deg/sec)	Time from LO (sec)
Stage I	Pitch	+0.28 -0.95	0.4 65.4 & 69.0	+0.22 -0.89	0.2 & 106.0
	Yaw	+0.67 -0.56	72.0 & 81.6 67.4	+0.76 -0.60	72.9 & 81.8 67.4
	Roll	+2.42 -1.54	0.1 9.1	+2.48 -1.62	0.1 9.1
Stage II	Pitch	+0.20 -0.99	1.0 65.0 & 68.7	+0.20 -0.98	1.0 65.3 & 68.7
	Yaw	+0.79 -0.48	72.7 & 81.9 67.7	+0.79 -0.48	72.3 & 81.7 67.4

*Bias removed.

TABLE IV-3 (continued)

Axis	Maximum Attitude Error* (deg)	Time from Liftoff (sec)
Pitch	+1.89 -1.26	108.0 69.5
Yaw	+0.86 -1.36	82.8 70.8
Roll	+1.31	108.7

*Bias removed.

Stage I gain change occurred at LO + 104.76 seconds, during which time adequate vehicle stability was maintained. The vehicle pitch attitude error prior to gain change was 0.64 degree up and reached a maximum of 1.9 degrees up approximately three seconds after gain change. The yaw attitude error changed from 0.1 degree right to a maximum of 0.6 degree right at seven seconds after gain change.

These attitude errors are attributed to changing gains and the reaction of the vehicle to changes in relative wind velocity and direction during this period.

B. STAGE II FLIGHT

1. Staging Transients

During staging, moderate sustainer vehicle rates and attitude errors were observed. The maximum attitude error, measured from the pre-BECO level, and the maximum vehicle rates are given in Table IV-4.

2. Stage II Attitude Errors and Biases

The pitch and yaw attitude errors are shown in Figs. IV-5 and IV-6, respectively; it should be noted that the roll attitude error remained constant at -0.10 degree after the staging transient. The predicted pitch and yaw attitudes are for the center-of-gravity displacement from the vehicle longitudinal axis and for the position of the roll thrust off the longitudinal axis. Additional biases from the predicted attitudes, -0.70 degree in pitch and +1.18 degrees in yaw, were caused by engine thrust

vector misalignment due to structural deformation at the engine gimbal assembly. These biases are of the same magnitude as those noted on previous flights and are within predicted limits.

TABLE IV-4

Maximum Staging Rates and Attitude Errors

Axis	From BECO to Stage Separation		From Stage Separation to Telemetry Blackout		From Telemetry Blackout to Plus One Second	
	Maximum Rates (deg/sec)	Time from BECO (sec)	Maximum Rates (deg/sec)	Time from BECO (sec)	Maximum Rates (deg/sec)	Time from BECO (sec)
Pitch						
Primary	+1.09 -1.27	0.573 0.071	+0.69 -2.53	0.706 0.718	-1.66	1.188
Secondary	+1.28 -1.37	0.573 0.071	+1.37 -2.36	0.708 0.686	-1.66	1.188
Yaw						
Primary	+1.18 -0.68	0.328 0.353	+2.07 -1.37	0.716 0.706	+1.57	1.366
Secondary	+0.89 -0.38	0.328 0.353	+2.65 -2.02	0.718 0.706	+1.67	1.366
Roll						
Primary	+0.60 -4.16	0.002 0.264	+0.49 -3.30	0.722 0.710	+0.69 -0.87	1.760 1.150
Secondary	+0.60 -4.16	0.002 0.264	+0.10 -3.30	0.723 0.710	+0.59 -0.77	1.708 1.123

Axis	Attitude Error (deg)	Time from LO (sec)
Pitch	-1.10	156.6
Yaw	+1.68	157.1
Roll	-1.73	155.9

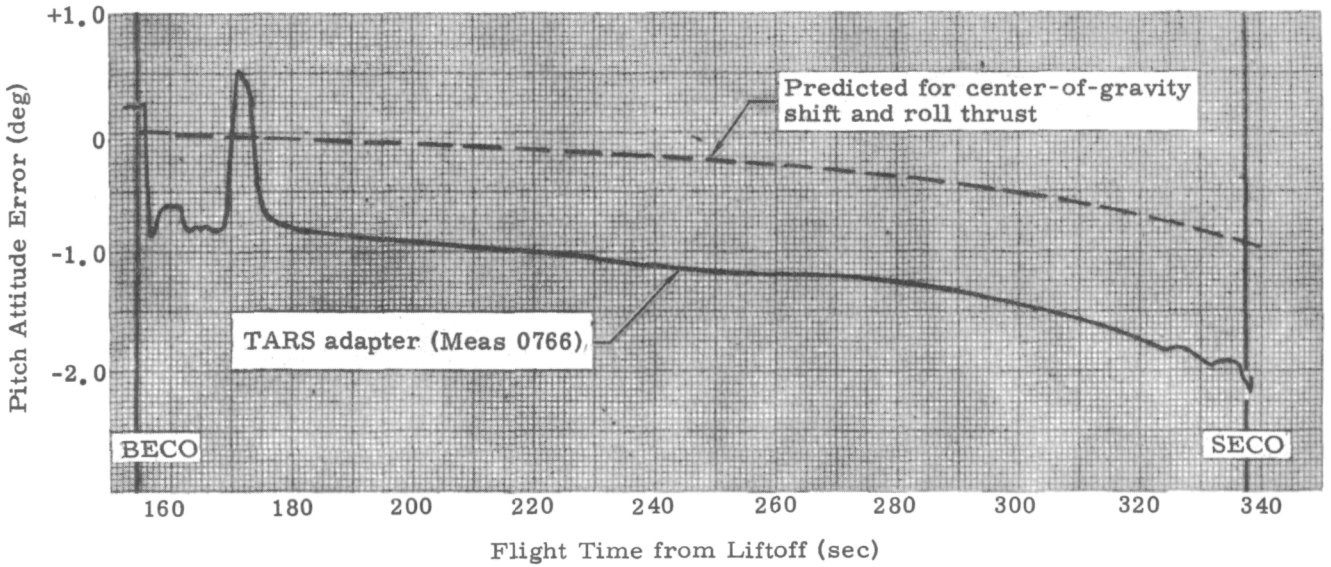

Fig. IV-5. Pitch Attitude Error During Stage II Flight

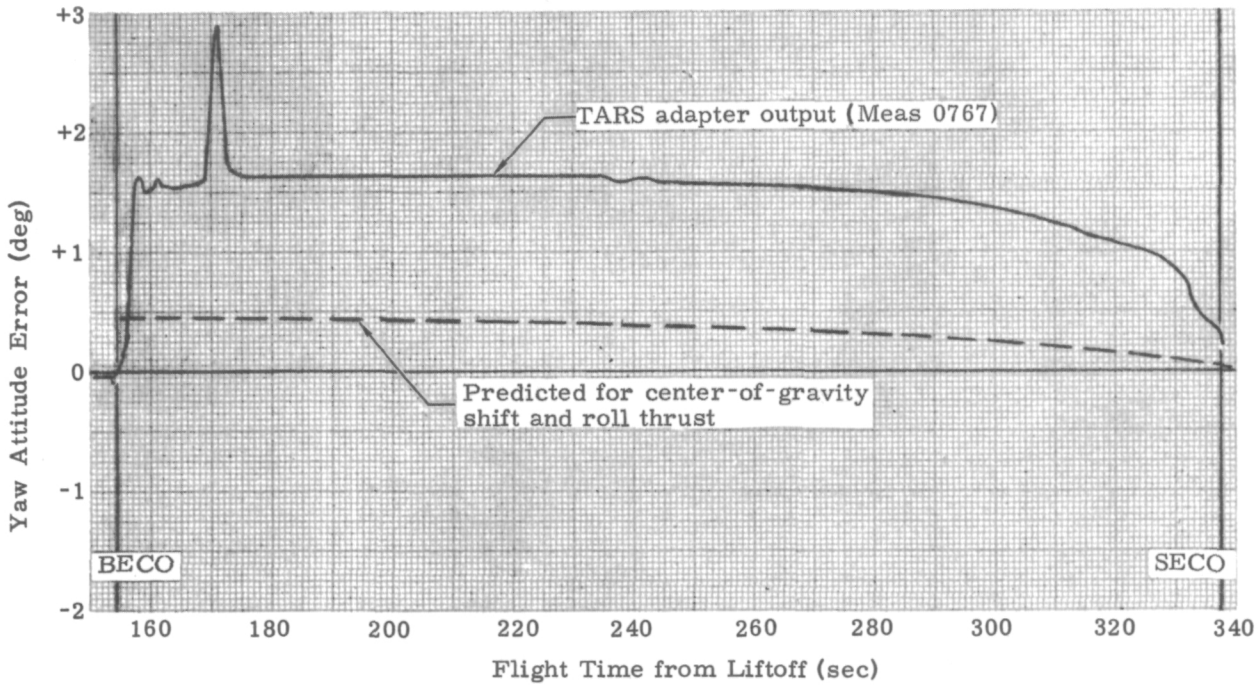

Fig. IV-6. Yaw Attitude Error During Stage II Flight

3. Response to Radio Guidance Commands

Response to the first pitch command consisted of a small nose-down command followed by a full 2.00 deg/sec nose-down command for 4.1 seconds. After the first 7.8 seconds of pitch guidance, all subsequent pitch commands were less than 0.31 deg/sec. Response to the first yaw command consisted of a nose-left command of 1.88 deg/sec for 1.5 seconds. After the first 5.7 seconds of yaw guidance, subsequent yaw commands were less than 0.06 deg/sec. The rate gyro signals substantiated correct response of the FCS to the guidance commands.

C. POST-SECO FLIGHT

Time histories of the pitch, yaw and roll primary and secondary attitude errors and rates while operating on primary system control are shown in Fig. IV-7. The maximum sustained rates measured during the period following SECO appear in Table IV-5.

TABLE IV-5

GT-8 Post-SECO Vehicle Rates

	Rate (deg/sec)	Time from SECO (sec)
Pitch Axis		
Maximum positive	+0.88	+0.7
Maximum negative	-0.38	+0.1
At insertion	-0.18	+20
At spacecraft separation	-0.09	+28.1
Yaw Axis		
Maximum positive	+0.39	+10.6
Maximum negative	-0.97	+0.8
At insertion	+0.29	+20
At spacecraft separation	0	+28.1

IV-13-1

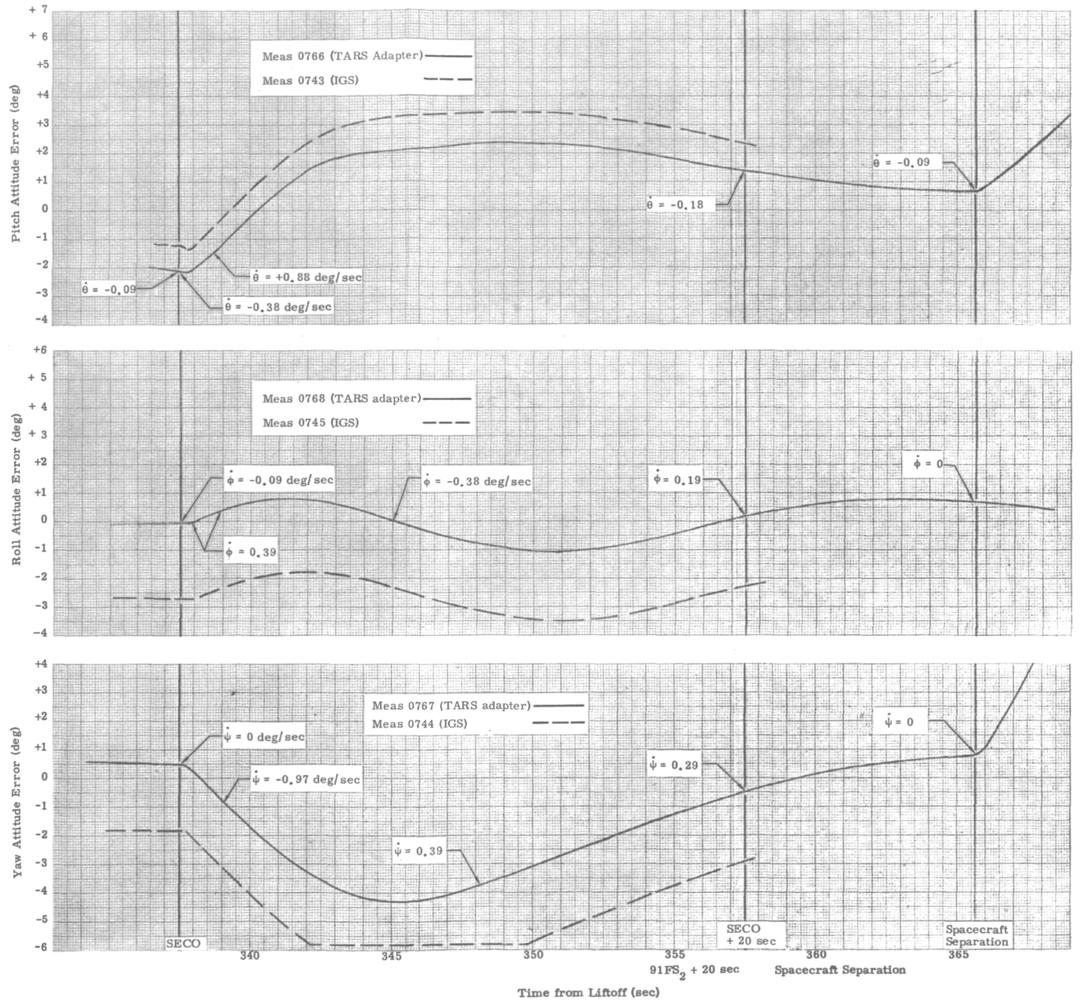

Fig. IV-7. Pitch, Roll, and Yaw Attitude Errors During Post-SECO Flight

TABLE IV-5 (continued)

Roll Axis		
	Rate (deg/sec)	Time from SECO (sec)
Maximum positive	+0.39	+0.4
Maximum negative	-0.38	+7.3
At insertion	+0.19	+20
At spacecraft separation	0	+28.1

There was a series of disturbances extraneous to the FCS which occurred between 3 and 7.5 seconds after $91FS_2$. The disturbances were noted predominantly on the low and high range accelerometers and on the rate gyros. However, in all cases the actuator and autopilot data indicate no signals through the autopilot and, similarly, no actuator responses.

In addition, another disturbance in the Stage II vehicle was noted at approximately 6.5 seconds after spacecraft separation. In contrast to the previous disturbances, this one was detected on the Stage II pitch and yaw actuator responses in addition to the accelerometer and rate gyro.

V. HYDRAULIC SYSTEM

Analysis of the telemetered data revealed that the GT-8 hydraulic system performed satisfactorily during Stage I and Stage II flight.

Prior to SFT, the engine-driven hydraulic pumps were replaced with newly cleaned units, thereby minimizing the probability of contamination during vehicle systems tests requiring hydraulic power. The newly installed pumps were checked with a Gaussmeter to verify free motion of the compensator.

A. STAGE I

1. Primary Subsystem

The final Stage I hydraulic system pressure and level check in the countdown was performed automatically by the sequencer. At T-180 seconds, function control A-7 initiated the motor-driven pump run, which pressurized the secondary system. Approximately 70 seconds later, AGE, using the motor pump, automatically selected and pressurized the primary system. Electric motor pump pressure was a normal 3110 psia at T-0. Engine start transients, starting at $87FS_1$ + 0.73 second, produced flow demands which dropped primary pressure to 2430 psia at $87FS_1$ + 0.87 second. Pressure recovery occurred immediately, indicating proper pump compensator response. The pressure overshoot on recovery peaked at 3370 psia at $87FS_1$ + 1.13 seconds. A steady-state pressure of 3050 psia was reached at $87FS_1$ + 1.7 seconds. There were no significant pressure perturbations either at lift-off or during flight. Pressure decayed normally during flight to 2790 psia at staging.

Prior to T-110 seconds, the static reservoir level was 55.6% full, and it decreased to a normal 35.6% full at T-0. The level increased during flight to 48% full at staging. This 12.4% increase is a result of normal fluid expansion with increasing fluid temperature.

The steady-state reservoir levels and the level changes during system pressurization were normal.

Primary and secondary system pressures and pressure switch actuation points are shown in Fig. V-1. A comparison of primary system pressure for GT-8 and GT-6A launches during engine start and holddown is presented in Fig. V-2.

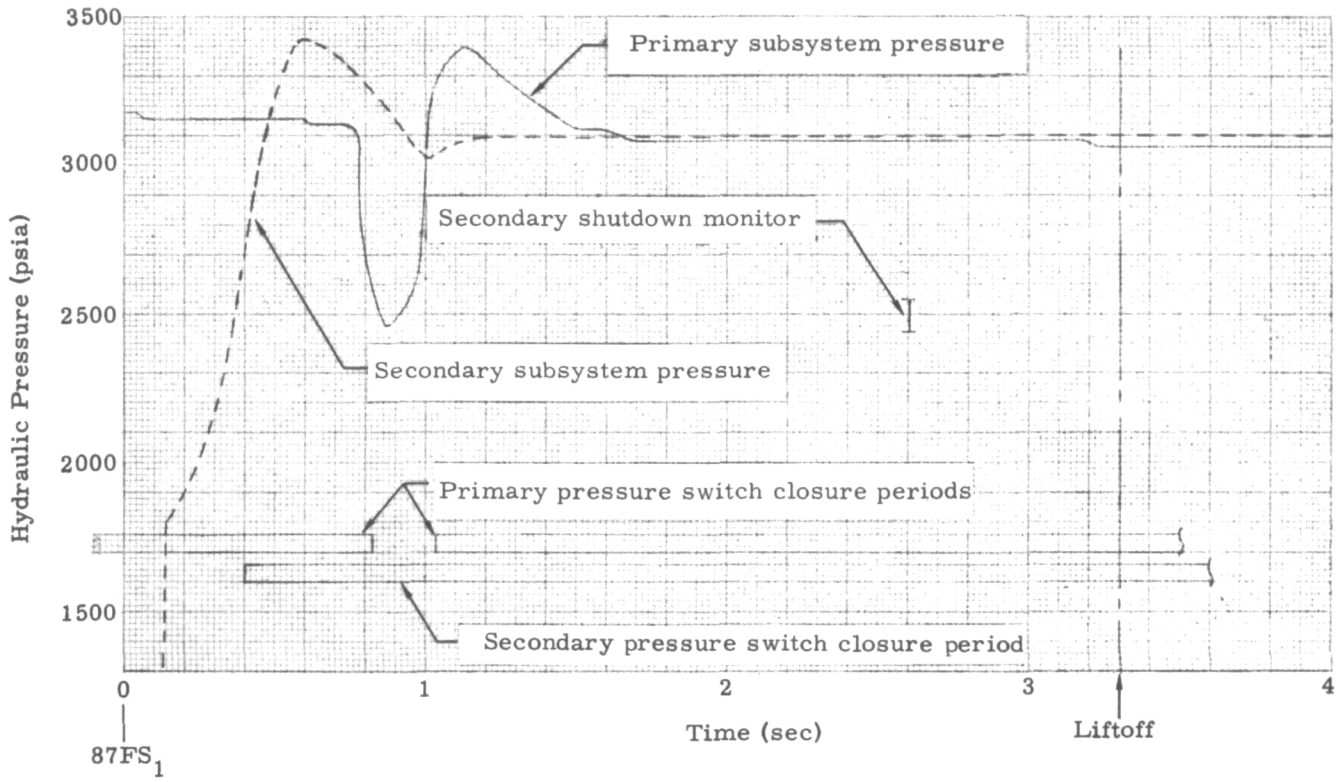

Fig. V-1. Stage I Hydraulic System Pressure Variation During Engine Start and Holddown

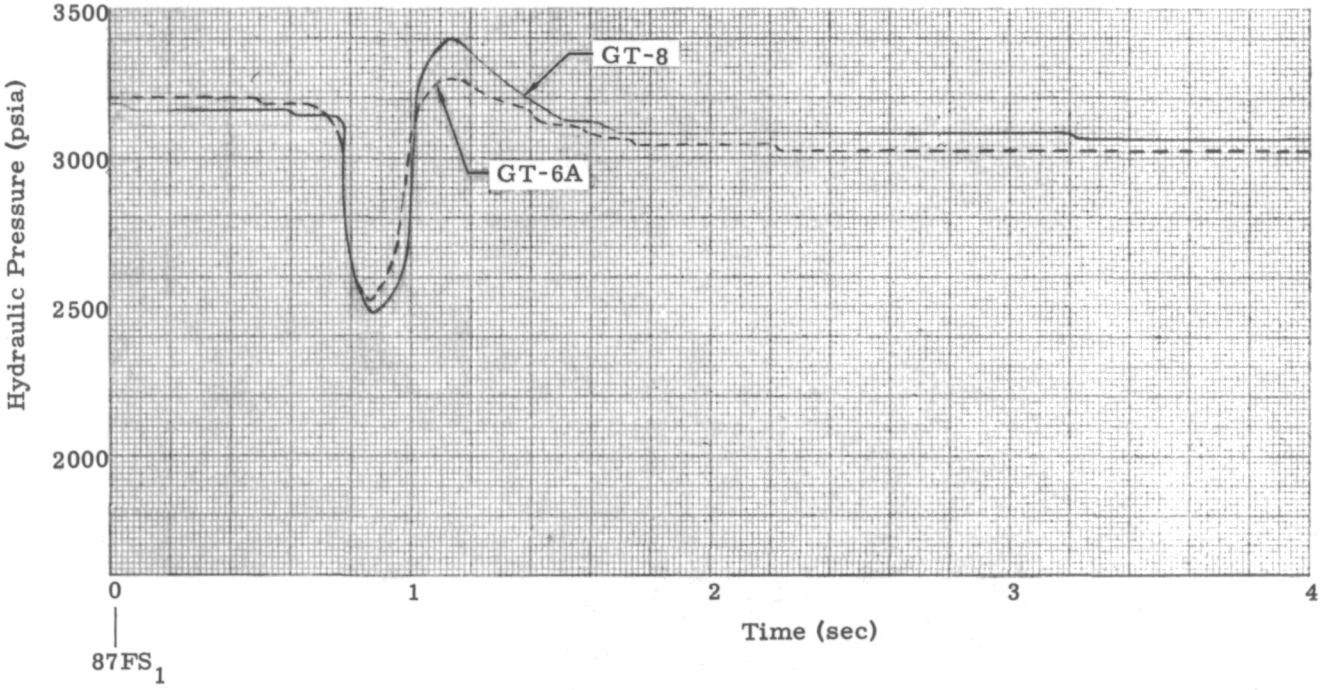

Fig. V-2. Comparison of Primary System Hydraulic Pressure During Engine Start and Holddown

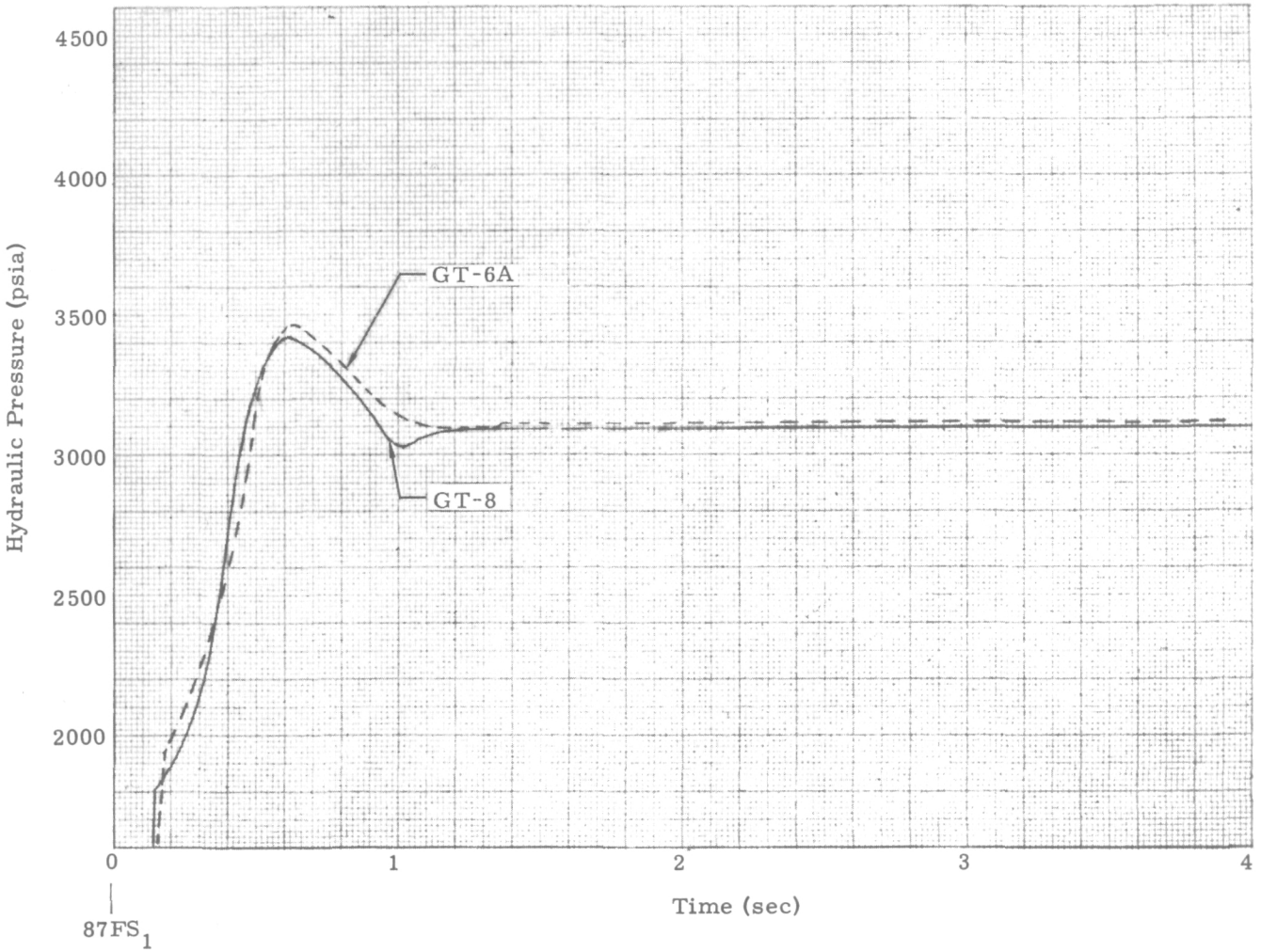

Fig. V-3. Comparison of Secondary System Hydraulic Pressure During Engine Start and Holddown

2. Secondary System

The final Stage I secondary hydraulic system pressure and reservoir level check was performed during a sequencer-initiated, motor-driven pump run from T-180 seconds to T-110 seconds. The indicated accumulator precharge was 1780 psia. Motor pump pressure was a normal 3040 psia at T-110 seconds.

The static reservoir level, which was a normal 54.6% full prior to pressurization at T-3 minutes, decreased to 30.2% full at T-110 seconds. These levels and the level changes during pressurization and depressurization of the system were normal.

At T-0 the system was unpressurized (soft). Pressure began to develop immediately as start cartridge energy rotated the engine turbine. Pressure overshoot reached a maximum of 3340 psia, indicating very good pump compensator response. A steady-state pressure of 2980 psia was reached at $87FS_1$ + 1.19 seconds. At the pressure shutdown interrogation point the pressure remained steady at 2980 psia.

There were no pressure perturbations during flight since the system remained in a standby condition. Pressure decayed normally during flight to 2810 psia at staging.

The reservoir level stabilized at 33.4% full after engine start, increasing during flight to 44.6% full at staging. This 11.2% increase is a result of normal fluid expansion with increasing fluid temperature.

A comparison of secondary system pressures during engine start and holddown for GT-8 and GT-6A launches is presented in Fig. V-3. The pressure values quoted were obtained from telemetered data. It has been determined that the primary and secondary pressure data readings are low by approximately 55 psia and 110 psia, respectively. This bias was due to a change in transducer outputs subsequent to calibration by the vendor. The magnitude of the error was determined by comparing vendor acceptance data on the Stage I pumps with telemetered data. The GT-8 curves plotted in Figs. V-1, V-2 and V-3 were corrected to include the respective bias.

B. STAGE II

The final Stage II hydraulic system pressure and level check was performed during a sequencer-initiated, motor-driven pump run from T-240 seconds to T-180 seconds; however, no data were recorded at this time.

During engine startup at staging, the indicated accumulator precharge was 1870 psia, and pressure overshoot was to 3910 psia.

Steady-state pressure after engine start was 2930 psia, decreasing to 2830 psia at SECO. No significant pressure perturbations occurred during flight. After SECO the pressure fluctuated with the engine rpm, a normal reaction to the low and variable turbine speeds occurring during this period.

The reservoir level was a normal 59.4% full prior to staging. After staging, the level stabilized at 35.8% full, gradually increasing to 39.2% full at SECO. This 3.4% increase is a result of normal fluid expansion with increasing fluid temperature.

The reservoir levels and changes during pressurization and depressurization of the system were normal.

VI. GUIDANCE SYSTEMS

A. RADIO GUIDANCE SYSTEM PERFORMANCE

1. Rate Beacon

Rate beacon performance was satisfactory. Good lock was maintained up to engine ignition and from approximately LO + 33 seconds to SECO + 52 seconds. The loss of lock at Stage I engine ignition is normal; relock occurs as the primary antenna is brought into favorable ground station view.

Values of the rate beacon telemetered functions during flight are listed in Table VI-1.

TABLE VI-1

RGS Telemetered Functions

Function	Meas	Maximum Value	Minimum Value
Rate beacon			
Received signal No. 1	0750	4.16 vdc*	4.10 vdc*
Phase detector	0751	2.96 vdc*	2.56 vdc*
Power out	0752	4.14 vdc*	4.12 vdc*
30-volt supply	0746	2.84 vdc	2.82 vdc
Pulse beacon			
Magnetron current	0753	3.42 vdc**	3.38 vdc**
AGC	0754	-8.0 dbm**	-35.7 dbm**
15-volt supply	0747	4.10 vdc	4.08 vdc
Decoder			
10-volt supply	0748	4.44 vdc	4.42 vdc

*Does not include normal periods of unlock.
**Does not include antenna crossover period.

2. Pulse Beacon

Pulse beacon performance also was satisfactory. Good lock* was maintained through Stage I engine ignition and up to approximately SECO + 54 seconds, well beyond spacecraft separation.

Normal oscillations during the antenna crossover period were observed in AGC from approximately LO + 30 seconds to LO + 73 seconds. During this time the minimum signal level received by the beacon was -55.8 dbm. A very small percentage of messages was not received by the pulse beacon in the period of peak AGC oscillations (which occurs during antenna crossover). This condition has occurred on five of the eight Gemini flights and is expected. The normal ground station signal level increase occurred at LO + 88 seconds and was observed on telemetry to be approximately 13 dbm.

Values of the pulse beacon telemetered functions during flight are listed in Table VI-1.

3. Decoder

Decoder performance was normal. Comparisons of the decoder telemetry data with the Burroughs computer-generated output data indicate that pitch and yaw steering signals and the SECO discrete were received and executed properly.

Values of the decoder telemetered functions are listed in Table VI-1.

4. Guidance Commands

a. Pitch steering

A profile of early closed-loop pitch steering in terms of Burroughs computer pitch steering commands, airborne decoder pitch steering commands, TARS gyro torquer monitor, and primary Stage II rate gyro output is shown in Fig. VI-1. The decoder pitch steering output is also shown in Fig. VI-2 for the entire Stage II flight period.

TARS discrete No. 3 (RGS enable) was issued at approximately LO + 161.65 seconds, thereby energizing the airborne guidance initiate relay. At the same approximate time, pitch program No. 3 was terminated. This effect can be observed on curves (c) and (d) of Fig. VI-1.

The initial decoder output command began at about LO + 168 seconds and built up to the maximum 2.0 deg/sec pitch-down. This command

* "Good lock" is defined as the condition in which no messages are missed by the pulse beacon. The ground station does not lose lock, however, unless a number of consecutive messages are missed.

VI-3
-2

VI-3-1

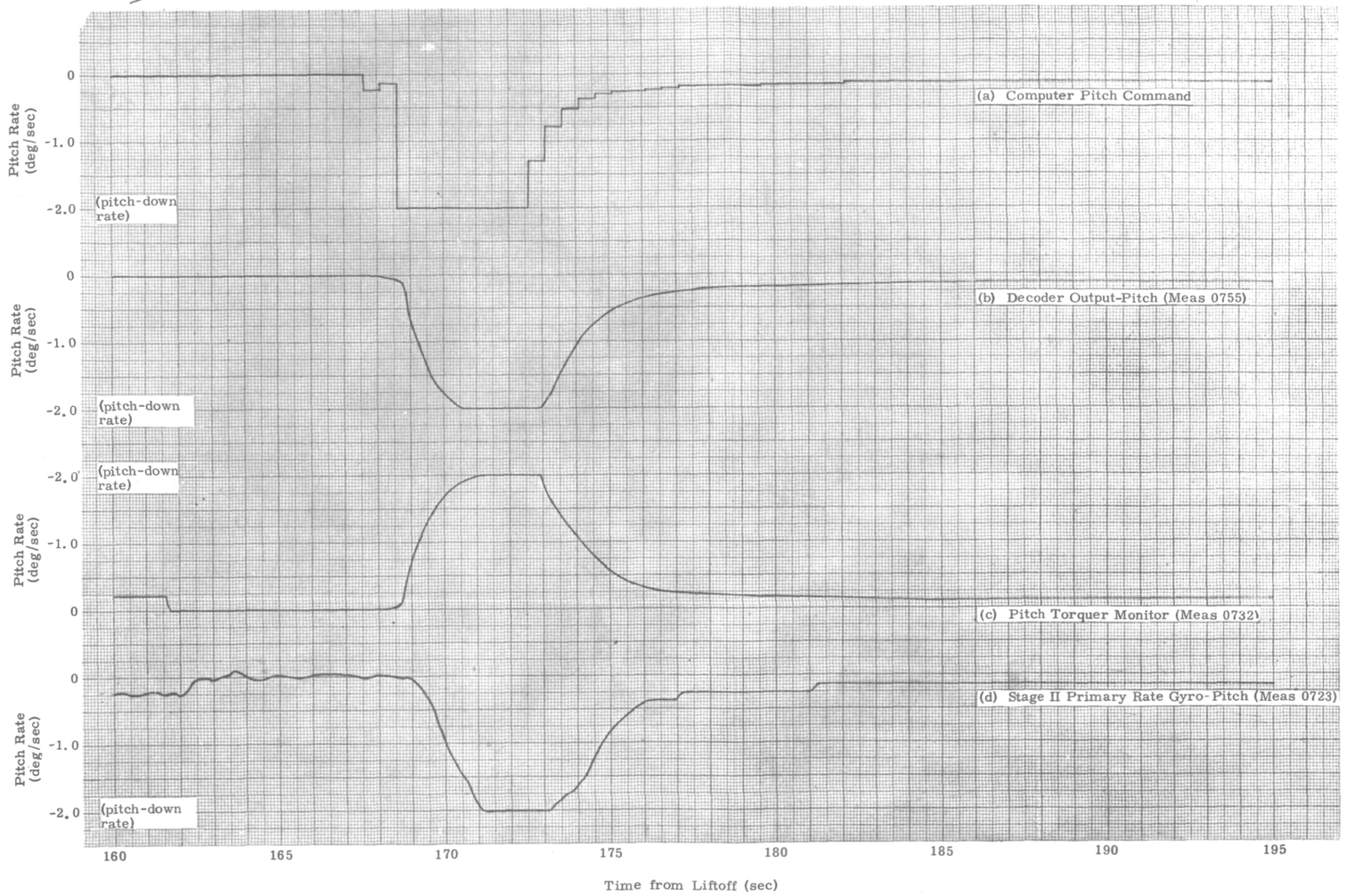

Fig. VI-1. GT-8 Stage II RGS Pitch Guidance Flight History

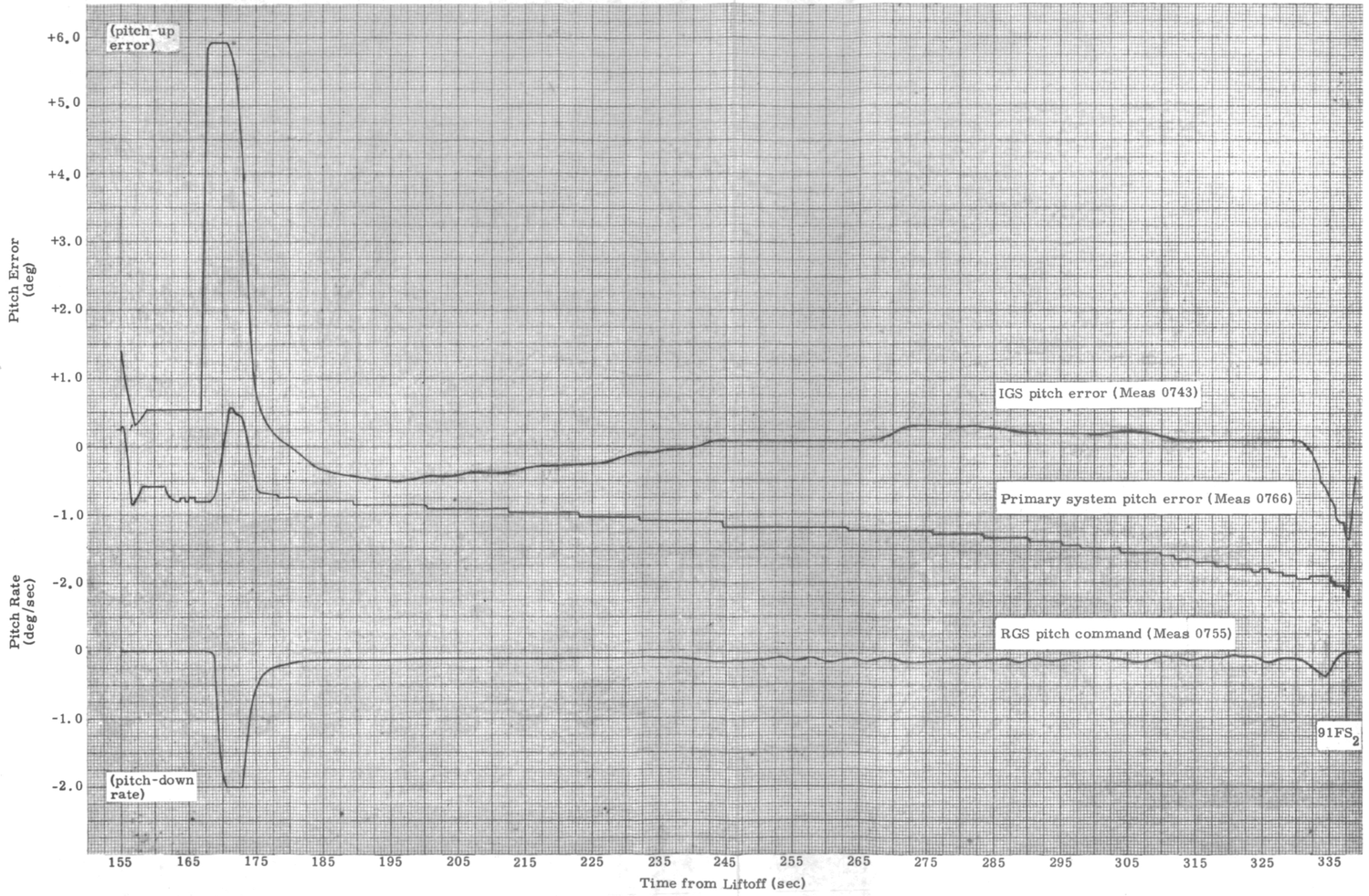

Fig. VI-2. Stage II IGS Pitch Flight History

was maintained for about 2.5 seconds, as can be seen in Fig. VI-1. Thereafter, the pitch steering command decreased to 0.20 deg/sec pitch-down within 8 seconds and remained between 0.05 and 0.20 deg/sec pitch-down until approximately SECO - 5.5 seconds. At this time, the pitch-down command began to increase, and it peaked at 0.35 deg/sec, just prior to normal termination of guidance steering. The decoder output correlated well with the Burroughs computer-generated output during this time period. Similar pitch-down commands just prior to SECO have been noted on previous flights. A good example is the GT-4 flight (Ref. 4) on which the pitch-down command peaked at approximately 0.40 deg/sec.

In the latter portion of Stage II flight, very small magnitude oscillations built up. These oscillations were similar to those on previous flights and have been attributed to atmospheric noise effects. The oscillations were approximately the same amplitude as those of the GT-6 and GT-7 flights but were much smaller than those of GT-5.

b. Yaw steering

Decoder yaw steering commands began at approximate LO + 168.68 seconds. The command peaked at the maximum 2.0 deg/sec yaw left at approximately LO + 170 seconds and remained there for approximately 0.5 second. Thereafter, the yaw command decreased to 0.05 deg/sec yaw left within 5 seconds. Subsequently, yaw commands remained within ± 0.05 deg/sec for the remainder of Stage II flight. The decoder yaw steering output is shown in Fig. VI-3 for the entire Stage II flight.

c. Discrete commands

The times for the computer-generated SECO/ASCO commands and the vehicle reactions are shown in Table VI-2.

TABLE VI-2

SECO/ASCO Events

Signal	Meas	Time from Liftoff (sec)
Ground station SECO	--	337.484 ± 0.003
Ground station ASCO	--	337.491 ± 0.003
Decoder discrete output	0777	337.516 ± 0.005
$91FS_2$	0519	337.536 ± 0.005
ASCO	0799	337.580 + 0.025

11-7-2

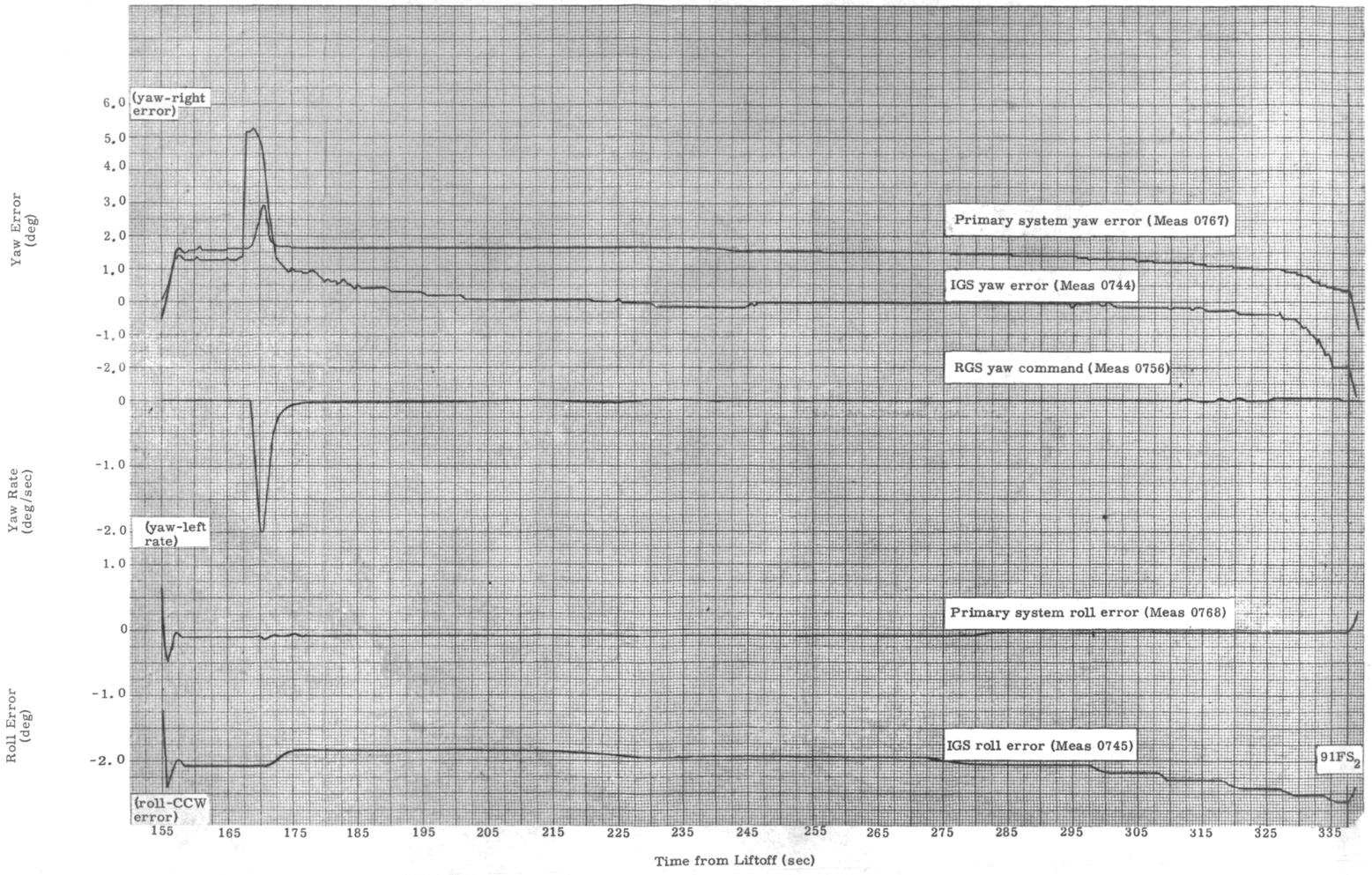

Fig. VI-3. Stage II IGS Yaw/Roll Flight History

The data shown in Table VI-2 indicate that the SECO time delay from ground station issuance to $91FS_2$ was 52 ± 8 milliseconds. The time delay between $91FS_2$ and ASCO reception was 44 ± 30 milliseconds.

B. SPACECRAFT INERTIAL GUIDANCE SYSTEM ASCENT PERFORMANCE

1. Prelaunch Nulls

The prelaunch IGS attitude error null signals were as follows:

Pitch	-0.031 degree
Yaw	-0.149 degree
Roll	+0.079 degree

These signals were well within the specification values of ± 0.37 degree in pitch and yaw and ± 0.25 degree in roll.

2. Stage I Performance

IGS performance during Stage I flight correlated well with the primary system, as shown by a comparison of IGS and corresponding primary system attitude errors in Figs. IV-2 through IV-4. The dispersions between IGS and primary system attitude errors at BECO are discussed in Chapter IV.

The IGS Stage I gain change discrete was issued at LO + 105.031 seconds ± 0.025 second, which was well within the specification time of 104.96 seconds, ± 1%.

3. Stage II Performance

IGS pitch, yaw and roll performance during Stage II Flight was normal. The attitude error dispersions which had built up between the IGS and primary system during Stage I flight in pitch, yaw and roll were apparent in the early portion of Stage II flight, as shown in Figs. VI-2 and VI-3.

a. Stage II pitch

IGS Stage II pitch attitude error appears in Fig. VI-2. Primary system pitch attitude error and RGS pitch steering commands are shown for comparison.

IGS closed-loop pitch guidance began at LO + 167.88 seconds. IGS pitch attitude error saturated at +5.91 degrees shortly thereafter and

remained on saturation for approximately 3.5 seconds. Figure VI-2 shows that, due to the RGS pitch rate command, the TARS pitch attitude error builds up during this same time period to about +0.56 degree. IGS pitch behavior during this period was normal and compares well with primary system behavior in correcting the vehicle trajectory errors.

As the RGS pitched the vehicle down, IGS pitch attitude error decreased to null within 10 seconds. For the remainder of Stage II flight, IGS pitch remained within limits of +0.30 to -0.55 degree until approximately SECO - 7 seconds. At this time, the IGS pitch attitude error, which had been trimmed out at approximately +0.10 degree, began to build-up in the negative direction; the attitude error was -1.34 degrees at SECO and was developed due to the RGS pitch-down command which was issued in this time. The IGS response appeared to be normal.

b. Stage II yaw

IGS Stage II yaw attitude error is shown in Fig. VI-3. Primary system yaw attitude error and RGS yaw steering commands are shown for comparison. Yaw steering began at the same time as pitch. The IGS yaw attitude error built up to about +5.28 degrees and remained at this approximate level for about 1.5 seconds. Figure VI-3 shows that the TARS yaw attitude error built up during this same time period to approximately +2.9 degrees due to the RGS yaw-left rate command. IGS yaw behavior during this period therefore appears to be normal and compares well with the primary system behavior in correcting the vehicle trajectory.

Thereafter, the IGS yaw attitude error decreased to +0.10 degree in approximately 35 seconds as the RGS command yawed the vehicle left. Subsequently, the IGS yaw attitude error remained within approximately +0.10 to -0.20 degree of null until about LO + 310 seconds. At this time, the IGS yaw attitude error began to slope in the negative direction, and by SECO it was approximately -1.96 degrees, which would be a GLV yaw-right command. The amplitude of the attitude error was not excessive, and the direction of the attitude error buildup was as expected due to cg drift. In Fig. VI-3 a similar effect is apparent both in primary attitude error (building up negatively) and in the small RGS yaw steering command (commands the GLV to yaw right).

c. Stage II roll

IGS roll attitude error for Stage II is shown in Fig. VI-3, with TARS roll attitude error shown for comparison. There was an apparent drift rate between TARS and IGS roll as shown by the increase in IGS roll output during Stage II flight. The drift rate was CCW, IGS with respect to TARS. The dispersion is predominantly due to TARS roll gyro g-sensitive drift; this type of drift has been noted on all flights to date.

VII. ELECTRICAL SYSTEM ANALYSIS

A. CONFIGURATION

The launch vehicle airborne electrical system components installed for the GLV-8 flight were similar to those used on GLV-6 and GLV-7 except for the flashing beacon light assembly, which was a special GLV-7 feature.

B. COUNTDOWN AND FLIGHT PERFORMANCE

The airborne electrical system functioned as designed during the launch and flight, with all parameters within specifications. Power transfer was comparatively smooth, and liftoff occurred without incident.

During staging, the APS current trace indicated that a Stage II engine start squib shorted to structure, maintaining a current increase of approximately 11 amperes until stage separation. Comparable staging shorts were encountered on GT-1, GT-2, GT-5 and GT-6 flights, and no staging shorts were encountered on GT-3, GT-4 and GT-7 flights.

Currents to the Stage II redundant shutdown squibs at SECO were detected on both APS and IPS traces. Squib operation was also confirmed by Meas 0521.

At spacecraft separation, the launch vehicle/spacecraft electrical interface was cut by a guillotine in the adapter. Interface signals on GT-8 indicated no shorts to structure, although guillotine shorts are normally expected and have occurred on all spacecraft separations to date.

A summary of electrical system parameters measured at power transfer and during flight is presented in Table VII-1.

TABLE VII-1

GLV-8 Launch Measurements

Meas	Parameter	At Power Transfer			At Liftoff	At $87FS_2/91FS_1$ (staging)			At $91FS_2$ (SECO)		
		Before	During	After		Before	During	After	Before	During	After
0800	IPS (volts)	29.8	28.0	29.4	29.4	29.2	28.9	29.4	29.7	28.8	29.7
0804	IPS (amps)	27.5	26.0	27.5	27.5	27.5	39.6	23.9	23.9	43.2	24.5
0801	APS (volts)	29.9	29.7	29.7	29.7	29.3	28.3	29.4	29.7	29.7	29.7
0805*	APS (amps)	28.1	28.1	28.1	23.3	26.9	40.3	25.7	19.0	21.5	20.9
0802	400 cycle, Phase A (volts)	113.9	113.9	113.9	114.0	113.9	113.8	113.9	113.9	113.9	113.9
0803	400 cycle, Phase A (cps)	400.1	400.1	400.1	400.1	400.1	400.0	400.1	400.1	400.1	400.1
0726	25-vdc power supply (volts)	25.2	25.2	25.2	25.2	25.2	25.2	25.2	25.2	25.2	25.2

*Including TARS heater cycling current.

VIII. INSTRUMENTATION SYSTEM

A. AIRBORNE INSTRUMENTATION

1. Prelaunch and Countdown Status

The airborne instrumentation system operated within specified limits during the GT-8 prelaunch testing and countdown. No components in the system were replaced after the simulated flight test.

Ambient checks during the launch countdown verified that all measurements were operating prior to T-0.

2. Data Acquisition

The measurement program for this launch consisted of 149 PCM analog signals and 42 PCM bilevel signals. All channels functioned throughout flight.

3. Instrumentation System Parameters

Instrumentation system parameters, as measured in flight, are compared with specified limits in Table VIII-1. All data were within the required limits.

4. Telemetry Signal Strength (244.3 mc)

Telemetry signal strength records indicated satisfactory signal levels for data acquisition from the launch vehicle from liftoff to approximately SECO + 150 seconds. The anticipated staging blackout lasted approximately 330 milliseconds.

The Cape Kennedy Tel II and Tel III ground stations monitored the entire flight of the launch vehicle. The Grand Bahama Island station acquired data from approximately LO + 49 seconds to the end of flight. The San Salvador station acquired data during Stage I flight at approximately LO + 83 seconds and during all of Stage II flight.

B. LANDLINE INSTRUMENTATION

1. Countdown Status

The landline instrumentation system operated satisfactorily from the start of propellant conditioning through the launch countdown up to liftoff. All instrumentation holdfire functions monitored in the blockhouse remained within specification throughout the countdown.

TABLE VIII-1

Instrumentation System Parameters

Meas	Description	Required PCM Count / Required Engineering Units	PCM Count / Engineering Units: At Liftoff	At 87FS$_2$/ 91FS$_1$	At 91FS$_2$	At SECO + 20
0810	5-volt power supply	203 ± 1	203	203	203	203
		5.00 V ± 0.035	5.004	5.004	5.004	5.004
0811	40-volt power supply	229 ± 3	227	227	227	227
		40.00 V + 0.64 - 0.44	39.84	39.84	39.84	39.84
0813	PCM mercury cell	73 ± 1	73	73	73	73
		1.335 to 1.375 V	1.355	1.355	1.355	1.355
0814	PCM mercury cell	73 ± 1	73	73	73	73
		1.335 to 1.375 V	1.355	1.355	1.355	1.355
0815	PCM mercury cell	73 ± 1	73	73	73	73
		1.335 to 1.375 V	1.355	1.355	1.355	1.355
0816	+30-volt power supply	162 ± 3	164	164	164	164
		29.92 to 30.06 V	30.01	30.01	30.01	30.01
0817	-30-volt power supply	216 ± 3	215	215	215	215
		-29.92 to -30.08	-30.02	-30.02	-30.02	-30.02

2. Data Acquisition

During propellant loading and launch countdown for GT-8, a total of 140 measurements consisting of 30 measurements on stripchart recorders for loading, 55 landline measurements on stripchart recorders for launch countdown, and 55 airborne measurements in real-time on chart recorders were monitored and recorded.

Data acquisition for all landline monitored data was 100%.

IX. RANGE SAFETY AND ORDNANCE

A. COMMAND CONTROL RECEIVERS

1. Countdown Performance

The command receiver shutdown and destruct and ASCO tests were successfully completed. Telemetry indicated a stable signal strength of approximately 115 microvolts from T-5 minutes through liftoff.

2. Flight Performance

Command receivers S/N 38 (APS) and S/N 9 (IPS) were flown on GLV-8. The Station 1 (Cape Kennedy) low power transmitter carrier signal strength rose to a peak of 1600 microvolts at LO + 30.8 seconds then fell to a flight low of approximately 50 microvolts at LO + 54.2 seconds. Station 1 switched from the low power to the high power transmitter at LO + 66.7 seconds, at which time the signal rose to a flight high of approximately 2400 microvolts then stabilized at approximately 110 microvolts. Switchover from Station 1 to Station 3 (Grand Bahama Island) occurred at LO + 119.5 seconds, and the carrier signal strength remained at approximately 100 microvolts. The switchover from Station 3 to Station 7 (Grand Turk) occurred at LO + 259.38 seconds, with the signal strength remaining at approximately 100 microvolts. The ASCO signal was issued by the command control receivers at LO + 337.58 seconds, at which time the carrier signal level was approximately 100 microvolts. The SECO signal preceded the ASCO signal by approximately 60 milliseconds.

B. MISTRAM

1. Countdown Performance

The MISTRAM open-loop checks with the MACK station were completed successfully. Telemetry data gave evidence of a signal imbalance in the transmit signals from the MACK station. From the start of range telemetry data at T-5 minutes until the MACK station shutdown at LO + 1.033 seconds, the calibration channel AGC voltage proportional was erratic, which is indicative of signal imbalance caused primarily by multipath.

2. Flight Performance

a. Airborne transponder

Transponder S/N 98 was flown on GLV-8. All transponder and ground station data indicate that performance was very good. The range

channel locked onto the Valkaria signal at LO + 7.73 seconds, and the calibrate channel locked on at LO + 8.08 seconds. There was a calibrate channel unlock from LO + 10.08 seconds until LO + 10.63 seconds; however, this occurred before the vehicle was above the horizon for the Valkaria station, and since there was no unlock in the range channel, there was no loss of data. Valkaria started active track at LO + 24.73 seconds and continued until handover to System II, which occurred at LO + 386.7 seconds. There was an approximate 0.5-second loss of data due to the staging plume.

b. MISTRAM I station (Valkaria)

The Valkaria station obtained reconstructible data from LO + 19 seconds to LO + 156 seconds and from LO + 156.5 seconds until LO + 386.7 seconds. The primary use of MISTRAM data for impact prediction is from T + 60 seconds until spacecraft separation. With the time of spacecraft separation at LO + 365.66 seconds, MISTRAM was used for a period of 305.66 seconds (97.1% of the time) as the source of impact prediction data. Utilization of the primary and secondary impact prediction plots is included in Table IX-1.

c. MISTRAM II station (Eleuthera)

The Eleuthera station operated intermittently in passive track from LO + 116 seconds through LO +155 seconds, operated in solid passive track from LO +156 seconds through LO + 388 seconds, operated in solid active track from LO + 389 seconds through LO + 460 seconds, and operated in intermittent active track from LO + 461 seconds through LO + 494 seconds. Eleuthera data were not used as an impact prediction source during this flight.

C. ORDNANCE

Stages I and II prevalves, Stage I engine start cartridges and drop weights ordnance operated satisfactorily.

Launch release ordnance nuts operated properly, with all nuts detonating as evidenced by recovery of all four holddown bolts and all lower launch nuts.

Stage separation explosive nuts and Stage II engine start cartridge ordnance operated as required. The TARS timer arm signal occurred at LO + 144.41 seconds, and the IPS staging arm timer was actuated at LO + 144.57 seconds. Both times were compatible with GLV-8 trend data on these timers.

TABLE IX-1

Range Safety Plotboards Impact Prediction

Primary Plotboard		Secondary Plotboard	
System	Usage Time (sec)	System	Usage Time (sec)
MISTRAM I	329.3	Mod III	307.3
Cape Kennedy FPS-16	54.4	Cape Kennedy FPS-16	10.0
Merritt Island TPQ-18	4.4	Merritt Island TPQ-18	19.2
Grand Bahama TPQ-18	4.3	Grand Bahama TPQ-18	21.2
Grand Turk TPQ-18	73.9	Grand Turk TPQ-18	53.7
Antigua FPS-16	63.2	Bermuda FPS-16	60.3
		Patrick AFB TPQ-18	28.2
Total	529.5	Total	499.9

X. MALFUNCTION DETECTION SYSTEM

A. CONFIGURATION

The malfunction detection system (MDS) hardware installed on GLV-8 for the launch countdown and flight on 16 March 1966 is presented in Table X-1.

TABLE X-1

MDS Components

Nomenclature	Part Number	Manufacturer	Serial Number
Rate switch package	PS830600015-027	Giannini	4019
Malfunction detection package	424-7569205-189	Martin	B020
Tank pressure transducers, Stage I	PS74600002-023	Servonics	Fuel A, 1122 Fuel B, 1124 Oxidizer A, 1132 Oxidizer B, 1114
Tank pressure transducers, Stage II	PS746000002-025	Servonics	Fuel A, 2120 Fuel B, 2124 Oxidizer A, 2117 Oxidizer B, 2118
Stage separation connectors	CCI8119A1-9 CC18119A1-6	Cannon	00112 00023
MDS engine switches, Stage I	284321	Aerojet	S/A 1 primary, 0000816 S/A 1 redundant, 0000815 S/A 2 primary, 0001238 S/A 2 redundant, 0000791
MDS engine switches, Stage II	711049-1	Aerojet	S/A 3 primary, 0000814 S/A 3 redundant, 0001240

Data analysis indicated proper performance of all the MDS hardware.

B. SYSTEM PERFORMANCE

Performance of the MDS during the countdown and flight of GLV-8 was satisfactory.

1. Engine Pressure Switches

Operation of the Stage I engine malfunction detection thrust chamber pressure switches (MDTCPS) and the Stage II engine malfunction detection fuel injector pressure switches (MDFJPS) for the flight is summarized in Table X-2. These switches are required to "make" in a pressure range of 540 to 600 psia and "break" in a pressure range of 585 to 515 psia. During the flight, the Stage I engine start transient was of sufficient amplitude and time duration to cause the S/A 2 MDTCPS switches to respond momentarily to the thrust chamber pressure. All MDS engine pressure switches operated properly and within specification requirements.

TABLE X-2

Flight Operation of MDS Engine Pressure Switches

	S/A 1 (Meas 0356)	S/A 2 (Meas 0357)	S/A 3 (Meas 0855)
Make (540 to 600 psia)	1641:00.030 at 595 psia	1641:00.021 at 575 psia	1643:37.661 *
Break (585 to 515 psia)	1643:36.969 at 580 psia	1643:36.980 at 535 psia	1646:40.065 *

*S/A 3 fuel injector pressure is not instrumented on the Gemini Launch Vehicle; hence, make and break pressures were not available.

2. Switchover

The MDS switchover circuitry functioned properly throughout the flight. There were no switchover commands and no switchover was executed--indicating proper performance of the switchover circuitry.

3. Vehicle Rate Detection

The spin motor rotation detectors (SMRDs) contained in the malfunction detection package functioned properly. The SMRDs monitor rate switch package (RSP) gyro rotational speed and thereby its rate sensing capability.

The rate switch package operated properly throughout the countdown and flight. There were no MDS rate switch operations during any portion of the flight from liftoff through SECO + 29 seconds. Table X-3 compares the maximum launch vehicle rates, measured during the period from liftoff through SECO, with the RSP switch settings. Presented in Table X-3 for the Stage II portion of the flight are the maximum high frequency rates (greater than 17 cps) and the maximum low frequency rates (less than 17 cps). Acceptance data on the rate switch gyros disclosed that they would not respond to the high frequency rate that occurred at staging, and telemetry data verified the proper operation of the rate switches to the rates of the launch vehicle.

TABLE X-3

Maximum Vehicle Rate Compared with Rate Switch Settings

	Axes	Stage I Flight	Flight Event	Stage II Flight	Flight Event
Rate switch settings (deg/sec)	Pitch	+2.5: -3.0	N/A	±10	N/A
	Yaw	±2.5	N/A	±10	N/A
	Roll	±20.0	N/A	±20	N/A
Maximum vehicle rates (deg/sec)	Pitch	-0.99	Wind shear	-2.53	Staging* (high frequency rate)
				-2.14	Guidance command (low frequency rate)
	Yaw	+0.79	Wind shear	+2.65	Staging* (high frequency rate)
				+1.67	Guidance command (low frequency rate)
	Roll	+2.48	Liftoff transient	-4.16	Staging* (high frequency rate)
				-2.4	Staging (low frequency rate)

*The staging rate occurs between stage separation and telemetry blackout.

Following SECO + 99.567 seconds (after spacecraft separation), there were two operations of the rate switches. The rate gyro outputs verified that the rate switch performance was in agreement with the RSP calibration data. Table X-4 summarizes the rate switch operation.

TABLE X-4

Rate Switch Operation

Specification Switch Operation Limits (deg/sec)	RSP Calibration Data		Time of Rate Switch Operation	Rate Gyro Output	
	Primary (deg/sec)	Redundant (deg/sec)		Primary (deg/sec)	Redundant (deg/sec)
Pitch close "A" and "B" switches (2.08 to 2.92)	2.61	2.50	SECO + 99.567 sec	2.58	2.60

4. Tank Pressure Sensors

All MDS tank pressure transducers operated properly throughout the countdown and flight. The maximum difference between the transducer pairs on each tank is presented in Table X-5.

TABLE X-5

Maximum Voltage and Pressure Differences Between Tank Pressure Transducer Pairs

	Maximum Difference			
	Volts (telemetry)	Percent of Transducer Full Range	Δ psi	Percent of Transducer Full Range
Stage I fuel	0.030	0.60	0.35	0.70
Stage I oxidizer	0.035	0.70	0.24	0.48
Stage II fuel	0.013	0.26	0.46	0.61
Stage II oxidizer	0.043	0.86	0.84	1.12

Figure X-1 presents the calibration curves for the Stage I fuel tank pressure transducer pairs (A and B) to clarify the percentage variations between voltages and psi (shown in Table X-5). The maximum difference of 0.86% of transducer full-range output voltage is well within the transducer and telemetry system errors.

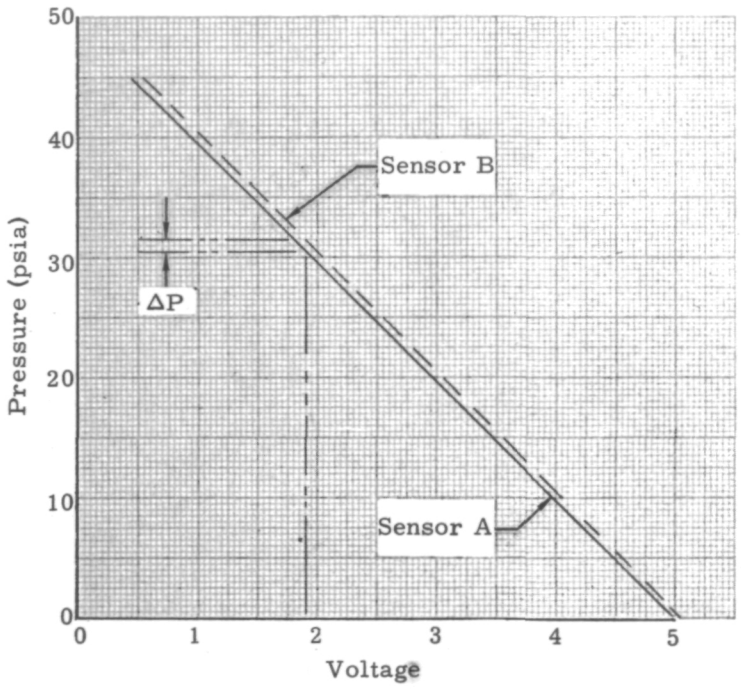

Fig. X-1. Calibration Curves for Stage I Fuel Tank Pressure Transducers

XI. CREW SAFETY

A. PRELAUNCH WINDS OPERATIONS

The upper atmosphere wind status for GT-8 was "go" throughout the prelaunch wind surveillance period. All forecasts and soundings released by the Air Weather Service were within the launch vehicle design wind criteria, and the maximum predicted wind induced loads were well within the launch winds go no-go criteria (no-go if predicted load exceeds limit load).

Prelaunch winds operations were smooth except for one coordination problem and one communication problem.

The Houston-MCC method of displaying punched card data transmitted from Baltimore was changed after the GT-6A flight. The new presentation method was coordinated with Martin and checked prior to the launch operations. However, on F-1 day, MCC had difficulty obtaining an acceptable trajectory plot. Houston personnel then requested Martin to change the digital trajectory program to provide twice the number of data points per trajectory. This change was incorporated, and the F-1 day trajectory was repeated and transmitted to Houston. The revised trajectory output proved acceptable.

The F-2 day, F-1 day, and the T-7 hour scheduled Datafax messages to Houston were delayed because of Datafax machine difficulties and an operator assignment problem at Houston. Martin-Baltimore has notified cognizant NASA officials of this problem and has arranged for an F-3 day test transmission for future flights.

The overall launch winds program is presented in Fig. XI-1, which indicates the data flow between Cape Kennedy, Martin-Baltimore and MCC-Houston. The GT-8 Air Weather Service wind profile releases are shown in Figs. XI-2 through XI-4. The prelaunch winds operations performed on each of the wind data releases are summarized in Table XI-1, which indicates run number, time of wind data release, operations performed, ratio of peak vehicle load to limit load, a wind in or out of specification statement, and the launch winds go or no-go status.

The T-0 hour sounding shown in Fig. XI-4 was not used for the prelaunch winds effort and is shown for reference only.

XI-2-2

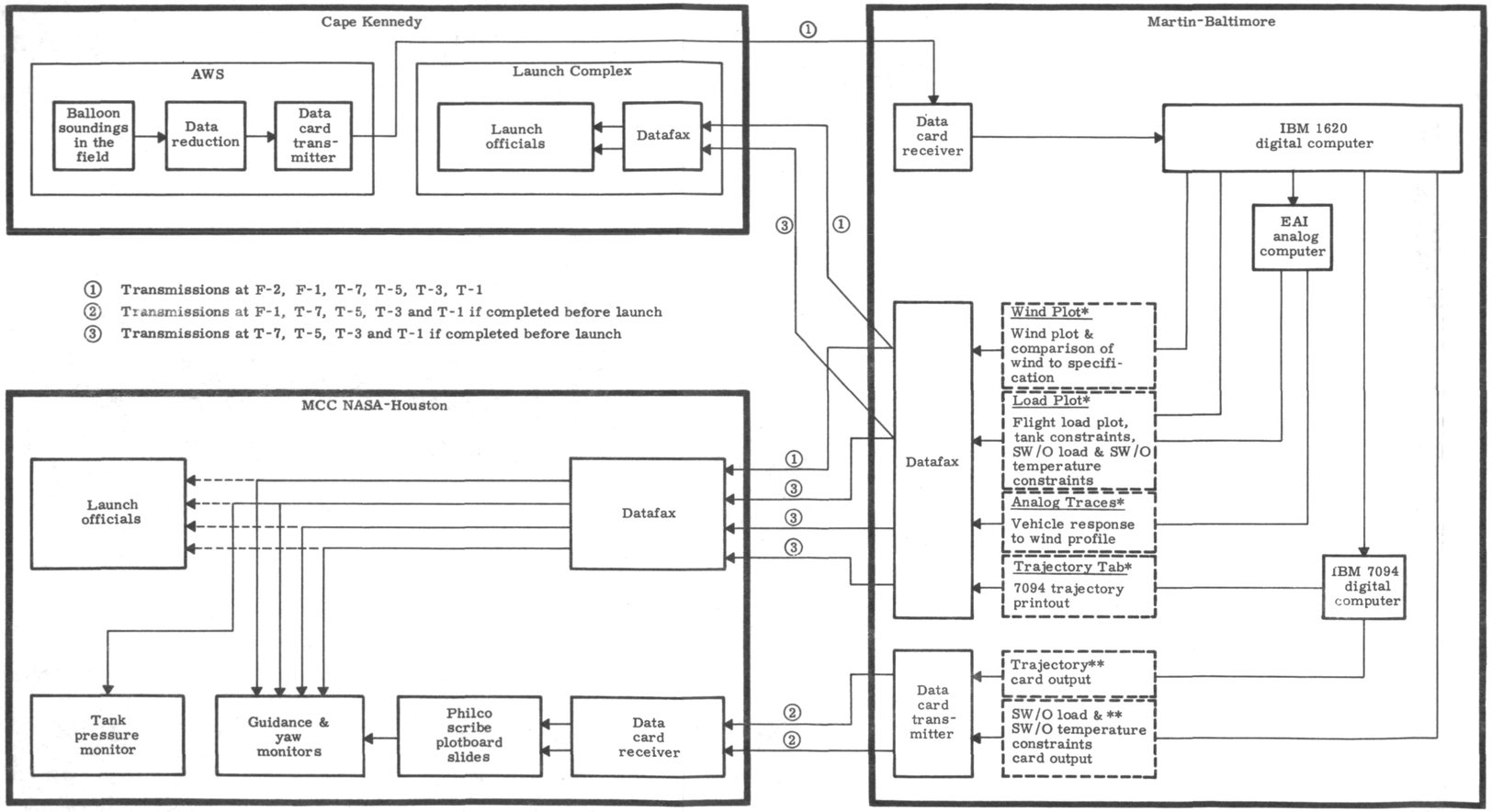

Fig. XI-1. Prelaunch Wind Operations

ER 13227-8

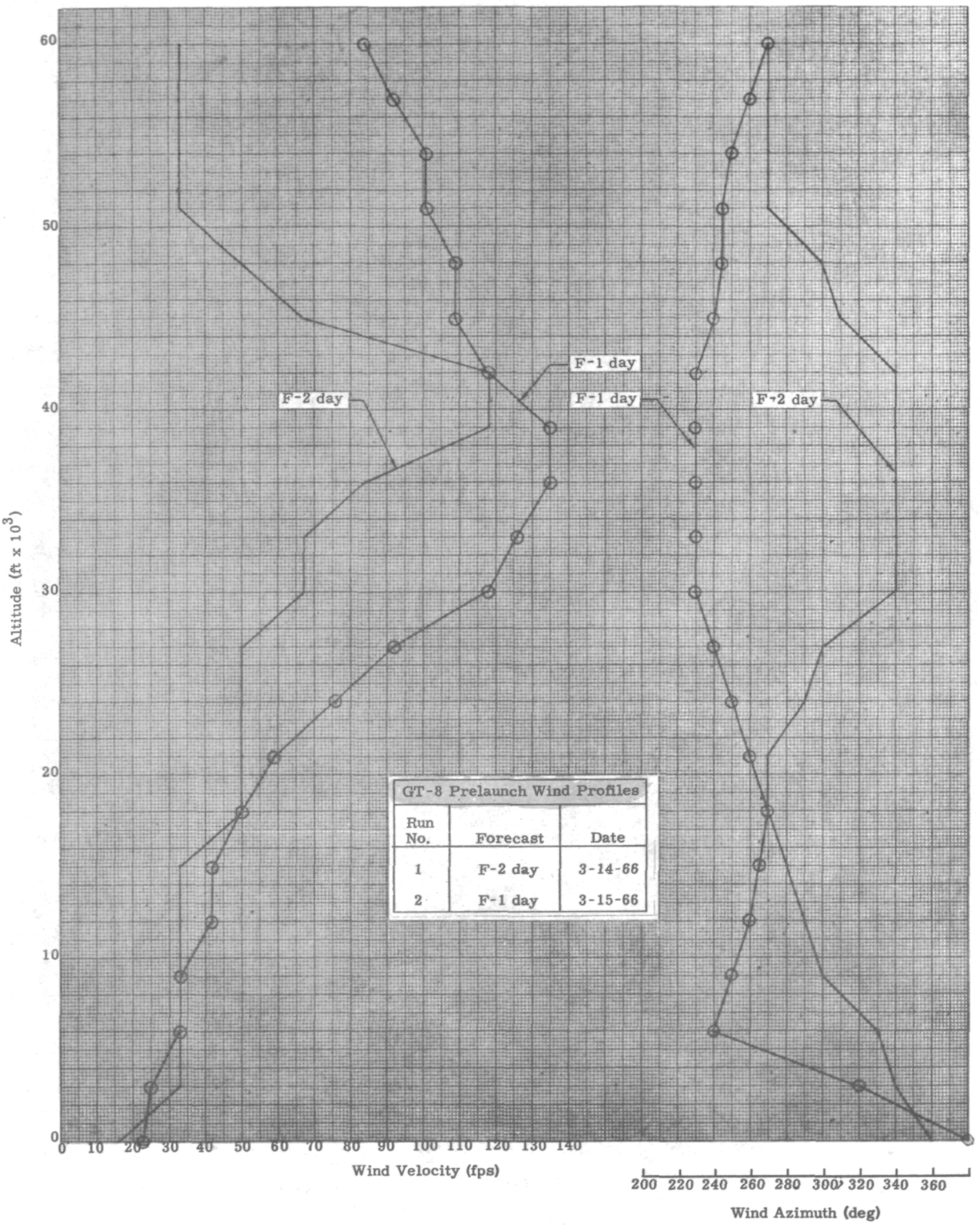

Fig. XI-2. F-2 and F-1 Day Wind Profiles

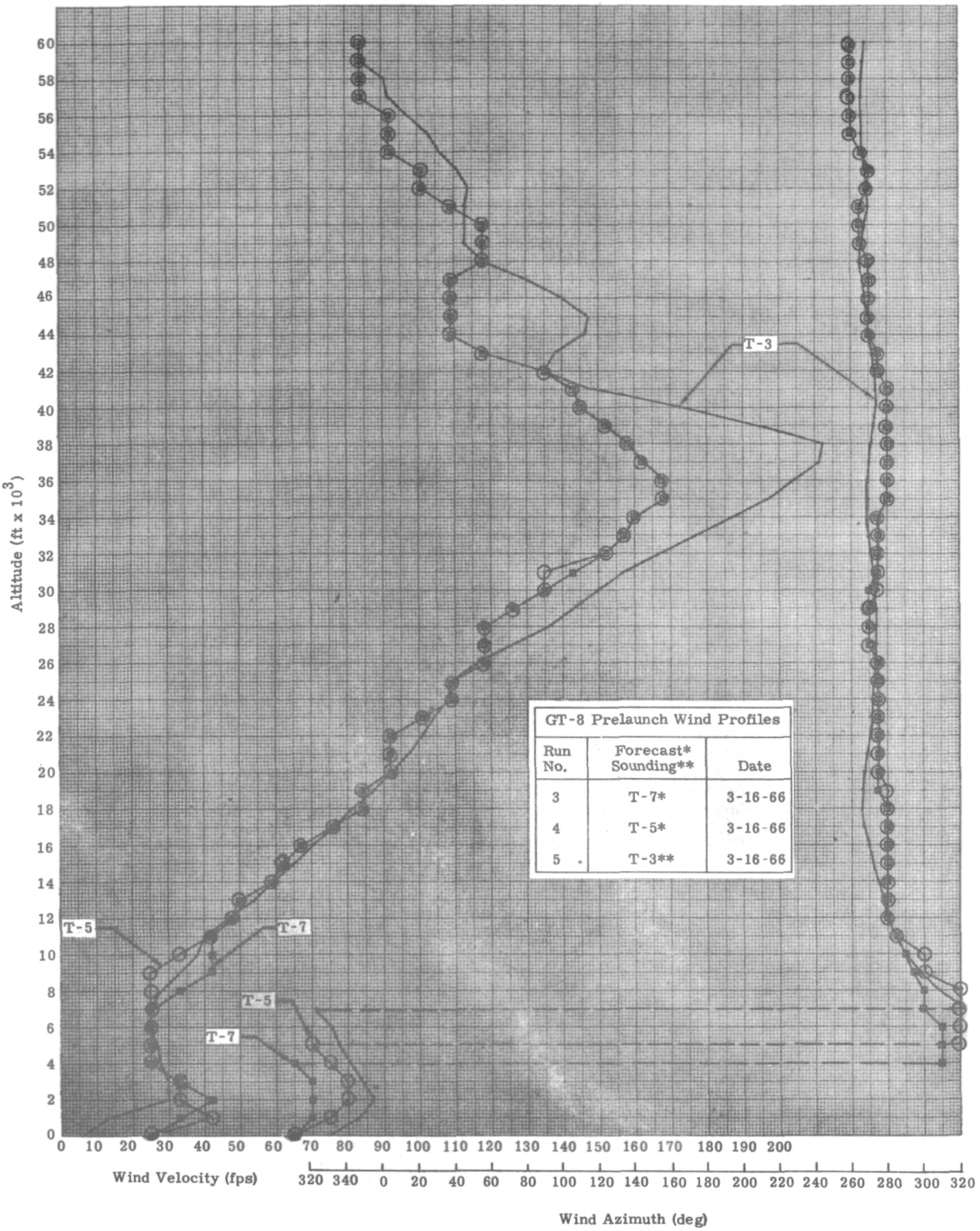

Fig. XI-3. T-7, T-5, and T-3 Hour Wind Profiles

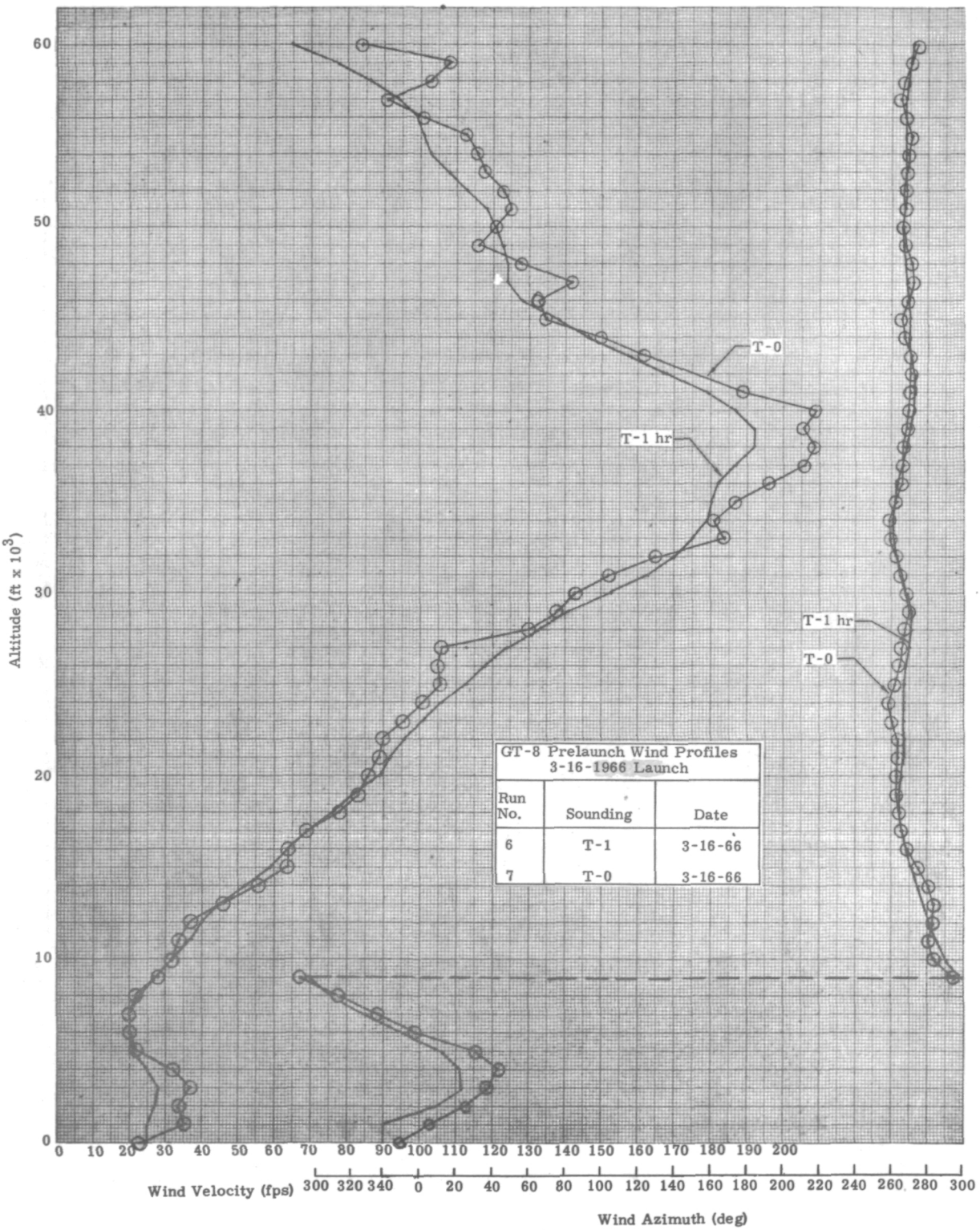

Fig. XI-4. T-1 and T-0 Hour Wind Profiles

TABLE XI-1

Summary of Prelaunch Winds Operations

Run No.	Time of Data Release to Martin-Baltimore	Operation
1	F-2 days 1100 EST 3-14-66	Wind comparison to specification. Wind in specification; status go.
2	F-1 days 1100 EST 3-15-66	Wind comparison to specification, trajectory, switchover load constraint and switchover temperature constraint were determined by computer programs. Wind in specification; status go.
3	T-7 hours 0450 EST 3-16-66	Wind comparison to specification, trajectory, vehicle loads, vehicle response, tank underpressure constraints, switchover load constraints, and switchover temperature constraint were determined by computer programs. Wind in specification; load ratio 0.79; status go.
4	T-5 hours 0650 EST 3-16-66	Wind data identical to T-7 hour release except for ground winds. No computer runs. Cape Kennedy and MCC-Houston notified by phone that there was no wind change.
5	T-3 hours 0850 EST 3-16-66	Wind comparison to specification, trajectory, vehicle loads, vehicle response, tank underpressure constraints, switchover load constraint, and switchover temperature constraint were determined by computer programs. Wind in specification; load ratio 0.83; status go.
6	T-1 hour 1050 EST 3-16-66	Wind comparison to specification. Launch occurred before other simulations were completed. Wind in specification; status go. Status phoned to Cape Kennedy and MCC-Houston.

B. SLOW MALFUNCTION MONITORING

1. Prelaunch Phase

Prelaunch activities started by scribing the F-1 day payload and trajectory predictions on the staff support room (SSR) 30 x 30 inch plotboards and the mission operations control room (MOCR) 10 x 10 foot scribing display. The F-1 day plotboard sheets and the scribed slide were then removed and stored for backup capability should events preclude utilizing F-0 day data.

The T-7 hour Martin-Baltimore predicted trajectory, the T-3 hour structure and temperature data and the performance prediction of Datafax transmission No. 4 from MRL-Cape Kennedy were used to scribe the launch day SSR plotboard sheets and MOCR slide. The decision to use the T-7 hour data was based on verbal notification from Martin-Baltimore that the T-5 hour sounding did not show any appreciable change from the T-7 hour data and that the T-3 hour data would be late (it was received approximately 30 min prior to liftoff). The performance switchover constraint was set at 200 pounds based on Datafax transmission No. 4. Prior to liftoff, verbal notification was received from Martin-Baltimore that indicated -247 pounds as the T-0 payload pad (PLP). NASA was notified of the change and agreed to go with the 200-pound switchover (SWO) lines. The countdown was normal at MCC-Houston, and the T-3 minute update from Burroughs was on time at the resumption of the count and agreed perfectly with the desired A_L of 99.9 degrees. Liftoff was within one second of the recommended liftoff time ($GMTLO_R$) of 1641:02 GMT, 3 March 1966.

2. Launch Phase

The trajectory predictions from Martin-Baltimore were very close to the actual flight results. For the first time, the lateral axis included the predicted roll thrust misalignment as well as wind effects. The pitch axis included the 1.34% low pitch program prediction. The RTCC stored constraint data and total scribing capability for displays were utilized on GT-8 for the first time. The scribing of constraints and trajectories by RTCC was excellent.

There were no equipment problems noted at MCC-Houston for the GT-8 mission. The overall operation was the smoothest to date.

a. Stage I

A roll attitude command of 0.72 deg CCW occurred at liftoff to compensate the roll thrust misalignment; the TARS and IGS were in perfect

agreement. No pitch or yaw thrust misalignment was depicted on the MCC-Houston SCRs (Figs. XI-5 and XI-6). The roll and pitch programs were initiated on time. The IGS roll program required approximately 0.1 degree more CCW roll than the TARS (see SCR No. 2, Fig. XI-6); the IGS pitch program was higher than the TARS pitch program for its duration (see SCR No. 1, Fig. XI-5). Based on the preflight prediction of the TARS programmer performance, both of the program anomalies were expected. The TARS roll attitude error displayed a buildup in CCW command of 0.24 degree to a total error of 0.96 degree to compensate for the thrust misalignment increase due to normal thrust buildup and other factors which change with time. Primary and secondary gain changes occurred on time.

The pitch trajectory ($\tilde{V}_I - \tilde{\gamma}_p$) display (Fig. XI-7) on plotboard VA was slightly lower at the peak and slightly higher at staging. The lateral trajectory ($\tilde{V}_Y - T_E$) display (Fig. XI-8) on plotboard IIIA was greater (-108 fps predicted versus -130 fps actual at BECO) than the Martin-Baltimore T-7 predictions. The changes noted in pitch were due to a change in winds aloft prior to liftoff. The monitors received verbal notification from Martin-Baltimore of the wind change as well as the T-3 hour wind profile Datafax from Baltimore and were expecting the small disparities on the displays.

b. Stage II

The pitch and yaw steering commands occurred on time and were normal for the initial conditions at staging. The pitch and lateral trajectories were normal from $\delta_6 = 1$ until after $\dot{V}/V_R = 0.9$ (approximately L/O + 330 seconds), when the flight path angle ($\tilde{V}_I - \gamma_p$) became slightly noisy and appeared to loft approximately 0.18 degree. This was compensated for by a W_{pn} nose-down command just prior to SECO.

SECO appeared as an overspeed cutoff on plotboard VA (see Fig. XI-7). The yaw cg shift caused a total 1.2 degree yaw attitude error shift over the Stage II portion of the flight.

c. Post SECO

Vehicle perturbations were very mild as observed on the MCC-Houston SCRs (see Figs. XI-5 and XI-6).

The roll axis displayed a low frequency oscillation of 0.055 cps with an amplitude of 1.44 degrees peak-to-peak from SECO until LOS.

	Stage II	Stage I	
	1-Sec Marks from Liftoff		1
Nose Down ↓	θ_{e_s} 743 ± 6°	θ_{e_s} 743 ± 6°	1
	SWO 872 - 874		2
—	Diff $\theta_{e_s} - \theta_{e_p}$ 743 - 766	Diff $\theta_{e_s} - \theta_{e_p}$ 743 - 766	2
	GCP 728		3
Stage II Nose Down ↑ Stage I ↓	δB_p GE/B ± 5°	$\dot{\theta}_c$ 732 MSB	3
	GCS 773		4
Nose Down ↓	ω_{pN} GE/B ±2°/sec	$\delta\theta_1$ 153 ± 5°	4
	Guid Init TARS 740		5
Nose Down ↓	$\dot{\theta}_g$ 755 ±2°/sec	$AP\theta_1$ 770 MSB	5
	δ_6 Guid Start GE/B		6
Stage I Nose Down ↑ Stage II ↓	ω_{ps} GE/B ±1°/sec	$\delta\theta_2$ 150 ± 5°	6
	δ_7 SSCO GE/B		7
Nose Down ↓	$\delta\theta$ 651 ± 3°	$AP\dot{\theta}_2$ 771 MSB	7
	SWO Command		8
Roll CW ↓	———	$\dot{\phi}_c$ 734 MSB	8

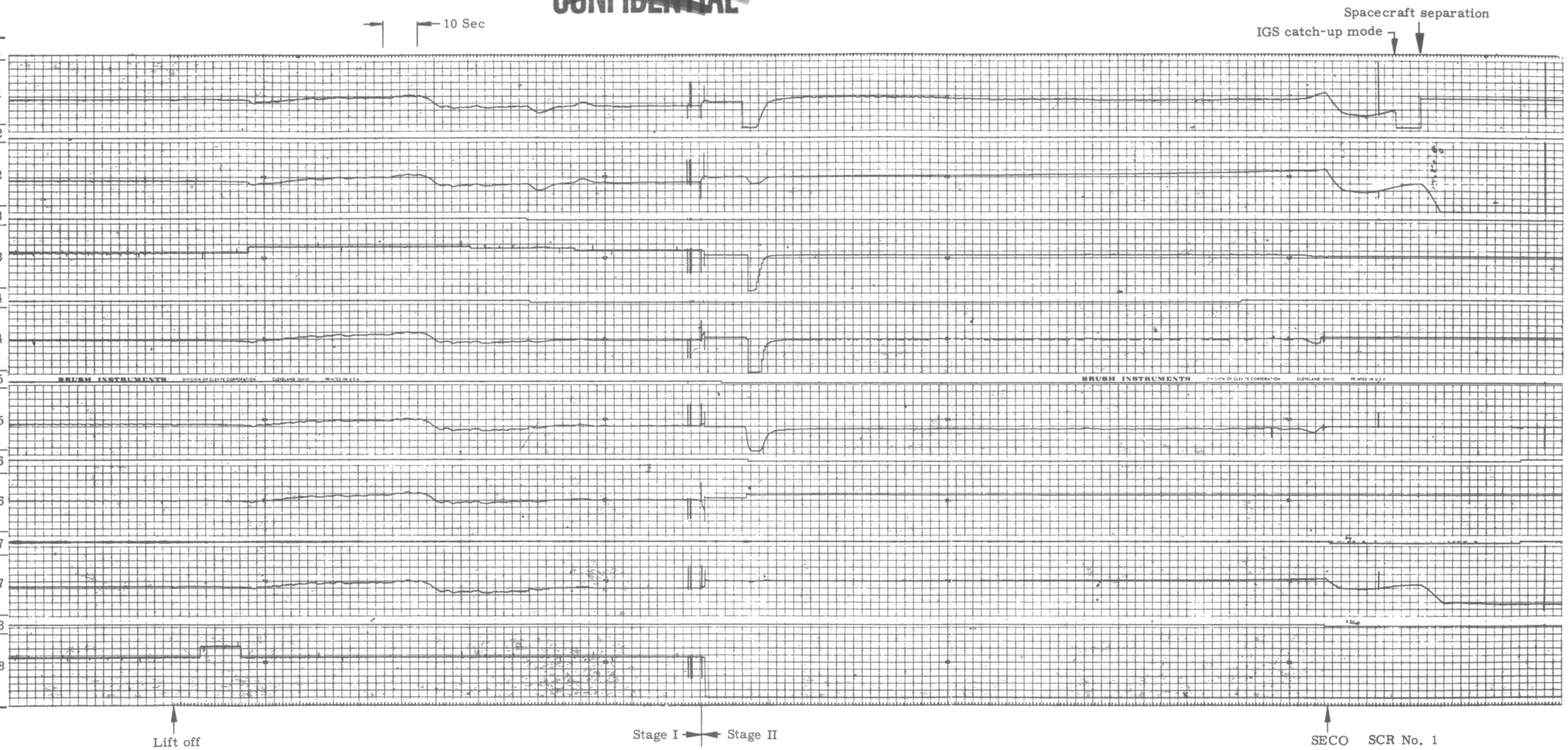

Fig. XI-5. Telemetry III Pitch Axis Recording

CONFIDENTIAL

XI-10-1

CONFIDENTIAL

XI-10-2

-3

CONFIDENTIAL

	Stage II	Stage I	
	1-Sec Marks from Liftoff		1
Roll CW ↓	ϕ_{e_s} 745	ϕ_{e_s} 745 ± 6°	1
—	SWO 872 or 874		2
	Diff 745 - 768	Diff 745 - 768	2
—	GCP 728		3
Yaw Right ↓	ψ_{e_s} 744	ψ_{e_s} 744 ± 6°	3
—	GCS 773		4
Yaw Roll Axis ↓	Diff ψ_{e_s} - ψ_{e_p} 744 - 767	Diff ψ_{e_s} - ψ_{e_p} 744 - 767	4
—	Guid Init TARS 740		5
Yaw Right ↓	↑ 2°/sec W_{YN} GE/B	$\delta\psi_1$ 152 ± 5°	5
—	δ_6 GE/B		6
Yaw Right ↓	↑ 2°/sec ψ_g 756	APψ_1 769 MSB	6
—	δ_7 SSCO GE/B		7
Yaw Right ↓	$\delta\psi$ 650 ± 3°	$\delta\psi_2$ 151 ± 5°	7
—	SWO Command		8
Roll CW ↓	$\delta\phi$ 652 ± 33°	APψ_2 772 MSB	8

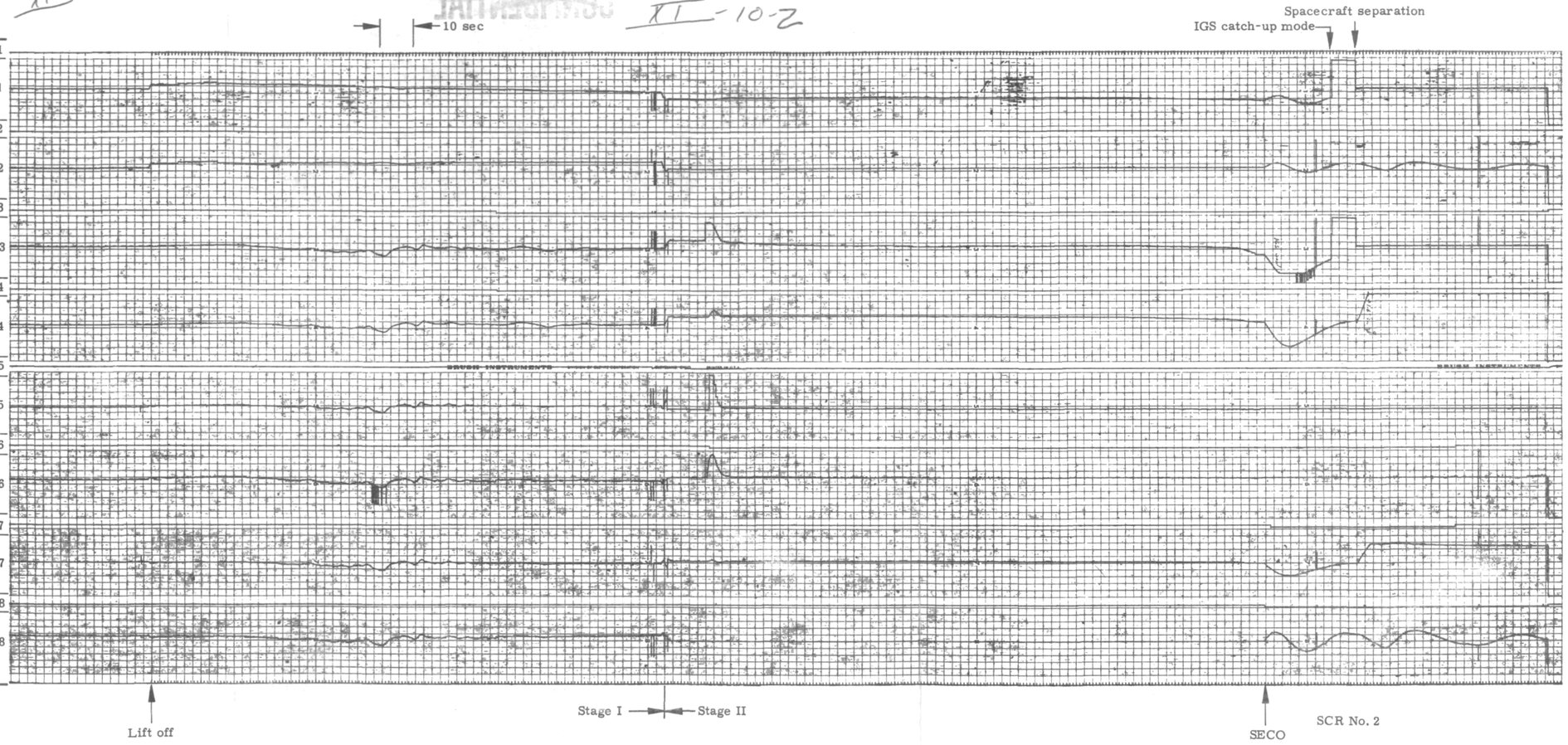

Fig. XI-6. Telemetry III Yaw-Roll Axis Recording

CONFIDENTIAL

CONFIDENTIAL

CONFIDENTIAL

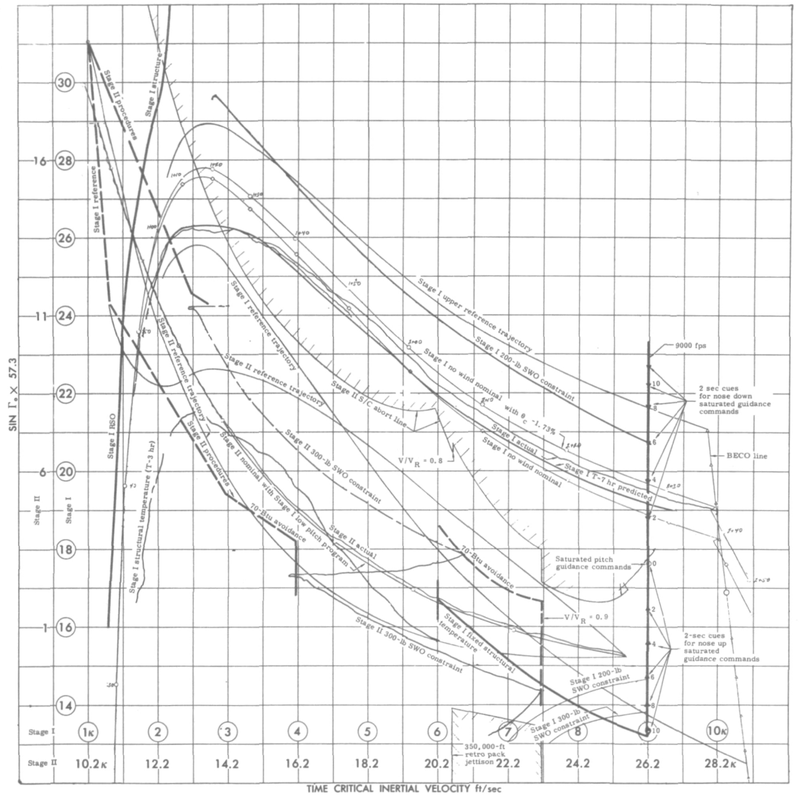

Fig. XI-7. Houston-MCC Plotboard V A, Pitch Plane

XI-12-2

CONFIDENTIAL

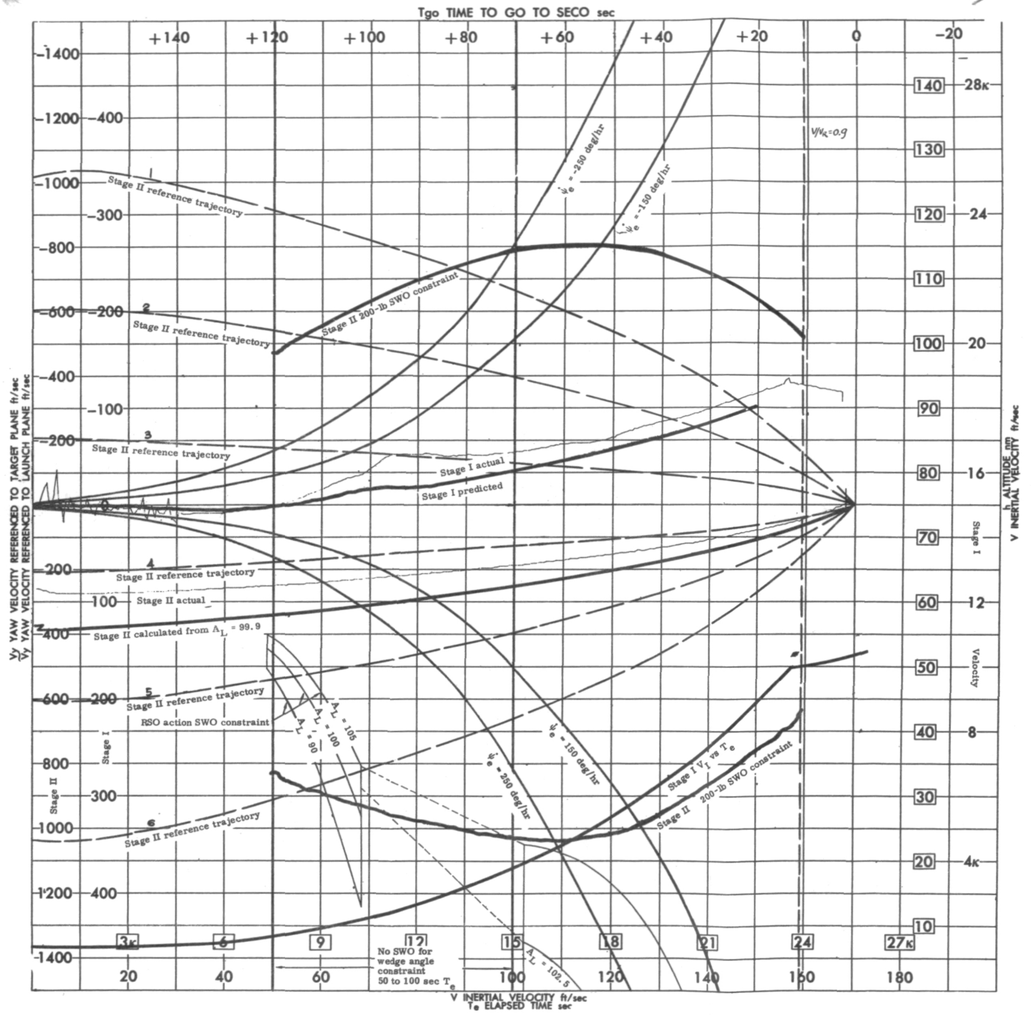

Fig. XI-8. Houston-MCC Plotboard III-A, Lateral Velocity

CONFIDENTIAL

The pitch axis initial rate was 0.62 deg/sec nose-up, decaying to 0 deg/sec and, at spacecraft separation, incurred a nose-up rate of 0.8 deg/sec.

The yaw axis average initial rate was 0.33 deg/sec nose-left, and at spacecraft separation it changed to 1.6 degrees nose-right.

XII. AIRFRAME SYSTEM

A. STRUCTURAL LOADS

Analysis of GT-8 flight data indicates that the loads experienced were well within the structural capability of the launch vehicle. The most critical loading occurred, characteristically, at pre-BECO, where the load aft of Station 320 reached 103.0% of design limit load in compression (DLL_c). Instrumentation for dynamic response data consisted of rate gyros and spacecraft accelerometers for lateral dynamic loads and axially mounted accelerometers for longitudinal dynamic loads. No major anomalies affecting the airframe occurred during flight. Unusually high amplitude axial oscillations occurred continuously during Stage II flight but were not considered to be detrimental.

1. Preignition

The 1 g deadweight distribution is the only contribution to steady axial loading in the preignition period. Ground winds were approximately 16 to 18 mph with gusts up to 22 mph from a direction of 333 to 340 degrees, resulting in steady bending loads of 153,000 in.-lb and wind induced oscillatory (WIO) loads of $\pm$ 860,000 in.-lb (Fig. XII-1) at Station 1224. The WIO response represents approximately 46% of the WIO design limit bending moment; Table XII-1 shows the comparison of GLV WIO loads to date.

TABLE XII-1

Comparison of WIO Loads

Flight	WIO Load at Station 1224 (% of WIO design limit bending moment)
GT-1	52
GT-2	5
GT-3	29
GT-4	3
GT-5	2
GT-7	40
GT-6A	2
GT-8	46

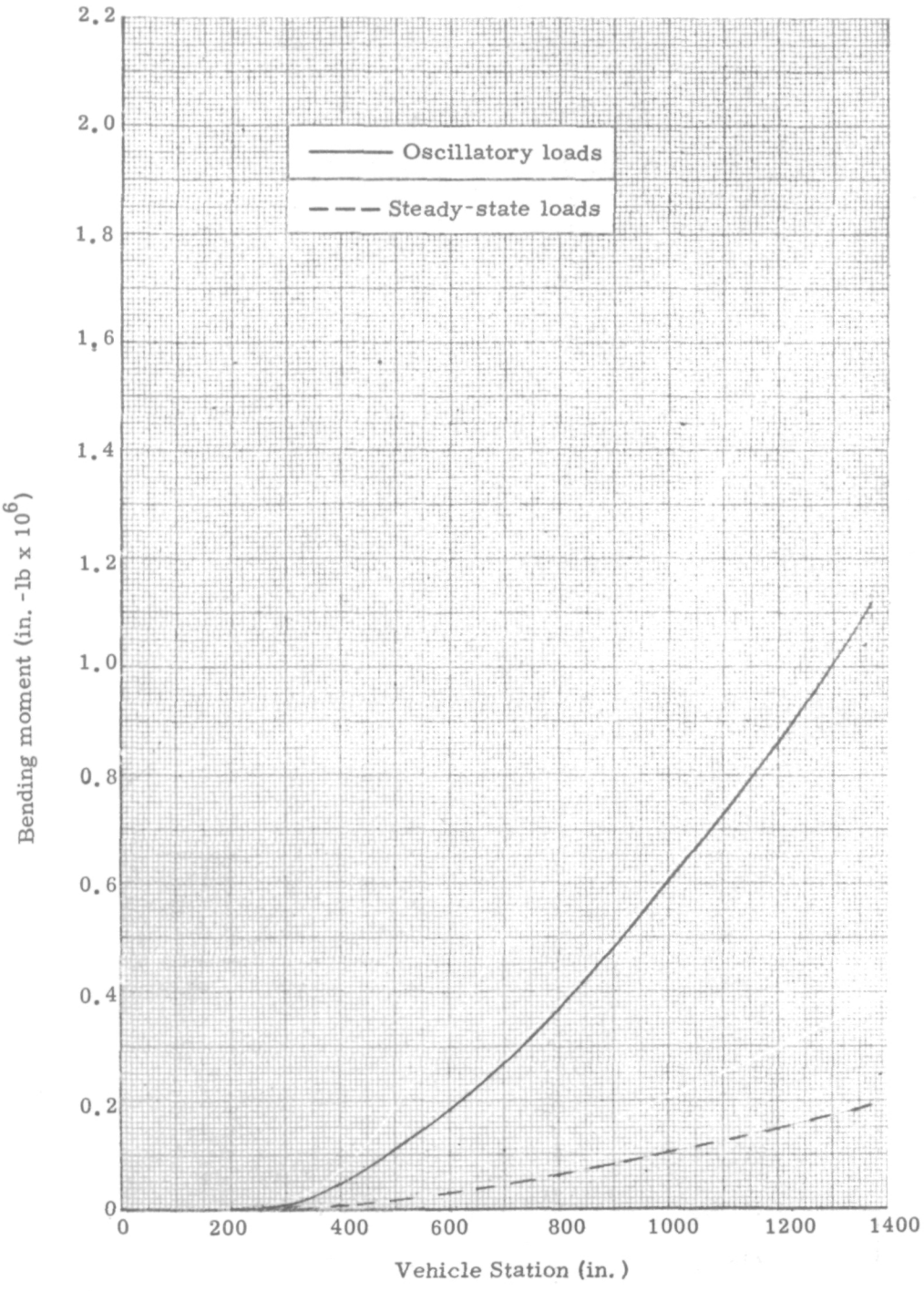

Fig. XII-1. Bending Moments Due to Ground Winds: Preignition

2. Launch Prerelease

Ignition transients were normal, and the attendant dynamic axial loads as measured by the BLH system are shown in Fig. XII-2 together with the steady axial load. The prerelease lateral dynamic loading was due to the combined effects of ground winds and engine start transients; this loading is shown in Fig. XII-3.

3. Launch Postrelease

A comparison (Table XII-2) of the GT-8 liftoff load factor with those of previous launches indicates that this flight experienced an initial steady acceleration which was somewhat lower than usual but within Stage I engine tolerances.

TABLE XII-2

Comparison of Liftoff Load Factors

Flight	Liftoff Load Factor (g)
GT-1	1.27
GT-2	1.27
GT-3	1.27
GT-4	1.27
GT-5	1.28
GT-7	1.26
GT-6A	1.25
GT-8	1.26

Dynamic deformation modes in evidence at postrelease consisted of the first and second structural bending and Stage I engine modes in the lateral plane and the first axial mode in the longitudinal direction. Frequency correlation between calculated and observed modes during the flight is given in Fig. XII-4; the resulting dynamic bending moment in the postrelease condition is shown in Fig. XII-5.

4. Stage I Flight

The most significant periods of Stage I flight for airframe loading occurred at Max C_{N_α} $q\alpha$ and at pre-BECO. Max C_{N_α} $q\alpha$ occurred at LO + 70 seconds, and maximum loading (pre-BECO) occurred at LO + 154 seconds.

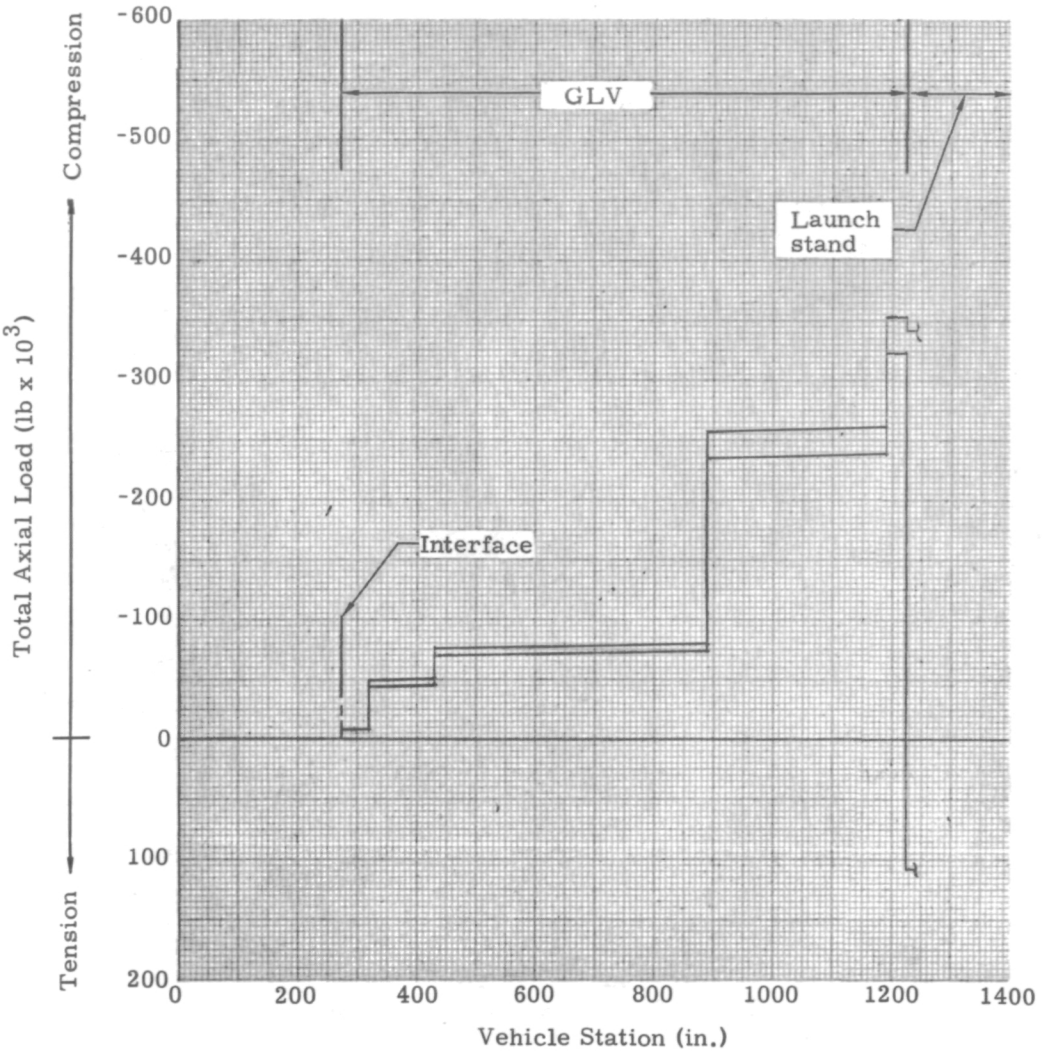

Fig. XII-2. Dynamic Axial Load Envelope: Prelaunch

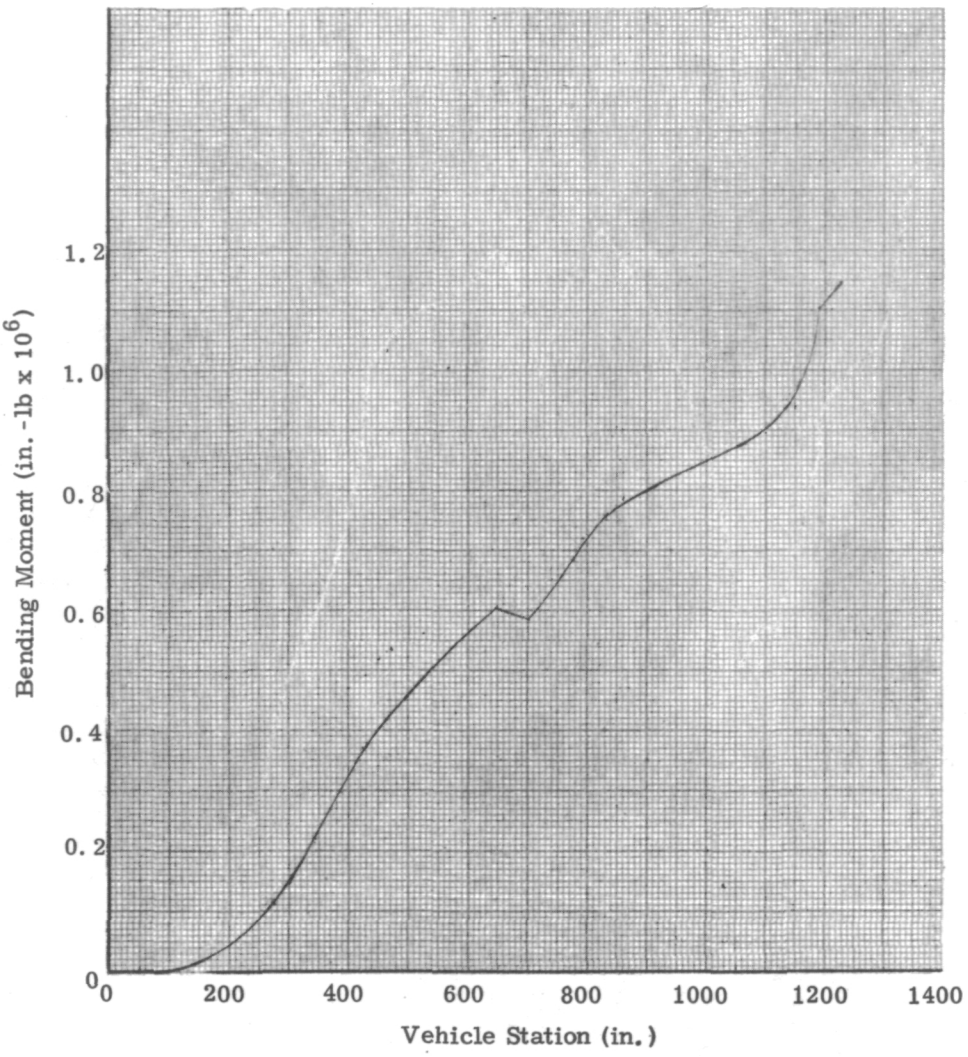

Fig. XII-3. Lateral Dynamic Bending Moment Envelope: Prerelease

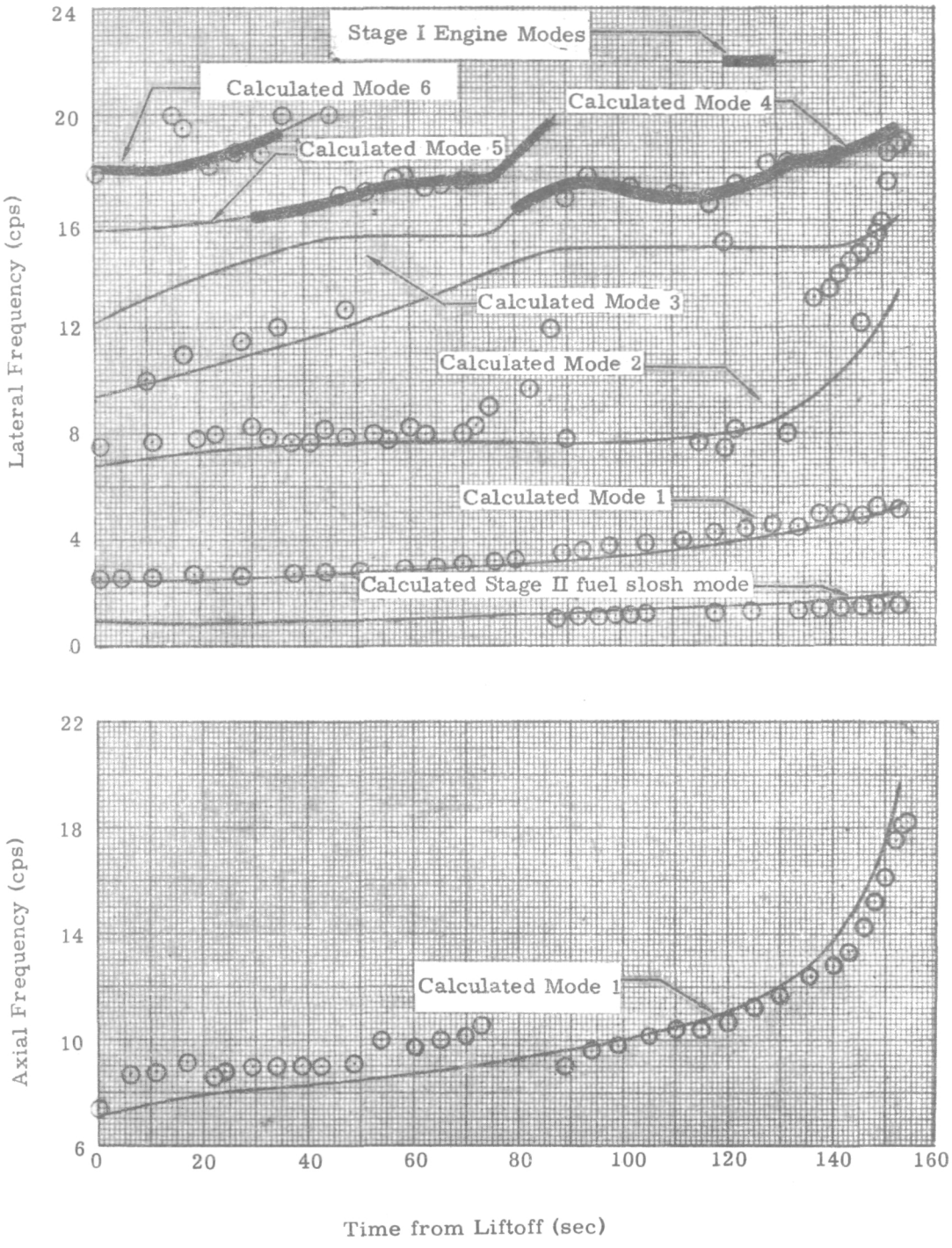

Fig. XII-4. Stage I Flight Vibration Frequency Correlation

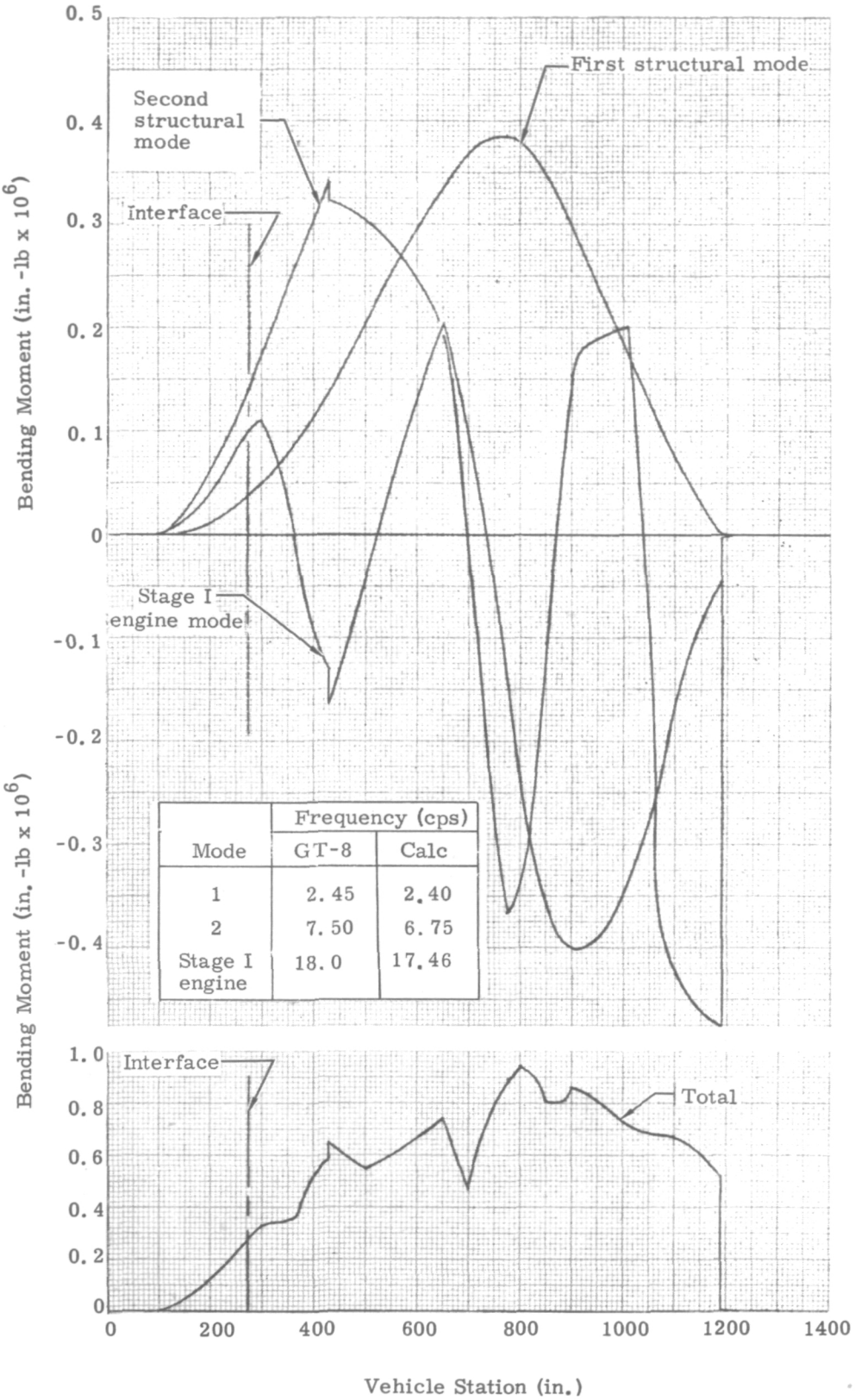

Fig. XII-5. Total Lateral Dynamic Load Envelope: Postrelease

Winds aloft were more severe than those experienced on previous Gemini launches. The wind magnitude at LO + 70 seconds was 76% of the design specification level, and the wind azimuth (right quartering) was closer to the critical azimuth than on any previous flight. The combined effects of high wind magnitude and near-critical wind azimuth with only a moderate reduction in dynamic pressure (resulting from the influence of increased spacecraft weight and slightly lower-than-predicted Stage I engine performance on velocity) resulted in a higher-than-average airframe loading at Max C_{N_α} $q\alpha$. This comparison is shown in Table XII-3.

TABLE XII-3

Structural Loads Comparison

Flight	At Max C_{N_α} $q\alpha$, Station 935 (% of DLL_c)	At Pre-BECO Station 320$^+$ (% of DLL_c)
GT-1	82.3	95.5
GT-2	80.1	100
GT-3	78.5	97
GT-4	85.4	101
GT-5	71.6	98.5
GT-7	72.8	98.5
GT-6A	74.8	103.6
GT-8	82.9	103.0

Dynamic bending moments obtained from the rate gyro responses in the Max C_{N_α} $q\alpha$ and pre-BECO regions of flight are shown in Figs. XII-6. and XII-7, respectively. Steady axial acceleration at pre-BECO is given in Table XII-4.

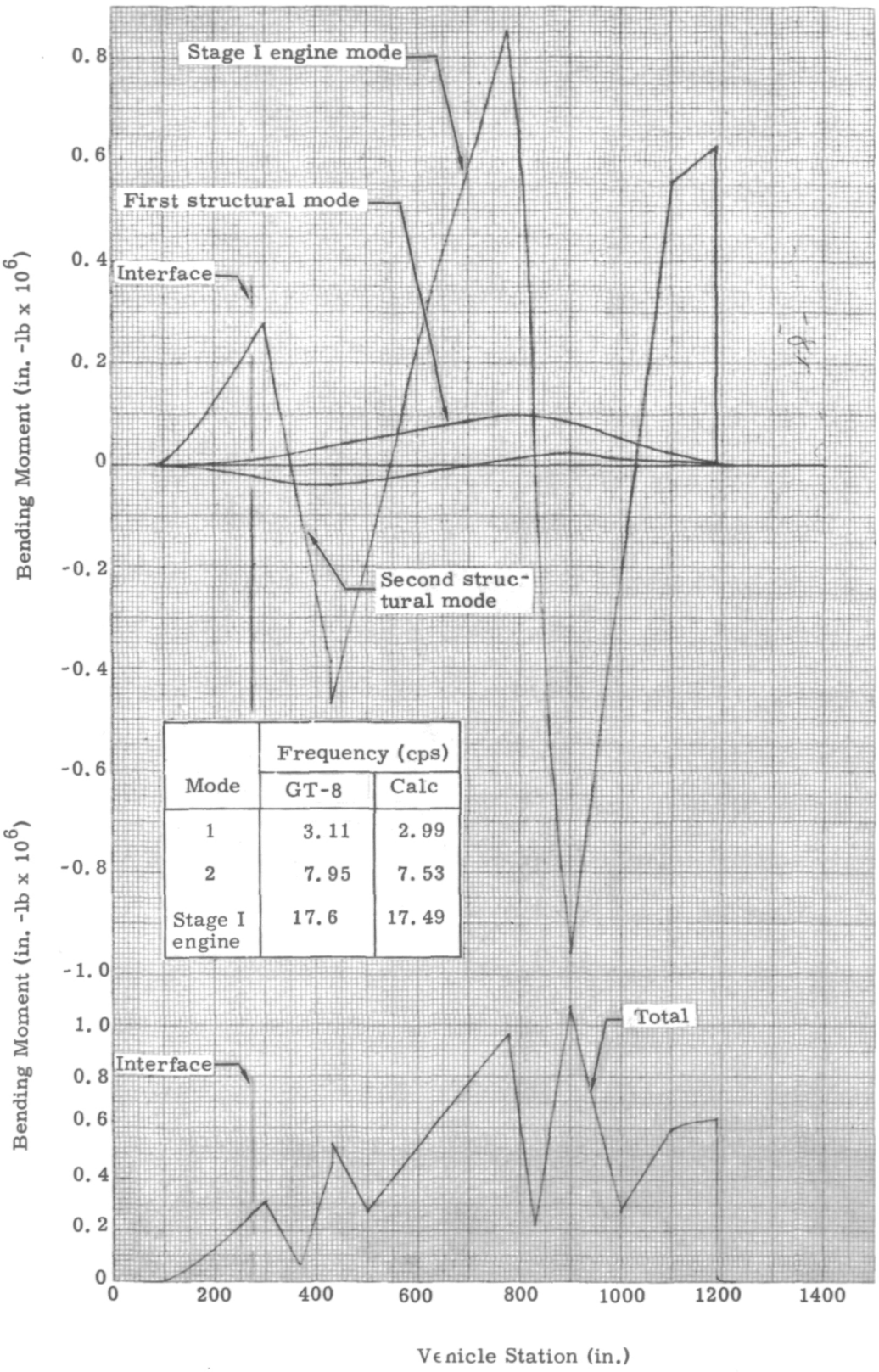

Mode	Frequency (cps)	
	GT-8	Calc
1	3.11	2.99
2	7.95	7.53
Stage I engine	17.6	17.49

Fig. XII-6. Total Lateral Dynamic Load Envelope: Max $C_{N_\alpha} q\alpha$

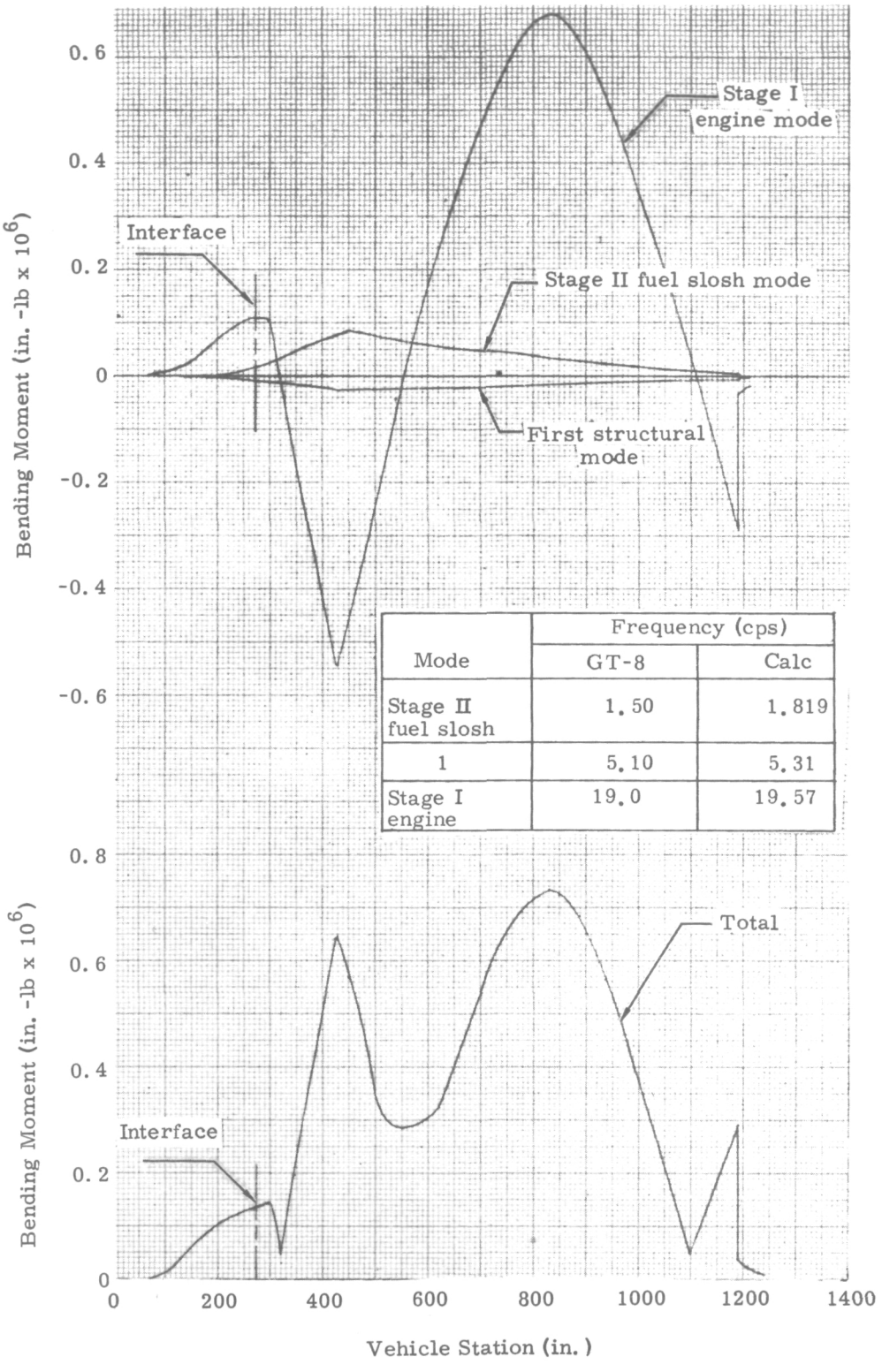

Mode	Frequency (cps)	
	GT-8	Calc
Stage II fuel slosh	1.50	1.819
1	5.10	5.31
Stage I engine	19.0	19.57

Fig. XII-7. Total Lateral Dynamic Load Envelope: Pre-BECO

TABLE XII-4

Steady Axial Accelerations at Pre-BECO

Flight	Pre-BECO Axial Acceleration (g)
GT-1	5.61
GT-2	5.69
GT-3	5.63
GT-4	5.63
GT-5	5.55
GT-7	5.56
GT-6A	5.46
GT-8	5.57

Lateral oscillations associated with the third structural and Stage I engine modes of the launch vehicle occurred intermittently prior to BECO. The dynamic loads resulting from the oscillations in these two modes, while significant, were comparable to those experienced on several previous flights (GT-2, GT-4, and GT-6A).

5. Stage II Flight

Propellant slosh oscillations, associated with the calculated Stage II fuel slosh mode, occurred continuously from LO + 220 seconds to LO + 320 seconds; the amplitude of the oscillations was small (± 0.09 deg/sec at LO + 285 seconds), as indicated by both pitch (predominant) and yaw rate gyros. In addition, first structural bending mode oscillations occurred continuously during the period from BECO to LO + 310 seconds, reaching a maximum amplitude of ± 0.2 deg/sec at LO + 239 seconds. This response was predominantly in the pitch plane and is attributed to Stage II engine operation.

Axial dynamic oscillations, with a frequency varying from 2.4 cps to 12.3 cps in the flight period of BECO + 20 seconds to SECO, also occurred during Stage II flight. The maximum amplitude attained was ± 0.24 g with a frequency of 10.2 cps at LO + 181 seconds at the spacecraft-launch vehicle interface. This response, although observed on previous flights at a much reduced amplitude, does not correspond to any theoretically determined frequency and is at present under investigation.

The steady axial acceleration at SECO is shown in Table XII-5 and was the lowest of any GLV flight. This is attributed to a combination of lower-than-predicted Stage II thrust level, low thrust level at SECO, increased spacecraft weight and trajectory differences. Stage II engine shutdown at SECO, as indicated by axial acceleration decay transients, was unusually rough.

TABLE XII-5

Steady Axial Accelerations at SECO

Flight	SECO Axial Acceleration (g)
GT-1	7.35
GT-2	7.70
GT-3	7.50
GT-4	7.42
GT-5	7.56
GT-7	7.23
GT-6A	7.33
GT-8	7.20

There were six indications of post-SECO disturbances on both the low range (± 0.5 g, Meas 0699) and high range (± 10 g, Meas 0670) axial accelerometers. The times of occurrence of these disturbances and their associated g levels were:

(1) 3.04 g peak-to-peak at SECO + 3.33 seconds

(2) 2.53 g peak-to-peak at SECO + 3.80 seconds

(3) 2.19 g peak-to-peak at SECO + 4.43 seconds

(4) 1.01 g peak-to-peak at SECO + 5.35 seconds

(5) 0.02 g peak-to-peak (Meas 0699) at SECO + 7.12 seconds

(6) 0.42 g peak-to-peak (Meas 0670) at SECO + 34.60 seconds

Spacecraft separation from the sustainer occurred at SECO + 28.10 seconds.

6. Total Airframe Loads

A summary of the total airframe loads (quasi-steady axial, dynamic axial and equivalent axial loads from quasi-steady and dynamic bending moments) for significant structural loading conditions at critical stations is presented in Table XII-6. Complete vehicle loading at significant flight times is shown in Figs. XII-8 through XII-12. The maximum load at any station and the loading condition for which it occurred are shown in Fig. XII-13.

TABLE XII-6

Summary of Total Airframe Loads

Flight Condition	Total Airframe Load (% of DLL_c at critical station)	Critical Station
Prerelease	71.3	1188*
Postrelease	78.8	1188*
Max C_{N_α} $q\alpha$ (LO + 70 sec)	82.9 & 90.9	935 & 1188*
Pre-BECO (LO + 154 sec)	103.0	320*
Pre-SECO (LO + 337 sec)	75.2	276.8*

*Just aft of station.

B. POGO

Analysis of GT-8 telemetry data showed that the POGO suppression devices (fuel accumulators and oxidizer standpipes) operated satisfactorily. No pressure oscillations associated with airframe structural resonances were detected in either the oxidizer or the fuel feedline until three seconds prior to BECO. At that time, sustained oscillations of significant amplitude (which are characteristic of the POGO phenomenon) occurred until Stage I engine shutdown. This occurrence is not altogether unexpected since the analytical analysis of Ref. 17 predicts that, in the final 5% of Stage I burn time, the first axial dynamic mode of the launch vehicle structure becomes increasingly unstable due to the increase in propellant line resonances and the rapidly increasing structural gain. However, this tendency toward instability in the last few seconds of Stage I flight has occurred on only one previous GLV flight (GT-1), which may be explained by the variation in structural damping from vehicle to vehicle.

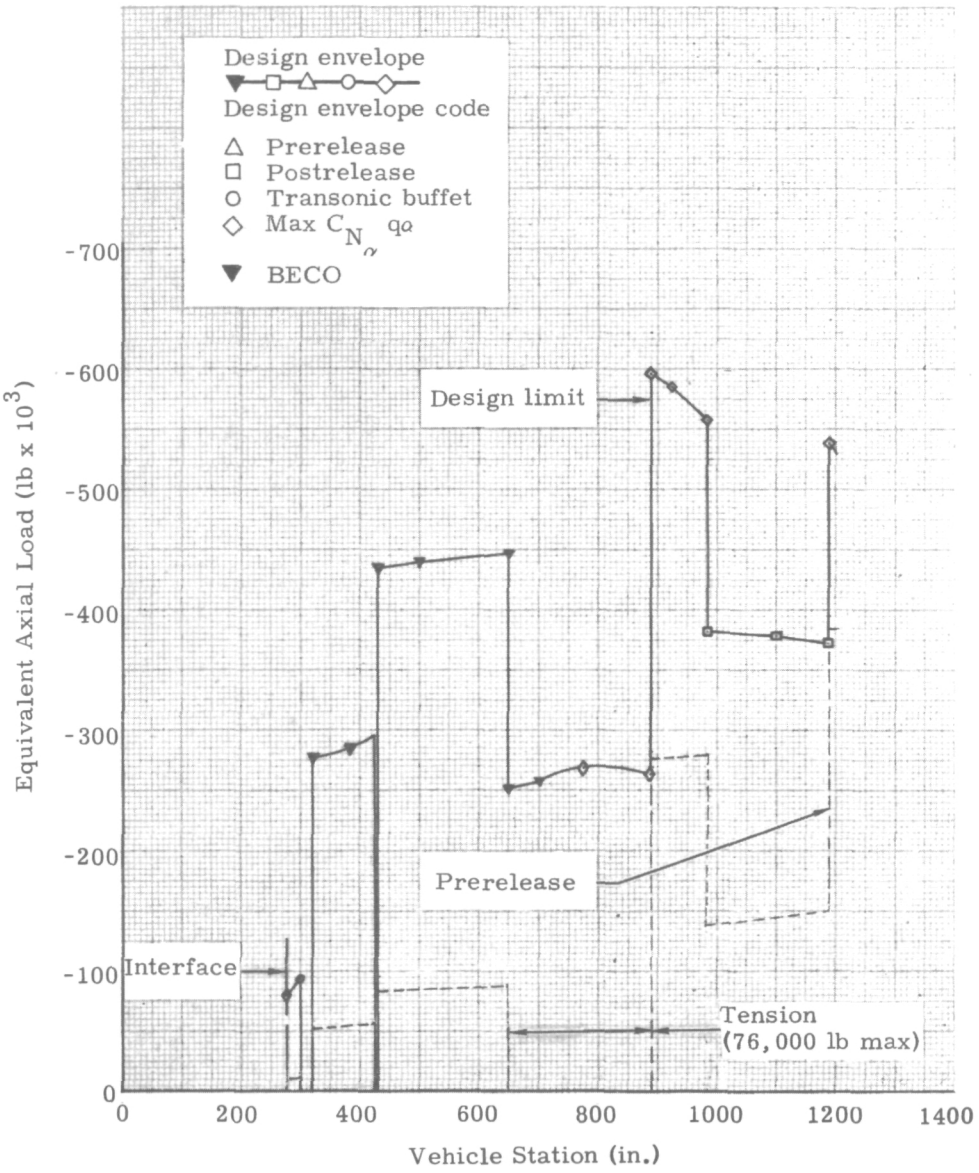

Fig. XII-8. Equivalent Axial Load: Prerelease

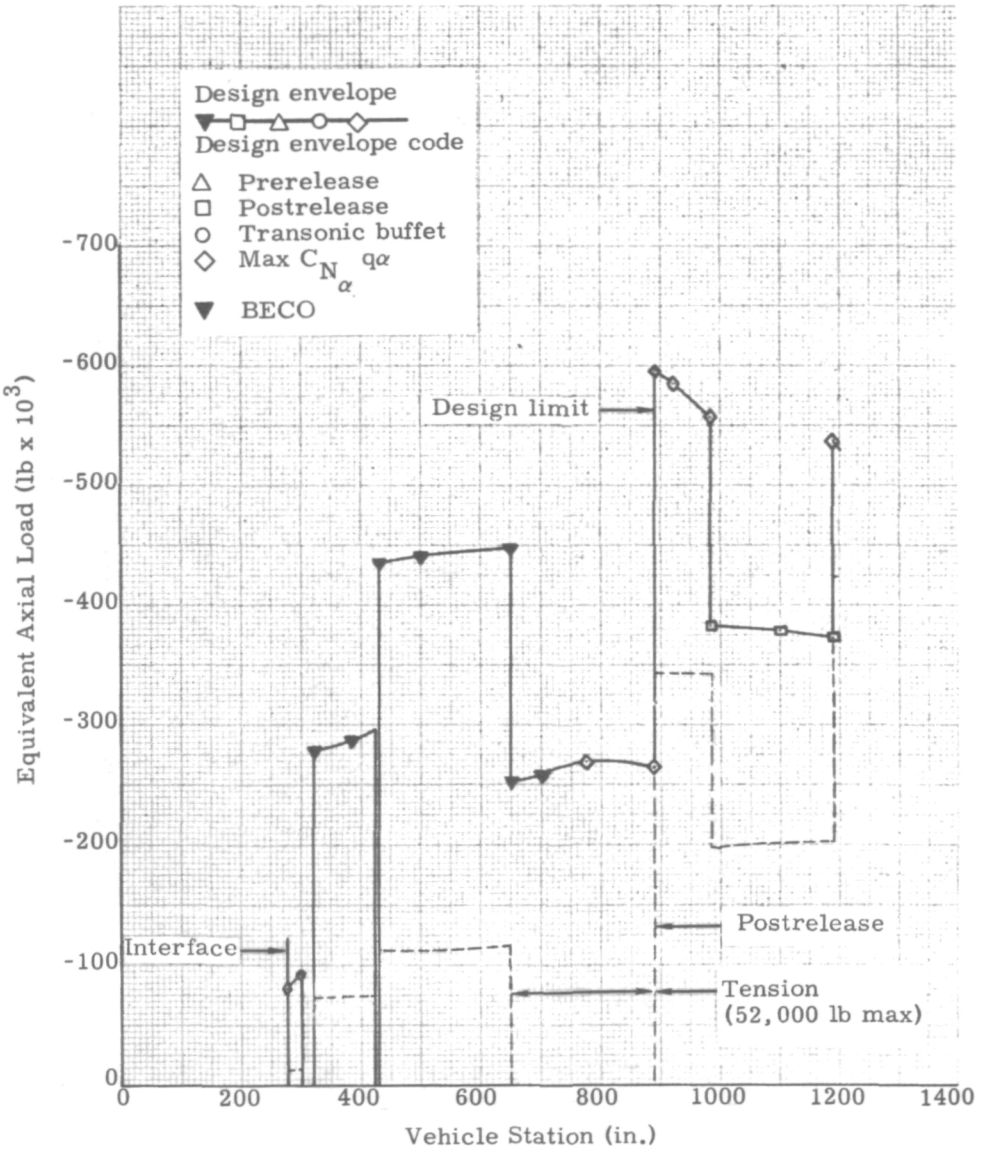

Fig. XII-9. Equivalent Axial Load: Postrelease

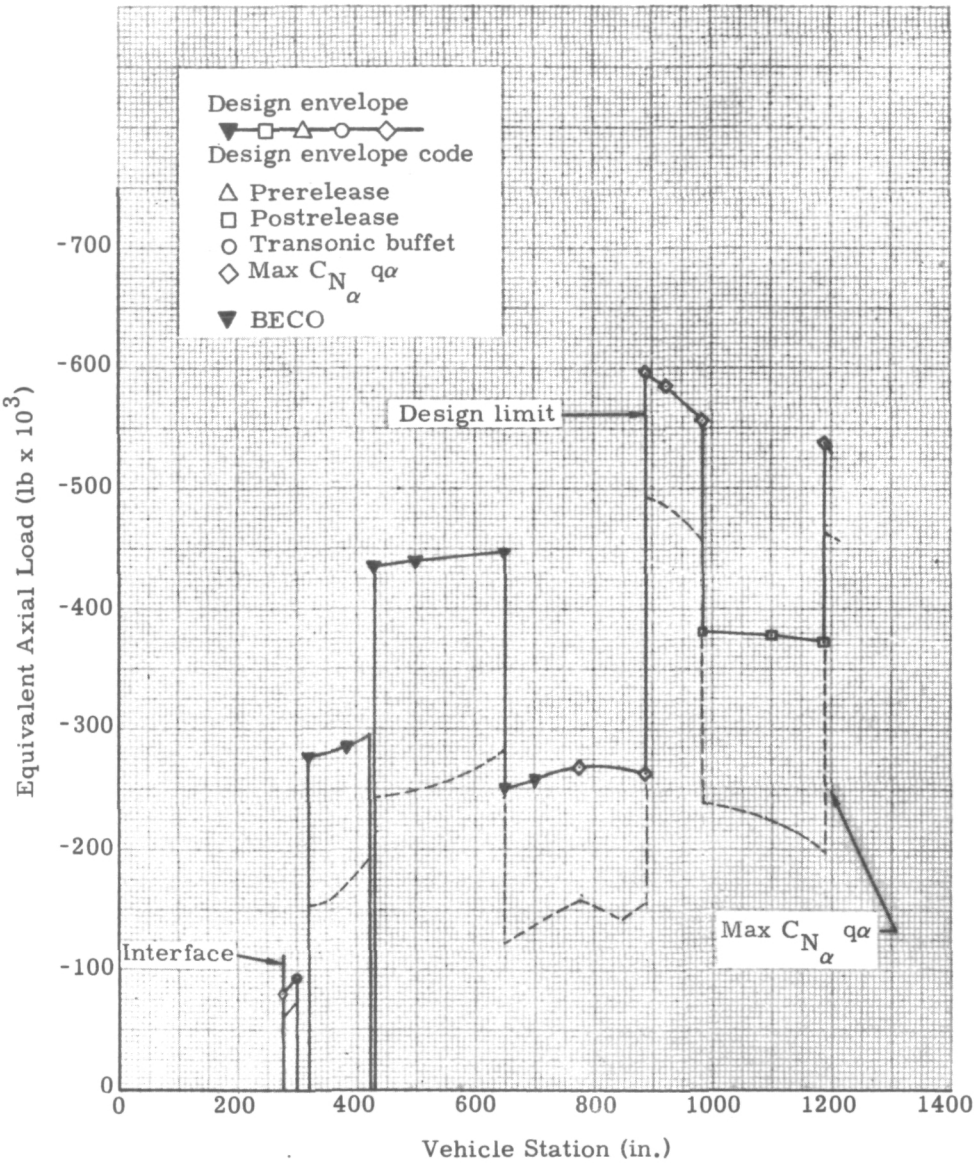

Fig. XII-10. Equivalent Axial Load: Max C_{N_α} $q\alpha$

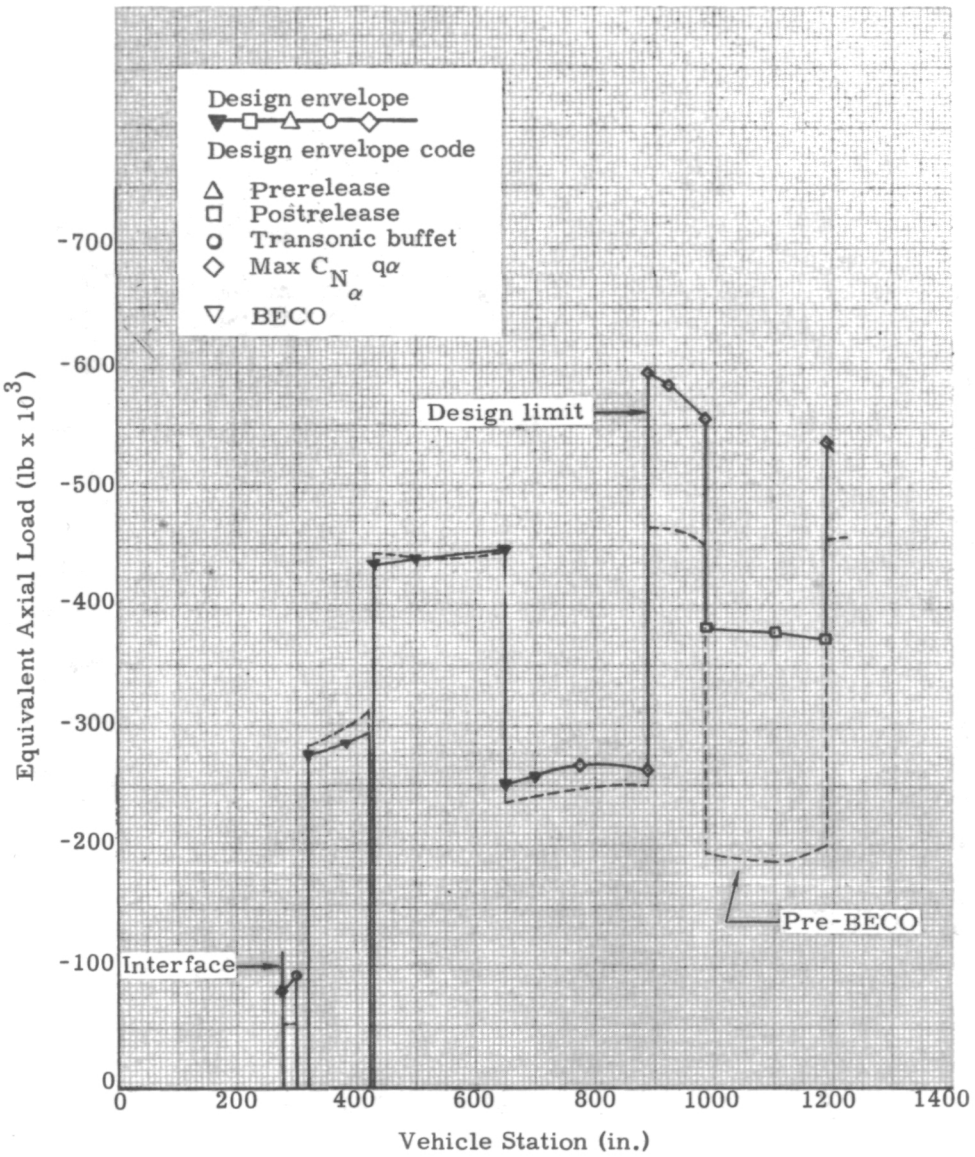

Fig. XII-11. Equivalent Axial Load: Pre-BECO

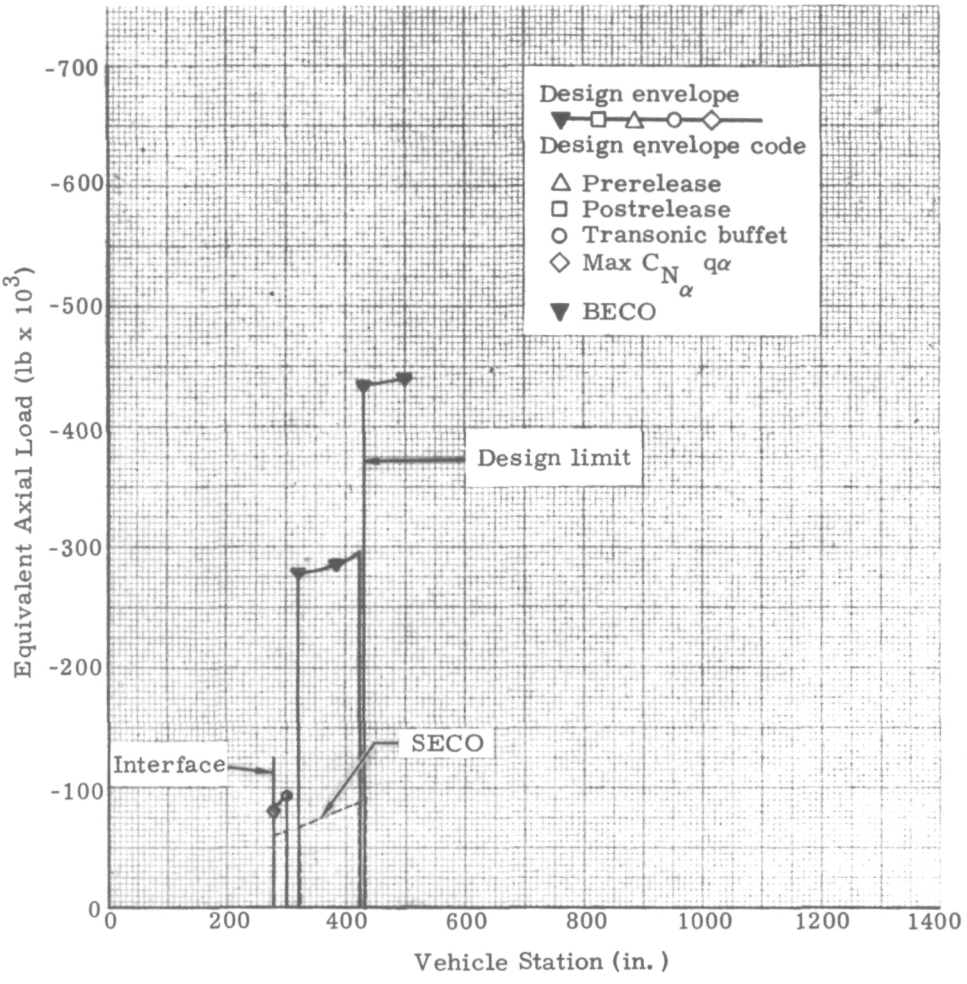

Fig. XII-12. Equivalent Axial Load: SECO

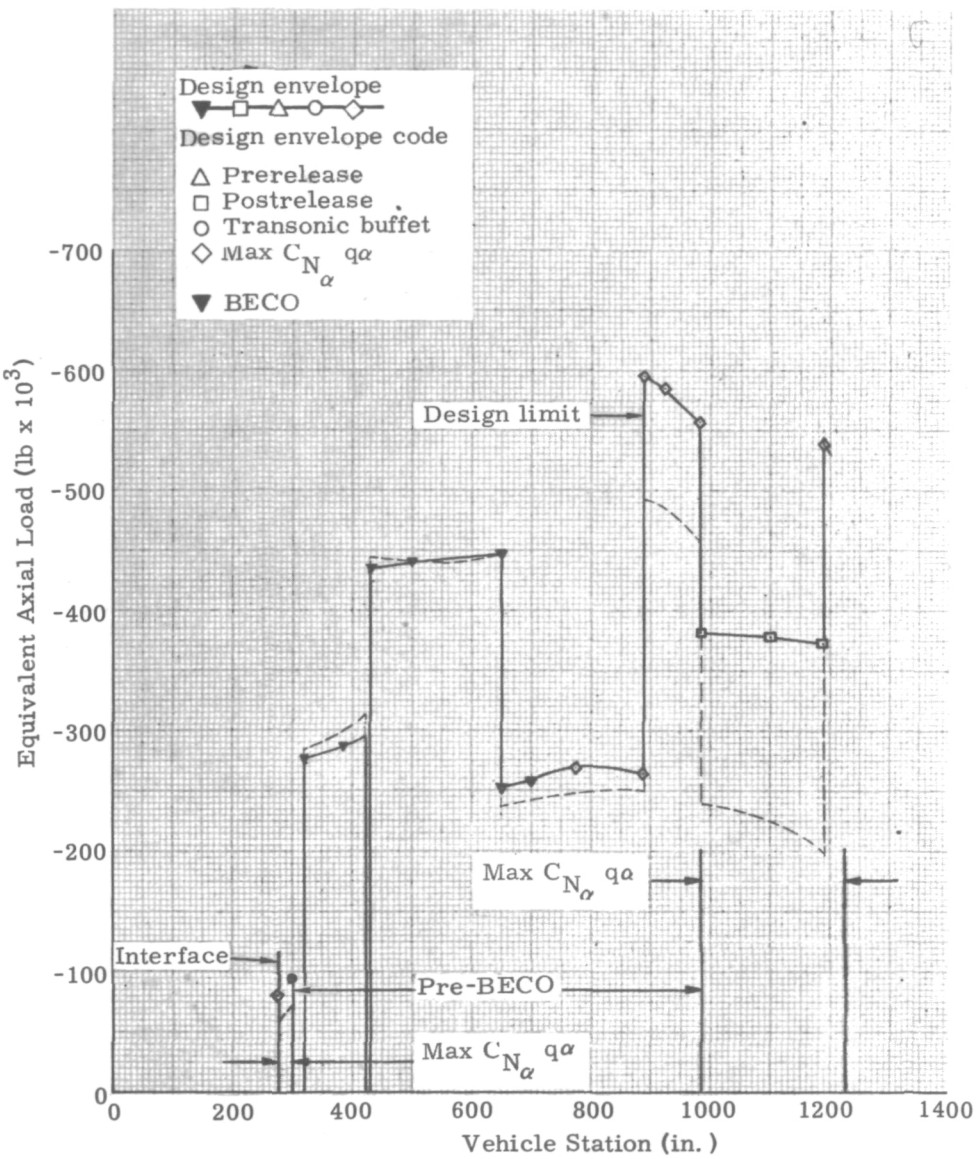

Fig. XII-13. Maximum Structural Load Envelope

Bandpass filtering of the analog reconstruction of PCM/FM telemetry (Meas 0670) indicates that the maximum intermittent longitudinal oscillation at the spacecraft-launch vehicle interface occurred at LO + 135.4 seconds. The amplitude of these oscillations was 0.215 g zero-to-peak with a response frequency of 12.4 cps. The maximum oscillation at the spacecraft-launch vehicle interface occurred at LO + 154.2 seconds and had an amplitude of 0.295 g zero-to-peak at 18.2 cps. This maximum amplitude was achieved for only one or two cycles of oscillation (approximately 0.07 second); for the most part, the oscillation was sustained at a level of 0.2 g zero-to-peak. The time history of POGO response amplitude for Compartments 1 and 5 is shown in Fig. XII-14.

Figure XII-15 is a comparison of longitudinal oscillations for the last four GLV flights. The occurrence of sustained oscillations in both Compartments 1 and 5 is shown in Fig. XII-16.

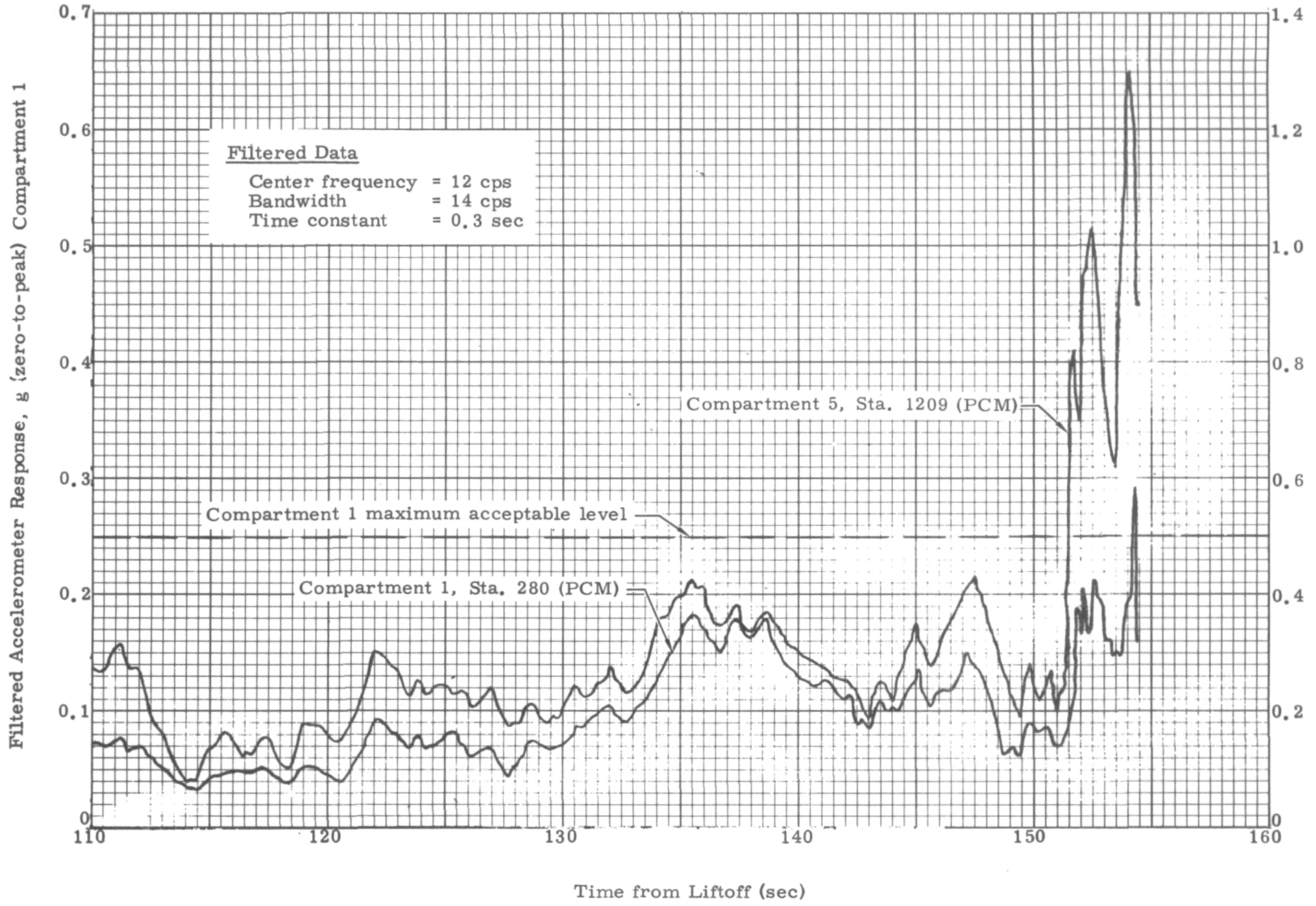

Fig. XII-14. Longitudinal Oscillations

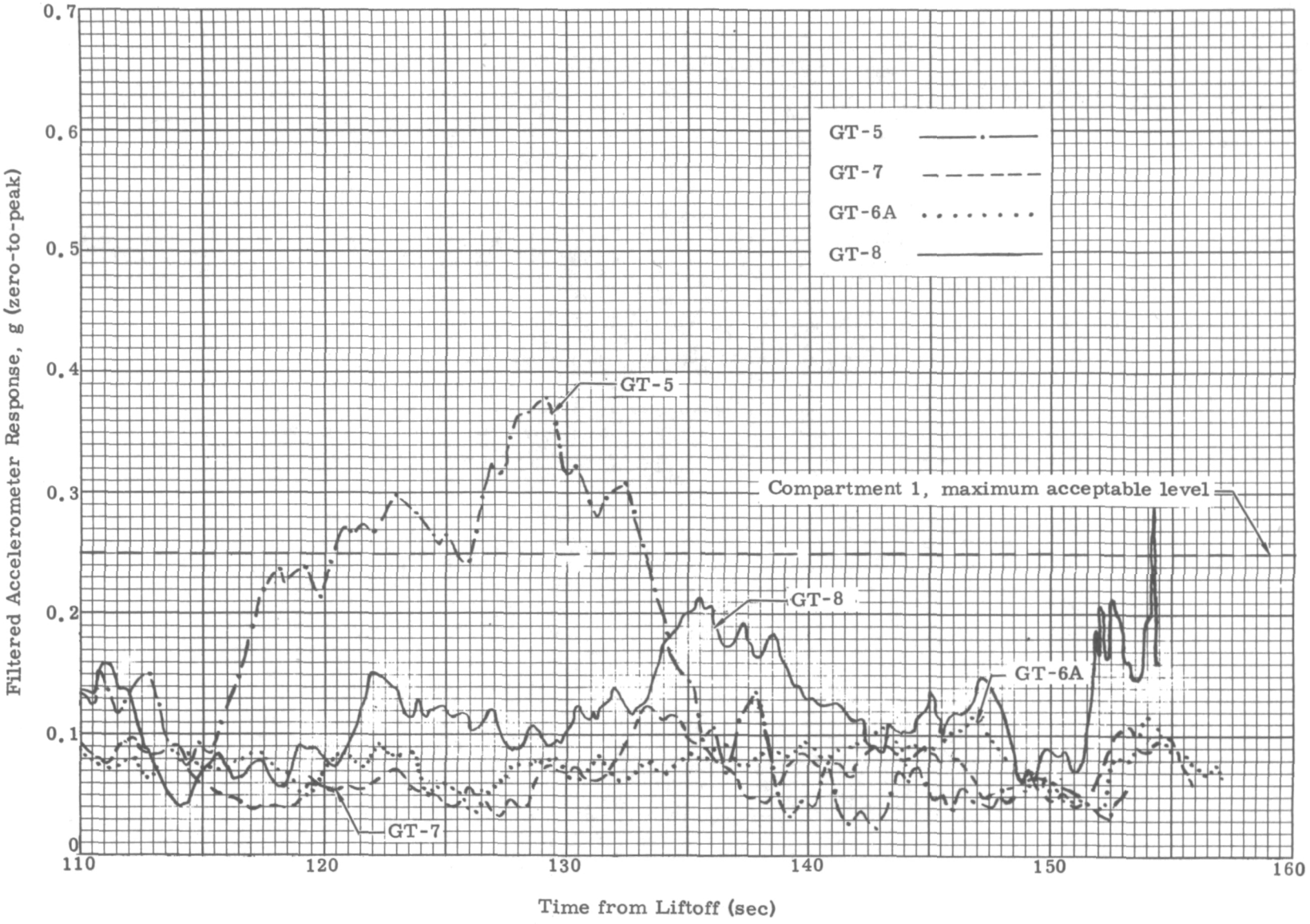

Fig. XII-15. Longitudinal Oscillations, Compartment 1 (Station 280)

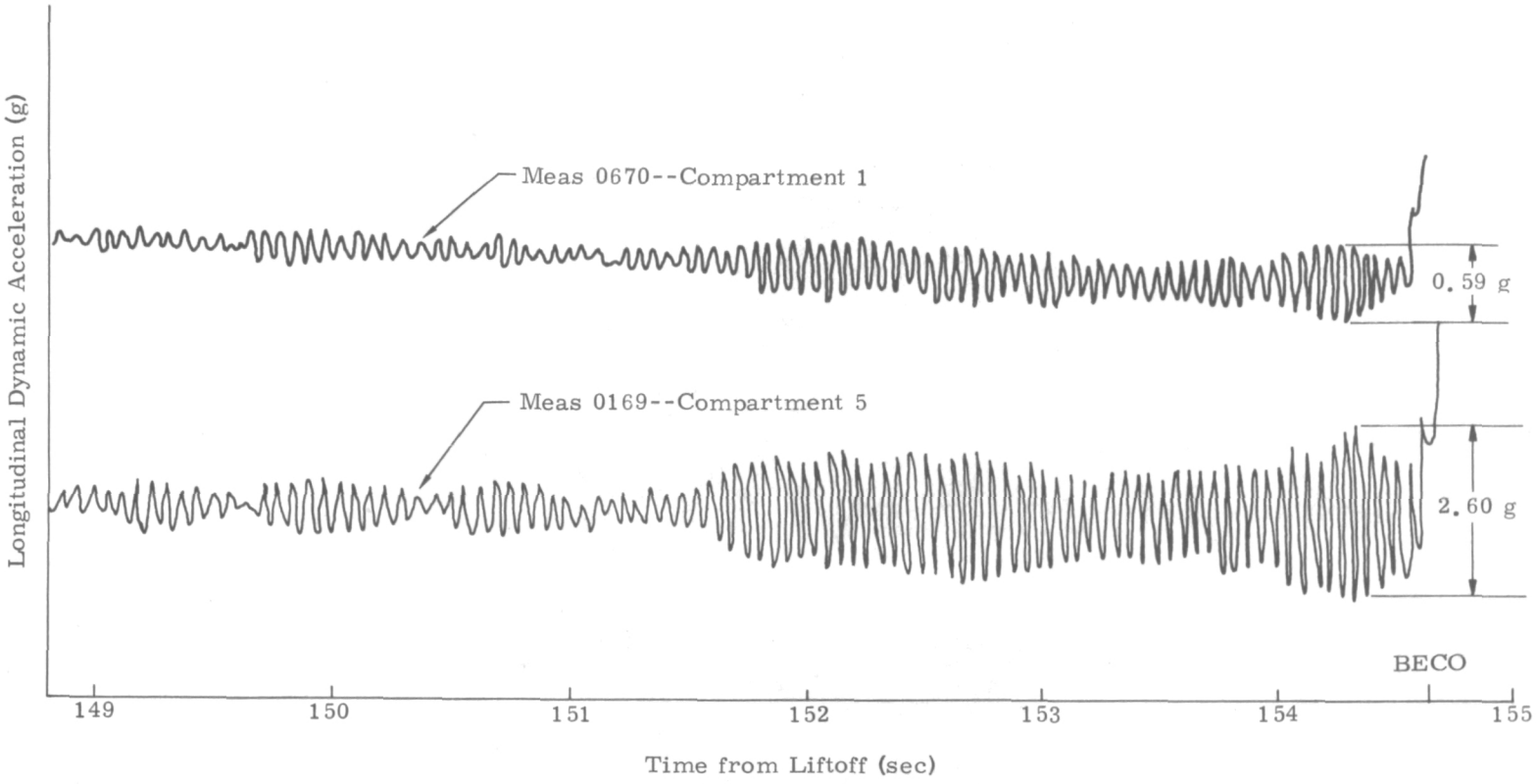

Fig. XII-16. GT-8 Sustained Longitudinal Oscillations Prior to BECO

XIII. AGE AND FACILITIES

A. MECHANICAL AGE

1. Precount Operations

The mechanical AGE utilized prior to countdown is primarily for transport and erection of Stages I and II. Both stages of GLV-8 were airlifted successfully to Cape Kennedy by B-377PG aircraft. During erection, all equipment functioned as designed.

2. Countdown and Launch Operations GLV-8 (March 16, 1966)

Analysis of magnetic tape recordings of functions carried through the umbilicals and inspection films confirm that all launch vehicle umbilicals separated cleanly in the planned sequence. The release times of the electrical umbilicals are presented in Table XIII-1.

TABLE XIII-1

Electrical Umbilical Disconnect Sequence

Umbilical Designation	Time of Disconnect (GMT)
3D1M/3D2M	1641:02.383
3D1E	1641:02.526
3D2E	1641:02.780
3B1E	1641:03.030
2B1E	1641:03.200
2B2E	1641:03.208

During launch, the spacecraft umbilical (Cable A) did not respond to the force exerted by the dropweight system, but immediately thereafter it was separated from the spacecraft by the static lanyard.

3. Post-Launch Operations

Mechanical AGE suffered no significant damage other than normal weather curtain tears and fraying. However, the weather curtains were disturbed one level higher on the erector than usual. This was caused by the prevailing north wind driving the blast cone effects up the erector.

B. ELECTRICAL AGE

Except for one anomaly during the FCS test, the launch and checkout equipment operated satisfactorily during prelaunch and launch operations. At T-60 minutes in the countdown, the TARS programmer test was performed using the CP 2650 recorder to indicate the values of the TARS torquer monitor voltages and program times of the roll and pitch programs. The torquer monitor voltage traces were 9.6 to 13.4% above nominal, indicating an out-of-specification condition. The test was rerun at T-32 minutes using airborne telemetry to measure the torquer monitor voltages; the telemetry indicated normal, in-specification voltages. Investigation of the CP 2650 recorder indicates that a variation in amplitude of the 20-kc oscillator power supply will cause a corresponding change in gain of the recorder; this is presently being analyzed.

C. MASTER OPERATIONS CONTROL SET (MOCS)

Analysis of the MOCS automatic sequence records shows that all functions were performed properly. The automatic countdown sequence was picked up at T-35 minutes and proceeded on schedule to the programmed hold at T-3 minutes. After a planned hold of 5 minutes and 54 seconds, the count was resumed and continued through a successful liftoff. MOCS T-0 occurred at 1640:59.037 GMT followed by TCPS "make" at T + 1.06 seconds. The following MOCS generated time functions occurred as specified:

TCPS + 1.6 seconds

TCPS + 1.8 seconds

TCPS + 2.0 seconds (fire launch nuts)

The launch operation through liftoff was completed in 3.352 seconds.

The recorders were changed to high speed at T-2 minutes. During the automatic portion of the count, the operation of the sequencer was compared to the real-time trace and patch list. All traces were checked for time of occurrence and were found to be correct and consistent with the planned operation of the sequencer.

D. FACILITIES

All facility items functioned properly throughout the launch and countdown.

1. Pad Damage

Damage to AGE and facility items caused by engine blast and heat was minor. All damaged items will be refurbished to their original configuration. A list of the most significant damaged items follows:

Complete Vehicle Erector

(1) Insulation on lines at base of CVE (east side) was damaged.

(2) Corrugated aluminum siding panels at east side of CVE at the 9-foot 8-inch, 26-foot 7-inch and 35-foot 4-inch levels were blown loose.

(3) L/V personnel elevator (west side) damage was as follows:

(a) Elevator door guard screen at the 9-foot 8-inch level entrance was blown loose.

(b) Elevator door at the third level was blown out of track.

(4) Spacecraft service elevator damage was as follows:

(a) Traveling cable duct was blown in and broken loose at the lower end.

(b) Overspeed governor cable tension device was damaged.

(c) Cam guide rail was bent at the 15-foot level.

(5) Ground strap on east pivot point was torn apart.

(6) Spacecraft cable raceway cover was damaged at the lower level (near southwest pivot).

(7) Electrical damage consisted of the following:

(a) J-box conduit at the 5-foot level on the east side was torn loose.

(b) Several lights and globes were broken at the lower levels.

(c) Light fixture under northeast corner of 26-foot 7-inch level was torn loose.

Complete Vehicle Umbilical Tower (CVUT)

(1) Level No. 1 white room air-conditioning duct insulation was damaged near the deck.

(2) Level No. 2 elevator cable guard screen was damaged.

(3) Level No. 3 elevator cable guard screen was bent.

Deck Area

(1) Flame shield on second stage erector (SSE) west leg lock was damaged.

(2) Deck grating was loose at the side of spacecraft elevator ramp.

(3) Floodlight damage was as follows:

(a) Floodlight standard on west side near CVUT was bent.

(b) Spray header support was bent outward from deck at the west side next to CVUT.

(4) Emergency shower frame and sides were bent on the east side.

(5) Portable erector control J-box and conduit were torn loose from the east side of CVUT near the deck.

XIV. RELIABILITY

Based on countdown experience through GLV-6, the average number of holds per countdown ($\bar{h}$) was calculated to be 0.100, i.e., one hold per ten countdowns. The probability of GLV-8 completing the countdown without a hold was predicted to be

$$P_{C/D}\ (\bar{h} = 0.1) = 0.90$$

Including the GLV-8 countdown, the average number of holds per countdown ($\bar{h}$) is shown in Table XIV-1 to be 0.091, i.e., one hold in 11 countdowns. The probability of GLV-9 completing countdown without a hold is predicted to be

$$P_{C/D}\ (\bar{h} = 0.091) = 0.913$$

$\bar{h}$ is based on countdown experience from T-240 minutes to T-0, except for the GLV-5 attempt, which was scrubbed at T-10 minutes. Spacecraft holds and SCF tests were not counted.

Countdown experience for all GLVs is included in Table XIV-1.

TABLE XIV-1

Countdown Data for 45-Day Report

Vehicle No.	Number of Countdowns	Number of Holds	Remarks
GLV-1	1	0	
GLV-2 (attempt)	1	0	3 S/C holds Tandem actuator failed after T-0
GLV-2	1	0	1 S/C hold
GLV-3	1	0	1 hold--not Martin's responsibility (oxidizer leak in Stage I engine transducer)
GLV-4	1	1	Erector stuck during lowering
GLV-5 (attempt)	1	0	1 S/C hold. Incomplete countdown--scrubbed at T-10 due to weather
GLV-5	1	0	
GLV-6 (attempt on 25 Oct 65)	0	0	Incomplete countdown--scrubbed at T-42 due to Agena failure
GLV-7	1	0	
GLV-6 (attempt on 12 Dec 65)	1	0	Umbilical failed (prematurely disconnected), and dust cap left in gas generator line--both after T-0
GLV-6 (launched on 15 Dec 65)	1	0	
GLV-8	1	0	
Total	11	1	

Note: Prediction for GT-9 based on data through GT-8.

*Based on Martin holds only.

XV. RANGE DATA

A. LAUNCH DATA DISTRIBUTION

1. Quick-Look Range Data

All available quick-look data were supplied by ETR to Martin-Baltimore as shown in Table XV-1.

The PCM serial FR600 magnetic tape was of excellent quality. The final formatted magnetic tape was of excellent quality and contained no redundancies. Except for approximately 330 milliseconds of transmission blackout during booster staging, the Tel II formatted tape showed only three bad data words from LO - 10 seconds to LO + 395 seconds. The Station 3 formatted tape was of comparable quality with only 18 bad words to LO + 420 seconds.

TABLE XV-1

Range Supplied Quick-Look Data

Description	Time Requested	Time Received (ETR)	Time Received (Baltimore)
Telemetry magnetic tapes:			
Tel II, PCM/FM FR600 (5 rolls)	T+1 hr	T+1 hr	T+8 hr
Station 1 formatted final (3 rolls)	T+9 hr	T+6 hr	T+12 hr

2. Martin Data

Test data and records acquired and generated by Martin at Cape Kennedy were received in Baltimore within two days after launch.

These data consisted of the following items:

(1) One set of quick-look records from RCA tape

(2) High speed records of engine parameters

(3) Landline records (events, Bristol, Multipoint and Sanborn) with associated calibrations

(4) BLH tabulations

(5) CP 2600 records (2612, 2650 and 2660)

(6) Sequencer records with code sheets

(7) Dub of Complex 19 landline magnetic tape

(8) Fuel and oxidizer loading records.

3. Range Data

All data supplied by the ETR are summarized in Table XV-2. The time requested for delivery to Martin-Canaveral (Ref. 6555th ATW Form 1-116, dated 9 March 1966) and the time received at Baltimore are shown in this table.

TABLE XV-2

Range Supplied Data

OD Item No.	Description	Time Requested (Canaveral)	Time Received (Baltimore)
5	Attitude, pitch, yaw and roll (camera)	3 CD	6 CD
8	Position, velocity, acceleration and special parameters (radar)	4 CD	13 CD
19	Position, velocity and acceleration MISTRAM I	5 CD	7 CD
20	Position, velocity, acceleration and special parameters, MISTRAM I and MISTRAM II	11 WD	10 WD
26	Best estimate of trajectory and special parameters	15 WD	18 WD
29.9	Function recordings, MISTRAM I	5 WD	6 WD
4.9	Function recordings, MISTRAM II	5 WD	6 WD

TABLE XV-2 (continued)

OD Item No.	Description	Time Requested (Canaveral)	Time Received (Baltimore)
1	Real-time computer facility selected sources	12 hr	24 hr
246	Quick-look reduction, trajectory parameters, KSC	1 CD	7 CD
64 (f)	Weather, Rawinsonde Stations 1, 4 and 29	6 hr	6 hr
64 (f)	Weather, Metroc Station 1, wind data	8 hr	5 WD
64 (f)	Weather, surface, Station 1	1 WD	6 hr
64 (f)	Weather, tower 700/701, Station 1	1 WD	6 hr
64 (f)	Weather, triple theodolite, Station 1	3 WD	1 WD
64 (f)	Weather, Metroc, Station 1 (200K)	3 WD	5 WD
1.5-2	Magnetic tape, serial PCM FR600 quick-look (Tel II)	1 hr	1 hr
1.5-2	Magnetic tape, serial PCM FR600 final (Tel II)	1 WD	1 WD
3.5-2	Magnetic tape, serial PCM FR600 (GBI)	3 CD	1 CD
2	Magnetic tape, formatted PCM quick-look (Tel II)	4 hr	*
3, 4	Magnetic tape, formatted PCM final (Tel II)	9 hr	6 hr
3, 4	Magnetic tape, formatted PCM (GBI)	1 CD	1 CD

*Not required, final received in 6 hours.

TABLE XV-2 (continued)

OD Item No.	Description	Time Requested (Canaveral)	Time Received (Baltimore)
1.5-7	Signal strength, center frequency recording (Tel II)	1 CD	7 CD
1.5-52	Signal strength, center frequency recording (Tel III)	1 CD	7 CD
3.5-6	Signal strength, center frequency recording (GBI)	3 CD	7 CD
4.5-3	Signal strength, center frequency recording (San Salvador)	**	5 CD
7.5-3	Signal strength, center frequency recording (Grand Turk)	3 CD	26 CD
91.5-4	Signal strength, center frequency recording (Antigua)	**	7 CD
1.11-1	Command control recording (Station 1)	3 WD	5 WD
1.11-5	Command control recording (Station 1)	3 WD	5 WD
1.11-6	Command control recording (Station 1)	3 WD	5 WD
3.11-1	Command control recording (GBI)	5 WD	5 WD
3.11-3	Command control recording (GBI)	5 WD	7 WD
7.11-1	Command control recording (Grand Turk)	5 WD	7 WD
7.11-3	Command control recording (Grand Turk)	5 WD	5 WD
91.11-1	Command control recording (Antigua)	**	5 WD

TABLE XV-2 (continued)

OD Item No.	Description	Time Requested (Canaveral)	Time Received (Baltimore)
1.11-4	Command control operators log (Station 1)	3 WD	15 WD
3.11-2	Command control operators log (GBI)	3 WD	15 WD
7.11-2	Command control operators log (Grand Turk)	3 WD	15 WD
1.11-25	Command antenna pointing data (Station 1)	5 CD	21 CD
3.11-25	Command antenna pointing data (GBI)	5 CD	21 CD
7.11-25	Command antenna pointing data (Grand Turk)	5 CD	8 CD
91.11-2	Command antenna pointing data (Antigua)	**	8 CD
1.18	Range safety plotboard charts	4 hr	5 WD
5.4.1.2	Propellant analysis report	2 WD	*
2.4-1	Preliminary test report	2 hr	5 WD
1.6-3	Command control field intensity, vertical polarization	3 WD	*
1.6-4	Command control field intensity, horizontal polarization	3 WD	*
1.6-62	Special FCA log	3 WD	3 WD
253	Vehicle engineering units (KSC NASA)	2 CD	7 CD
266	Vehicle computer words (KSC NASA)	1 CD	7 CD
249	Vehicle bilevels (KSC NASA)	1 CD	7 CD

*Data not received by 11 April 1966.
**Supplemental data received.

CD = Calendar days
WD = Working days

4. Agency/Contractor Supplied Data

Table XV-3 presents data received from associated contractors and NASA-MSC.

TABLE XV-3

Agency/Contractor Supplied Data

Description	Supplier	Received (Baltimore)
Mod III radio guidance system	GE-Syracuse	1 CD
Spacecraft ascent mode	NASA	9 CD
Spacecraft bilevel events	NASA	9 CD
Spacecraft Mode 2 ascent	NASA	12 CD
Spacecraft time history	NASA	12 CD
Spacecraft rates and attitude control	NASA	16 CD

B. FILM COVERAGE

Photographic coverage of the GT-8 launch (16 March 1966) was good; however, the high altitude tracking coverage was partially obscured by a thin cloud cover. Table XV-4 contains a listing of the films obtained from the fixed and the tracking cameras.

The 70-mm tracking films (Items 1.2-40 and 1.2-41) were reviewed for information pertaining to the booster staging event. The portion of film received for item 1.2-41 did not include the staging event, and item 1.2-40 was not clear enough to observe particles from the normal break-up of the transportation section.

TABLE XV-4

Film Coverage and Disposition

OD Item No.	Description	Footage (ft)	Time Received (Baltimore)
1.2-10 16mm fixed	Missile centered, movement at launch, 50-ft tower 19-5	110	5 WD
1.2-13 16mm fixed	Spacecraft centered, launch sequence, 50-ft tower 19-7A	75	6 WD
1.2-14 16mm fixed	Explosive bolts and first motion, Stage 2 umbilical	127	6 WD
1.2-15 16mm fixed	Explosive bolts and first motion, 50-ft tower 19-7A	130	8 WD
1.2-16 16mm fixed	Engine area centered, east launch ring	150	7 WD
1.2-17 16mm fixed	Engine area centered, west launch ring	140	7 WD
1.2-18 16mm fixed	Engine bells centered, north launch ring	120	7 WD
1.2-19 16mm fixed	Engine bells centered, south launch ring	115	8 WD
1.2-20 16mm fixed	3D1E and 3D2E umbilical plugs, umbilical tower, first level	75	7 WD
1.2-21 16mm fixed	2DFVT umbilical plug, umbilical tower, second level	130	7 WD
1.2-22 16mm fixed	1DOVT umbilical plug, umbilical tower, fourth level	150	6 WD
1.2-23 16mm fixed	3B1E and associated umbilical plugs, umbilical tower, fifth level	139	7 WD
1.2-24 16mm fixed	2B1E and associated umbilical plugs, umbilical tower, sixth level	134	7 WD
1.2-25 16mm fixed	Umbilical boom 3, "J" bars and lanyards, umbilical tower, sixth level	208	6 WD
1.2-26 16mm fixed	Spacecraft upper umbilical plug, top umbilical tower, level No. 1	145	8 WD
1.2-27 16mm fixed	Spacecraft lower umbilical, top umbilical tower, level No. 2	125	7 WD
1.2-31 16mm tracking	Spacecraft centered, LO to LOV, U191L122	390	7 WD
1.2-34 16mm tracking	Missile centered, LO to LOV, U102R6	270	6 WD
1.2-36 16mm tracking	Engine centered to missile centered, first acquisition to LOV, U112L24	260	5 WD
1.2-37 16mm tracking	Engine centered to missile centered, first acquisition to LOV, U29R46	276	5 WD
1.2-38 16mm tracking	Engine centered to missile centered, first acquisition to LOV, U247L116	282	6 WD
1.2-40 16mm tracking	Missile centered, first acquisition to staging (ROTI) RTCB	128	6 WD
1.2-40 70mm tracking	Missile centered, first acquisition to staging (ROTI) RTCB	983	16 CD
1.2-41 16mm tracking	Missile centered, first acquisition to staging (ROTI) RTMB	16	7 WD
1.2-41 70mm tracking	Missile centered, first acquisition to staging (ROTI) RTMB	116	9 CD
1.2-44 16mm tracking	Missile centered, airborne coverage (C-54)	280	7 WD
1.2-45 16mm tracking	Missile centered, airborne coverage (C-54)		*

*Data not received by 11 April 1966

CD = Calendar days
WD = Working days

XVI. PRELAUNCH AND COUNTDOWN OPERATIONS

A. PRELAUNCH

1. Simulated Flight Test

The GT-8 simulated flight test (SFT) was performed successfully on 10 March 1966 in accordance with the Martin Test Procedure (Ref. 9). For monitoring and training, the backup crew was in the spacecraft during the primary and secondary runs.

The countdown for the secondary run was started at T-45 minutes (1230 EST) and was completed successfully at T+6 minutes (1321 EST).

During the recycle period in preparation for the primary run, a power failure occurred at the command transmitter building at Cape Kennedy and subsequently delayed the test for approximately 2-1/2 hours.

The primary run was picked up at T-3 minutes (1655 EST) and was successfully completed at T+6 minutes (1704 EST).

During the F-1 day preparation, on 14 March 1966, the launch date was rescheduled to 16 March 1966 due to electrical and mechanical problems encountered by the Atlas standard launch vehicle and the Gemini spacecraft.

2. Precountdown Activities

The precountdown tests were started, with power being applied to the launch vehicle at 0840 EST on 15 March 1966. The range sequencer was picked up at T-725 minutes (1630 EST), and the precountdown tests were completed successfully, with the range sequencer being secured at T-530 minutes (1945 EST). Propellant loading was delayed approximately two hours because McDonnell personnel were troubleshooting the spacecraft heater and communication circuits.

Oxidizer loading started at 0050 EST on 16 March 1966 and was completed at 0235 EST. Fuel loading was started at 0318 and was completed at 0422 EST.

The range sequencer was restarted on schedule at T-530 minutes at 0245 EST on 16 March.

At approximately T-360, while bringing up hydraulics to support the Stage I primary rate gain test, a malfunction occurred which prevented pressurization of the Stage I primary hydraulic system. After

evaluation, subsequent runs were performed, and the malfunction did not reoccur. Based on test data and the AGE console operator observations, the transient malfunction was isolated to either the hydraulic system test select valve or the electric motor-driven pump. Since both components are used for ground test only, the countdown continued. Investigation of the probable cause is being conducted at the Martin-Baltimore facility.

B. LAUNCH COUNTDOWN

The launch countdown was picked up on schedule at 0735 EST on 16 March 1966. The 240-minute countdown was performed in accordance with the Martin Test Procedure (Ref. 10). The countdown progressed smoothly, and astronaut ingress occurred at approximately T-120 minutes.

The Atlas-Agena was successfully launched at T-95 minutes (1000 EST).

Review of the data from the TARS programmer/guidance command test revealed that the pitch torquer monitor voltage traces on the CP 2650 recorder were out of specification. Subsequent rerun and review of the real-time telemetry data indicated proper in-specification values. An out-of-calibration condition on the CP 2650 recorder was confirmed, and an investigation will be performed to determine the cause of the problem.

The countdown continued normally, and the programmed hold was initiated automatically at T-3 minutes to adjust for proper liftoff time. The hold was in effect for 5 minutes and 54 seconds. The countdown was resumed at T-3 minutes (1137: 59 EST), and liftoff occurred on schedule at 1141 EST for a successful launch.

The countdown schedule is shown in Fig. XVI-1.

XVI-3-1

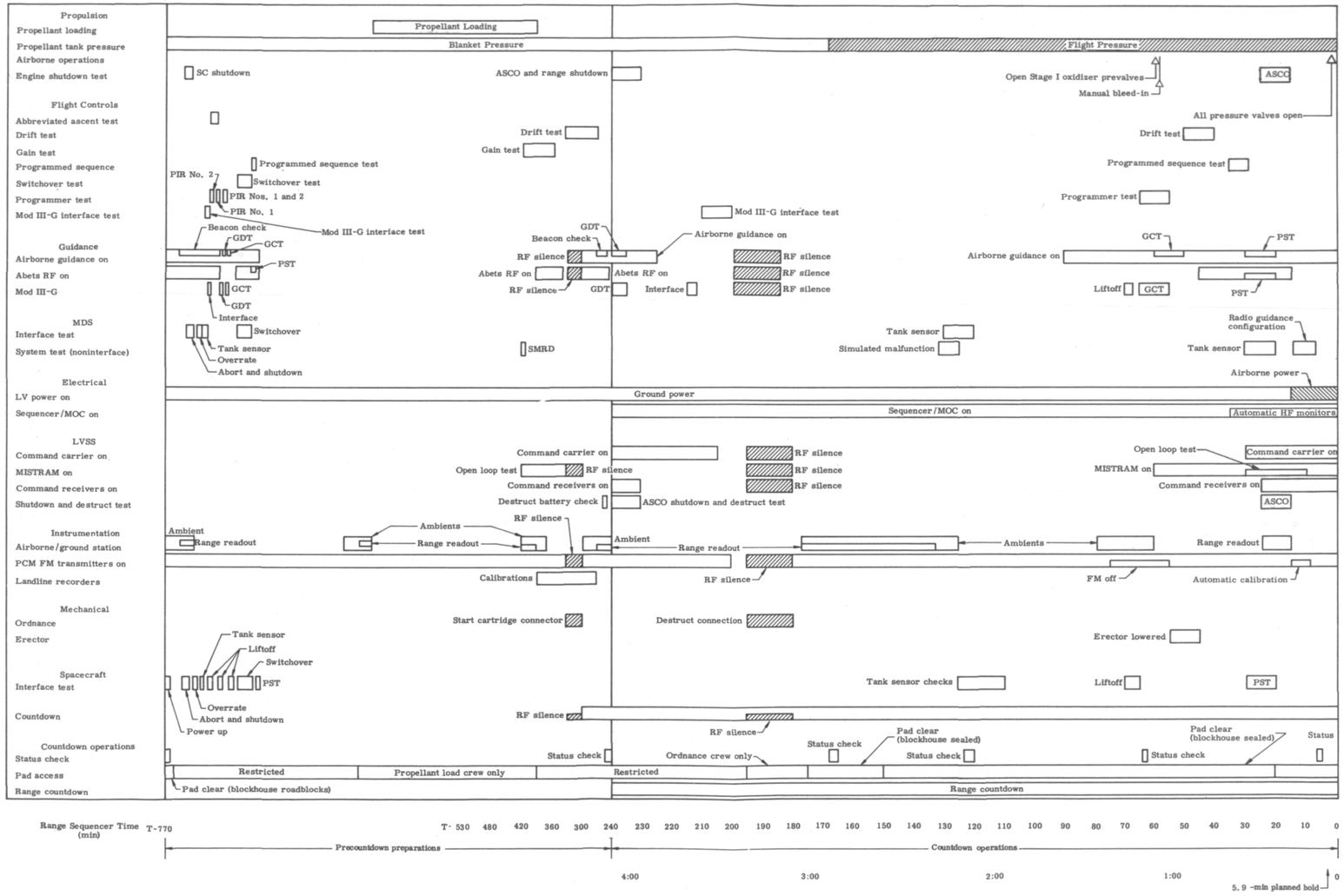

Fig. XVI-1. Planned Precount and Countdown

XVII. CONFIGURATION SUMMARY

A. LAUNCH VEHICLE SYSTEMS DESCRIPTION

The Gemini Launch Vehicle (GLV) is a modified two-stage Titan II intercontinental ballistics missile (ICBM) which has been "man rated" for Gemini usage. The propulsion system in each stage uses hypergolic (self-igniting upon mixture) propellants. Modifications to the basic Titan II vehicle to achieve the "man rated" GLV follow:

(1) Addition of a completely redundant malfunction detection system (MDS).

(2) Replacement of the Titan II inertial guidance system (IGS) with the Mod III-G radio guidance system (RGS).

(3) Addition of a three-axis reference system (TARS) to provide attitude reference and open-loop programming to the autopilot.

(4) Addition of a secondary flight control system (FCS).

(5) Addition of a secondary Stage I hydraulic system.

(6) Addition of the capability of switchover to the secondary guidance, flight control, and hydraulic systems.

(7) Provision of redundancy in electrical sequencing by APS and IPS power.

(8) Provision of an engine shutdown capability from the spacecraft.

(9) Provision of a 120-inch diameter cylindrical skirt forward of the Stage II oxidizer tank for mating the spacecraft to the launch vehicle.

(10) Removal of the retrorockets, vernier rockets and associated equipment.

(11) Addition of fuel line spring-piston accumulators and oxidizer line tuned standpipes for suppression of POGO vibrations.

(12) Capability for redundant Stage II engine shutdown (GLV-3 and up).

Significant GLV-8 changes from the GLV-7 configuration are listed in Table XVII-1.

TABLE XVII-1

GLV-8 Modifications

System	Significant Changes from GLV-7
Structures	1. Eliminate low pressure helium leak test before hydro test on Stages I and II propellant tanks 2. Visibility cutout provided in receptacle support fairings for pad disconnects 3D1M and 3D2M*
Propulsion	1. Improved Stage II engine injector (GEMSIP) incorporated
Flight controls	1. Time of gain change No. 1 changed from LO + 110 seconds to LO + 105 seconds. The 0.5- to 10-second delay timer was eliminated
Guidance	None
Hydraulics	1. Dummy engine driven pumps used in testing. Newly cleaned pumps installed at ETR prior to SFT 2. Tandem actuator position transducer revised to use more reliable 2N2222 transistors
Electrical	1. Flashing beacon lights not provided 2. Breakwire and index marking added to pad disconnects 3D1M and 3D2M* 3. Stiffeners added to telemetry antenna
Malfunction detection	1. Alignment scribe marks added to Stages I and II separation connector
Instrumentation	None
Range safety and ordnance	None
AGE	1. Landline Meas 4601 (Stage II fuel tank temperature) not recorded on magnetic tape. Meas 2643 (Stage II hydraulic pump thermal switch) added to magnetic tape 2. Holdfires HF A2 (PCS launch mode) and HF D6 (Stage I flame bucket pressure monitor) removed

*These items were incorporated on GLV-6 at ETR.

A detailed description of all GLV systems is presented in Martin Engineering Report, "Launch Vehicle No. 4 Flight Evaluation" (Ref. 4).

B. MAJOR COMPONENTS

The two major GT-8 components were as follows:

(1) Spacecraft

(a) Manufacturer: McDonnell Aircraft Corporation

(b) Serial Number: Spacecraft Number 8

(2) Gemini Launch Vehicle

(a) Manufacturer: Martin Company

(b) Serial Number: GLV-8

(c) Air Force Serial Number: 62-12563.

Figure XVII-1 shows the general arrangement of the GLV.

XVII-4-2

XVII-4-3

LAUNCH VEHICLE UMBILICAL SYSTEMS INTERFACE

CODE	FUNCTION	SYSTEM	LOCATION
28A	AIR COND.	GUIDANCE AIR COND. STG II	STA. 371.522 QUAD I 62½° OFF BL.O
52BOV	OXID. VENT	OXID. STG II	STA. 371.522 QUAD. II 65° OFF BL.O
282E	ELECTRICAL	ELECTRICAL STG II	STA 402.472 QUAD. II 80½° OFF BL.O
28IE	ELECTRICAL	ELECTRICAL STG II	STA 402.472 QUAD II 65½° OFF BL.O
28FVT	FUEL VENT TOPPING	FUEL STAGE II	STA. 406.491 QUAD II 84° 20' OFF BL.O
52BFV	FUEL VENT	FUEL STG II	STA. 404.472 QUAD II 37½° OFF BL.O
53BH	HYDRAULIC	HYDRAULIC STG II	STA 470.125 QUAD II 15° OFF BL.O
▲ 3BA	AIR CONDITIONING	ENGINE AREA STG II	STA 474.875 QUAD II 30° OFF BL.O
53BF	FUEL FILL AND DRAIN	FUEL STG II	STA 492.250 QUAD II 15° OFF BL.O
3BFD	FUEL PRESS. SEQ. VALVE DRAIN	FUEL STG II	STA 492.250 QUAD II 30° OFF BL.O
53BO	OXID. FILL AND DRAIN	OXID STG II	STA 492.250 QUAD II 72° OFF BL.O
3BIE	ELECTRICAL	ELECTRICAL STG II	STA 492.250 QUAD II 45° OFF BL.O
ICIFD	TUBO-PUMP FUEL DRAIN	FUEL STG I	STA 554.750 QUAD II 17½ OFF BL.O
ICOD	TUBO-PUMP OXID. DRAIN	OXID STG I	STA 554.750 QUAD I 17½ OFF BL.O
SIDOV	OXID. VENT	OXID STG I	STA 530.727 QUAD II 60° OFF WL 60.0
S2DFV	FUEL VENT	FUEL STG I	STA 963.326 QUAD II 40° OFF BL.O
3DIM	MALFUNCTION DETECTION SYS.	MALFUNCTION STG I	STA 214.873 QUAD I 36 3/4° OFF BL.O
3D2M	MALFUNCTION DETECTION SYS.	MALFUNCTION STG I	STA 214.873 QUAD III 36½° OFF BL.O
3DIE	ELECTRICAL	ELECTRICAL STG I	STA 1216.691 QUAD II 20° OFF BL.O
53DF	FUEL FILL AND DRAIN	FUEL STG I	STA 1243.560 QUAD I
53DFD	FUEL DRAIN - PRE-VALVE	FUEL STG I	STA 1244.123 QUAD III
53DOD	OXID. DRAIN - PRE-VALVE	OXID. STG I	STA 1250.560 QUAD II
53DIH	HYDRAULIC SUPPLY AND RETURN	HYDRAULIC STG I PRIMARY	STA 1255.835 QUAD I
53DO	OXID. FILL AND DRAIN	OXID. STG I	STA 1249.560 QUAD IV
2BOVT	OXID. VENT TOPPING	OXID. STG II	STA. 351.802 QUAD II 4° OFF WL 60
IDOVT	OXID. VENT TOPPING	OXID. STG I	STA 630.727 QUAD II 60° OFF BL.O
2DFVT	FUEL VENT TOPPING	FUEL STAGE I	STA 963.326 QUAD II 50° OFF BL.O
3D2E	ELECTRICAL	ELECTRICAL STG I	STA 1216.691 QUAD II 60° OFF BL.O
53D2H	HYDRAULIC SUPPLY AND RETURN	HYDRAULIC STG I SECONDARY	STA 1255.835 QUAD II
▲ 3D10C	OXID. REMOTE CHARGING SYSTEM	OXID. STG. I	STA. 1224.311 QUAD III 22½° OFF B.L.O.
▲ 3D20C	OXID. REMOTE CHARGING SYSTEM	OXID. STG. I	STA. 1224.311 QUAD III 17½° OFF B.L.O.

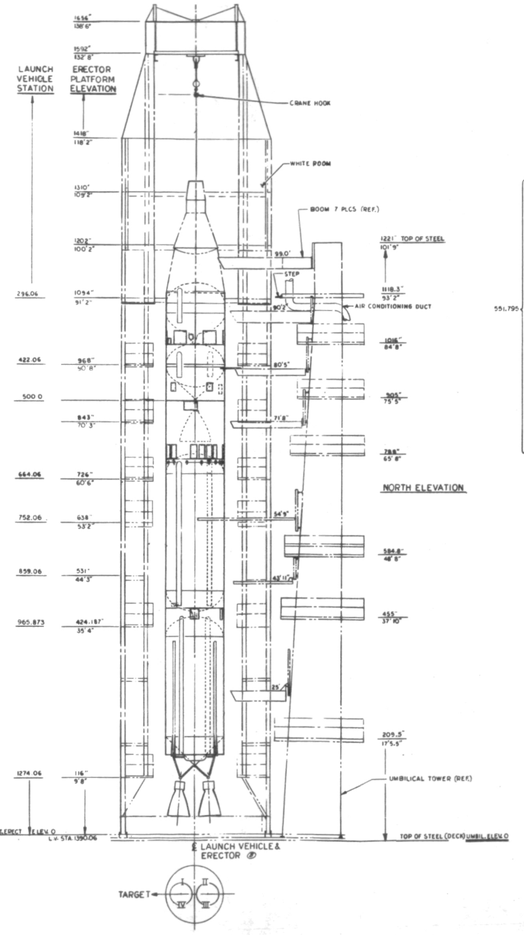

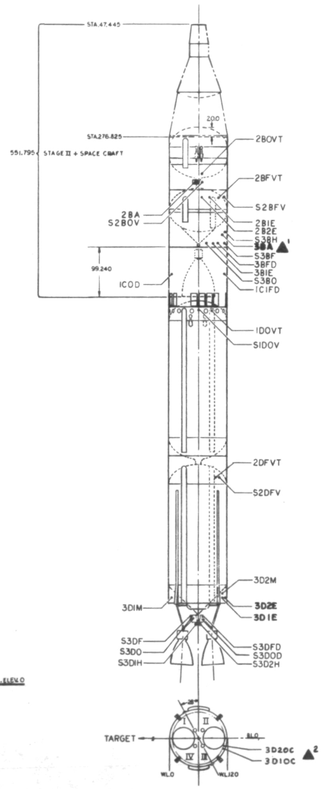

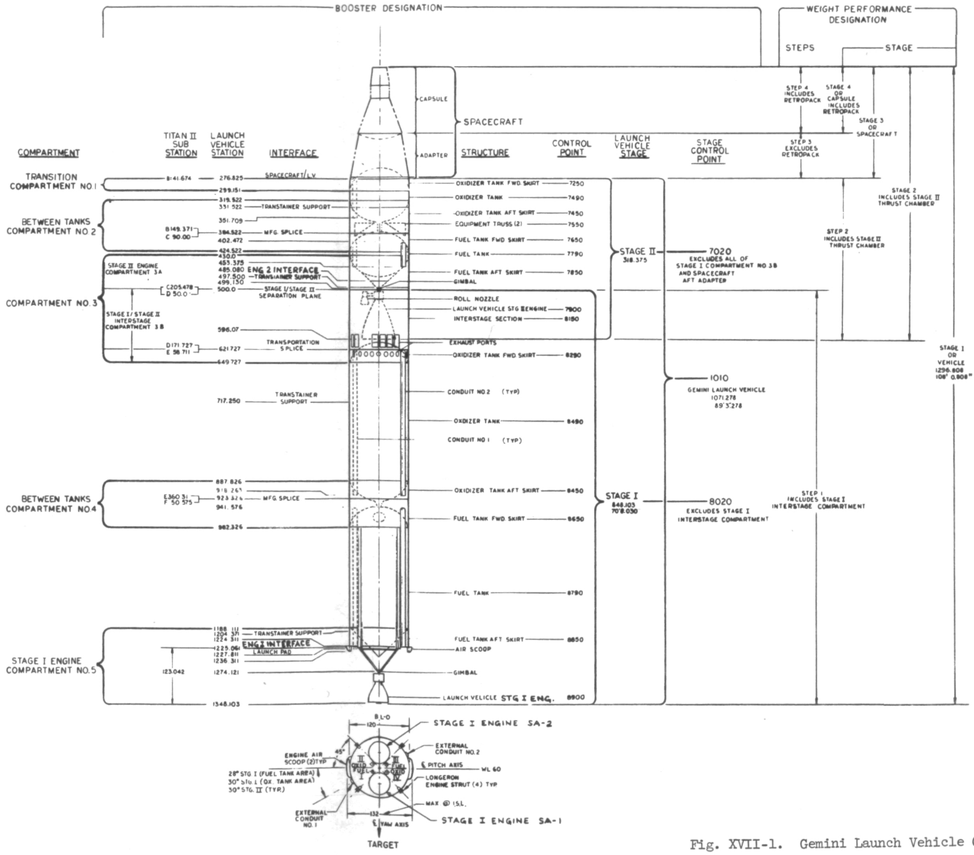

4. ▲2 GLV 4 & UP
3. ▲ GLV 1 THRU 4 ONLY
2. THIS DRAWING RELEASES NO PARTS REF. ONLY.
1. NEW GEMINI LAUNCH VEHICLE DRAWING

NOTE

Fig. XVII-1. Gemini Launch Vehicle General Arrangement

XVIII. REFERENCES

1. "Launch Vehicle No. 6 Flight Evaluation." Engineering Report 13227-6, Martin Company, Baltimore, Maryland, February 1966. Confidential

2. "Launch Vehicle No. 7 Flight Evaluation." Engineering Report 13227-7, Martin Company, Baltimore, Maryland, January 1966. Confidential

3. "Launch Vehicle No. 5 Flight Evaluation." Engineering Report 13227-5, Martin Company, Baltimore, Maryland, October 1965. Confidential

4. "Launch Vehicle No. 4 Flight Evaluation." Engineering Report 13227-4, Martin Company, Baltimore, Maryland, July 1965. Confidential

5. "Launch Vehicle No. 3 Flight Evaluation." Engineering Report 13227-3, Martin Company, Baltimore, Maryland, May 1965. Confidential

6. "Launch Vehicle No. 2 Flight Evaluation." Engineering Report 13227-2, Martin Company, Baltimore, Maryland, March 1965. Confidential

7. "Launch Vehicle No. 2 Launch Attempt Evaluation." Engineering Report 13227-2X, Martin Company, Baltimore, Maryland, January 1965. Confidential

8. "Launch Vehicle No. 1 Flight Evaluation." Engineering Report 13227-1, Martin Company, Baltimore, Maryland, May 1964. Confidential

9. "Martin-Canaveral Test Procedure." 424-876-ETR, Revision F.

10. "Martin-Canaveral Test Procedure." 424-875-ETR, Revision O.

11. "GT-8 Pre-flight Test Report." LV-326-8, Martin Company, Baltimore, Maryland, March 1966. Confidential

12. "Gemini Launch Vehicle Performance Specification." MB-1046, SCN-11, Martin Company, Baltimore, Maryland, March 1966. Confidential

13. Letter from SSD to MMB, dated 19 October 1965, subject: "Transmittal of RGS Dispersions for GT-6."

14. "Flight Weight Coordination Report, Post-Flight Weight, GT-8." LV-165-8B, Martin Company, Baltimore, Maryland, 12 April 1966.

15. "Subsystem Engineering Analysis YLR 87-AJ-5 and YLR 91-AJ-5 Rocket Engines." AGC 521-3.15 Q-15, Aerojet-General Corporation, Sacramento, California, 22 July 1964. Confidential

16. "Master Measurements List." LV-220, Revision N, Martin Company, Baltimore, Maryland, 24 January 1966.

17. "GLV Longitudinal Oscillation Instability Study--POGO." Engineering Report 13374, Martin Company, Baltimore, Maryland, December 1964.

18. "The Analytical Feasibility of ATC Removal." LV-402, Martin Company, Baltimore, Maryland.

APPENDIX A

SUMMARY OF GEMINI LAUNCHES

A-2-2

CONFIDENTIAL

Summary of Gemini Launches

Mission	Launch Date and Time (hr EST)	Launch Vehicle Payload (lb)	Burning Time Stage I (sec)	Burning Time Stage II (sec)	Inertial Velocity (fps) BECO	Inertial Velocity (fps) SECO	Inertial Velocity (fps) SECO + 20 Sec	Altitude (ft) BECO	Altitude (ft) SECO	Altitude (ft) SECO + 20 Sec	Inertial Flight Path Angle (deg) BECO	Inertial Flight Path Angle (deg) SECO	Inertial Flight Path Angle (deg) SECO + 20 Sec	Time in Orbit ③ (hr) Stage II	Time in Orbit ③ (hr) Spacecraft	Orbit (naut mi) Apogee	Orbit (naut mi) Perigee	Launch Evaluation Report Number
GT-1	4-8-64 1100	7029 ①	157.5	185.3	9,752	25,679	25,786	208,262	531,500	528,184	20.00	0.0	-0.03	95.2 ① (64 orbits)	95.2 ① (64 orbits)	173	86.6	ER 13227-1
GT-2	1-19-65 0904	6890 ②	155.1	180.4	9,916	25,611	25,738	229,743	546,960	526,380	26.219	-2.4523	-2.3431	N/A ②	N/A ②	N/A ②	N/A ②	ER 13227-2X ④ ER 13227-2
GT-3	3-23-65 0924	7112	155.8	181.3	9,981	25,587	25,688	224,777	531,477	532,338	21.79	0.0	0.0323	18 (13 orbits)	4.6 (3 orbits)	121	87	ER 13227-3
GT-4	6-3-65 1016	7868	155.7	181.3	9,844	25,670	25,745	214,775	531,522	532,886	18.66	-0.0235	0.059	47.7 (34 orbits)	97.7 (66 orbits)	152.3	87	ER 13227-4
GT-5	8-21-65 0900	7947	156.8	179.7	9,848	25,713	25,806	215,607	531,276	531,118	19.90	-0.0279	-0.0129	72 (51 orbits)	190.9 (127.9 orbits)	189	87	ER 13227-5
GT-7	12-4-65 1430	8085	159.1	181.4	10,049	25,735	25,789	207,088	529,583	529,738	18.66	0.0500	0.0285	66 (46.6 orbits)	330.6 (219.8 orbits)	177.1	87	ER 13227-7
GT-6A	12-15-65 0837	7821	160.4	181.6	9,992	25,634	25,728	202,186	529,891	530,201	17.94	0.08	-0.054	31 (21 orbits)	25.8 (17.1 orbits)	140.4	87	ER 13227-6
GT-8	3-16-66 1141	8351	157.9	182.9	9,917	25,663	25,736	209,005	527,191	526,600	19.34	-0.141	-0.02	29 (21.1 orbits)	10.7 (7 orbits)	148.2	86.9	ER 13227-8

① Spacecraft and Stage II inserted into orbit as a unit.

② Suborbital mission (spacecraft impact 2125 miles downrange).

③ Inertial orbit.

④ Launch attempt report.

CONFIDENTIAL

CONFIDENTIAL

ER 13227-8

MARTIN MARIETTA

CONFIDENTIAL